Theoretical and Experimental Investigation of the Equilibrium and Dynamic Interfacial Behavior of Mixed Surfactant Solutions

by

Michael Mulqueen

Submitted to the Department of Chemical Engineering
in partial fulfillment of the requirements for the degree of

Doctor of Philosophy in Chemical Engineering

at the

MASSACHUSETTS INSTITUTE OF TECHNOLOGY

September 2001

Author .....
Department of Chemical Engineering
August 20, 2001

Certified by. .....
Daniel Blankschtein
Professor
Thesis Supervisor

Accepted by .....
Daniel Blankschtein
Chairman, Department Committee on Graduate Students

Theoretical and Experimental Investigation of the Equilibrium and Dynamic Interfacial Behavior of Mixed Surfactant Solutions

by

Michael Mulqueen

Submitted to the Department of Chemical Engineering
on August 20, 2001, in partial fulfillment of the
requirements for the degree of
Doctor of Philosophy in Chemical Engineering

Abstract

In many commercial applications involving surfactants, the desired properties are controlled by both the equilibrium and the dynamic interfacial behavior. In particular, surfactant adsorption at air-water interfaces causes the surface tension to decrease, which, for example, can control the spreading properties of a liquid, and hence, is important in practical applications involving the use of paints and pesticides, as well as in the manufacturing of photographic films. Similarly, surfactant adsorption at oil-water interfaces causes the interfacial tension to decrease, which, for example, can enhance the ability of surfactant solutions to remove oily soil from dirty surfaces (fabric, hair, skin, etc.) during cleaning applications.

A predictive, molecular-thermodynamic theory capable of modeling the behavior of surfactants at solution interfaces would help minimize the need for costly and time-consuming experimentation associated with the development of surfactant products based on a trial-and-error approach. Furthermore, this theory should encompass mixtures of surfactants, since their use in industrial applications is widespread, whether intentionally, to take advantage of synergism between the surfactant components in a mixture, or simply because it is too costly to mass produce a single, pure surfactant. With this as motivation, a molecularly-based theoretical framework to model both the equilibrium and the dynamic adsorption of surfactant mixtures at both the air-water interface and the oil-water interface has been developed.

The equilibrium air-water surface equation of state is based on a two-dimensional, nonideal gas-like monolayer model of the adsorbed surfactant molecules. For nonionic surfactants, two types of interactions were accounted for: (i) repulsive, steric interactions, which were modeled using a hard-disk treatment, and (ii) attractive, van der Waals interactions, which were modeled using a virial expansion, truncated to second order in surfactant surface concentration. Since both the hard-disk size and the second-order virial coefficients characterizing these interactions can be deduced from the known molecular structures of the surfactants, this surface equation of state

contains no experimentally determined parameters. This nonionic surface equation of state was subsequently modified to incorporate electrostatic effects associated with charged surfactants. For mixtures that contain only a single ionic surfactant species, the electrostatic contribution to the surface equation of state was computed using a Gouy-Chapman based approach, which also included a Stern layer of counterion exclusion. This electrostatic description assumes that all of the electrostatic charge on the adsorbed surfactant molecules is located on a single two-dimensional charge layer. The Gouy-Chapman model was then extended to mixtures that contain multiple ionic surfactants, or surfactants that contain multiple charged groups (such as zwitterionic surfactants) by treating the case of multiple, two-dimensional charge layers at the interface. This extended theoretical framework is capable of treating any number of surfactant components containing any number of charged groups, without requiring any experimentally determined parameters for the mixture.

To relate the surfactant surface concentration and the surface tension to the bulk surfactant concentration and composition, an adsorption isotherm was utilized that contains one experimentally determined parameter for each surfactant component in the mixture, which can be determined from one surface tension measurement on a single surfactant solution of each surfactant component. The resulting theory does not contain any mixture dependent experimentally determined parameters, and hence, no experiments are required on the mixed surfactant solutions. Good agreement was found between the theoretical predictions and the experimental surface tension, surface concentration, and surface composition values obtained from the literature for mixtures containing nonionic, ionic, and zwitterionic surfactants.

The equilibrium air-water surface equation of state was then generalized to treat the case of surfactants adsorbed at the oil-water interface. This was done by eliminating the van der Waals attractive interactions between the hydrophobic tails of the adsorbed surfactant molecules, reflecting the compatibility of the hydrocarbon oil phase and the hydrocarbon surfactant tails. Note that the other surfactant molecular parameters, such as the hard-disk size, are the same for the air-water surface case and the oil-water interface case. To test the validity and range of applicability of this theory, the decane-water interfacial tension of surfactant solutions selected specifically for this purpose was measured using a ring tensiometer, and good agreement was found between the theoretical predictions and the experimental values, including those obtained from the literature.

The equilibrium air-water surface equation of state was subsequently utilized as the basis for a theoretical framework of dynamic surfactant adsorption capable of predicting the surface tension, surface concentration, and surface composition, all as a function of time. In addition to the complete prediction of these dynamic profiles, a simplified timescale analysis was utilized to quickly predict the timescale for adsorption of each surfactant component present in the mixture. This timescale analysis is also valuable in that it provides a relationship between the chemical structure of a surfactant molecule and its dynamic properties. To test the validity and range of applicability of the dynamic interfacial theory, the dynamic surface tension of a surfactant mixture chosen specifically for this purpose was measured using a pendant bubble tensiometer, and good agreement was found between the theoretical predic-

tions and the experimental results.

Finally, in order to facilitate the use of the theories developed as part of this thesis by industrial researchers, and to create a better link between this academic work and commercial applications, the various theoretical frameworks developed in this thesis were incorporated in two user-friendly computer programs, Program SURF and Program DYNAMIC, for industrial use. It is hoped that the theoretical developments presented in this thesis, including the two computer programs, will facilitate the design and optimization of surfactant solutions of practical relevance having the desired interfacial properties by reducing the need for relatively costly and time-consuming experimentation.

Thesis Supervisor: Daniel Blankschtein
Title: Professor

Acknowledgments

I owe a great deal of gratitude to a number of people who have helped me throughout my journey at MIT and the completion of this thesis. First of all, I would like to thank, my advisor, Professor Daniel Blankschtein. This thesis could not have been completed without his hard work and dedication. Furthermore, I thank the members of my thesis committee –Professor William Deen and Professor Alan Hatton– for their guidance and for making my thesis committee meetings an enjoyable and educational exchange of ideas.

I would also like to thank all of the current and former members of the Blankschtein group, including: Nancy Diggs, Anat Shiloach, Ginger Tse, Daniel Kamei, Peter Moore, Hua Tang, Betty Yu, Isaac Reif, Vibha Srinivasan, Hua Tang, Arthur Goldsipe, Henry Lam, and Joseph Kushner. In addition to the many technical discussions that we have all shared about each others research, the group has been a source of friendship during my years at MIT. Even a partial list of all of the good times that we have shared would turn this thesis into a two volume set. I am often amazed at how much fun we have had together and your company will truly be missed.

On a more personal note, I would like to thank Samantha Arrington for bringing a ton of Southern warmth and friendliness up here to the cold North, for taking me places I otherwise would not have gone, and for surrounding me with dogs. I thank Bill Jeffrey for giving me countless opportunities to get away from MIT while still being able to have meaningful technical discussions interspersed with Monty Python jokes without it being too nerdy. I thank Vivek "Sir Blue" Sujan for turning the gym into a home-away-from-home, as well as the other gym buddies, including: Tony "Hardy" Caola, Paul "Hunter" Duchnowski, Jason "Tito" James, Shawn "the Big U" Mowry, Tim "Hard Core" Pigeon, and Chris "Air Force One" Spadaccini, for countless number of spots. Finally, I thank my mother and father for starting me out on the right track and for making everything possible. They, along with my brother and grandmother, have given me a place where I always feel welcome, and the importance of that can not be overstated.

Contents

List of Figures

List of Tables

Chapter 1

Introduction

1.1 Background and Motivation

Surfactants are molecules having a unique molecular architecture consisting of a hydrophilic (water-loving) group, referred to as the "head", and a hydrophobic (water-fearing) group, referred to as the "tail". The tail commonly consists of a hydrocarbon chain, while the head can be of the nonionic, ionic, or zwitterionic variety. The covalent bond between the head and the tail constrains these dissimilar chemical groups to remain together, leading to the interesting and unique behavior exhibited by surfactants in aqueous solutions. Two very important characteristics of surfactants, driven by their simultaneous hydrophilic and hydrophobic character, are: (i) their tendency to accumulate at interfaces (for example, air-water or oil-water), with their hydrophobic tails pointing out of the aqueous solution into the less polar air or oil phases, and (ii) their tendency to form aggregates (known as micelles) in the bulk of the aqueous solution, in which the hydrophobic tails cluster together in the micellar core, which can be viewed as a "micro-phase of oil". Micellization generally occurs at surfactant concentrations which exceed a critical surfactant concentration, referred to as the Critical Micelle Concentration (CMC).

There are many important industrial and commercial applications that exploit these unique surfactant characteristics. Surfactant accumulation at interfaces lowers the interfacial tension which is important in detergency, coating and wetting pro-

cesses, enhanced oil recovery, and emulsification. Surfactant accumulation at interfaces also provides a mass transport barrier in corrosion protection and evaporative-loss reduction, and also affects the stability of foams.[1–10] In these and other practical applications, surfactant mixtures are commonly utilized, because: (i) they often exhibit properties that are superior to those attained utilizing the individual, single surfactants, (ii) environmental and health concerns often dictate the mixing of known and approved surfactants rather than the use of a totally new surfactant, and (iii) it is often too costly to mass produce and purify a single, pure surfactant.[11] Furthermore, different types of surfactants (which include nonionic, ionic, or zwitterionic surfactants), or mixtures of different types of surfactants, are commonly employed.

As stressed below in Section 1.2, a central goal of this thesis is the prediction of interfacial properties, namely, the prediction of the surface tension and the amount of each type of surfactant adsorbed at the interface, for various surfactant solutions. As further motivation for the work presented in this thesis, a number of important processes where the interfacial properties are important are described below. It should be noted that for processes that occur over a relatively short time period (relative to the rate of adsorption of the surfactant), it is the dynamic interfacial properties that are important. On the other hand, for processes that occur over a relatively long time period, only the equilibrium interfacial properties are important. Both the equilibrium and the dynamic interfacial properties of surfactant solutions will be addressed in this thesis.

1.1.1 Examples of Practical Applications of Surfactants where Interfacial Properties are Important

1.1.1.1 Detergency

The most common commercial use of surfactants is in soaps and detergents for cleaning purposes, with current US annual sales in the $10 billion range.[2] Although this is an old industry, price pressures, environmental concerns, new cleaning techniques, and the competitive drive for new products makes this an active area of research.[3]

In general, the removal of oily soil from surfaces (e.g., fabric, hair, skin, etc.) is a complex process involving both equilibrium and kinetic processes. There are three major known mechanisms involved in the removal of oily soil from solid surfaces by a surfactant solution: "roll-up", "necking" or emulsification, and solubilization.[2,4] In the "roll-up" process, the contact angle of an oil droplet (in this case the "soil" that needs to be removed from the solid surface) is increased until no contact exists between the oil and the solid surface (see Figure 1-1). The equilibrium contact angle, θ, is given by the Young equation:

$$\cos(\theta) = \frac{\sigma_{WS} - \sigma_{OS}}{\sigma_{OW}} \tag{1.1}$$

where σ_{WS}, σ_{OS}, and σ_{OW} are the water/solid, oil/solid, and oil-water interfacial tensions, respectively. Complete, spontaneous removal of the oily soil can theoretically occur only if the contact angle is 180°; however, in practice, this process occurs at smaller contact angles due to hydraulic and buoyancy forces.[2] Accordingly, one can control the "roll-up" process by controlling the interfacial tensions in Eq. (1.1) with the use of surfactants.

Necking is a kinetic process in which part of the oily soil is removed when the oil-water interfacial tension is lowered sufficiently such that hydraulic currents in the bath or buoyancy forces can raise and remove a portion of the oil droplet, forming an emulsion (see Figure 1-2). Since additional oil-water surface area is being created, one of the keys to this process is the reduction of the oil-water interfacial tension (that is, the amount of free energy per unit area required to create this additional surface area). The last mechanism, solubilization, is one where the oil molecules dissolve into the water bath, diffuse to a micelle, and become solubilized in the hydrophobic micellar core. Although surfactants that are directly adsorbed onto the oily soil on the solid surface play less of a role in the solubilization mechanism, part of the free energy required to form the suspension of microscopic oil droplets with surfactants adsorbed at their oil-water interfaces, often referred to as a microemulsion, is given by the oil-water interfacial tension. Accordingly, any attempt to model the solubilization

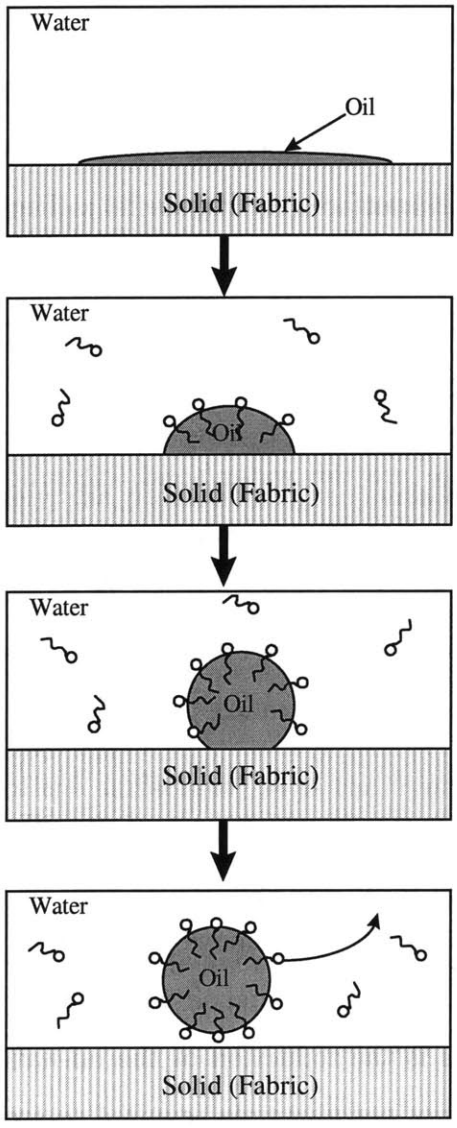

Figure 1-1: Schematic representation of the roll-up process for the removal of an oily soil. As surfactant molecules adsorb at the oil-water interface, the contact angle increases (due to a reduction in the oil-water interfacial tension) until a cutoff value of 180° is reached. At that point, the oily drop is essentially no longer in contact with the fabric, and can be removed by hydraulic or buoyancy forces.

mechanism will require an estimation of this interfacial tension.

1.1.1.2 Wetting and Coating

In many commercial applications, such as painting, photographic film manufacturing, pesticide delivery, and detergency (where the solid surface (fabric) needs to be fully wetted by the solution in order for the processes described in Section 1.1.1.1 to occur), it is desired that a liquid solution spread on a solid substrate. For this to occur spontaneously, the spreading coefficient, S, must be greater than zero. S is defined as the difference between the work of adhesion and the work of cohesion and is given by:

$$S = \sigma_S - \sigma_L - \sigma_{LS} \tag{1.2}$$

where σ_S is the solid/air surface tension, σ_L is the liquid/air surface tension, and σ_{LS} is the liquid/solid interfacial tension.[5] Once again, the prediction and manipulation of surface or interfacial tensions is required in order to understand the wetting and coating process.

1.1.1.3 Crude Oil Recovery

When trying to remove crude oil from underground reservoirs, much of the oil (on the order of 50% to 70%)[6] remains trapped by capillary forces in the pores of the rock formation. With the use of surfactant solutions, part of this oil can be recovered by the reduction of the oil-water interfacial tension and the resulting decrease of the capillary forces.[6–8] Here, oil is being removed from rocks instead of from fabrics, where it can later be recovered from the solution and used. As in detergency, the oil-water interfacial tension is a central input for the modeling of the crude oil recovery process.

1.1.1.4 Foam Stability

In many commercial applications, one desires to generate solutions exhibiting high foaming ability. High-foam applications include household cleaning agents, dust prevention, and fire-fighting.[9] Alternatively, in other applications, the prevention of foam-

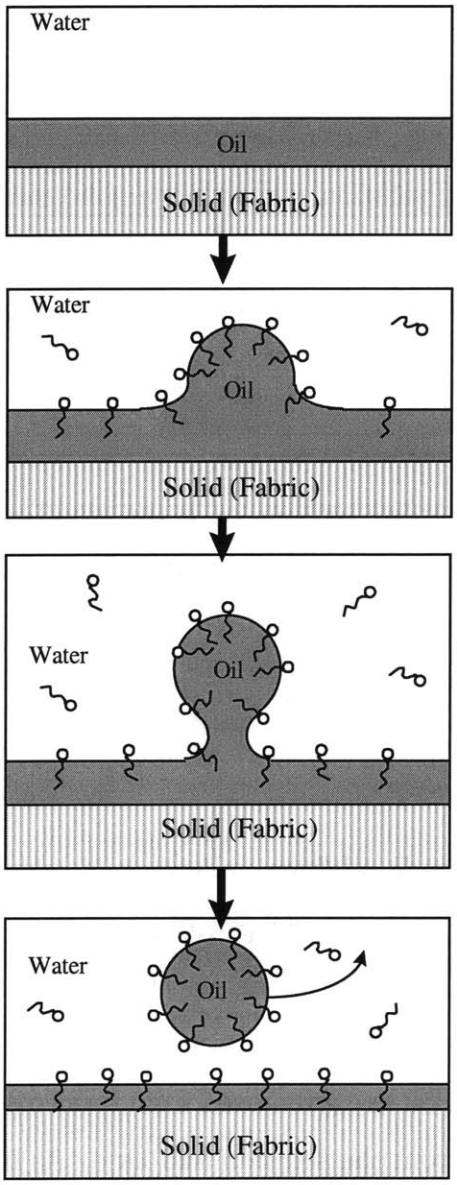

Figure 1-2: Schematic representation of the necking process for the removal of an oily soil. As surfactant molecules adsorb at the oil-water interface, the interfacial tension decreases. This lowers the free energy required for hydraulic or buoyancy forces to remove part of the oil as an emulsion droplet.

ing is desired. Low-foam applications include automatic dishwashers and laundry machines. Surfactants are involved in the foam stabilization process in two ways. First, their adsorption at the air-water interface lowers the surface tension, thus reducing the free energy per unit area required to create the additional surface area of the foam lamella. In addition, the surfactant molecules adsorbed on the two layers of the thin film that makes up the foam lamella can repel each other, either through electrostatic or steric interactions, thus keeping the film from draining to a point where it becomes so thin that it ruptures (see Figure 1-3).[1,10] Clearly, one could destabilize a foam by adding a more surface active surfactant that did not display such repulsive interactions (for example, a nonionic surfactant with a relatively small head). This surfactant could then displace any foam stabilizing surfactants at the lamella surface, causing a collapse of the foam system. Once again, a method to control and predict surface tension and surfactant adsorption at the air-water surface is required to understand and control foam stability.

1.2 Thesis Objectives

The central objective of this thesis is to develop molecularly-based theoretical frameworks to describe and predict both the equilibrium and the dynamic adsorption of surfactants at interfaces (air-water and oil-water), including the resulting lowering of surface and interfacial tensions. As discussed in Section 1.1, the interfacial properties of solutions containing surfactants, and in particular those containing mixtures of surfactants, have important practical implications. Therefore, the development of a quantitative, molecularly-based thermodynamic theory capable of predicting the interfacial properties of aqueous solutions containing mixtures of surfactants would be extremely valuable for the design and optimization of new surfactant formulations having the desired interfacial properties. The availability of such a theory would also reduce the need for tedious and time consuming trial-and-error type experimentation.

A detailed review of previous work, as it relates to each chapter, is presented in the Introductions to each of the following chapters. It should be stressed from

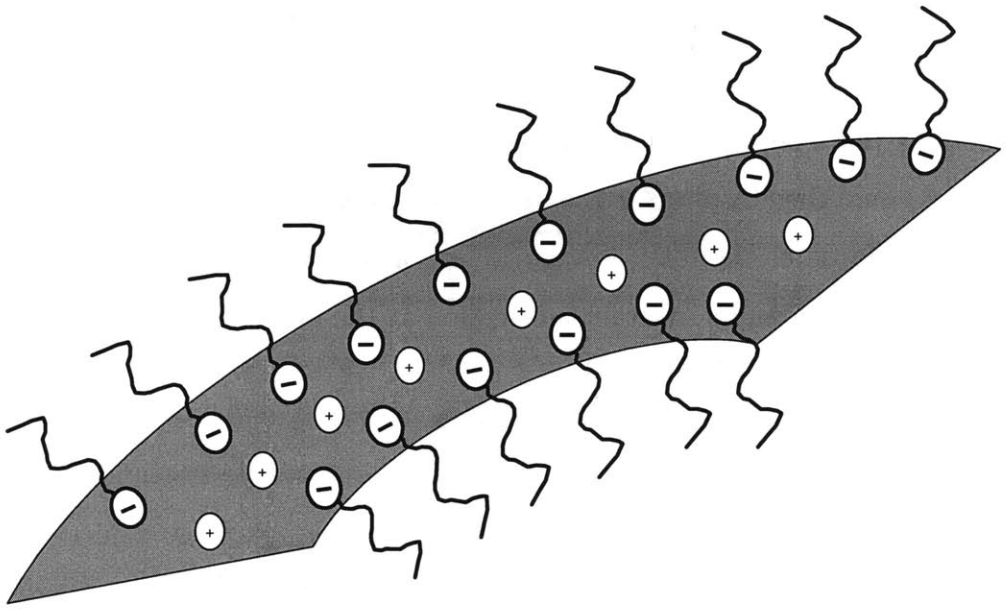

Figure 1-3: Schematic representation of a thin-film lamella stabilized by anionic surfactants adsorbed at the film surfaces.

the outset that the most commonly utilized models to describe the equilibrium adsorption of surfactants, the Langmuir and the Frumkin models, are semi-empirical in nature. That is, the various parameters in these models must be determined by fitting to experimental measurements. The most commonly utilized theory to model the adsorption of mixed surfactant systems is the Regular Solution Theory (RST). This theory contains an additional fitted parameter for each binary surfactant mixture of interest. The inclusion of a mixture dependent experimentally determined parameter is extremely significant. For example, if one is considering two surfactants and wants to predict the interfacial behavior of the binary mixture, one would have to conduct only one experiment on that pair of surfactants. On the other hand, if one is considering ten surfactants and wants to predict the interfacial behavior of all the $(10 \times 9)/2 = 45$ possible binary mixtures, one would have to conduct 45 sets of experiments on the 45 possible pairs of surfactants, which is clearly a very daunting task. However, if one utilizes a theoretical framework that contains no mixture dependent experimentally determined parameters, one could create a library of surfactants for which any possible mixture could be considered without the need to perform any additional experiments. This is, in fact, the approach taken in this thesis.

In contrast to the majority of previously developed theories describing the adsorption of surfactants at interfaces, the theoretical framework developed in this thesis utilizes the molecular structures of the surfactant, rather than experimentally determined parameters, as inputs. Specifically, this thesis builds upon the theory developed earlier by Nikas, et al.,[12] which modeled the *equilibrium* adsorption of *nonionic* surfactants at the *air-water interface* by treating the adsorbed surfactant molecules as a two-dimensional, nonideal gas interacting through repulsive, steric interactions and attractive, van der Waals interactions. Since both of these interactions were modeled using the molecular structures of the surfactants as inputs, the resulting surface equation of state does not contain any experimentally determined parameters, while the adsorption isotherm contains just one experimentally determined parameter (the standard-state chemical potential difference between a surfactant molecule adsorbed at the interface and one in the bulk aqueous phase) for each single surfac-

tant component comprising the mixture. Note that there are no mixture dependent, experimentally determined parameters in this theory.

This thesis adds to the previously developed hard-disk model the effect of electrostatic interactions in the case of ionic or zwitterionic (dipolar) surfactants. In Chapter 2, a Gouy-Chapman based description is utilized to model the electrostatic effects in the case of a single ionic surfactant where all of the charge at the interface is located in a single, two-dimensional charge layer. In Chapter 3, the Gouy-Chapman description is extended to model the case of multiple charged layers at the interface (corresponding, for example, to a single zwitterionic surfactant or to a mixture of a zwitterionic and an ionic surfactant). In Appendix A, the effect of relaxing two of the assumptions of the Gouy-Chapman model (that the ions have zero physical size in the aqueous region, and that the dielectric constant is uniform throughout this region) is investigated. In Appendix B, the sensitivity of the predictions made using the theoretical framework developed in Chapters 2 and 3 to the surfactant molecular parameters is discussed. In Appendix C, the prediction of interfacial phase transitions made utilizing the theoretical framework developed in Chapters 2 and 3 is discussed in detail.

In Chapter 4, the theoretical framework is extended further to model the adsorption of surfactants at the oil-water interface. In all cases, the theoretical predictions were validated through a comparison with experimental measurements. In the case of the equilibrium adsorption of the various surfactants considered in Chapters 2 and 3, there is sufficient experimental data in the literature to carry out these comparisons. However, the availability of experimental interfacial tension data for surfactant mixtures adsorbed at the oil-water interface is extremely limited. Consequently, as discussed in Chapter 4, oil-water interfacial tensions were measured using the pendant bubble method for a pair of surfactants chosen specifically to test the validity and range of applicability of the theoretical framework presented in Chapter 4.

In Chapter 5, the equilibrium description developed in Chapters 2 and 3 is utilized as the basis for the development of a theoretical framework to predict the dynamic adsorption of surfactants for solutions below the CMC. In Appendix D, this theoret-

ical framework is extended further to predict the dynamic adsorption of surfactants from a micellar solution (that is, above the CMC). In Chapter 6, the theory developed in Chapter 5 is tested experimentally. As in the case of mixtures of surfactants adsorbed at the oil-water interface discussed in Chapter 4, the availability of experimental dynamic surface tension data for surfactant mixtures is extremely limited. Consequently, as discussed in Chapter 6, dynamic surface tensions were measured for a pair of surfactants, again chosen specifically to test the validity and range of applicability of the theoretical framework presented in Chapter 5.

In Chapter 7, the previous theoretical developments are implemented in two user-friendly computer programs, SURF and DYNAMIC, which can be used by industrial researchers to facilitate the selection and optimization of surfactants for various practical applications requiring desired interfacial properties. Finally, a summary of the thesis as well as a discussion of possible future research directions are presented in Chapter 8.

Chapter 2

Prediction of Equilibrium Surface Tension and Surface Adsorption of Aqueous Surfactant Mixtures Containing Ionic Surfactants

2.1 Introduction

As discussed in Chapter 1, the interfacial properties (specifically, the interfacial adsorption and the interfacial tension) of aqueous solutions containing surfactants determine and control performance in many practical applications, and in particular, surfactant *mixtures* are almost always utilized.[11] Therefore, the development of a quantitative, molecularly-based thermodynamic theory capable of predicting the interfacial properties of aqueous solutions containing mixtures of surfactants would be extremely valuable for the design of new surfactant formulations having the desired interfacial properties. The availability of such a theory would also reduce the need for tedious and time consuming trial-and-error type experimentation. One should also keep in mind that, as will be shown in Chapter 5, even for systems which do not attain thermodynamic equilibrium at the interface, a fundamental understanding of

the equilibrium interfacial behavior is needed in order to properly model and predict the dynamic interfacial behavior.[13]

The adsorption of a *single, nonionic surfactant* species at the water/air interface has been studied theoretically in the past by numerous investigators (for comprehensive reviews of this topic, see Refs. 1, 14, 15, 16, 17). More recently, the interfacial behavior of *nonionic surfactant mixtures* has been investigated theoretically by several researchers (for a recent comprehensive review, see Ref. 11). In particular, the Langmuir adsorption isotherm has been utilized extensively to model the adsorption of a single surfactant species at an interface,[13] and requires two experimentally-fitted parameters, the maximum surfactant adsorption and an adsorption constant related to the free energy of adsorption. However, the empirical generalization of the Langmuir adsorption isotherm to mixtures of surfactants has been shown to be thermodynamically inconsistent.[18,19] A thermodynamically consistent extension of the Langmuir adsorption isotherm to mixed surfactant solutions has been developed based on the assumption of ideal mixing in the mixed surfactant monolayer,[20] and therefore, does not account for the nonideal synergistic or antagonistic behaviors of the mixed surfactant monolayer which are often observed experimentally. Nonideal theoretical treatments of the mixed surfactant monolayer based on regular solution theory, first suggested by Ingram,[21] and subsequently developed by Rosen and coworkers[22,23] and by Holland and coworkers,[11,24] and further developed by Nguyen and Scamehorn,[25] all make use of an additional, experimentally-fitted empirical parameter *for each surfactant pair* (the so called surface interaction parameter), and thus require experimental inputs (specifically, surface tension measurements) of the surfactant mixtures to determine these parameters. Other empirical theories, such as those which utilize surface activity coefficients,[26] or the more general *nonideal adsorbed solution* theory,[27] which allows for the variation of the surface beta interaction parameter with surface pressure, also require surface tension measurements of the surfactant mixtures to determine the experimentally-fitted parameters for each surfactant mixture considered.

Previous theoretical studies of *ionic surfactants* at interfaces are all based on some empirical surface equation of state (EOS) for uncharged surfactants which is

subsequently generalized to incorporate the ionic surfactant character by modeling the free energy required to charge the monolayer in the presence of the various ionic species in the diffuse region of the double layer. For example, Davies[28] utilized the non-electrostatic Langmuir surface EOS in conjunction with the Gouy-Chapman[29,30] electrostatic description of the ionic diffuse region of the double layer. Subsequently, Borwanker and Wasan[31] improved the Davis model by replacing the Langmuir surface EOS with the Frumkin surface EOS, which adds a third fitted parameter describing possible lateral interactions among the surfactant species in the monolayer, to model the non-electrostatic contribution to the surface equation of state. Others have concentrated on improving the electrostatic Gouy-Chapman model describing the distribution of ionic species in the diffuse region of the double layer. For example, Stern[32] incorporated a distance of closest approach of the ionic species present in the diffuse region of the double layer, the so-called "Stern layer". More recently, Kalinin and Radke[16] allowed for a fraction of the counterions to bind to the adsorbed ionic surfactant species. In a similar spirit, Warszynski et al.[33] allowed for the counterions themselves to adsorb in the monolayer along with the ionic surfactant species. Note that in all these previous studies of the adsorption of ionic surfactants at interfaces, the non-electrostatic contribution to the surface equation of state was modeled in an empirical manner, and as such, relied on at least two or three experimentally-fitted parameters. In addition, all of the theoretical work described above has dealt exclusively with the adsorption behavior of single ionic surfactants at interfaces. The extension of these theories to mixtures of surfactants would require the introduction of new empirical parameters to model the non-electrostatic contribution to the multicomponent surface EOS, which in turn, would demand additional experiments on the mixed surfactant solutions in order to fit these additional parameters.

In contrast to the previous theories which are all based on empirical non-electrostatic surface equations of state, in this chapter, I present a theoretical description of ionic/nonionic surfactant adsorption at the aqueous solution/air interface which relies on *a molecularly-based, non-electrostatic surface equation of state* developed by Nikas et al.[12] Specifically, this surface EOS is utilized to obtain a non-electrostatic

adsorption isotherm which requires only one experimentally-determined parameter for each individual surfactant species comprising the mixture. More importantly, because of its molecular nature, this surface EOS and associated adsorption isotherm can be extended to surfactant mixtures containing any number of components without introducing any additional parameters, thus requiring *no experimental inputs on the mixed surfactant solutions.* In the spirit of previous theoretical descriptions, the electrostatic contribution to the surface EOS is modeled using the Gouy-Chapman description of the diffuse region of the double layer, modified by the inclusion of a Stern layer with no surfactant counterion binding or counterion adsorption in the monolayer. The treatment of surfactant mixtures consisting of surfactants containing multiple charge groups, for example, zwitterionic surfactants, will be presented in Chapter 3. The results of these calculations indicate that this simplified theoretical description of the ionic aqueous solution provides an adequate model for the relatively dilute surfactant solutions considered here.

In general, the theoretical modeling of the adsorption of surfactants at interfaces can be divided into two main approaches: the *two-dimensional solution* model, where the solvent is considered explicitly, and the *two-dimensional gas* model, where the adsorbed surfactant molecules are assumed to be present in a monolayer at the interface with the solvent modeled as a continuum background.[34] For the theoretical framework presented in this chapter, a two-dimensional, nonideal gas model is utilized.[12] Two important advantages of this approach include: (i) the model parameters can be related explicitly to the molecular structures of the surfactants present in the solution, and (ii) the model can be readily extended to multicomponent surfactant mixtures *without adding any additional parameters.* The interfacial model is then combined with a recently-developed molecular-thermodynamic theory of the bulk surfactant mixture solution behavior capable of predicting micelle and surfactant monomer concentrations as a function of the total bulk surfactant concentration and solution composition.[35–37] Using this combined theoretical approach, surface tensions and surfactant monolayer concentrations and compositions can be predicted as a function of the total bulk surfactant concentration and solution composition, both

below and above the critical micelle concentration (CMC) of the surfactant mixture.

As will be shown in Section 2.2, the theoretical approach presented here requires the specification of four molecular characteristics (only two for nonionic surfactants) for each surfactant species comprising the surfactant mixture. These include: (i) the number of carbons in the surfactant hydrocarbon tail, (ii) the molecular cross-sectional area of the surfactant hydrophilic head, (iii) the valence (for ionic surfactants), and (iv) the distance of closest approach between the centers of charge of the adsorbed surfactant and its counterion (for ionic surfactants). Characteristics (i), (ii), and (iii) can be determined from the known molecular structure of the surfactant hydrophobic tail and hydrophilic head, while the determination of characteristic (iv) also requires knowing the chemical structure of the counterion, including hydration. In addition, the standard-state chemical potential difference corresponding to a surfactant molecule in the monolayer and in the bulk solution is also needed for each surfactant species comprising the surfactant mixture. In principle, this quantity can also be estimated theoretically from a detailed description of the interactions of the surfactant molecules with the surrounding aqueous medium in the monolayer and in the bulk solution.[38,39] However, due to the uncertainties associated with this estimation, this quantity will be determined here by fitting one experimentally measured surface tension value to the predicted one for each surfactant species comprising the surfactant mixture (for details, see Section 2.3.2).

It is important to stress that in extending this theory from single surfactants to surfactant mixtures containing any number of components, no additional empirical parameters are introduced and no assumption of ideal mixing is made. Using the theoretical approach presented in this chapter, one could create a library of single surfactants from which the mixture interfacial properties could then be predicted for any possible permutation of surfactant mixtures. Eliminating the need for experiments on all the possible realizable surfactant mixtures can considerably facilitate the design and optimization of surfactant mixtures exhibiting the desired interfacial behavior.

The remainder of the chapter is organized as follows. The theory of adsorption

at the aqueous solution-air interface for nonionic and ionic surfactants both below and above the critical micelle concentration of the surfactant mixture is presented in Section 2.2. This theory is utilized in Section 2.3 to predict surface tensions and surface adsorptions for several single as well as mixed surfactant systems, including a comparison of these predictions with available experimental measurements from the literature. The surfactant systems examined include single surfactant aqueous solutions of sodium dodecyl sulfate (SDS), dodecyl maltoside (C_{12}Maltoside), and dodecyl hexa(ethylene oxide) ($C_{12}E_6$), as well as binary surfactant aqueous solutions of SDS/$C_{12}E_6$ and SDS/C_{12}Maltoside. Finally, in Section 2.4, concluding remarks are presented.

2.2 Theory

2.2.1 Surface Equation of State and Adsorption Isotherm for Mixtures of Nonionic Surfactants

A molecularly-based surface equation of state for aqueous solutions containing mixtures of nonionic surfactants was developed by Nikas et al.[12] using a kinetic (gas-like) treatment of the surfactant molecules which are adsorbed at the solution-air interface. A brief overview of this theory, including some new insights, is presented here as an introduction to the treatment of ionic surfactants described in Section 2.2.2, and also, because any nonionic surfactants present in the mixture will be modeled using this theory. The theory by Nikas et al. assumes that the interactions operating between the surfactant molecules at the interface are not sufficiently strong so as to induce long-range ordering or segregation among the adsorbed species. An examination of possible phase transitions in the monolayer driven by attractive interactions between the adsorbed surfactant molecules will be presented in Appendix C. Two types of interactions between the nonionic surfactant molecules which are adsorbed at the interface are accounted for in this theory: (i)repulsive, steric interactions between the surfactant heads and/or tails (depending on their relative size), and (ii) attractive,

van der Waals interactions between the surfactant tails.

The Gibbs interfacial model[14] forms the basis for this thermodynamic treatment. Specifically, a two-dimensional planar Gibbs dividing interface is chosen within the actual three-dimensional interfacial region at a position where the Gibbs surface excess number of solvent (water) molecules,N_{w}^{σ}, vanishes. Recall that the Gibbs surface excess number of molecules of type i, N_i^{σ}, is defined as follows:[14]

$$\frac{N_i^{\sigma}}{A} \equiv \Gamma_i \equiv \int_{-\infty}^{0} [n_i(x) - n_i^{v}]\mathrm{d}x + \int_{0}^{\infty} [n_i(x) - n_i^{\mathrm{w}}]\mathrm{d}x \tag{2.1}$$

where A is the area of the planar Gibbs dividing interface, Γ_i is the surface excess number density of molecules of type i (referred to hereafter as the surface concentration of molecules of type i), x is the distance perpendicular to the interface, such that the aqueous phase lies on the side of positive x, $n_i(x)$ is the number density of molecules of type i located at position x, n_i^{w} is the bulk aqueous number density of molecules of type i (limiting value of $n_i(x)$ as $x \to \infty$), and n_i^{v} is the bulk vapor number density of molecules of type i (limiting value of $n_i(x)$ as $x \to \infty$). Note that the integrands in Eq. (2.1) are non-zero solely within the interfacial region, that is, in the region where $n_i(x)$ is different than the bulk number density of molecules of type i in the corresponding phase, n_i^{w} or n_i^{v}. Therefore, the integrations in Eq. (2.1) may be carried out only over the interfacial region without affecting the values of N_i^{σ} or Γ_i.

In the monolayer model for nonionic surfactants adsorbed at an interface, all the Gibbs surface excess number of surfactant molecules are assumed to be present in a two-dimensional monolayer located at the interface. In the vapor phase ($x < 0$), the number density of surfactant molecules vanishes since it is assumed that the surfactants are completely non-volatile. In the liquid phase ($x > 0$), the number density of surfactant molecules is constant at the bulk value, n_i^{w}. At the interface itself ($x = 0$), the number density of surfactant molecules behaves like a delta function since the treatment is that of a two-dimensional monolayer. Mathematically, the local number density distribution of a non-volatile nonionic surfactant of type i can be

written as follows:

$$n_i(x) = \begin{cases} 0, & \text{for} \quad x < 0 \\ \left[\frac{\eta_i}{A}\right]\delta(x) + n_i^{\mathrm{w}}, & \text{for} \quad x \geq 0 \end{cases} \tag{2.2}$$

where $\delta(x)$ is the delta function, and η_i is the number of surfactant molecules of type i in the monolayer. Substituting Eq. (2.2) in Eq. (2.1) and integrating yields:

$$\eta_i = N_i^{\sigma} \tag{2.3}$$

In other words, in this description, the Gibbs surface excess number of surfactant molecules of type i, N_i^{σ}, is equal to the number of surfactant molecules of type i present in the monolayer, η_i.

In Eq. (2.2), the monolayer is assumed to be positioned at the Gibbs dividing surface (x=0). This assumption is physically reasonable since one expects the monolayer to be located within the relatively thin interfacial region, such that the hydrophilic surfactant heads are in the polar, aqueous environment while the hydrophobic surfactant tails are in the non-polar, vapor environment. Note that an extremely precise choice of the position of the Gibbs dividing surface is not essential, since small changes in this position have a negligible effect on the value of the surface concentration of surfactant molecules of type i, Γ_i. For example, for $C_{12}E_6$ at a bulk aqueous concentration of 10^{-8} mol/cm^3 (which corresponds to a surface tension of approximately 45 dyn/cm), changing the position of the Gibbs dividing surface by 10Å changes the value of the $C_{12}E_6$ surface concentration, $\Gamma_{C_{12}E_6}$, by (10^{-8}mol/cm^3) $\times$ (10×10^{-8}cm) $= 10^{-15}$mol/cm^2. This difference is much smaller than the actual $C_{12}E_6$ surface excess of 2×10^{-10} mol/cm^2 determined experimentally using the Gibbs method through surface tension data as a function of bulk aqueous $C_{12}E_6$ concentration.[14] Accordingly, the predictions generated using this theoretical framework are quite insensitive to the assumption that the surfactant monolayer is located at the Gibbs dividing surface. In addition, note that it is assumed that the air in the vapor phase is inert as well as not surface active.

In the context of the monolayer model, one can develop a surface equation of state by accounting for the various types of interactions between the surfactant molecules present in the monolayer. Steric interactions are accounted for by treating each surfactant molecule as a hard-disk having an area equal to the larger of the cross-sectional areas of the surfactant head or tail. For surfactants having a compact, well-defined head, such as SDS, the head cross-sectional area can be estimated from the surfactant head molecular structure using known bond lengths and angles. For surfactants having a polymeric-like head, such as those of the poly (ethylene oxide) variety, an average head cross-sectional area can be estimated using a Monte-Carlo simulation approach, as described in detail previously.[12] The estimation of the head area size is discussed further in Section 2.3.

Attractive, van der Waals surfactant tail-tail interactions are treated as a perturbation to the hard-disk repulsions using an expansion in surfactant surface concentration truncated at second order. As described in Ref. 12, the second-order virial coefficient, B_{ij}, characterizing the attractive van der Waals interaction between a surfactant molecule of type i and another of type j, can be calculated theoretically as:

$$B_{ij} = \pi \int_{d_{ij}}^{\infty} \left[1 - \exp\left(\frac{-u_{ij}(r)}{\mathrm{k_B}T} \right) \right] \mathrm{d}r \tag{2.4}$$

where u_{ij} is the two-particle inter-molecular potential, for which an estimate is given by Salem.[40] A similar calculation of the second-order virial coefficients will be implemented here.

Accounting for the steric and attractive interactions as described above, the surface EOS of aqueous solutions of surfactant mixtures that include *only nonionic species* can be written as follows:[12]

$$\Pi = \mathrm{k_B}T \left\{ \frac{\sum_{i=1}^{n} N_i^{\sigma}}{A - \sum_{i=1}^{n} N_i^{\sigma} a_i} + \frac{\pi \left(\sum_{i=1}^{n} N_i^{\sigma} r_i \right)^2}{\left(A - \sum_{i=1}^{n} N_i^{\sigma} a_i \right)^2} + \sum_{ij=1}^{n} B_{ij} \frac{N_i^{\sigma} N_j^{\sigma}}{A^2} \right\} \tag{2.5}$$

where Π is the surface pressure, defined as the difference between the surface tension

of the pure solvent, σ_0, and that of the solution, σ, that is, $\Pi = \sigma_0 - \sigma$, k_B is the Boltzmann constant, T is the absolute temperature, A is the area of the interface, n is the number of surfactant species, and a_i and r_i are the hard-disk area and radius of surfactant molecules of type k, respectively. In Eq. (2.5), $\sum_{ij=1}^{n}$ denotes summation over all possible pairs of surfactant species, while avoiding double-counting. For the aqueous surfactant solutions examined in this chapter, σ_0 is the surface tension of pure water, taken to be 72dyn/cm at 25°C.[41]

As expected, the surface pressure is an intensive property, and consequently, Eq. (2.5) can be rewritten solely in terms of intensive variables. Specifically,[12]

$$\Pi = k_B T \left\{ \frac{1}{a - \sum_{i=1}^{n} x_i^{\sigma} a_i} + \frac{\pi \left(\sum_{i=1}^{n} x_i^{\sigma} r_i \right)^2}{\left(a - \sum_{i=1}^{n} x_i^{\sigma} a_i \right)^2} + \sum_{ij=1}^{n} B_{ij} \frac{x_i^{\sigma} x_j^{\sigma}}{a^2} \right\} \tag{2.6}$$

where a is the area per adsorbed surfactant molecule, defined as $a \equiv A / \sum_{i=1}^{n} N_i^{\sigma}$, and x_i^{σ} is the surface mole fraction of surfactant molecules of type i, defined as $x_i^{\sigma} = N_i^{\sigma} / \sum_{k=1}^{n} N_k^{\sigma}$.

The surface equation of state, Eq. (2.6), expresses the surface pressure, Π, (and hence the surface tension, $\sigma = \sigma_0 - \Pi$) as a function of the surface concentration and composition, $1/a$ and x_i^{σ}, respectively. However, it is the bulk solution concentration and composition that is typically known or controlled experimentally. To relate the surface concentration and composition to the bulk concentration and composition, one can invoke the thermodynamic diffusional equilibrium between the surfactant molecules adsorbed at the interface and those present in the bulk aqueous solution using the theoretical framework described below.

The excess surface free energy, F^{σ}, can be calculated by integrating the surface pressure, Π, with respect to surface area, A, utilizing the fact that, in general, the free energy must approach ideal behavior at infinite dilution. Specifically,[12]

$$F^{\sigma} = F^{\sigma,id} - \int_{\infty}^{A} \left(\Pi - \Pi^{id} \right) dA \tag{2.7}$$

where $\Pi^{id} = k_B T \sum_{k=1}^{n} N_k^\sigma / A$ is the ideal surface pressure, and $F^{\sigma,id}$ is the corresponding ideal excess surface free energy, given by:[12]

$$F^{\sigma,\mathrm{id}} = \sum_{k=1}^{n} N_k^\sigma \left(\tilde{\mu}_k^{\sigma,0} + \mathrm{k}T \ln \left(\frac{\Pi^{\mathrm{id}}}{\Pi_0} \right) + \mathrm{k_B}T \ln x_k^\sigma \right) \tag{2.8}$$

where x_k^σ is the surface mole fraction of surfactant molecules of type k, and $\tilde{\mu}_k^{\sigma,0}$ is the standard-state chemical potential of surfactant molecules of type k at a reference pressure, Π_0. Note that the reference pressure is arbitrarily chosen to be 1 dyn/cm, since *cgs* units are used throughout this thesis. Note also that the choice of the reference pressure will affect the numerical value of the standard-state chemical potential, but will not affect the final predicted surface tensions or surface adsorptions.

Finally, the surface chemical potential of surfactant molecules of type i, μ_i^σ, can be calculated by differentiating the excess surface free energy, F^σ, in Eq. (2.8) with respect to the excess number of surfactant molecules of type i adsorbed at the interface, N_i^σ, at constant interfacial area, A, temperature, T, pressure, P, and number of surfactant molecules of type $j \neq i$ adsorbed at the interface, $N_{j\neq i}^\sigma$. Specifically, for nonionic surfactants, μ_i^σ is given by:[12,34]

$$\mu_i^\sigma = \left(\frac{\partial F^\sigma}{\partial N_i^\sigma} \right)_{A,T,P,N_{j\neq i}^\sigma} \tag{2.9}$$

$$= \tilde{\mu}_i^{\sigma,0} + k_B T \left(1 + \ln \left(\frac{\Pi^{id}}{\Pi_0} \right) + \ln x_i^\sigma \right) - \int_{\infty}^{A} \left(\frac{\partial \left(\Pi - \Pi^{id} \right)}{\partial N_i^\sigma} \right)_{A,T,P,N_{j\neq i}^\sigma} \mathrm{d}A$$

Using the surface equation of state, Eq. (2.5), in Eq. (2.9) and integrating yields:[12]

$$\mu_i^\sigma = \mu_i^{\sigma,0} + \mathrm{k_B}T \left\{ \ln \left(\frac{x_i^\sigma}{a - \sum_{k=1}^{n} x_k^\sigma \mathrm{a}_k} \right) + \frac{\mathrm{a}_i + 2\pi \mathrm{r}_i \sum_{k=1}^{n} x_k^\sigma \mathrm{r}_k}{a - \sum_{k=1}^{n} x_k^\sigma \mathrm{a}_k} + \right. \tag{2.10}$$

$$+ \left. \frac{\pi \mathrm{a}_i \left(\sum_{k=1}^{n} x_k^{\sigma} \mathrm{r}_k \right)^2}{\left(a - \sum_{k=1}^{n} x_k^{\sigma} \mathrm{a}_k \right)^2} + \frac{2}{a} \sum_{k=1}^{n} B_{ik} x_k^{\sigma} \right\}$$

where $\mu_i^{\sigma,0} \equiv \tilde{\mu}_i^{\sigma,0} + \mathrm{k_B}T \{1 + \ln(\mathrm{k_B}T/\Pi_0)\}$ has been introduced for convenience.

At thermodynamic diffusional equilibrium, the surface chemical potential of a surfactant molecule of type i, μ_i^{σ} in Eq. (2.10), can then be set equal to an appropriate expression for the bulk aqueous chemical potential of a surfactant molecule of type i (either as a monomer or in a micelle), μ_i^{w}, for each surfactant type i, to determine the excess amount of surfactant adsorbed on the surface, that is,

$$\mu_i^{\sigma} = \mu_i^{\mathrm{w}} \tag{2.11}$$

For a reasonably dilute surfactant solution, that is, below and slightly above the CMC, where the bulk intermicellar and micelle-monomer interactions are negligible, the bulk aqueous chemical potential of surfactant monomers of type i can be modeled using ideal solution theory. * Specifically,[12,35]

$$\mu_i^{\mathrm{w}} = \mu_i^{\mathrm{w},0} + \mathrm{k_B}T \ln(x_{1i}^{\mathrm{w}}) \approx \mu_i^{\mathrm{w},0} + \mathrm{k_B}T \ln\left(\frac{n_{1i}^{\mathrm{w}}}{n_{\mathrm{w}}^{\mathrm{w}}}\right) \tag{2.12}$$

where $\mu_i^{\mathrm{w},0}$ is the bulk aqueous standard-state chemical potential of surfactant monomers of type i in the infinite dilution limit, and x_{1i}^{w} is the bulk aqueous mole fraction of surfactant monomers of type i and is defined as $x_{1i}^{\mathrm{w}} = n_{1i}^{\mathrm{w}} / \left(n_{\mathrm{w}}^{\mathrm{w}} + \sum_{j=1}^{n} n_j^{\mathrm{w}} \right) \approx n_{1i}^{\mathrm{w}}/n_{\mathrm{w}}^{\mathrm{w}}$, where n_{1i}^{w}, n_j^{w}, and $n_{\mathrm{w}}^{\mathrm{w}}$ are the bulk aqueous concentration (as a number density) of surfactant monomers of type i, the total bulk aqueous concentration of surfactant molecules of type j in either monomeric or micellar form, and the bulk aqueous concentration of water molecules, respectively. Note that the bulk aqueous concentration of water, $n_{\mathrm{w}}^{\mathrm{w}}$ is approximately a constant and equal to that of pure water since the

*The ideal solution chemical potential model provides a very good approximation to the more complex, non-ideal expression for the bulk surfactant monomer chemical potential that was used in Refs. 35 and 36.

surfactant solutions are dilute. Note also that although micelles do no adsorb at the interface, they nevertheless effect the solution surface properties indirectly by affecting the surfactant monomer concentration.

For any given total bulk aqueous surfactant concentration, $n_{\text{tot}} \equiv \sum_{k=1}^{n} n_k^{\text{w}}$, and bulk aqueous solution composition, α^{soln}, temperature, T, and pressure, P, a recently developed molecular-thermodynamic theory of bulk micellization[35–37] is utilized to calculate $n_{1i}^{\text{w}}(n_{\text{tot}}, \alpha^{soln}, T, P)$ for each surfactant type i. A detailed description of the calculational procedures can be found in Refs. 35–37. The calculated n_{1i}^{w} values can then be used in Eq. (2.12) to compute $\mu_i(n_{\text{tot}}, \alpha^{soln}, T, P)$.

Using Eqs. (2.10) and (2.12) in Eq. (2.11) finally yields:

$$\ln\left(\frac{n_{1i}^{\text{w}}}{n_{\text{w}}^{\text{w}}}\right) = \frac{\Delta\mu_i^0}{k_B T} + ln\left(\frac{x_i^\sigma}{a - \sum_{k=1}^{n} x_k^\sigma a_k}\right) + \frac{a_i + 2\pi r_i \sum_{k=1}^{n} x_k^\sigma r_k}{a - \sum_{k=1}^{n} x_k^\sigma a_k} \qquad (2.13)$$

$$+ \frac{\pi a_i \left(\sum_{k=1}^{n} x_k^\sigma r_k\right)^2}{\left(a - \sum_{k=1}^{n} x_k^\sigma a_k\right)^2} + \frac{2}{a}\sum_{k=1}^{n} B_{ik} x_k^\sigma$$

where $\Delta\mu_i^0 \equiv \mu_i^{\sigma,0} - \mu_i^{\text{w},0}$is the standard-state chemical potential difference of surfactant molecules of type i at the surface and in the bulk aqueous solution. Note that Eq. (2.13) represents a system of n equations, one for each surfactant type present in the mixture. The quantities $\Delta\mu_i^0$ are the only parameters in the theory that are not calculated by direct molecular modeling. Instead, $\Delta\mu_i^0$ can be found by performing a single experimental surface tension measurement at a known total bulk aqueous surfactant concentration for each individual surfactant type present in the mixture, and then fitting the solution of Eqs. (2.6) and (2.13) to the measured surface tension value. Specifically, one can first determine the surface pressure, Π, from the surface tension measurement using $\Pi = \sigma_0 - \sigma$. This value of the surface pressure can then be used in Eq. (2.6) for a particular single surfactant i to determine a, the interfacial

area per molecule, with knowledge of the temperature, T, the pressure, P, the head area size, a_i, and the second-order virial coefficient, B_{ii}. Note that, in this case, the surface mole fraction of surfactant molecules of type i, x_i^σ, is unity, while the surface mole fractions of all the other surfactant types, $x_{j\neq i}^\sigma$, vanish since only a single surfactant type, i, is present in the system. This value of a can then be used in Eq. (2.13) to determine $\Delta\mu_i^0$ (see Section 2.3 for a discussion of the recommended total bulk surfactant concentration to be used for this surface tension measurement). Note that once $\Delta\mu_i^0$ is determined in this manner for each surfactant type present in the mixture, *no additional experimental measurements involving the surfactant mixture are necessary.*

For mixtures containing only nonionic surfactants, since Eq. (2.13) represents a system of n equations, and there are $n+1$ unknown quantities (a and $\{x_1^\sigma,...,x_n^\sigma\}$), this system of equations can be solved uniquely along with the additional constraint that $\sum_{i=1}^{n} x_i^\sigma = 1$. The values of a and $\{x_1^\sigma,...,x_n^\sigma\}$ found by solving Eq. (2.13) can then be used in Eq. (2.6) to predict the equilibrium surface pressure, Π, and hence the equilibrium surface tension, $\sigma = \sigma_0 - \Pi$, as a function of n_{tot}, α^{soln}, T, and P. The extension of this theory to mixtures containing ionic surfactants is discussed next in Section 2.2.2.

2.2.2 Surface Equation of State and Adsorption Isotherm For Mixtures Containing Ionic Surfactants

The spatial distribution of all the ionic species (ionic surfactants and their counterions) is modeled here as consisting of an adsorbed charged monolayer at the interface and a diffuse ionic cloud in which, at equilibrium, thermal diffusion is balanced by electrostatic interactions between the ionic species and the charged monolayer,[14,1,28] as modeled by Gouy and Chapman.[29,30] It is assumed hereafter that the ionic surfactants are fully dissociated. In other words, although the ionic surfactants and their inorganic counterions interact through attractive Coulombic forces, they do not remain bound together as a single entity. This is expected to be valid for organic

salts, such as SDS considered here, but may not be valid for organic fatty acids at low pH where a certain fraction of the fatty acids may remain undissociated.[14] In addition, this description treats all the ions in the bulk aqueous solution as point charges having no physical excluded volume, except for a minimum distance of closest approach (the so-called Stern-layer described below). Furthermore, the diffuse layer and the surface are treated as having uniform, "smeared" three- and two-dimensional local charge densities, respectively, and it is assumed that the ions interact through a structureless solvent having a uniform dielectric constant. For a review of this type of electrostatic theoretical description, see Ref. 14 and references therein. The effects of ion size and dielectric constant saturation on the diffuse region of the Gouy-Chapman model will be examined in Appendix A.

As in the nonionic surfactant case, the Gibbs model forms the basis for this thermodynamic treatment (see Section 2.2.1). However, in the ionic surfactant case, the interfacial region (the region where the actual local number density of ions is significantly different than that in the bulk aqueous solution) is wide compared to the size of the various ionic solutes. This is a result of the diffuse layer forming the so-called *electrical double layer* (see Figure 2-1 for an illustration).[14] In the context of this diffuse layer model, two different quantities related to the surface excess number of ions can be defined: η_i, the number of molecules of type i actually adsorbed in the monolayer, and λ_i, the excess number of molecules of type i in the diffuse layer, as described in detail by Hachisu[42] (see Eq. (2.14) below for a mathematical description). As in the nonionic surfactant case, it is assumed that the position of the surfactant monolayer is the same as that of the Gibbs dividing surface ($x = 0$). As explained in Section 2.2.1, this is physically reasonable, and variations of this position that are of the order of the size of the surfactant molecules will have a negligible effect on the predictions of this model.

Similar to the nonionic surfactant case, in the vapor phase ($x < 0$), the local surfactant number density vanishes, and at the monolayer ($x = 0$), the local surfactant number density exhibits the behavior of a delta function. However, in the Stern layer (extending from the monolayer at $x = 0$ to the Stern surface at $x = \mathrm{d}$), the local sur-

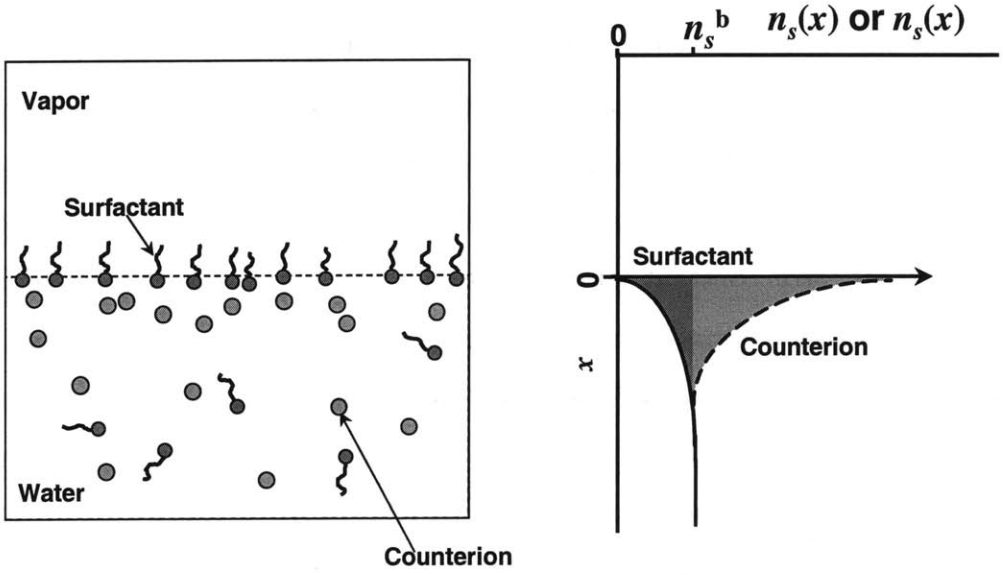

Figure 2-1: Schematic illustration of the air-water interfacial region of an ionic surfactant solution (left) and the corresponding local number densities of both the surfactant molecules (solid line) and counterions (dashed lines) as a function of the distance from the interface (right). In the plot on the left, the dark shaded region corresponds to the (negative) surface excess concentration of surfactant molecules in the diffuse region, the light shaded region corresponds to the (positive) surface excess concentration of the counterions, and the arrow at $x = 0$ indicates a delta function which corresponds to the surface excess concentration of surfactant molecules in the two-dimensional monolayer. Note that, for simplicity, the Stern region is not shown in this illustration.

factant number density vanishes due to steric repulsions with the surfactant molecules adsorbed in the monolayer. In the aqueous environment near the monolayer ($x > \mathrm{d}$), the local surfactant number density, $n_{surfactant}(x)$, is lower than that of the bulk aqueous surfactant number density, $n^{\mathrm{w}}_{surfactant}$, due to the electrostatic repulsions with the similarly charged surfactant molecules present in the monolayer. As the distance from the monolayer, x, increases, these electrostatic repulsions decrease in magnitude, and therefore, the local surfactant number density increases, approaching an asymptote at the bulk aqueous surfactant number density far away from the monolayer ($x \to \infty$). Similar to the surfactant, the counterions are assumed to be non-volatile requiring $n_{counterion}(x)$ to vanishes in the vapor phase ($x < 0$). However, as stated earlier, the counterions are assumed not to be present at all in the monolayer. Accordingly, there is no delta function at the monolayer ($x = 0$) for the counterions. Moreover, as in the surfactant case, the steric repulsions between the counterions and the surfactant molecules adsorbed in the monolayer require that the local counterion number density vanishes in the Stern layer ($0 < x < \mathrm{d}$). Since the counterions have a charge that is opposite to that of the surfactant molecules adsorbed in the monolayer, they are attracted electrostatically to the monolayer, leading to an increase in the local counterion number density, $n_{counterion}(x)$, near the monolayer ($x > \mathrm{d}$). Far away from the monolayer ($x \to \infty$), this attractive interaction vanishes, and the local counterion number density approaches the bulk aqueous counterion number density, $n^{\mathrm{w}}_{counterion}$.

In this treatment of the Stern-layer, it is assumed that neither the surfactant molecules nor the counterions are present in a region of thickness d near the monolayer (at $x = 0$), and that the value of d corresponds to the size of the counterion. Physically, one could argue that a different value of d should be used for the surfactant molecules since, in general, they have a different size. Or, possibly, one may want to allow for the presence of surfactant in the Stern-layer, since surfactant molecules will at some point need to traverse the Stern layer in order to adsorb at the monolayer. However, one should keep in mind that the concentration of surfactant in the aqueous region near the monolayer is inherently quite low due to the electrostatic repulsions with the similarly charged monolayer. Accordingly, changing the distance of closest

approach of the surfactant molecules should have a negligible effect on the final predictions of this model. Using the same value of d for both the surfactants and the counterions allows us to obtain a closed-form mathematical expression for the surface pressure (see Section 2.2.2.1) while introducing very little error.

Mathematically, the two quantities, η_i and λ_i, can be expressed as follows:

$$\frac{\eta_i}{A} \equiv \lim_{\varepsilon \to 0} \int_{-\varepsilon}^{+\varepsilon} (n_i(x) - n_i^{\mathrm{w}}) \mathrm{d}x = \lim_{\varepsilon \to 0} \int_{-\varepsilon}^{+\varepsilon} n_i(x)\, \mathrm{d}x \tag{2.14}$$

and

$$\frac{\lambda_i}{A} \equiv \lim_{\varepsilon \to 0} \int_{\varepsilon}^{\infty} (n_i(x) - n_i^{\mathrm{w}}) \mathrm{d}x \tag{2.15}$$

Combining η_i and λ_i [Eqs. (2.14) and (2.15)] yields the conventional Gibbs surface excess number of molecules of type i, N_i^{σ}, for the case where no surfactant or counterion molecules are present in the vapor phase, that is,

$$\eta_i + \lambda_i = A \int_{0}^{\infty} (n_i(x) - n_i^{\mathrm{w}}) \mathrm{d}x = N_i^{\sigma} \tag{2.16}$$

It is important to recognize that η_i is the number of molecules of type i held at the surface by the hydrophobic effect, while λ_i is the contribution to the Gibbs surface excess number of molecules of type i, N_i^{σ}, due to the competition between the electrostatic interactions, associated with the ions actually adsorbed in the monolayer and those dispersed in the bulk aqueous solution, and the thermal energy of the ions. Note again that since the integrands in Eqs. (2.15) and (2.16) vanish outside the interfacial region, the integrations need not extend to infinity, but instead, can terminate at any distance, x, outside of the interfacial region.

As discussed above, it is assumed that the adsorption process is driven primarily by the hydrophobic effect, and therefore, that only the organic, surface-active ions are physically adsorbed in the monolayer, while their inorganic counterions are present only in the diffuse region of the double layer. In other words, if i is an inorganic counterion, then $\eta_i \approx 0$ and $\lambda_i \approx N_i^{\sigma}$. The organic surface-active ions are present

in both the monolayer and the diffuse layer.[42] However, to a good approximation, $\lambda_i << \eta_i$, and therefore,

$$\eta_i \approx N_i^{\sigma} \tag{2.17}$$

for all the organic surface-active ions. The approximation in Eq. (2.17) is not necessary; however, it greatly simplifies the mathematical calculations which follow, and was found to have a negligible effect on the final predictions. Accordingly, Eq. (2.17) will be used hereafter to model the organic, surface-active ions.

As will be discussed in Section 2.2.2.2, determining the adsorption isotherm for ionic surfactants is more complex than for nonionic surfactants due to the requirement of electroneutrality. Indeed, instead of simply considering an isolated ionic surfactant and requiring that it be at thermodynamic, diffusive equilibrium in both the bulk aqueous phase and in the surface phase, one must consider the diffusive equilibrium of an electroneutral combination of the surfactant ion and its counterion. In other words, at equilibrium, the sum of the chemical potentials of the two ions comprising that electroneutral combination must be the same in both the bulk aqueous phase and the surface phase. This is analogous to the treatment of phase equilibrium of ionic species in two coexisting bulk, three-dimensional phases.[43]

2.2.2.1 Surface Equation of State for Solutions Containing Ionic Surfactants Below the CMC

The effect of electrostatic interactions on the surface pressure, Π, is accounted for here by incorporating it as an additive contribution.[14,1,28] Specifically,

$$\Pi = \Pi_{\mathrm{NI}} + \Pi_{\mathrm{elec}} \tag{2.18}$$

where Π_{NI} is the contribution to the surface pressure resulting from all non-electrostatic interactions, and Π_{elec} is the contribution to the surface pressure arising from the electrostatic interactions. This implicitly assumes that electrostatic interactions can be decoupled from all other interactions, an assumption which may break down for very highly-charged interfaces or in the presence of polyelectrolytes at the interface,

since long-range ordering may exist under these conditions. In other words, the nonionic contribution, Π_{NI}, can be calculated by treating the surfactant molecules as if they were not charged, as described above in Section 2.2.1, and then adding to that the excess surface free energy per unit area associated with charging the ionic surfactants and their counterions, captured in Π_{elec}.[14]

As described in Section 2.2.1, for the nonionic surfactants, the non-electrostatic contribution to the surface pressure, Π_{NI}, which includes repulsive hard-disk and attractive van der Waals interactions is given by [see Eq. (2.5)]:

$$\Pi_{\mathrm{NI}} = \mathrm{k_B}T \left\{ \frac{\sum_{i=1}^{n} \eta_i}{A - \sum_{i=1}^{n} \eta_i a_i} + \frac{\pi \left(\sum_{i=1}^{n} \eta_i \mathrm{r}_i \right)^2}{\left(A - \sum_{i=1}^{n} \eta_i a_i \right)^2} + \sum_{ij=1}^{n} B_{ij} \frac{\eta_i \eta_j}{A^2} \right\} \tag{2.19}$$

now written in terms of the variables η_i, rather than N_i^{σ}, since η_i represents the actual number of surfactant molecules of type i in the monolayer itself [see Eq. (2.14)].

The first step in calculating the electrostatic contribution to the surface pressure, Π_{elec}, is to model the equilibrium spatial distribution of ions in the diffuse region of the double layer, and then to calculate the resulting electrostatic potential. First, the aqueous region is divided into two parts, a Stern layer and a diffuse layer, as described earlier in Section 2.2.2. In the Stern layer, the charge density vanishes due to the steric exclusion of any ions, and therefore, the Poisson equation reduces to:

$$\frac{\mathrm{d}^2\Psi}{\mathrm{d}x^2} = \frac{-4\pi\rho_{\mathrm{elec}}}{\varepsilon_{\mathrm{s}}} = 0 \quad , \text{for} \quad 0 \leq x \leq \mathrm{d} \tag{2.20}$$

where Ψ is the electrostatic potential, ρ_{elec} is the local charge density, and ε_s is the dielectric constant in the Stern layer, which was estimated to have an effective value of 42 (see Section 2.3.1).

The spatial distribution of ionic species in the diffuse layer is assumed to be described by the Boltzmann distribution, given by:

$$n_i(x) = n_i^{\mathrm{w}} \exp\left(-\frac{z_i e \Psi(x)}{k_B T} \right) \tag{2.21}$$

where z_i is the valence of ions of type i, n_i^w is the bulk aqueous number density of ions of type i, and e is the charge of a proton. The distribution in Eq. (2.21) arises from the balance between the entropic-driven tendency for a uniform ion number density and the electrostatic-driven tendency for the ions to order themselves with respect to the charged monolayer. An important approximation regarding Eq. (2.21) is that the ions in the bulk aqueous solution are point charges, having no excluded volume. This approximation is expected to be valid for electrolyte solutions that are reasonably dilute and will be discussed further in Appendix A. Combining Eq. (2.21) with the Poisson equation (in cgs units) yields the governing equation of the diffuse layer, that is, the familiar Poisson-Boltzmann equation:[14,28,44]

$$\frac{d^2\Psi}{dx^2} = \frac{-4\pi\rho_{elec}}{\varepsilon} = \frac{-4\pi e}{\varepsilon}\sum_{i=1}^{n} z_i n_i(x) \tag{2.22}$$

$$= \frac{-4\pi e}{\varepsilon}\sum_{i=1}^{n} z_i n_i^w \exp\left(\frac{-z_i e\Psi(x)}{kT}\right) \quad , \quad \text{for} \quad x > d$$

where ε is the dielectric constant in the diffuse region, assumed to be that of pure water. Two important approximations leading to Eq. (2.22) include: (i) treating the ions in the bulk aqueous solution with a uniform, smeared, charge density, ρ_{elec}, and (ii) assuming that the dielectric constant, ε, is uniform throughout the diffuse region. This latter assumption will be examined in detail in Appendix A. Equations (2.20) and (2.22) are two second-order ordinary differential equations for Ψ, thus requiring four boundary conditions for their solution (two for each equation). The first boundary condition can be obtained by relating the electric field, -$d\Psi/dx$, to the surface charge density, $\hat{\sigma}$,[45] leading to:

$$\left.\frac{d\Psi}{dx}\right|_{x=0} = \frac{-4\pi\hat{\sigma}}{\varepsilon_s} \tag{2.23}$$

The second boundary condition can be obtained by arbitrarily choosing a distance infinitely far from the interface as the reference point of the electrostatic potential.

Specifically, the electrostatic potential is chosen to vanish at infinity, that is,

$$\Psi\left(x \to \infty\right) = 0 \tag{2.24}$$

The third boundary condition can be obtained by requiring that the electrostatic potential, Ψ, be continuous across the Stern boundary at x=d, namely, that

$$\Psi\left(x = d^{-}\right) = \Psi\left(x = d^{+}\right) \tag{2.25}$$

where $\Psi(x=\mathrm{d}^{-})$ denotes the electrostatic potential at x=d in the Stern layer, and $\Psi(x=\mathrm{d}^{+})$ denotes the electrostatic potential at x=d in the diffuse layer. The final boundary condition can be found by relating the electric field at the boundary between the Stern and the diffuse layers (x=d) as follows:

$$\varepsilon_s \left.\frac{d\Psi}{dx}\right|_{x=d^{-}} = \varepsilon \left.\frac{d\Psi}{dx}\right|_{x=d^{+}} \tag{2.26}$$

Note that in utilizing Eq. (2.26) it has been assumed that the counterions do not bind or adsorb onto the Stern layer. Integrating Eq. (2.20) twice, and using Eqs. (2.23) and (2.25) as boundary conditions, yields the solution for the electrostatic potential in the Stern layer. Specifically,

$$\frac{\mathrm{d}\Psi}{\mathrm{d}x} = -\frac{4\pi\hat{\sigma}}{\varepsilon_{\mathrm{s}}}, \text{for} \quad 0 \le x \le \mathrm{d} \tag{2.27}$$

and

$$\Psi = \Psi_{\mathrm{d}} + \frac{4\pi\hat{\sigma}}{\varepsilon_{\mathrm{s}}}\left(\mathrm{d} - x\right), \text{for} \quad 0 \le x \le \mathrm{d} \tag{2.28}$$

where $\Psi_{\mathrm{d}} \equiv \Psi(x = d)$ is the value of the electrostatic potential at the boundary between the Stern layer and the diffuse layer.

The solution to the electrostatic potential in the diffuse layer can be found by integrating Eq. (2.22) once to solve for $\mathrm{d}\Psi/\mathrm{d}x$, and using the fact that the electric field vanishes at infinity (as a result of the entire system being electroneutral). This

yields:

$$\left(\frac{\mathrm{d}\Psi}{\mathrm{d}x}\right)^2 = \frac{8\pi \mathrm{k_B}T}{\varepsilon}\sum_{i=1}^{n} n_i^{\mathrm{w}}\left(\exp\left(\frac{\mathrm{z}_i \mathrm{e}\Psi}{\mathrm{k}T}\right) - 1\right) \tag{2.29}$$

If only monovalent ions are present, that is, if $|\mathrm{z}_i = 1|$, which corresponds to the ionic surfactant SDS considered in this chapter, Eq. (2.29) reduces to:[14]

$$\left(\frac{\mathrm{d}\Psi}{\mathrm{d}x}\right)^2 = \frac{8\pi \mathrm{k_B}T n^{\mathrm{w}}}{\varepsilon}\left[2\sinh\left(\frac{\mathrm{e}\Psi}{2\mathrm{k_B}T}\right)\right]^2$$

$$\frac{\mathrm{d}\Psi}{\mathrm{d}x} = -\frac{2\mathrm{k_B}T\kappa}{\mathrm{e}}\sinh\left(\frac{\mathrm{e}\Psi}{2\mathrm{k_B}T}\right) \tag{2.30}$$

where $n^{\mathrm{w}} \equiv \sum_{cations} n_i^{\mathrm{w}} = \sum_{anions} n_i^{\mathrm{w}}$, and $\kappa^{-1} \equiv \sqrt{\frac{k_B T \varepsilon}{8\pi n^{\mathrm{w}} e^2}}$ is the familiar Debye-Hückel screening length. Note that the negative square root was used above in Eq. (2.30) since, in the case of a positively-charged monolayer, Ψ will be positive, leading to a positive value of $\sinh(\mathrm{e}\Psi/2\mathrm{k}_B\mathrm{T})$, resulting in a negative value of $(\mathrm{d}\Psi/\mathrm{d}x)$. This is expected physically, since the potential, Ψ, is positive near the interface, and should decrease to zero with increasing distance from the monolayer. Similarly, for a negatively-charged monolayer, Ψ will be negative, resulting in a positive value of $(\mathrm{d}\Psi/\mathrm{d}x)$. In addition, note that if multivalent ions are present, the analysis which follows must be done numerically, as described in Section 2.2.2.4.

By combining Eqs. (2.26) and (2.27), the surface charge density, $\hat{\sigma}$, can be expressed as follows:

$$\hat{\sigma} = \frac{-\varepsilon}{4\pi}\left.\frac{\mathrm{d}\Psi}{\mathrm{d}x}\right|_{x=\mathrm{d}^+} \tag{2.31}$$

Combining Eqs. (2.30) and (2.31) yields:

$$\hat{\sigma} = \left(\frac{\varepsilon\kappa}{4\pi}\right)\left(\frac{2\mathrm{k_B}T}{\mathrm{e}}\right)\sinh\left(\frac{\mathrm{e}\Psi_{\mathrm{d}}}{2\mathrm{k_B}T}\right) \tag{2.32}$$

Finally, solving Eq. (2.32) for Ψ_d, and combining with Eq. (2.28), one obtains the

following expression for the potential at x=0, Ψ_0:

$$\Psi_0 = \frac{2k_B T}{e} \ln \left| \frac{2\pi e\hat{\sigma}}{\varepsilon \kappa k_B T} + \sqrt{1 + \left(\frac{2\pi e\hat{\sigma}}{\varepsilon \kappa k_B T} \right)^2} \right| + \frac{4\pi d\hat{\sigma}}{\varepsilon_s} \tag{2.33}$$

Note that the first term in the right-hand-side of Eq. (2.33) results from the distribution of the ions in the diffuse layer, and the second term results from the Stern layer.

The electrostatic contribution to the surface pressure, Π_{elec}, is the free energy per unit area required to build up the charge in the monolayer, in the presence of the counterions, from zero surface charge density, to a surface charge density of $\hat{\sigma} = \sum_{i=1}^{n} ez_i\eta_i/A$, given by the following integral:[14,46]

$$\Pi_{elec} = \hat{\sigma}\Psi_0 \Big|_{\sum_{i=1}^{n} ez_i\eta_i/A} - \int_0^{\sum_{i=1}^{n} ez_i\eta_i/A} \Psi_0(\hat{\sigma})\, d\hat{\sigma} \tag{2.34}$$

Inserting the expression for Ψ_0, given in Eq. (2.33), into Eq. (2.34) yields the following expression for the electrostatic contribution to the surface pressure:

$$\Pi_{elec} = \left(\frac{\varepsilon\kappa}{4\pi} \right) \left(\frac{2k_B T}{e} \right)^2 \left[\cosh\left(\frac{e\Psi_0}{2k_B T} \right) - 1 \right] + \frac{2\pi d}{\varepsilon_s} \left(\frac{\sum_{i=1}^{n} ez_i\eta_i}{A} \right)^2 \tag{2.35}$$

The first term in the right-hand-side of Eq. (2.35) is the electrostatic term in the familiar Davies equation of state.[28,44] The second term in the right-hand-side of Eq. (2.35) is the new contribution from the Stern layer. Note that if the Stern layer is removed by setting d = 0, the original Davis term is recovered.

Using Eq. (2.32) to calculate $\cosh(e\Psi_0/2kT)$, and then utilizing this result in

Eq. (2.35) yields:

$$\Pi_{\text{elec}} = \left(\frac{\varepsilon\kappa}{\pi}\right)\left(\frac{k_BT}{e}\right)^2\left[\sqrt{1+\left(\frac{2\pi e}{\varepsilon\kappa k_BT}\right)^2\left(\frac{\sum_{i=1}^{n} ez_i\eta_i}{A}\right)^2}-1\right] \tag{2.36}$$

$$+\ \frac{2\pi \mathrm{d}}{\varepsilon_s}\left(\frac{\sum_{i=1}^{n} ez_i\eta_i}{A}\right)^2$$

Equation (2.36) provides an expression for the electrostatic contribution to the surface pressure written explicitly in terms of the various numbers of surfactant molecules present in the monolayer, η_i. Note that although the various excess number of ions in the diffuse layer, λ_i, do not appear explicitly in Eq. (2.36), their existence is accounted for through the integral in Eq. (2.34), and therefore, they do contribute to the electrostatic surface pressure, Π_{elec}. Electroneutrality dictates that the excess number of counterions is not independent of the excess number of surface active species present in the monolayer (see Ref. 42 for a more detailed discussion of this topic).

The total surface pressure, Π, can now be obtained by combining Eqs. (2.19) and (2.36). Specifically,

$$\Pi = \mathrm{k_B}T\left\{\frac{1}{\alpha-\sum_{i=1}^{n}\xi_i\mathrm{a}_i}+\frac{\pi\left(\sum_{i=1}^{n}\xi_i\mathrm{r}_i\right)^2}{\left(\alpha-\sum_{i=1}^{n}\xi_i\mathrm{a}_i\right)^2}+\sum_{ij=1}^{n}B_{ij}\frac{\xi_i\xi_j}{\alpha^2}\right\} \tag{2.37}$$

$$+\ \left(\frac{\varepsilon\kappa}{\pi}\right)\left(\frac{\mathrm{k_B}T}{\mathrm{e}}\right)^2\left[\sqrt{1+\left(\frac{2\pi\mathrm{e}}{\varepsilon\kappa\mathrm{k_B}T}\right)^2\left(\sum_{i=1}^{n}\frac{\mathrm{ez}_i\xi_i}{\alpha}\right)^2}-1\right]+\frac{2\pi\mathrm{d}}{\varepsilon_\mathrm{s}}\left(\sum_{i=1}^{n}\frac{\mathrm{ez}_i\xi_i}{\alpha}\right)^2$$

where $\alpha \equiv A/\sum_{i=1}^{n}\eta_i$ and $\xi_i \equiv \eta_i/\sum_{j=1}^{n}\eta_j$ are intensive variables, and represent the area per surfactant molecule actually adsorbed in the monolayer and the fraction of

molecules of type i actually adsorbed in the monolayer, respectively. Note that if all the surfactant species are nonionic, then z_i=0, and η_i=N_i^σ (since there is no diffuse layer, that is, λ_i=0) for each i. In that case, Eq. (2.37) reduces to the original equation of state for nonionic surfactants, Eq. (2.19), or equivalently, Eq. (2.5). Consequently, Eq. (2.37) serves as a general equation of state for both single ionic and nonionic surfactants, as well as for their mixtures.

2.2.2.2 Surface Chemical Potential for Ionic Surfactant Solutions Below the CMC

As an illustration of the application of the theoretical framework developed so far, an aqueous solution containing only one monovalent ionic surfactant species (denoted by subscript s) and its oppositely-charged counterion (denoted by subscript c), along with an arbitrary number of nonionic surfactants is considered. In particular, this would apply to an aqueous solution of a single ionic surfactant, such as SDS, or to an aqueous solution containing a binary mixture of a single ionic surfactant and a single nonionic surfactant, such as the binary mixtures of SDS–$C_{12}E_6$ and SDS–C_{12}Maltoside considered in this chapter. Attention is also restricted to systems that do not contain any added salt.

The use of electroneutral combinations of ions constitutes a common approach to theoretically model phase equilibrium of electrolytes in bulk solutions.[43] As stated in Section 2.2.2, one can treat phase equilibrium of charged species by requiring that the sum of the chemical potentials of each ion in an electroneutral combination be equal in all the phases that are in thermodynamic diffusional equilibrium. For example, consider two phases, α and β. One can use the following equation to describe the diffusional equilibrium of an electroneutral combination of the surfactant, s, and its counterion, c, between these two phases:

$$\mu_s^\alpha + \mu_c^\alpha = \mu_s^\beta + \mu_c^\beta \tag{2.38}$$

Defining the sum of the chemical potentials of ions s and c by μ_{sc}, that is, μ_{sc}=μ_s+μ_c,

Eq. (2.38) can be rewritten as follows:

$$\mu_{sc}^{\alpha} = \mu_{sc}^{\beta} \tag{2.39}$$

Physically, μ_{sc} represents the incremental rate of change of the free energy when equal amounts of species s and species c are added to the corresponding phase. Mathematically, this can be expressed as follows for the surface phase:*

$$\mu_{sc}^{\sigma} = \left(\frac{\partial F^{\sigma}}{\partial N_s^{\sigma}}\right)_{T,P,A,N_{j\neq s,c}^{\sigma}} = \left(\frac{\partial F^{\sigma}}{\partial N_c^{\sigma}}\right)_{T,P,A,N_{j\neq s,c}^{\sigma}} \tag{2.40}$$

since $dN_s^{\sigma}|_{T,P,A,N_{j\neq s,c}^{\sigma}} = dN_c^{\sigma}|_{T,P,A,N_{j\neq s,c}^{\sigma}}$ in order to maintain electroneutrality (that is, any change in s must be accompanied by an equal change in c if the amount of all other species are held constant). In Eq. (2.40), the term $N_{j\neq s,c}^{\sigma}$ denotes the number of molecules in the surface phase of all types other than s and c.

Utilizing Eq. (2.40), the surface chemical potential of surfactant ion s and counterion c , μ_{sc}^{σ}, can be written as follows:

$$\mu_{sc}^{\sigma} = \left(\frac{\partial F^{\sigma}}{\partial N_s^{\sigma}}\right)_{T,P,A,N_{k\neq s,c}^{\sigma}} = \left(\frac{\partial F^{\sigma}}{\partial \eta_s}\right)_{T,P,A,\eta_{k\neq s}} \left(\frac{\partial \eta_s}{\partial N_s^{\sigma}}\right)_{T,P,A,N_{k\neq s,c}^{\sigma}} \tag{2.41}$$

Using the approximation given in Eq. (2.17) that $\eta_s \approx N_s^{\sigma}$, it follows that:

$$\left(\frac{\partial \eta_s}{\partial N_s^{\sigma}}\right)_{T,P,A,N_{k\neq s,c}^{\sigma}} = 1 \tag{2.42}$$

Using Eq. (2.42) in Eq. (2.41) then yields:

$$\mu_{sc}^{\sigma} = \left(\frac{\partial F^{\sigma}}{\partial N_s^{\sigma}}\right)_{T,P,A,N_{k\neq s,c}^{\sigma}} \approx \left(\frac{\partial F^{\sigma}}{\partial \eta_s}\right)_{T,P,A,\eta_{k\neq s}} \tag{2.43}$$

*The excess surface free energy used here is defined as F^{σ}=F-F^{V}-F^{L}+PV^{V}+PV^{L}, where F is the total Helmholtz free energy of the system, F^{V} and F^{L} are the Helmholtz free energies of the vapor and liquid phases, respectively, and V^{V} and V^{L} are the volumes of the vapor and liquid phases, respectively. Accordingly, the pressure, P, is held constant in the differentiation of Eq. (2.40) (see Ref. 34 for a detailed discussion).

Note that $\eta_c = 0$ in this model (see Section 2.2), and therefore, does not need to be held constant in the second partial derivative in Eq. (2.43). In analogy to the derivation for nonionic surfactants presented in Section 2.2.1 (see Eq. (2.9)), the surface chemical potential of an ionic surfactant s with its counterion c, μ_{sc}^{σ}, can be expressed as follows:

$$\mu_{sc}^{\sigma} = \frac{\partial}{\partial N_s^{\sigma}} \left(F^{\sigma,\mathrm{id}} - \int_{\infty}^{A} (\Pi - \Pi^{\mathrm{id}})\, \mathrm{d}A \right)_{A,T,P,N_{k\neq s,c}^{\sigma}} \tag{2.44}$$

$$= \frac{\partial}{\partial \eta_s} \left(F^{\sigma,\mathrm{id}} - \int_{\infty}^{A} (\Pi - \Pi^{\mathrm{id}})\, \mathrm{d}A \right)_{A,T,P,\eta_{k\neq s}}$$

$$= \mu_{sc}^{\sigma,0} + \mathrm{k_B}T \left(1 + \ln\left(\frac{\Pi^{\mathrm{id}}}{\Pi_0} \right) + \ln \xi_s \right) - \int_{\infty}^{A} \left(\frac{\partial \left(\Pi - \Pi^{\mathrm{id}} \right)}{\partial \eta_s} \right) \mathrm{d}A$$

where $\mu_{sc}^{\sigma,0}$ is the standard-state surface chemical potential at a reference surface pressure, Π_0, chosen arbitrarily to be 1 dyn/cm, $\Pi^{\mathrm{id}} = \mathrm{k_B}T \sum_{k=1}^{n} \eta_k / A$ is the ideal surface pressure, and $F^{\sigma,id}$ is the corresponding ideal surface free energy (for details, see Section 2.2.1). Using the expression for Π given in Eq. (2.37) in Eq. (2.44), one obtains the following expression for the surface chemical potential, μ_{sc}^{σ}:

$$\mu_{sc}^{\sigma} = \mu_{sc}^{\sigma,0} + \mathrm{k_B}T \left\{ \ln\left(\frac{\xi_s}{\alpha - \sum_{k=1}^{n} \xi_k \mathrm{a}_k} \right) + \frac{\mathrm{a}_s + 2\pi \mathrm{r}_s \sum_{k=1}^{n} \xi_k \mathrm{r}_k}{\alpha - \sum_{k=1}^{n} \xi_k \mathrm{a}_k} \right. \tag{2.45}$$

$$\left. + \frac{\pi \mathrm{a}_s \left(\sum_{k=1}^{n} \xi_k \mathrm{r}_k \right)^2}{\left(\alpha - \sum_{k=1}^{n} \xi_k \mathrm{a}_k \right)^2} + \frac{2}{\alpha} \sum_{k=1}^{n} B_{sk} \xi_k \right\} +$$

$$+ \quad 2k_B T z_s \ln \left\{ \frac{2\pi e^2}{\varepsilon \kappa k_B T \alpha} z_s \xi_s + \sqrt{1 + \left(\frac{2\pi e^2}{\varepsilon \kappa k_B T \alpha} z_s \xi_s \right)^2} \right\} + \frac{4\pi d \left(z_s e\right)^2}{\varepsilon_s} \frac{\xi_s}{\alpha}$$

In Eq. (2.45), $\sum_{k=1}^{n}$ denotes summation over all the surfactant species, one ionic and the remaining nonionic. In deriving Eq. (2.45), only the presence of one ionic surfactant species was considered, and therefore, there are no summations in the last two terms in Eq. (2.45), since they originate from the electrostatic interactions.

As expected, for a nonionic surfactant ($z_s = 0$), the electrostatic contribution in Eq. (2.45) vanishes (and since there is no counterion in that case, μ_{sc}^{σ} would be replaced by μ_i^{σ}). In addition, note that Eq. (2.45) yields the same results for an anionic ($z_s = 1$) or cationic ($z_s = -1$) surfactant. This is expected, since physically, there is no inherent difference between anionic and cationic surfactants in the context of the theoretical description presented here.

2.2.2.3 Bulk Aqueous Chemical Potential for Ionic Surfactant Solutions Below the CMC

For solutions containing ionic surfactants at concentrations below the CMC, the system is sufficiently dilute (typically, less than, or on the order of, 10 millimolar) that the ideal solution approximation may be invoked. Note that below the CMC, all of the added surfactant molecules are present as monomers. As a result, the bulk aqueous ionic surfactant monomer concentration, n_{s1}^{w}, is equal to the bulk aqueous concentration of ionic surfactant, n_s^{w}. Therefore, the bulk aqueous chemical potential of a surfactant molecule s and its counterion c, μ_{sc}^{w}, can be expressed as follows:

$$\mu_{sc}^{w} = \mu_{sc}^{w,0} + k_B T \ln \left(\frac{n_s^{w}}{n_w^{w}} \right) + k_B T \ln \left(\frac{n_c^{w}}{n_w^{w}} \right) \tag{2.46}$$

where $\mu_{sc}^{w,0}$ is the corresponding standard-state bulk aqueous chemical potential, and n_c^{w} is the bulk aqueous concentration of counterion c. Although electrostatic interactions are long-ranged in nature, the use of the ideal-solution approximation (which

assumes negligible interactions between the solute molecules) is justified in this case since the solutions are sufficiently dilute. Indeed, the inclusion of non-ideality in the context of a Debye-Hückel activity coefficient model[43] was found to have a negligible effect on the theoretical predictions of the model presented in this chapter. In the absence of added salt containing the counterion c, it follows that $n_s^{\mathrm{w}} = n_c^{\mathrm{w}}$ in order to ensure bulk electroneutrality, in which case Eq. (2.46) can be rewritten as follows:

$$\mu_{sc}^{\mathrm{w}} = \mu_{sc}^{\mathrm{w},0} + 2\mathrm{k_B}T \ln\left(\frac{n_s^{\mathrm{w}}}{n_{\mathrm{w}}^{\mathrm{w}}}\right) \tag{2.47}$$

Equating the bulk aqueous chemical potential, μ_{sc}^{w}, from Eq. (2.47), and the surface chemical potential, μ_{sc}^{σ}, from Eq. (2.45), yields the required thermodynamic diffusional equilibrium condition. Specifically,

$$\begin{aligned} 2\ln\left(\frac{n_s^{\mathrm{w}}}{n_{\mathrm{w}}^{\mathrm{w}}}\right) &= \frac{\Delta\mu_{sc}^{0}}{\mathrm{k_B}T} + \ln\left(\frac{\xi_s}{\alpha - \sum_{k=1}^{n}\xi_k \mathrm{a}_k}\right) + \frac{\mathrm{a}_s + 2\pi \mathrm{r}_s \sum_{k=1}^{n}\xi_k \mathrm{r}_k}{\alpha - \sum_{k=1}^{n}\xi_k \mathrm{a}_k} \\ &+ \frac{\pi \mathrm{a}_s \left(\sum_{k=1}^{n}\xi_k \mathrm{r}_k\right)^2}{\left(\alpha - \sum_{k=1}^{n}\xi_k \mathrm{a}_k\right)^2} + \frac{2}{\alpha}\sum_{k=1}^{n} B_{sk}\xi_k \\ &+ 2\mathrm{z}_s \ln\left|\frac{2\pi \mathrm{e}^2}{\varepsilon\kappa \mathrm{k_B}T\alpha}\mathrm{z}_s\xi_s + \sqrt{1 + \left(\frac{2\pi \mathrm{e}^2}{\varepsilon\kappa \mathrm{k_B}T\alpha}\mathrm{z}_s\xi_s\right)^2}\right| + \frac{4\pi \mathrm{d}\,(\mathrm{z}_s \mathrm{e})^2}{\mathrm{k_B}T\varepsilon_{\mathrm{s}}}\frac{\xi_s}{\alpha} \end{aligned} \tag{2.48}$$

As in the nonionic surfactant case, the standard-state chemical potential difference, $\Delta\mu_{sc}^{0} \equiv \mu_{sc}^{\sigma,0} - \mu_{sc}^{\mathrm{w},0}$, is an unknown constant parameter that can be determined by a single surface tension measurement at a known concentration of the single ionic surfactant, s, as described in Section 2.2.1. For an aqueous solution of one ionic surfactant and $n-1$ nonionic surfactants, Eq. (2.48) for the ionic surfactant, along with the system of $n-1$ equations given in Eq. (2.13) for the nonionic surfactants, can be

combined with the additional constraint that $\sum_{i=1}^{n} \xi_i = 1$ to yield a total of n+1 equations. The solution of this set of $n+1$ equations then yields the equilibrium values of the $n+1$ unknowns: α and $\{\xi_1, ..., \xi_n\}$. These values can then be utilized in the surface equation of state, Eq. (2.37), to predict the equilibrium surface pressure, Π, and therefore, the equilibrium surface tension, $\sigma = \sigma_0 - \Pi$, of the surfactant solution.

2.2.2.4 Ionic Surfactant Solutions Above the CMC

For surfactant solutions above the CMC, the theoretical model for ionic surfactants presented in Sections 2.2.2.1 – 2.2.2.2 is further complicated by the electrostatic interactions involving the charged micelles. This may include electrostatic interactions between the charged micelles and the charged surfactant monomers, between the charged micelles and the charged surface, and between the charged micelles and other micelles. In keeping with the spirit of the Gouy-Chapman model, one would have to include electrostatic interactions between the micelles and the surface in the Poisson-Boltzmann equation (see Eq. (2.22)). Similarly, electrostatic intermicellar and micelle-monomer interactions in the bulk aqueous region should be included in the bulk aqueous chemical potential model, Eq. (2.46). The modeling of such ionic interactions in the bulk aqueous solution and in the diffuse region of the double layer would require a more detailed model than that based on the Gouy-Chapman theory.

In view of the above, the discussion will be restricted to micellar solutions that are sufficiently dilute such that the various electrostatic interactions involving charged micelles are unimportant (see below). In that case, the electrostatic surface pressure model presented in Section 2.2.2.1, as well as the bulk aqueous chemical potential model presented in Section 2.2.2.2, are still applicable. This is similar to the neglect of *non-electrostatic interactions* involving micelles in the nonionic surfactant case presented in Section 2.2.1 and Ref. 12. In addition, note that the surface properties often do not vary much above the CMC, and therefore, one is primarily interested in predicting surface tension and surface adsorption over a relatively dilute surfactant concentration range below and slightly above the CMC. To determine the surfactant concentration range where the neglect of micellar interactions constitutes an accept-

able approximation, the Debye-Hückel screening length, κ^{-1}, provides an estimate of the length scale for the decay of the electrostatic interactions within the surfactant solution.[43,47] In other words, the electrostatic effects associated with a charged particle or charged surface will be significantly reduced at a distance which is several Debye-Hückel screening lengths away. If the average distance between micelles, estimated by $n_{mic}^{-1/3}$ (where n_{mic} is the micelle number density), is much larger than the Debye-Hückel screening length, κ^{-1}, then on average, the electrostatic effects of a micelle on the surface (or on a surfactant monomer, or another micelle) are expected to be small, since the average distance between a micelle and the surface (or between a micelle and a surfactant monomer, or between two micelles) will be sufficiently large in that case. In other words, as long as

$$n_{mic}^{-1/3} >> \kappa^{-1} \tag{2.49}$$

to a good approximation, the various electrostatic interactions involving micelles may be neglected. The inequality in Eq. (2.49) is satisfied for the aqueous ionic surfactant solutions considered in this chapter having total bulk aqueous surfactant concentrations as large as approximately 10 times the CMC. Figure 2-2 shows an example of the variation of the ratio of the Debye-Hückel screening length, κ^{-1}, and the average intermicellar distance, $n_{mic}^{-1/3}$, as a function of the total bulk aqueous surfactant concentration, $n_{\rm tot}$, for an aqueous binary mixture of 10% SDS and 90% $C_{12}E_6$ at 25°C. The micelle number density was predicted using the bulk molecular-thermodynamic theory of micellization described in Refs. 35-37. Figure 2-2 indicates that below the CMC (indicated by the arrow), the intermicellar distance is infinite, and therefore, $\kappa^{-1}/n_{mic}^{-1/3}$ vanishes. Above the CMC, as the total bulk aqueous surfactant concentration, $n_{\rm tot}$, increases, the intermicellar distance decreases (as more micelles form), thus increasing the value of $\kappa^{-1}/n_{\rm mic}^{-1/3}$. However, even at concentrations ten times larger than the CMC, the ratio remains small compared to unity (approximately 0.1). As illustrated by this example, even if electrostatic interactions involving micelles are neglected, the theory developed here should still be applicable over the surfactant

concentration range that is relevant for many of the practical applications involving ionic surfactants.

Figure 2-3 shows a schematic illustration of the bulk micellar solution when Eq. (2.49) is satisfied. The area surrounded by box A represents a region in the bulk aqueous solution were the electrostatic effects associated with the charged micelles are negligible. Accordingly, the chemical potential of a surfactant monomer of type s inside the region of Box A may be modeled by the ideal solution approximation, that is,

$$\mu_s^{\mathrm{w}} = \mu_s^{\mathrm{w},0} + \mathrm{k_B}T \ln\left(x_{s1}\right) = \mu_s^{\mathrm{w},0} + \mathrm{k_B}T \ln\left(\frac{n_{s1}^{\mathrm{w}}}{n_{\mathrm{w}}^{\mathrm{w}}}\right) \tag{2.50}$$

where x_{s1} and n_{s1}^{w} are the bulk aqueous mole fraction and concentration, respectively, of *surfactant monomers* of type s which can be predicted as a function of the total bulk aqueous surfactant concentration, n_{tot}, and bulk aqueous solution composition, α^{soln}, using the bulk molecular-thermodynamic theory discussed in Refs. 35–37. In the absence of added salt, the number density of the counterions in region A is equal to the number density of the ionic surfactant monomers in order to maintain electroneutrality in region A. The chemical potential of the counterions in region A can therefore be written as follows:

$$\mu_c^{\mathrm{w}} = \mu_c^{\mathrm{w},0} + \mathrm{k_B}T \ln\left(x_{s1}\right) = \mu_c^{\mathrm{w},0} + \mathrm{k_B}T \ln\left(\frac{n_{s1}^{\mathrm{w}}}{n_{\mathrm{w}}^{\mathrm{w}}}\right) \tag{2.51}$$

where the counterion mole fraction, x_c, has been replaced by x_{s1} as explained above. Equations (2.50) and (2.51) yield the same expression for $\mu_{sc}^{\mathrm{w}} \equiv \mu_s^{\mathrm{w}} + \mu_c^{\mathrm{w}} = \mu_{sc}^{\mathrm{w},0} + 2k_BTln\left(x_{1s}\right)$ as that given in Eq. (2.47) for the bulk aqueous chemical potential, with the exception that, above the CMC, the surfactant *monomer* concentration differs from the *total* surfactant concentration.

In addition, above the CMC, the effect of the charged micelles on the surface equation of state and on the surface chemical potentials must also be examined. In the remainder of this section, two different methods for treating the micelle-surface electrostatic interactions are considered. In the first method, the Poisson-Boltzmann model is utilized, and the charged micelles are treated as just another ionic species

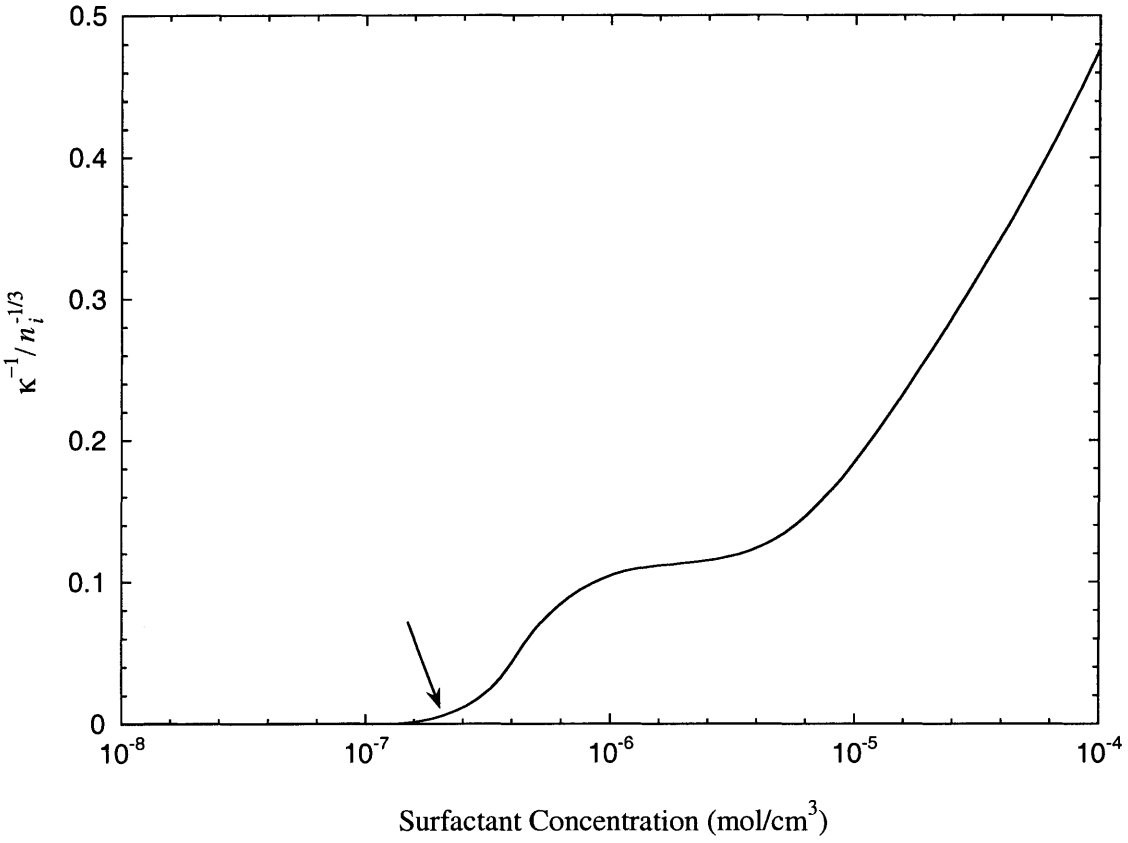

Figure 2-2: Variation of the ratio of the Debye-Hückel screening length, κ^{-1}, and the average intermicellar distance, $n_{mic}^{-1/3}$, with total bulk aqueous surfactant concentration, $n_{SDS}^{w} + n_{C_{12}E_6}^{w}$, for an aqueous binary surfactant mixture of 10% SDS and 90% $C_{12}E_6$ at 25°C. Note that below the CMC (indicated by the arrow), the intermicellar distance is infinite, and therefore, the ratio vanishes. Above the CMC, as the total surfactant concentration increases, the intermicellar distance decreases (as more micelles form), thus increasing the ratio. However, even at concentrations ten times larger than the CMC, the ratio remains small compared to unity.

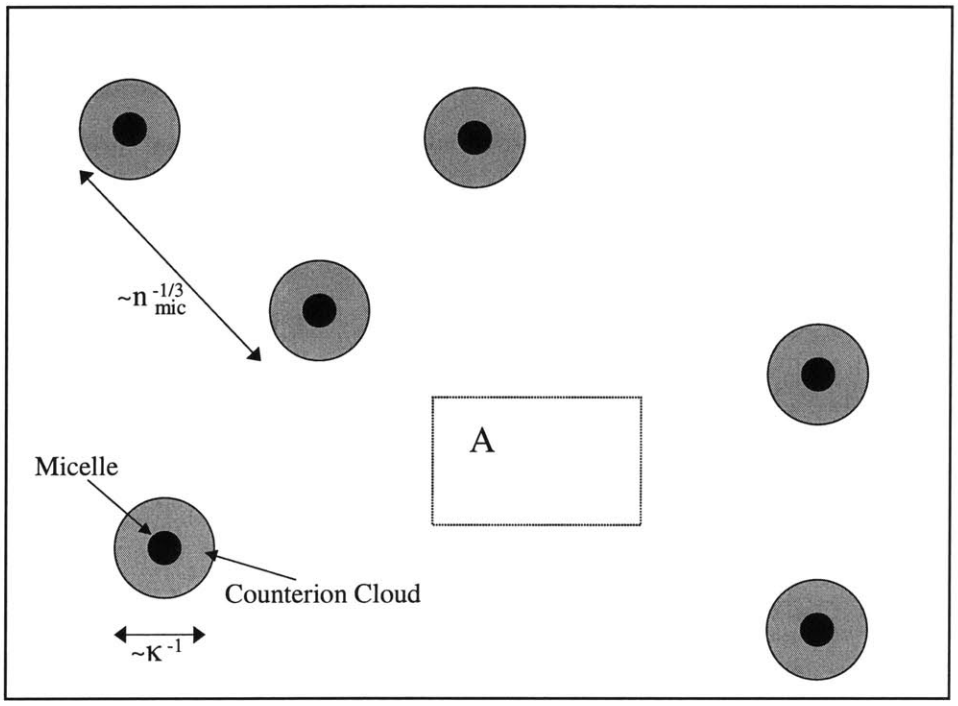

Figure 2-3: Schematic illustration of a bulk micellar solution consisting of a single ionic surfactant species and its counterions when the Debye-Hückel screening length, κ^{-1}, is much smaller than the intermicellar distance, $n_{mic}^{-1/3}$ (see text for details).

present in the diffuse region of the double layer. In the second method, the presence of the charged micelles is neglected altogether. The first and second methods provide upper and lower bounds, respectively, for the effect of the micellar electrostatic interactions on the surface properties of the surfactant solution. Moreover, for a micellar solution not too far above the CMC (where the inequality in Eq. (2.49) is valid), both methods yield similar results. Consequently, when the micellar concentration is small and Eq. (2.49) is therefore valid, neglecting the contribution of the charged micelles to the surface equation of state represents a reasonable approximation.

In the first method for the treatment of micelle-surface electrostatic interactions, the charged micelles can be included in the Poisson-Boltzmann model by simply treating them as any other ionic species. Specifically, the Poisson-Boltzmann equation (see Eq. (2.22)) takes the following form:

$$\frac{d^2\Psi}{dx^2} = \frac{-4\pi e}{\varepsilon}\sum_{i=1}^{n} z_i n_i(x) = \frac{-4\pi e}{\varepsilon}\left\{ z_s n_{s1}^{w} exp\left(\frac{-z_s e\Psi}{k_B T}\right) + z_c n_c^{w} exp\left(\frac{-z_c e\Psi}{k_B T}\right) \right.$$

$$\left. + \; z_{mic} n_{mic}^{w} exp\left(\frac{-z_{mic} e\Psi}{k_B T}\right)\right\} \tag{2.52}$$

where n_{s1}^{w} is the bulk aqueous monomer number density of the single ionic surfactant, s, (that is, far away from the charged interface), n_c^{w} is the bulk aqueous number density of the counterion, c, n_{mic}^{w} is the bulk aqueous number density of micelles, and z_{mic} is the total valence of the micelle. Note that for simplicity, Eq. (2.52) was written for a monodisperse micelle population. The extension of Eq. (2.52) to a polydisperse micelle population is straightforward. The three terms on the right-hand side of Eq. (2.52) correspond to the three different ionic species present in the solution: the monomers, the counterions, and the micelles. Note that n_{s1}^{w}, n_{mic}^{w}, and z_{mic} can be predicted using the bulk molecular-thermodynamic theory of micellization discussed above.[35–37] The validity of including the charged micelles in the Poisson-Boltzmann model in this manner will be discussed below. Note that since the micelles are not

monovalent, the closed form solution of the Poisson-Boltzmann equation derived in Section 2.2.2.1 is not applicable. Instead, a numerical solution to Eq. (2.52) is utilized as follows. Integrating Eq. (2.52) once, and then using the fact that the electric field, $(\mathrm{d}\Psi/\mathrm{d}x)$ vanishes at infinity yields:

$$\left(\frac{\mathrm{d}\Psi}{\mathrm{d}x}\right)^2 = \frac{-8\pi \mathrm{k_B}T}{\varepsilon}\left\{n_{s1}^{\mathrm{w}}\left(\exp\left(\frac{-\mathrm{z}_s\mathrm{e}\Psi}{\mathrm{k_B}T}\right)-1\right)+n_c^{\mathrm{w}}\left(\exp\left(\frac{-\mathrm{z}_c\mathrm{e}\Psi}{\mathrm{k_B}T}\right)-1\right)\right.$$

$$\left. + \; n_{\mathrm{mic}}^{\mathrm{w}}\left(\exp\left(\frac{-\mathrm{z}_{\mathrm{mic}}\mathrm{e}\Psi}{\mathrm{k_B}T}\right)-1\right)\right\} \tag{2.53}$$

The electrostatic potential at the Stern layer, Ψ_d, can be found as a function of the number of surfactant molecules in the monolayer, η_s, by numerically solving the following equation for Ψ_d using any one of the many numerical techniques for solving one equation for one unknown quantity:[48]

$$\hat{\sigma}^2 = \left(\frac{-\varepsilon}{4\pi}\left.\frac{d\Psi}{dx}\right|_{x=d}\right)^2 = \frac{\varepsilon k_B T}{2\pi}\left\{n_{s1}^{\mathrm{w}}\left(exp\left(\frac{z_s e\Psi_d}{k_B T}\right)-1\right)\right. \tag{2.54}$$

$$\left. + \; n_c^{\mathrm{w}}\left(exp\left(\frac{z_c e\Psi_d}{k_B T}\right)-1\right)+n_{mic}^{\mathrm{w}}\left(exp\left(\frac{z_{mic} e\Psi_d}{k_B T}\right)-1\right)\right\}$$

where $\hat{\sigma} = ez_s\eta_s/A$ is the surface charge density. Once Ψ_d is known, the surface electrostatic potential, Ψ_0, can be determined using Eq. (2.28). Finally, the electrostatic surface pressure, Π_{elec}, can be found by numerically integrating Eq. (2.34), and the total surface pressure can be found using $\Pi = \Pi_{\mathrm{NI}} + \Pi_{\mathrm{elec}}$, where Π_{NI} is given by Eq. (2.19). The surface chemical potential of the ionic surfactant s and counterions c, μ_{sc}^{σ}, can then be found by integrating Eq. (2.44).

Physically, it is anticipated that this method of including the charged micelles in the Poisson-Boltzmann model should overestimate the electrostatic effects of the

micelles on the surface monolayer, since it assumes that all the ions are uniformly smeared out in the bulk aqueous solution (that is, it does not include the possibility of "counterion binding" to the micelles, and also does not account for the electrostatic intermicellar interactions). In reality, one would expect a fraction of the counterions to be ordered around the micelles, thus lowering the effective charge of each micelle. Furthermore, the effect of the relatively large size of the micelles, which should further reduce the ability of the micelles to screen the surface electrostatic charge, is not taken into account here. Hence, this first method does not represent a realistic approximation to the actual system, but rather serves as an upper bound for the effect of electrostatic interactions between the charged micelles and the charged surface monolayer.

As an alternative, one can underestimate the electrostatic effects of the charged micelles on the charged surface monolayer by completely neglecting the effect of the charged micelles on the surface equation of state, as was done in Sections 2.2.2.1-2.2.2.2. This should serve as a lower bound for the effect of the electrostatic interactions between the charged micelles and the charged surface monolayer. Figure 2-4 shows a comparison of the two methods, with (—) and without (– – –) micelles in the Poisson-Boltzmann model for the surface equation of state, for the surface tension, σ, as a function of the total bulk aqueous surfactant concentration, n_{tot}, for an aqueous binary mixture of 10% SDS and 90% $C_{12}E_6$ at 25°C. Note that for dilute micellar solutions (n_{tot} is less than approximately $5 \times 10^{-6} mol/cm^3$, which is 10 times the CMC of $5 \times 10^{-7} mol/cm^3$) where the inequality in Eq. (2.49) is satisfied, the two methods yield identical results (the full and the dashed lines in Figure 2-4 are indistinguishable). This supports the previous assertion that electrostatic interactions between the micelles and the charged surface are negligible for dilute micellar solutions. For more concentrated micellar solutions, Figure 2-4 shows that the two methods deviate, suggesting that electrostatic interactions between the charged micelles and the charged surface monolayer become increasingly important as n_{tot} increases. In that case, a more complex theory is required to make accurate predictions at these higher surfactant concentrations. Note that at higher n_{tot} values ($n_{\text{tot}} > 5 \times 10^{-6} mol/cm^3$),

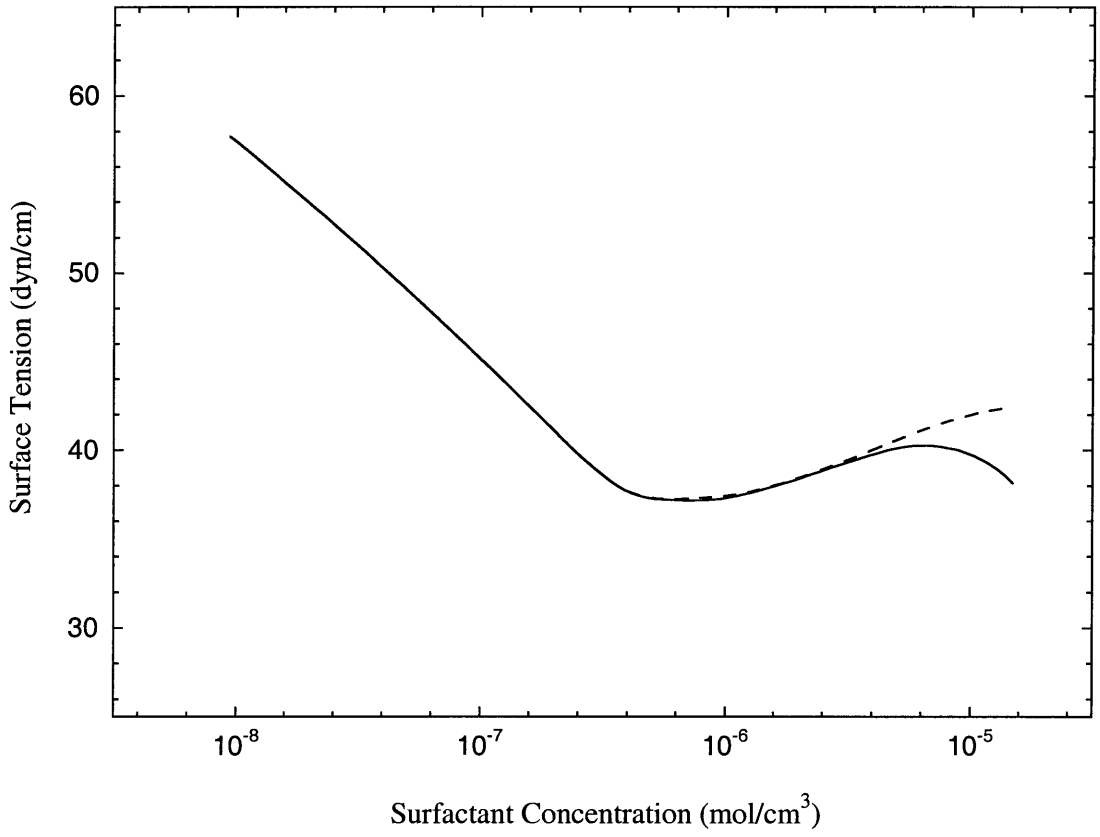

Figure 2-4: Illustration of the effect of micelle-surface electrostatic interactions on the predicted surface tension vs. total bulk aqueous surfactant concentration, $n^{\mathrm{w}}_{SDS} + n^{\mathrm{w}}_{C_{12}E_6}$, for an aqueous binary surfactant mixture of 10% SDS and 90% $C_{12}E_6$ at 25°C. Predictions were made by including (solid) and neglecting (dashed) micellar electrostatic interactions with the charged surface in the Poisson-Boltzmann model.

accounting for the presence of the ionic micelles on the surface equation of state leads to increased electrostatic screening. This enhanced electrostatic screening allows more ionic surfactant molecules to adsorb at the surface, leading to an overall increase in the total number of surfactant molecules at the surface, and therefore, resulting in an increase in the non-electrostatic contribution to the surface pressure, Π_{NI}. This, in turn, results in higher total surface pressure, Π, or equivalently, a lower surface tension, $\sigma = \sigma_0 - \Pi$, when charged micelles are accounted for in the surface equation of state (see Figure 2-4).

2.3 Results and Discussion

2.3.1 Calculation of Molecular Parameters

The surface tension, surface concentration, and surface composition were predicted for aqueous solutions containing either SDS, $C_{12}E_6$, and C_{12}Maltoside, as well as for aqueous solutions containing binary mixtures of SDS–$C_{12}E_6$ and SDS–C_{12}Maltoside. The corresponding hard-disk head area sizes, a_i, hard-disk radii, r_i, Stern-layer thickness, d, second-order virial coefficients, B_{ii} and B_{ij}, and standard-state chemical potential differences, $\Delta\mu_i^0$, are listed in Tables 2.1 and 2.2. An analysis of the sensitivity of the theoretical predictions to the values of these parameters is presented in Appendix B. The estimation of a_i for C_iE_j nonionic surfactants was discussed in detail previously,[24] and was used here to determine the value of 42Å^2 for $C_{12}E_6$. The hard-disk head area of the C_{12}Maltoside nonionic surfactant was obtained through small angle neutron and X-ray scattering experiments performed by Dupuy et al.[49] Their experiments determined that the effective head-area size depends on the curvature of the micelle surface. The head-area size used here for the surface equation of state, 32Å^2, corresponds to the experimentally determined value at a point of minimal surface curvature since the solution-air interface is flat. The head-area size used in the bulk, micellization model, 58Å^2, corresponds to that in a spherical micelle. The hard-disk head area of the SDS surfactant calculated by the bond angles and lengths

of the sulfate group has been previously determined[36,50] to be 25Å^2. The Stern-layer thickness, d, for SDS was also calculated using the geometry of the sulfate group as well as the size of the sodium counterion. For the dielectric constant in the Stern layer, ε_s, the value of 42 suggested by Bockris and Reddy[47] which is in reasonable agreement with experimental measurements[51] has been utilized. Note that a 10% change in the value of ε_s results in a change of less than 1% in the final predicted surface tension. Accordingly, the results are not extremely sensitive to the precise value of ε_s with the approximate value utilized here providing sufficient accuracy. The second-order virial coefficients were computed using the determined head-area sizes as described in Ref. 12. As described in Section 2.2.1, the standard-state chemical potential differences, $\Delta\mu_i^0$, were calculated by fitting *one* measured surface tension value for each *single* surfactant solution considered. The bulk aqueous surfactant concentrations, n_{tot}, chosen for this fit are $5.4 \times 10^{-6} mol/cm^3$ for SDS, $1.7 \times 10^{-8} mol/cm^3$ for $C_{12}E_6$, and $6.1 \times 10^{-8} mol/cm^3$ for C_{12}Maltoside. Since the theoretically predicted surface tensions were found to be in good agreement with the experimentally measured surface tensions (see below), the precise choice of n_{tot} for the fit is quite arbitrary and does not greatly affect the theoretical predictions. However, in general, it is recommended to choose a surfactant concentration, n_{tot}, below the CMC. In that case, any inaccuracy in the prediction of the CMC and surfactant monomer concentration by the bulk molecular-thermodynamic theory of micellization will not have a strong influence on the value of the bulk aqueous chemical potential, since below the CMC, all the surfactant is present in monomeric form. Moreover, one should also avoid extremely low surfactant concentrations, where the percent uncertainty in the surface pressure measurement is large due to the low value of the surface pressure.

2.3.2 Comparison with Experimental Surface Tension and Adsorption Measurements

Experimentally measured surface tensions and surface concentrations and compositions (measured directly using neutron scattering) were reported[52] for single surfac-

Table 2.1: Values of the hard-disk areas, a_i, second-order virial coefficients, B_{ii}, Stern layer thickness, d, and standard-state chemical potential differences, $\Delta\mu_i^0$, corresponding to the three surfactants C_{12}Maltoside, $C_{12}E_6$, and SDS.

Surfactant i	a_i (Å^2)	B_{ii} (Å^2)	d (Å)	$\Delta\mu_i^0$ (k_BT)
C_{12}Maltoside	32	-157	–	-48.6
$C_{12}E_6$	42	-77	–	-53.0
SDS	25	-367	4.05	-59.0

Table 2.2: Values of the second-order virial coefficients, B_{ij}, for the two binary combinations corresponding to the three surfactants C_{12}Maltoside, $C_{12}E_6$, and SDS.

Surfactant Pair	B_{ij} (Å^2)
C_{12}Maltoside–SDS	-225
$C_{12}E_6$–SDS	-135

tant aqueous solutions of SDS, C_{12}Maltoside, as well as for binary surfactant aqueous solutions of SDS–C_{12}Maltoside. Experimentally measured surface tensions were reported[36,50] for single surfactant aqueous solutions of SDS and $C_{12}E_6$, as well as for binary surfactant aqueous solutions of SDS–$C_{12}E_6$. All of the reported measurements were conducted at 25°C.

The surface tension predictions were made by first predicting the monolayer concentrations of both surfactants through a simultaneous solution of Eq. (2.13), for either the nonionic surfactant $C_{12}E_6$, or the nonionic surfactant C_{12}Maltoside, and Eq. (2.48) for the ionic surfactant SDS. For these two binary surfactant systems, Eqs. (2.13) and (2.48) reduce to:

$$\ln\left(\frac{n_{1B}^{\mathrm{w}}}{n_{\mathrm{w}}^{\mathrm{w}}}\right) = \frac{\Delta\mu_A^0}{\mathrm{k_B}T} + \ln\left(\frac{\xi_B}{\alpha - \xi_A \mathrm{a}_A - \xi_B \mathrm{a}_B}\right) + \frac{\mathrm{a}_B + 2\pi \mathrm{r}_B\left(\xi_A \mathrm{r}_A + \xi_B \mathrm{r}_B\right)}{\alpha - \xi_A \mathrm{a}_A - \xi_B \mathrm{a}_B}$$

$$+ \frac{\pi \mathrm{a}_B\left(\xi_A r_A + \xi_B r_B\right)^2}{\left(\alpha - \xi_A \mathrm{a}_A - \xi_B \mathrm{a}_B\right)^2} + \frac{2}{\alpha}\left(B_{BA}\xi_A + B_{BB}\xi_B\right) \tag{2.55}$$

and

$$2\ln\left(\frac{n_{1A}^{\mathrm{w}}}{n_{\mathrm{w}}^{\mathrm{w}}}\right) = \frac{\Delta\mu_A^{\sigma}}{\mathrm{k_B}T} + \ln\left(\frac{\xi_A}{\alpha - \xi_A \mathrm{a}_A - \xi_B \mathrm{a}_B}\right) + \frac{\mathrm{a}_A + 2\pi \mathrm{r}_A\left(\xi_A \mathrm{r}_A + \xi_A \mathrm{r}_A\right)}{\alpha - \xi_A \mathrm{a}_A - \xi_B \mathrm{a}_B}$$

$$+ \frac{\pi \mathrm{a}_A\left(\xi_A \mathrm{r}_A + \xi_B \mathrm{r}_B\right)^2}{\left(\alpha - \xi_A \mathrm{a}_A - \xi_B \mathrm{a}_B\right)^2} + \frac{2}{\alpha}\left(B_{AA}\xi_A + B_{AB}\xi_B\right) \tag{2.56}$$

$$+ 2\mathrm{z}_A \ln\left|\frac{2\pi \mathrm{e}^2}{\varepsilon\kappa \mathrm{k_B}T\alpha}\mathrm{z}_A\xi_A + \sqrt{1 + \left(\frac{2\pi \mathrm{e}^2}{\varepsilon\kappa \mathrm{k_B}T\alpha}\mathrm{z}_A\xi_A\right)^2}\right| + \frac{4\pi \mathrm{d}\left(\mathrm{z}_A \mathrm{e}\right)^2}{\mathrm{k_B}T\varepsilon_{\mathrm{s}}}\frac{\xi_A}{\alpha}$$

where the subscript A refers to SDS and the subscript B refers to $C_{12}E_6$ or C_{12}Maltoside. First, the values of n_{1A}^{w} and n_{1B}^{w} are predicted for a given total bulk aqueous surfactant concentration, n_{tot}, and bulk aqueous solution composition, α^{soln}, using the

bulk molecular-thermodynamic theory of micellization discussed earlier in Section 2.2 and Refs. 35–37. Subsequently, Eqs. (2.55) and (2.56) can be solved for the two unknown quantities, α and ξ_A (note that ξ_B can be eliminated using $\xi_A + \xi_B = 1$) using a two-dimensional Newton-Raphson technique.[48] For the single nonionic surfactant cases ($C_{12}E_6$ or C_{12}Maltoside), α is determined by solving Eq (2.55) alone, with the constraint that ξ_A=0 and ξ_B=1. For the single ionic surfactant case (SDS), α is determined by solving Eq (2.56) alone with the constraint that ξ_A=1 and ξ_B=0. The surface pressure, Π, and the corresponding surface tension, $\sigma = \sigma^0 - \Pi$, are finally calculated using Eq. (2.37), which for this binary system reduces to:

$$\Pi = k_B T \left\{ \frac{1}{\alpha - \xi_A a_A - \xi_B a_B} + \frac{\pi \left(\xi_A r_A + \xi_B r_B\right)^2}{\left(\alpha - \xi_A a_A - \xi_B a_B\right)^2} \right. \tag{2.57}$$

$$\left. + B_{AA}\frac{\xi_A \xi_A}{\alpha^2} + B_{AB}\frac{\xi_A \xi_B}{\alpha^2} + B_{BB}\frac{\xi_B \xi_B}{\alpha^2} \right\}$$

$$+ \left(\frac{\varepsilon\kappa}{4\pi}\right)\left(\frac{2k_B T}{e}\right)^2 \left[\sqrt{1 + \left(\frac{4\pi}{\varepsilon\kappa}\right)^2 \left(\frac{e^2}{2k_B T}\right)^2 \left(\frac{z_A \xi_A}{\alpha}\right)^2} - 1\right] + \frac{2\pi d}{\varepsilon_s}\left(\frac{e z_A \xi_A}{\alpha}\right)^2$$

In Figure 2-5, the predicted surface tensions as a function of total bulk aqueous surfactant concentration, n_{tot}, are compared to the experimentally measured surface tensions of aqueous solutions of the single surfactants SDS (▲), $C_{12}E_6$ (■), and C_{12}Maltoside (●). In Figure 2-6, the predicted surface tensions as a function of total bulk aqueous surfactant concentration, n_{tot}, are compared to the experimentally measured surface tensions of aqueous binary surfactant mixtures of SDS and $C_{12}E_6$ at solution compositions, $\alpha^{soln} \equiv n^w_{SDS} / \left(n^w_{SDS} + n^w_{C_{12}E_6}\right)$, of 0.05 (■), 0.4 (●), and 0.9 (▲). In Figure 2-7, the predicted surface tensions as a function of total bulk aqueous surfactant concentration, n_{tot}, are compared to the experimentally measured surface tensions of aqueous binary surfactant mixtures of SDS and C_{12}Maltoside at solution compositions, $\alpha^{soln} \equiv n^w_{SDS} / \left(n^w_{SDS} + n^w_{C_{12}Maltoside}\right)$, of 0.2 (■), 0.5 (●), and

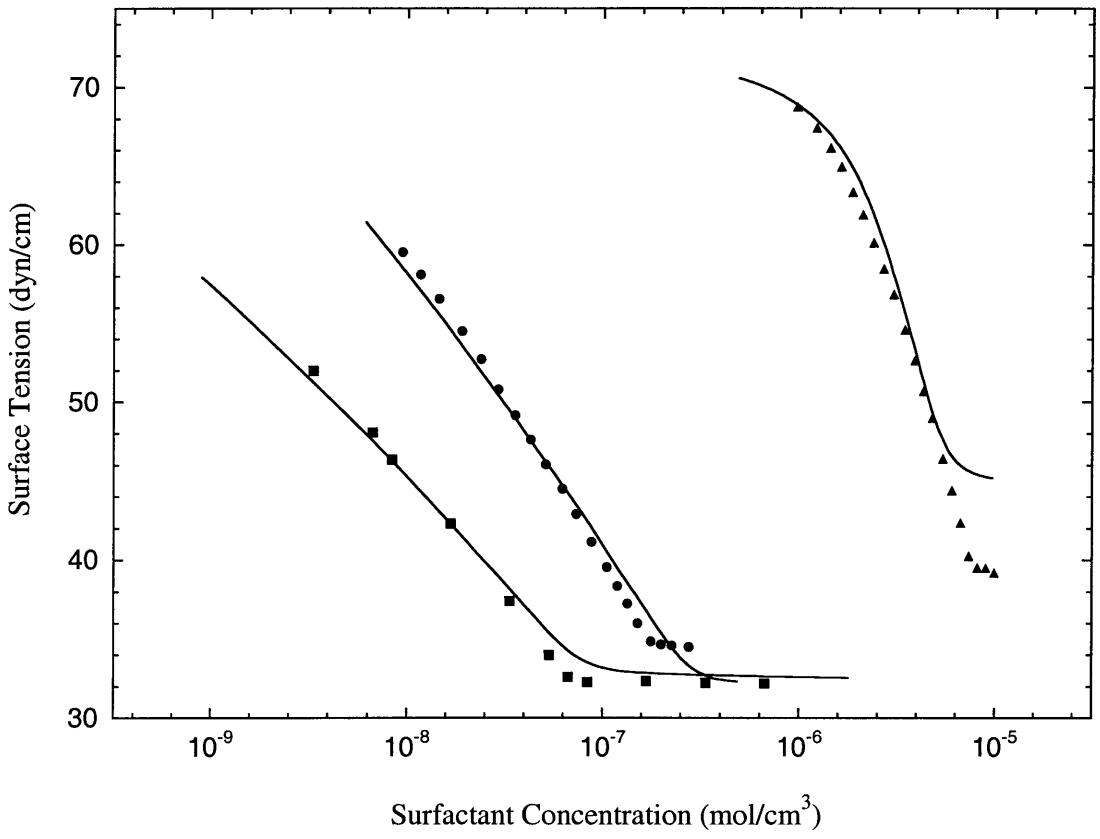

Figure 2-5: Predicted (various lines) and measured (various symbols) surface tensions, σ, as a function of the total bulk aqueous surfactant concentration, n_i^{w}, of single surfactant aqueous solutions of SDS (▲), $C_{12}E_6$ (■), and C_{12}Maltoside (●) at 25°C. The reported experimental uncertainty is within 0.1 dyn/cm.

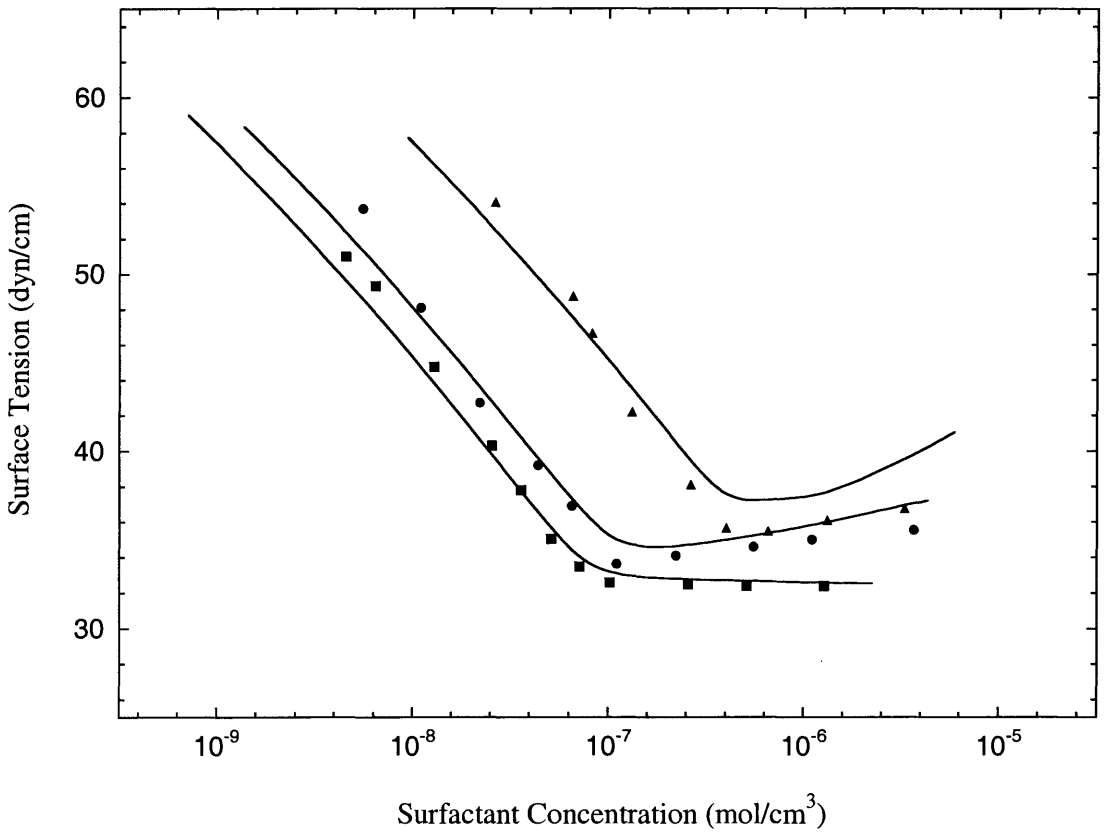

Figure 2-6: Predicted (various lines) and measured (various symbols) surface tensions, σ, as a function of the total bulk aqueous surfactant concentration, $n^{\mathrm{w}}_{SDS} + n^{\mathrm{w}}_{C_{12}E_6}$, of aqueous solutions containing binary mixtures of SDS and $C_{12}E_6$ at 25°C, at bulk aqueous solution compositions, $\alpha^{soln} \equiv n^{\mathrm{w}}_{SDS}/(n^{\mathrm{w}}_{SDS} + n^{\mathrm{w}}_{C_{12}E_6})$, of 0.05 (■), 0.4 (●), and 0.9 (▲). The reported experimental uncertainty is within 0.1 dyn/cm.

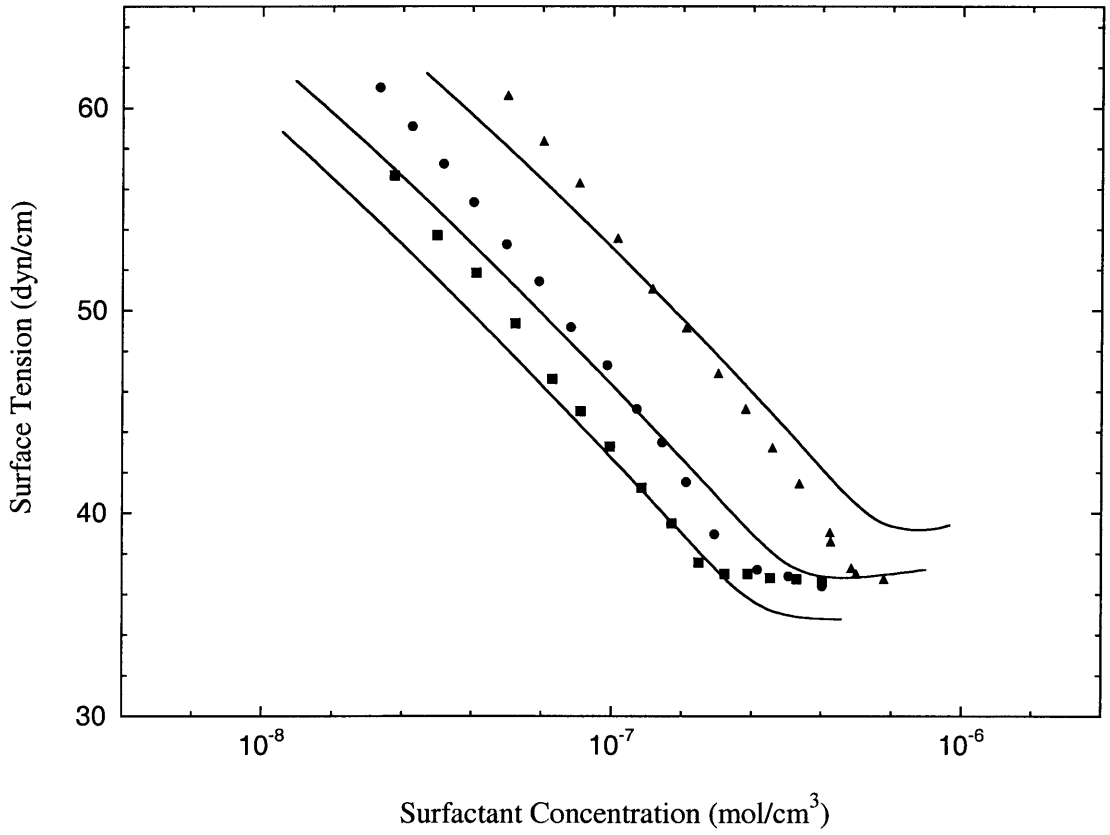

Figure 2-7: Predicted (various lines) and measured (various symbols) surface tensions, σ, as a function of the total bulk aqueous surfactant concentration, $n^{w}_{SDS} + n^{w}_{C_{12}Maltoside}$, of aqueous solutions containing binary mixtures of SDS and C_{12}Maltoside at 25°C, at bulk aqueous solution compositions, $\alpha^{soln} \equiv n^{w}_{SDS}/(n^{w}_{SDS} + n^{w}_{C_{12}Maltoside})$, of 0.2 (■), 0.5 (●), and 0.8 (▲). The reported experimental uncertainty is within 0.1 dyn/cm.

0.8 (▲). Note that the reported experimental uncertainty in the surface tension measurements is better than, or on the order of, 0.1 dyn/cm, which is smaller than the size of the symbols used in Figures 2-5 through 2-7. Figures 2-5 through 2-7 show that the predicted surface tensions are in good agreement with the experimentally measured values, both for the single surfactants (which contain the one fitted parameter, $\Delta\mu_i^0$), as well as for the binary surfactant mixtures (*which contain no additional fitted parameters*). One area of only marginal agreement between the predicted and the experimental surface tension values is for the ionic surfactant SDS above the CMC (see ▲'s in Figure 2-5). For the SDS system, the predicted surface tensions above the CMC are larger than the experimentally measured values. This can be explained by the fact that the bulk molecular-thermodynamic theory of micellization utilized here under-predicts the CMC for this ionic surfactant. This, in turn, leads to a predicted SDS monomer concentration that is too low, resulting in too low of a bulk aqueous chemical potential of the SDS monomers, which leads to an under-prediction of the SDS surface concentration, and hence, to an under-prediction of the surface pressure (which corresponds to the observed over-prediction of the surface tension in Figure 2-5). Since the slope of the surface tension vs. $\log_{10}(n_{\text{tot}})$ curve for SDS is very steep, the small difference between the predicted and the experimentally measured CMC has a relatively large effect on the difference between the predicted and the experimentally measured surface tensions above the CMC. This error could be reduced by improving the bulk molecular-thermodynamic theory of micellization for ionic surfactants, an endeavor which is currently in progress.[53]

Figures 2-8 through 2-10 show a comparison of the predicted and the experimentally measured values (using neutron scattering[52]) of the monolayer concentration of SDS, Γ_{SDS} (▲, — — —), and C_{12}Maltoside, $\Gamma_{C_{12}Maltoside}$ (●, ———), as a function of the surface pressure, Π, for solution compositions, α^{soln}, of 0.2 (Figure 2-8), 0.5 (Figure 2-9), and 0.8 (Figure 2-10). The theoretical predictions, for Γ_{SDS} and for $\Gamma_{C_{12}Maltoside}$, are in reasonable agreement with the experimental values, typically within 0.3×10^{10}mol/cm^2. Note that this difference is within the error range of the neutron scattering measurements which is reported to be on the order

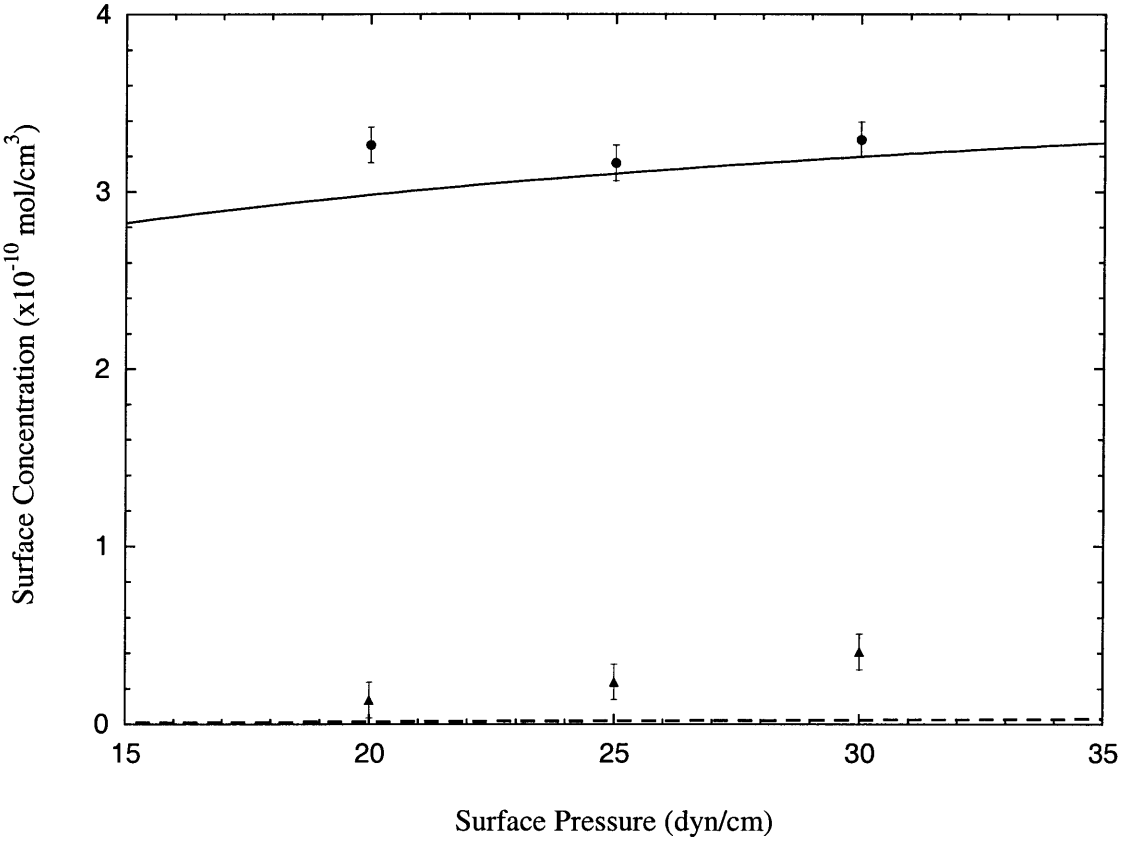

Figure 2-8: Predicted (various lines) and measured (various symbols) surface concentrations of SDS, Γ_{SDS} (▲, — — —), and C_{12}Maltoside, $\Gamma_{C_{12}Maltoside}$ (●, ———), as a function of surface pressure, Π, at a bulk aqueous solution composition, α^{soln}, of 0.2 for aqueous solutions containing binary mixtures of SDS and C_{12}Maltoside at 25°C. The reported experimental uncertainty is on the order of 0.1×10^{10}mol/cm^2.

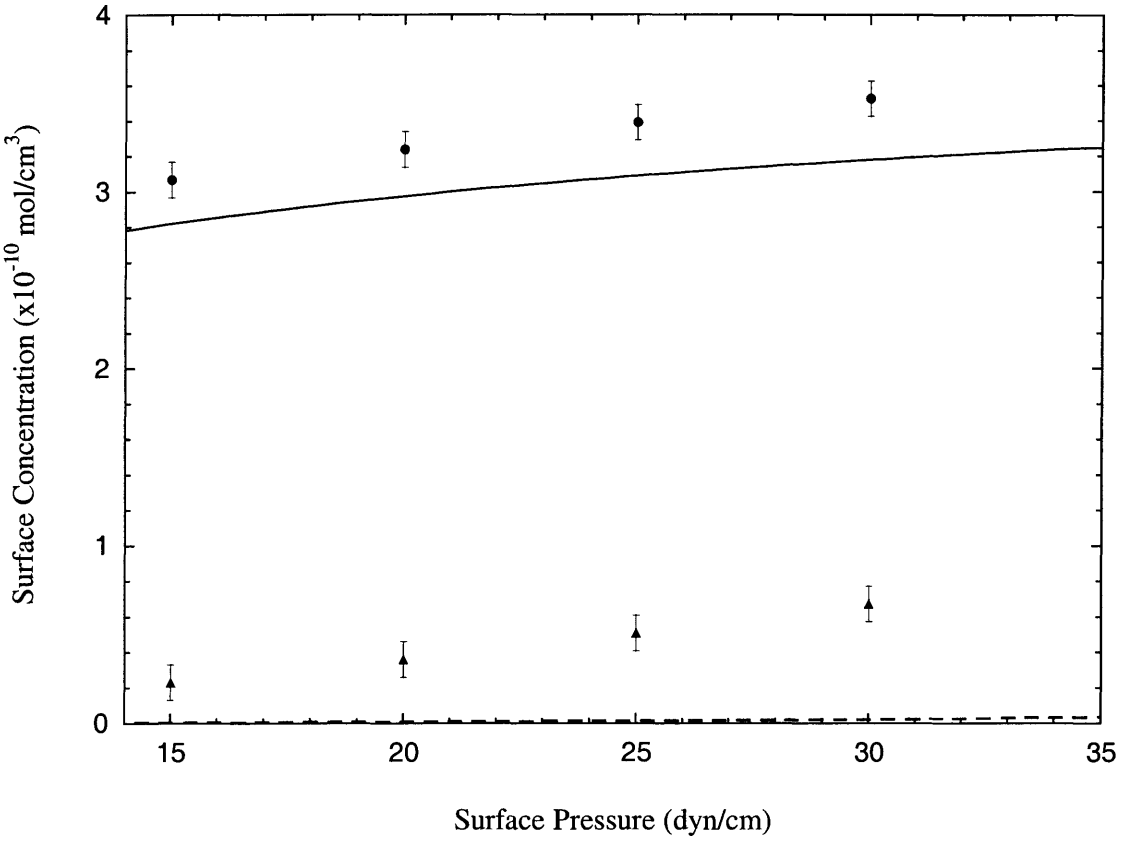

Figure 2-9: Predicted (various lines) and measured (various symbols) surface concentrations of SDS, Γ_{SDS} (▲, — — —), and C_{12}Maltoside, $\Gamma_{C_{12}Maltoside}$ (●, ———), as a function of surface pressure, Π, at a bulk aqueous solution composition, α^{soln}, of 0.5 for aqueous solutions containing binary mixtures of SDS and C_{12}Maltoside at 25°C. The reported experimental uncertainty is on the order of 0.1×10^{10}mol/cm^2.

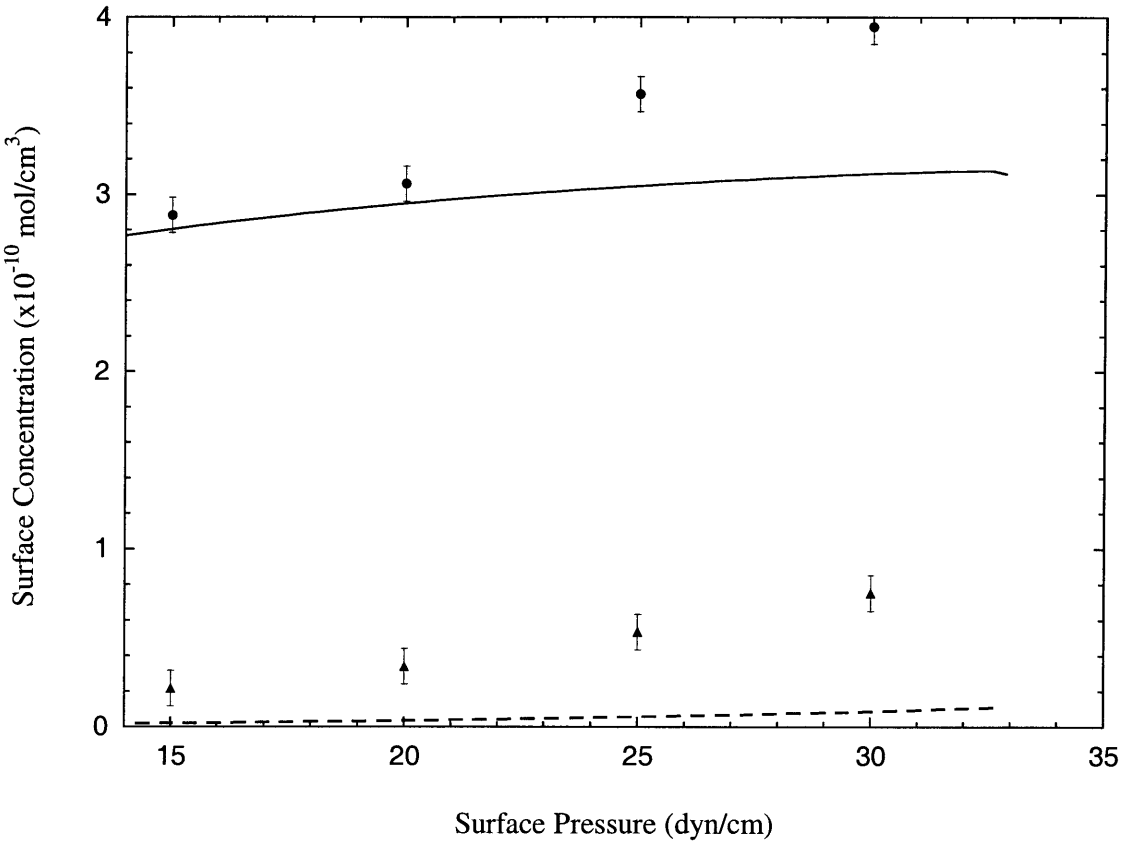

Figure 2-10: Predicted (various lines) and measured (various symbols) surface concentrations of SDS, Γ_{SDS} (▲, — — —), and C_{12}Maltoside, $\Gamma_{C_{12}Maltoside}$ (●, ———), as a function of surface pressure, Π, at a bulk aqueous solution composition, α^{soln}, of 0.8 for aqueous solutions containing binary mixtures of SDS and C_{12}Maltoside at 25°C. The reported experimental uncertainty is on the order of 0.1×10^{10}mol/cm^2.

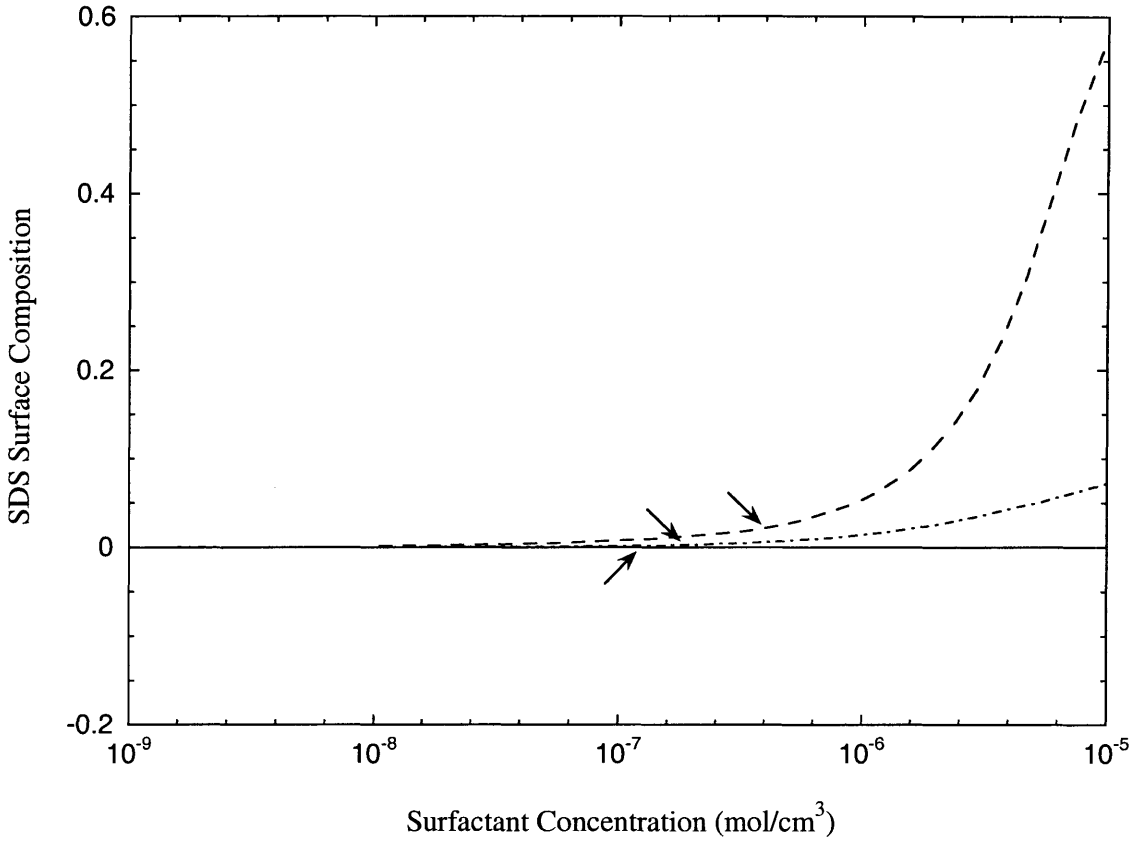

Figure 2-11: Predicted surface composition (mole fraction of SDS in the monolayer), ξ_{SDS}, as a function of total bulk aqueous surfactant concentration, $n^{w}_{SDS} + n^{w}_{C_{12}E_6}$, of aqueous solutions containing binary surfactant mixtures of SDS and $C_{12}E_6$ at 25°C at bulk aqueous solution compositions, α^{soln}, of 0.05 (———), 0.4 (- – - – -), and 0.9(— — —). The three arrows indicate the predicted mixture CMC's corresponding to the three solution compositions considered.

of 0.1×10^{10}mol/cm^2.[52]

Figure 2-11 shows the predicted surface composition, ξ_{SDS}, as a function of total bulk aqueous surfactant concentration at solution compositions, α^{soln}, of 0.05 (———), 0.4 (- – - – -) and 0.9 (— — —) for an aqueous binary surfactant mixture of SDS and $C_{12}E_6$ at 25°C. The predicted CMC's of each solution, $8.9 \times 10^{-8} mol/cm^3$ for 5% SDS, $1.3 \times 10^{-7} mol/cm^3$ for 40% SDS, and $3.4 \times 10^{-7} mol/cm^3$ for 90% SDS, are indicated by the three arrows corresponding to the three solution compositions considered in Figures 2-11. No experimental measurements of the surface composition or concentration are currently available for this system. Nevertheless, it is interesting to note that at very low total bulk aqueous surfactant concentrations, n_{tot}, the composition of the monolayer is mostly $C_{12}E_6$ ($\xi_{SDS} \approx 0$), due to the fact that $C_{12}E_6$ is much more surface active than SDS. The higher surface activity of $C_{12}E_6$ relative to SDS is also reflected by the fact that, for an aqueous solution of $C_{12}E_6$, the total bulk aqueous surfactant concentration, n_{tot}, at which the surface tension begins to decrease significantly from that of pure water is significantly lower than that for which an aqueous solution of SDS shows the same surface tension lowering (see Figure 2-5). However, at the CMC's of the SDS–$C_{12}E_6$ mixed surfactant solutions for the 40% and 90% SDS cases, ξ_{SDS} increases sharply. This can be explained physically by noting that below the surfactant mixture CMC, the bulk aqueous surfactant monomer composition, $\alpha_1 \equiv n^{\text{w}}_{1SDS} / \left(n^{\text{w}}_{1SDS} + n^{\text{w}}_{1C_{12}E_6}\right)$, is equal to the bulk aqueous solution composition, α^{soln}, since all the surfactant molecules are present in monomeric form. Above the CMC, the bulk aqueous surfactant monomer composition, α_1, as predicted by the bulk molecular-thermodynamic theory of micellization,[35–37] deviates from the bulk aqueous solution composition, α^{soln}. In this case, α_1 increases due to the fact that $C_{12}E_6$, which has a lower CMC than SDS, partitions preferentially into the $C_{12}E_6$-SDS mixed micelles, thus leaving a higher fraction of SDS in monomeric form. As a result, there are relatively fewer $C_{12}E_6$ molecules available to adsorb at the surface, leading to an increase in the relative amount of SDS at the surface (since the surfactant molecules at the interface are in equilibrium with those in the bulk). This sharp change in surface composition near the CMC

was also predicted theoretically[12] for mixtures containing only nonionic surfactants -a trend that was qualitatively verified experimentally for similar C_iE_j type surfactants.[54] Note that in Figure 2-11, the 5% SDS solution contains too little SDS to exhibit this effect.

2.4 Conclusions

A theoretical framework to model surfactant adsorption at the air-solution interface was presented for aqueous solutions containing mixtures of ionic and nonionic surfactants. This theory can predict the surface tension and surfactant surface concentration and composition of these solutions both below and above the CMC. A comparison of the theoretical predictions with experimental surface tension and surfactant surface concentration measurements for aqueous solutions containing binary surfactant mixtures of SDS–$C_{12}E_6$ and SDS–C_{12}Maltoside shows good agreement.

The theory presented in this chapter utilizes a molecularly-based surface equation of state developed in the context of a nonideal two-dimensional adsorbed gas model. Nonideal interactions that are accounted for include: (i) steric, excluded-area interactions between the adsorbed surfactant molecules treated as hard-disks, (ii) attractive, van der Waals interactions between the surfactant tails that are incorporated through a virial expansion truncated at second order in surfactant surface concentration, and (iii) electrostatic interactions in the case of ionic surfactants. All the parameters appearing in this surface equation of state for the mixed surfactant monolayer can be estimated from the known molecular characteristics of the surfactants. These molecular parameters include the valences of the ionic surfactants, the cross-sectional areas of the surfactant molecules, the distance of closest approach between the absorbed ionic surfactants and their counterions, and the second-order virial coefficients, which can be calculated from the known number of carbons in the surfactant hydrocarbon tails and their cross-sectional areas. *In contrast with other existing theories for mixtures of surfactants at interfaces, there are no mixture-dependent experimentally-fitted, empirical parameters in the mixture surface equation of state presented in this*

chapter.

The resulting surface equation of state can be combined with a description of the bulk aqueous surfactant solution chemical potential, including a single experimentally-determined parameter, the difference in the standard-state chemical potential of a surfactant molecule at the surface and in the bulk aqueous solution, for each single surfactant present in the mixture, to predict the total amount and composition of adsorbed surfactant. This can then be combined with the surface equation of state to predict the surface tension. The standard-state chemical potential difference for each surfactant species can be determined from a single surface tension measurement. No additional parameters are required for the mixed surfactant solutions. This greatly reduces the amount of experimentation that would be required to predict the interfacial behavior of mixed surfactant solutions.

Surfactant mixtures having multiple charge layers, including mixtures of ionic surfactants or zwitterionic surfactants, will be discussed in Chapter 3, and investigations into modifying the relatively simple Poisson-Boltzmann model utilized in this chapter to describe the diffuse region will be discussed in Appendix A. Furthermore, as will be shown in Chapter 4, the theoretical methodology presented in this chapter can also be extended to the oil-water interface, where the surfactant behavior is expected to be analogous to that at the air-water interface, but with a reduction in the attractive van der Waals interactions between the adsorbed surfactant hydrocarbon tails. In addition, in Chapters 5 and 6, the theoretical framework for the equilibrium adsorption of surfactants developed in this chapter will be used as a basis for a diffusion limited dynamic adsorption model capable of predicting the surface concentration and composition, as well as the surface tension, as a function of time. Finally, the theory presented in this chapter can be implemented in relatively fast, user-friendly computer programs (see Chapter 7) that may be utilized to reduce the need for time-consuming and tedious experimentation when developing surfactant-based products having the desired interfacial properties.

Chapter 3

Prediction of Equilibrium Surface Tension and Surface Adsorption of Aqueous Surfactant Mixtures Containing Zwitterionic Surfactants

3.1 Introduction

As discussed in Chapter 1 and Section 2.1, the development of a quantitative, molecularly-based thermodynamic theory capable of predicting the interfacial properties of aqueous solutions containing surfactants (and in particular, surfactant mixtures) would be extremely valuable for the design of new surfactant formulations exhibiting the desired interfacial behavior, since the availability of such a theory would also alleviate the need for tedious and time consuming trial-and-error type experimentation. In this chapter, the theoretical framework developed in Chapter 2 is extended to treat mixtures containing zwitterionic surfactants.

Among the various types of surfactants, those of the zwitterionic type are of

particular practical interest because: (i) they are commonly utilized in commercial formulations, particularly in personal care products (including soaps, shampoos, and lotions), where they are typically found to be less irritating to the skin,[55] and (ii) they often exhibit significant synergism (that is, strong, favorable interactions) at the interface when mixed with ionic surfactants, while comparably little synergism is observed when mixed with nonionic surfactants.[52,56] This varying degree of synergism, in addition to being of practical importance, should also provide a useful test of the predictive capabilities of any theory developed to describe the interfacial behavior of aqueous mixtures containing zwitterionic surfactants. Accordingly, a comparison between the predicted interfacial behavior of a zwitterionic-ionic aqueous surfactant mixture and that of a zwitterionic-nonionic aqueous surfactant mixture should provide a stringent test of the theoretical framework presented in this chapter.

In Chapter 2, a theoretical framework was presented to predict the interfacial properties of aqueous mixtures of nonionic and ionic surfactants at the air-aqueous solution interface. There, it was assumed that all the charges associated with the ionic surfactant molecules adsorbed in the monolayer are located at a single, two-dimensional charge layer. In this chapter, the theoretical framework of Chapter 2 is extended to model interfaces that contain *multiple*, two-dimensional electrostatic charge layers, such as those that may result from the adsorption of a single zwitterionic surfactant (two charge layers), or of a binary mixture of zwitterionic and ionic surfactants (three charge layers). This new theoretical framework will allow for the quantitative prediction of the extent of interfacial synergism that results from the adsorption of zwitterionic, ionic, and nonionic surfactants at the air-aqueous solution interface.

The interfacial behavior of surfactants has been investigated theoretically by numerous researchers (see Section 2.1 for more detailed background, as well as for a comparison between the theoretical treatment presented in this thesis and other theoretical treatments). Two important differences between previous theoretical treatments of surfactant adsorption and the theory presented here are that: (i) our theoretical description is molecularly based, relying explicitly on the chemical structures of the

various surfactants species adsorbed at the interface, and as such, the resulting surface equation of state *does not contain any experimentally determined parameters*, while the adsorption isotherm contains *only one* experimentally determined parameter for each surfactant species, and (ii) the theory can be applied to mixtures that contain *any number* of surfactant components without introducing any additional experimentally determined parameters, and therefore, no additional experiments on the mixed surfactant solutions are required. This is to be contrasted with other popular models of single surfactant adsorption, such as the Langmuir or the Frumkin based models,[28,57,58] which require two or more experimentally determined parameters to model the adsorption of a single surfactant species. Moreover, when applied to surfactant mixtures, our theory has a notable advantage over other popular models of mixed surfactant adsorption at interfaces which are based on the Regular Solution Theory (RST) approach.[11,21–25] These RST based approaches all contain experimentally determined parameters which require measurements on the mixed surfactant solutions. Accordingly, the theoretical framework presented here significantly reduces the amount of experimentation required to predict the interfacial behavior of *mixed* surfactant solutions.

The surface equation of state developed in Chapter 2 and in this chapter is based on a two dimensional kinetic gas-like treatment of the adsorbed surfactant monolayer.[34] The non-electrostatic contribution to this surface equation of state includes two types of interactions:[12] (i) steric repulsions, which are included using a hard-disk model, and (ii) van der Waals attractions which are modeled using a virial expansion in surface concentration, truncated to second order. Electrostatic effects, which form an additive contribution to the surface pressure, are treated using the Gouy-Chapman[28,44,29,30] description of the diffuse region of the electrostatic *double layer*. The electrostatic description is further refined by including a Stern layer,[32] that is, a region where the counterions in the aqueous, diffuse region cannot penetrate due to steric repulsive interactions with the adsorbed surfactant heads. Furthermore, it is assumed that the charges of the adsorbed surfactant molecules that form the monolayer are contained in multiple charge layers. For example, in the case of a single

zwitterionic surfactant species, there are two charge layers corresponding to the positive and negative charges associated with the dipolar moiety. This is to be contrasted with the single charge layer used in the original Gouy-Chapman treatment to model the adsorption of a single ionic surfactant species.[57]

The theoretical approach presented in this chapter requires the specification of four molecular characteristics for each surfactant species present in the solution. These include: (i) the number of carbons in the surfactant hydrocarbon tail, (ii) the molecular cross-sectional area of the surfactant hydrophilic head, (iii) the valence and position of each charged group in the surfactant head, and (iv) the distance of closest approach between the centers of charge of an adsorbed surfactant molecule and its counterion. Characteristics (i), (ii), and (iii) can be determined from the known molecular structure of the surfactant hydrophobic tail and hydrophilic head, while the determination of characteristic (iv) also requires knowing the chemical structure and size of the counterion, including hydration. Note that requirement (iv) does not apply in the case of zwitterionic surfactants, and requirements (iii) and (iv) do not apply in the case of nonionic surfactants. In addition, the difference in the standard-state chemical potentials of a surfactant molecule in the monolayer and in the bulk solution is needed for each surfactant species, which can be determined from one surface tension measurement for each single surfactant species present in the solution.

The remainder of the chapter is organized as follows. The theory of adsorption at the air-aqueous solution interface for nonionic, ionic, and zwitterionic surfactants below the critical micelle concentration of the surfactant solution is presented in Section 3.2. This theory is then utilized in Section 3.3 to predict the surface tension and surface concentration and composition of several single as well as mixed surfactant systems, and these predictions are compared with available experimental measurements from the literature. The surfactant systems examined include: (i) single surfactant aqueous solutions of dodecyl maltoside (C_{12}Maltoside), dodecyl betaine (C_{12}Betaine), and sodium dodecyl sulfate (SDS), (ii) binary surfactant aqueous solutions of C_{12}Maltoside-C_{12}Betaine and C_{12}Betaine-SDS, and (iii) a ternary surfactant aqueous solution of C_{12}Maltoside-C_{12}Betaine-SDS. Finally, concluding remarks are

presented in Section 3.4.

3.2 Theory

3.2.1 The Gibbs Interfacial Model and Theoretical Assumptions

The Gibbs interfacial model forms the basis of our molecular-thermodynamic treatment.[14] Specifically, a two-dimensional, planar Gibbs dividing surface is chosen within the actual three-dimensional interfacial region at a position where the Gibbs surface excess number of solvent (water) molecules, N_{w}^{σ}, vanishes. Recall that the Gibbs surface excess number of molecules of type i, N_i^{σ}, is defined as follows:

$$\frac{N_i^{\sigma}}{\mathrm{A}} \equiv \Gamma_i \equiv \int_{-\infty}^{0} [n_i(x) - n_i^{\mathrm{v}}]\mathrm{d}x + \int_{0}^{\infty} [n_i(x) - n_i^{\mathrm{w}}]\mathrm{d}x \tag{3.1}$$

where A is the area of the planar Gibbs dividing interface, Γ_i is the surface excess number density of molecules of type i (referred to hereafter as the surface concentration of molecules of type i), x is the distance perpendicular to the interface, such that the aqueous phase lies on the side of positive x, $n_i(x)$ is the number density of molecules of type i located at position x, $n_i^{\mathrm{w}}$is the bulk aqueous number density of molecules of type i (limiting value of $n_i(x)$ as $x \to \infty$), and n_i^{v} is the bulk vapor number density of molecules of type i (limiting value of $n_i(x)$ as $x \to -\infty$).

As was discussed in more detail in Section 2.2, it is assumed that the adsorbed surfactant molecules form a monolayer which is positioned at the Gibbs dividing surface ($x = 0$). The first integral on the right-hand side of Eq. (3.1) can be neglected since on the vapor side of the monolayer ($x < 0$), both the local number density, $n_i(x)$, and the bulk vapor number density, n_i^{v}, vanish because the surfactant molecules are assumed to be non-volatile.

When surfactants containing a net charge (ionic surfactants) are present in the solution, an electrostatic diffuse layer is formed in the aqueous region near the mono-

layer where thermal diffusion is balanced by the long-range electrostatic interactions between the ionic species in the solution and the charged monolayer (see Section 2.2.2). In the electrostatic treatment presented here, it is assumed that zwitterionic surfactants, which posses no net charge, do not contribute to the formation of a diffuse region. In other words, it is assumed that the concentration of zwitterionic surfactants is uniform throughout the aqueous region extending from the Stern layer to infinity. This is reasonable because the local electric field generated in the aqueous region by the ionic surfactants adsorbed in the monolayer interacts much more strongly with other ionic species (ionic surfactants or counterions) than with the zwitterionic surfactants. In addition, if only surfactants possessing no net charge are present in the solution (for example, nonionic and zwitterionic surfactants, as well as their mixtures), then no local electric field, and therefore, no diffuse layer, is generated in the aqueous region when these surfactants adsorb at the monolayer (see Section 3.2.3.2 for a more detailed explanation).

In modeling surfactant electrostatic effects, it is assumed hereafter that the charged surfactant molecules and their counterions are fully dissociated. In other words, although the charged surfactants and their inorganic counterions interact through attractive Coulombic forces, it is assumed that they do not remain bound together as a single entity. This is expected to be valid for organic salts, such as SDS considered here, but may not be valid for organic fatty acids at low pH where a certain fraction of the fatty acids may remain undissociated. Furthermore, it is also assumed that there is no binding of ions (including H^+ or OH^-) to the charged groups of the zwitterionic surfactants. This last assumption may not be valid at very high or very low pH's depending on the surfactant. Our description treats all the ions in the bulk solution as point charges having no physical excluded volume, except for a minimum distance of closest approach (the so-called Stern layer described below). In addition, the diffuse region is treated as having a uniform, "smeared" three-dimensional local charge density, and the ions are assumed to interact through a structureless solvent having a uniform dielectric constant. The assumptions that: (i) the ions in the diffuse region can be treated as point ions, and (ii) the dielectric constant is uniform, are

discussed further in Appendix A.

Each charge-containing surfactant present in the monolayer is modeled as having an electrostatic charge (or charges) located at particular position(s) on the surfactant head. For example, an anionic or cationic surfactant has a single charge, and a zwitterionic surfactant has two charges. Note that, in principle, the theory presented here can be applied to model surfactants that contain any number of charge groups. It is assumed that the discrete charges on the heads of the adsorbed surfactant molecules can be smeared in the two directions parallel to the interface, forming a set of L two-dimensional charge layers, where L is equal to the sum of the number of charge groups on each of the surfactant molecules present in the monolayer (see Figure 3-1 for an illustration). For example, if only one ionic surfactant species is present, then there is only one charge layer, which when combined with the diffuse region, forms the familiar electrostatic *double layer*.[57] If a binary mixture comprising an ionic and a zwitterionic surfactant is present, then there are three charge layers within the monolayer (as depicted schematically in Figure 3-1). As discussed in Section 3.1, a Stern layer (that is, a region between the last charge layer (layer L) and the diffuse region where counterions are excluded by steric repulsive interactions with the surfactant molecules adsorbed in the monolayer.[32]) is also included (see Figure 3-1). The position of the Stern layer is approximated here by the distance that the longest surfactant head extends into the aqueous region plus the radius of the counterion (see Figure 3-1). Note that for the surfactant mixtures considered in this chapter, the surfactant heads are quite similar in length, and the resulting monolayers are compact (see Section 3.4). Note also that if one considered a surfactant mixture containing a small amount of a surfactant having a relatively long head, then one may need to assume a smaller effective Stern layer thickness. In addition, one could also treat multiple counterion types having different sizes (leading to multiple Stern layer thicknesses) by generalizing the equations developed in this chapter, and then solving them numerically. However, such an analysis is not necessary here, with the equations presented below leading to a closed-form analytical equation for the surface pressure (see Section 3.2.3).

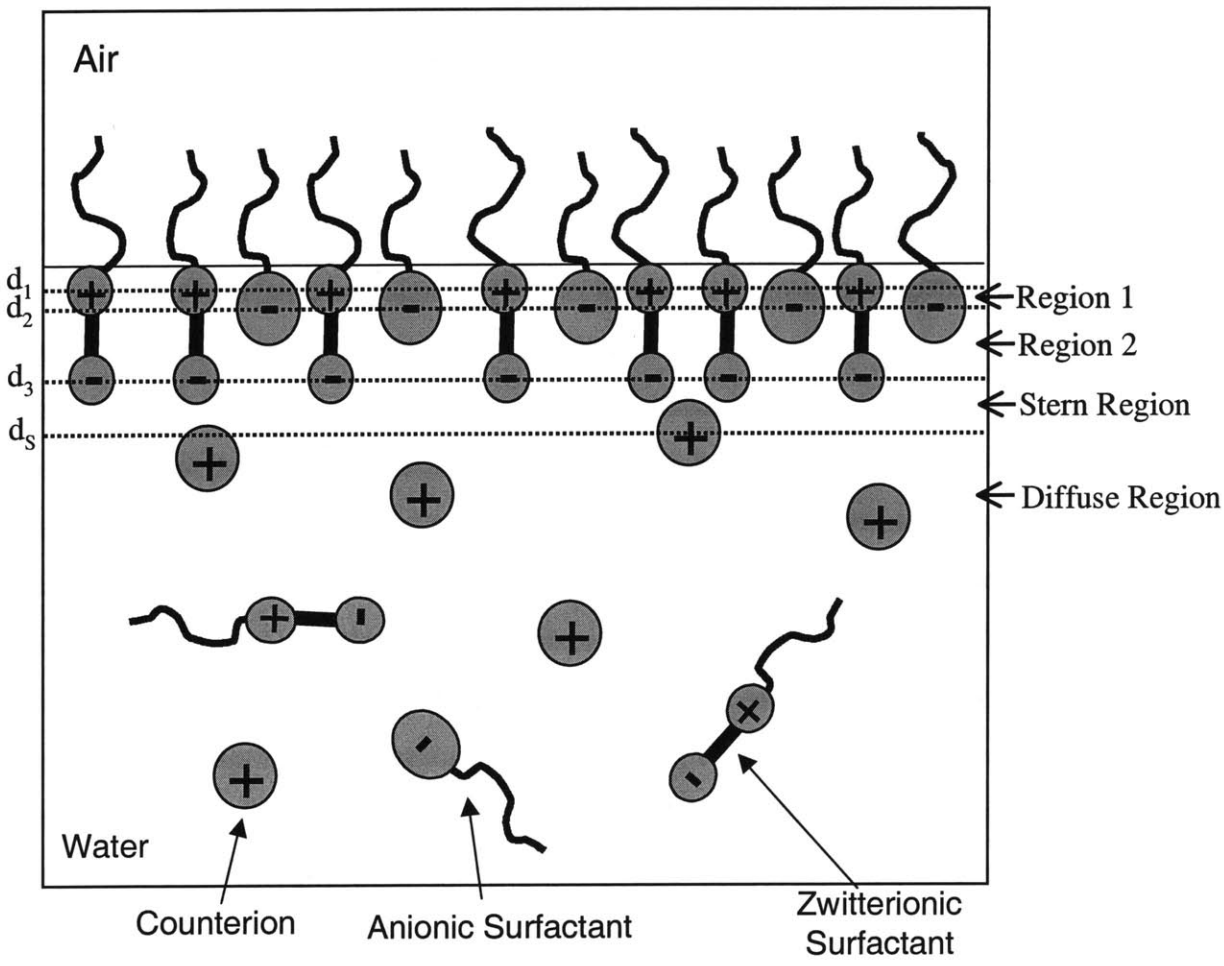

Figure 3-1: Schematic illustration of the adsorption of a zwitterionic and a monovalent anionic surfactant from an aqueous solution at the air-solution interface. Note that, in this case, there are three, two-dimensional charge layers (Layers 1, 2, and 3, corresponding to the positive charge on the zwitterionic head, the negative charge on the anionic head, and the negative charge on the zwitterionic head, respectively); two regions between the three charge layers (Regions 1 and 2); a Stern Region; and a Diffuse Region.

In the context of the diffuse layer model presented here, two different quantities related to the surface excess number of ions of type i can be defined: η_i, the number of molecules of type i actually adsorbed in the monolayer, and λ_i, the excess number of molecules of type i in the diffuse region, as described in detail by Hachisu.[42] Specifically, η_i and λ_i can be expressed as follows:

$$\frac{\eta_i}{A} \equiv \lim_{\varepsilon \to 0} \int_{-\varepsilon}^{+\varepsilon} (n_i(x) - n_i^{\mathrm{w}}) \mathrm{d}x = \lim_{\varepsilon \to 0} \int_{-\varepsilon}^{+\varepsilon} n_i(x)\, \mathrm{d}x \tag{3.2}$$

and

$$\frac{\lambda_i}{A} \equiv \lim_{\varepsilon \to 0} \int_{\varepsilon}^{\infty} (n_i(x) - n_i^{\mathrm{w}}) \mathrm{d}x \tag{3.3}$$

By combining Eqs. (3.1)-(3.3), one finds that, in general,

$$N_i^{\sigma} = \eta_i + \lambda_i \tag{3.4}$$

However, as stated above, for a surfactant having no net charge (for example, a non-ionic or a zwitterionic surfactant), there are no net Coulombic interactions between the charged monolayer and the surfactant molecules in the bulk solution. As a result, the local surfactant number density everywhere in the aqueous region, $n_i(x > 0)$, is equal to the bulk surfactant number density, $\mathrm{n}_i^{\mathrm{w}}$, which leads to $\lambda_i = 0$ in Eq. (3.3). In that case, Eq. (3.4) indicates that:

$$N_i^{\sigma} = \eta_i \tag{3.5}$$

For an ionic surfactant, λ_i does not vanish, but as discussed in Section 2.2.2, $\lambda_i << \eta_i$, and, to a good approximation, one still obtains:

$$N_i^{\sigma} \approx \eta_i \tag{3.6}$$

In our description, it is further assumed that the counterions do no adsorb directly

in the monolayer. Accordingly, for the counterions, $\eta_i = 0$, leading to:

$$N_i^{\sigma} = \lambda_i \tag{3.7}$$

3.2.2 Notation Conventions

In the analysis presented below, the following notation conventions will be used. The various charge layers comprising the monolayer, described above, will be numbered from 1 to L, such that layer 1 is closest to the air side of the air-solution interface, with the corresponding positions of each layer denoted as d_1, d_2,...,d_L (see Figure 3-1 for an example when $L = 3$). The regions between the charge layers will be numbered from 1 to $L - 1$ such that region 1 is between charge layer 1 and charge layer 2, etc. The subscript S will refer to the Stern region, and the subscript D will refer to the diffuse region. In addition, Greek letter subscripts will be utilized to index the various charge layers and the corresponding inter-charge layer regions. For example, d_ϕ will denote the position of charge layer ϕ, σ_ϕ will denote the charge density of charge layer ϕ, and $\sum_{\phi=1}^{L}$ will denote the summation over charge layers 1 to L. In addition, the symbol ζ_i^ϕ will denote the valence of surfactant molecules of type i located at layer ϕ. For example, a zwitterionic surfactant of type i with a positive charge at the first layer and a negative charge at the third layer will be characterized by $\zeta_i^1 = 1$, $\zeta_i^2 = 0$, and $\zeta_i^3 = -1$. Accordingly, using this notation, it follows that the charge density of charge layer, ϕ, is given by:

$$\sigma_\phi = \sum_{i=1}^{n} e\zeta_i^\phi \eta_i \Big/ A \tag{3.8}$$

where e is the proton charge and A is the area of the monolayer. Note also that using this notation, the valence of surfactant molecules of type i, z_i, is given by:

$$z_i = \sum_{\phi=1}^{L} \zeta_i^\phi \tag{3.9}$$

As expected, Eq. (3.9) indicates that $z_i = 0$ for zwitterionic surfactants. Although the theoretical analysis presented in this section can be applied to any number of

surfactant species, each containing any number of charge groups, Section 3.3 will focus on a few specific cases corresponding to the surfactant systems of interest in this chapter.

To simplify the presentation that follows, a different notation will be used to represent the electrostatic potential in the various regions of interest. Specifically, $\Psi_\phi(x)$ will denote the electrostatic potential in the ϕ^{th} inter-charge layer region ($\mathrm{d}_\phi \leq x \leq \mathrm{d}_{\phi+1}$), $\Psi_S(x)$ will denote the electrostatic potential in the Stern region ($\mathrm{d}_L \leq x \leq \mathrm{d}_S$), and $\Psi_D(x)$ will denote the electrostatic potential in the diffuse region ($x \geq \mathrm{d}_S$). Accordingly, the total electrostatic potential function, $\Psi(x)$, is given by:

$$\Psi(x) = \begin{cases} \Psi_\phi(x), & \text{for} \quad \mathrm{d}_\phi \leq x \leq \mathrm{d}_{\phi+1} \\ \Psi_S(x), & \text{for} \quad \mathrm{d}_L \leq x \leq \mathrm{d}_S \\ \Psi_D(x), & \text{for} \quad x \geq \mathrm{d}_S \end{cases} \tag{3.10}$$

3.2.3 Calculation of the Surface Pressure

3.2.3.1 Calculation of the Non-Electrostatic Surface Pressure

The effect of electrostatic interactions on the surface pressure, $\Pi = \sigma_0 - \sigma$, where σ_0 is the surface tension of the pure solvent (water, for which the experimental value of 72dyn/cm at 25°C is adopted[14]), and σ is the surface tension in the presence of the surfactant monolayer, is accounted for here by incorporating it as an additive contribution.[28,14] Specifically,

$$\Pi = \Pi_{\mathrm{NI}} + \Pi_{\mathrm{elec}} \tag{3.11}$$

where Π_{NI} is the contribution to the surface pressure resulting from all non-electrostatic interactions, and Π_{elec} is the contribution to the surface pressure arising from the electrostatic interactions. Equation (3.11) assumes that the electrostatic interactions can be decoupled from all other interactions, an assumption that may break down in the case of very highly-charged interfaces for which electrostatically-induced long-range correlations may develop.

As has been described in Chapter 2,[12] the non-electrostatic contribution to the

surface pressure, Π_{NI}, which includes repulsive hard-disk and attractive van der Waals interactions, can be modeled as follows:

$$\Pi_{NI} = k_B T \left\{ \frac{\sum_{i=1}^{n} \eta_i}{A - \sum_{i=1}^{n} \eta_i a_i} + \frac{\pi \left(\sum_{i=1}^{n} \eta_i r_i \right)^2}{\left(A - \sum_{i=1}^{n} \eta_i a_i \right)^2} + \sum_{ij=1}^{n} B_{ij} \frac{\eta_i \eta_j}{A^2} \right\} \tag{3.12}$$

where k_B is the Boltzmann constant, T is the absolute temperature, r_i and a_i are the hard-disk radius and area of surfactant molecules of type i, respectively, and B_{ij} is the second-order virial coefficient corresponding to surfactant molecules of type i and j. In Eq. (3.12), $\sum_{i=1}^{n}$ denotes summation over all the surfactant species present at the interface, and $\sum_{ij=1}^{n}$ denotes summation over all possible pairs of surfactant species, while avoiding double counting. Note that in the development of this non-electrostatic model, steric interactions are assumed to operate on a single plane. In other words, the surfactant molecules are treated as two-dimensional disks, rather than as more complex three-dimensional structures. This approximation is made in order to develop a simplified working model, and was previously shown to yield good results.[12]

3.2.3.2 Calculation of the Electrostatic Potential

Next, the electrostatic potential, $\Psi(x)$, and the electrostatic contribution to the surface pressure, Π_{elec}, are calculated. As will be shown in detail below, this is accomplished by first determining the electrostatic potential corresponding to the various inter-charge layer regions comprising the monolayer, $\Psi_\phi(x)$ where $\phi = 1$ to $L - 1$, as well as the electrostatic potential corresponding to the Stern and the diffuse regions, $\Psi_S(x)$ and $\Psi_D(x)$, respectively, by solving the governing electrostatic equations, along with the appropriate two boundary conditions at each charge layer (which are based on the continuity of the electrostatic potential and the discontinuity of the electric field across a charged two-dimensional surface).[59] Once the electrostatic potential, $\Psi(x)$, is known everywhere [see Eq. (3.10)], the electrostatic contribution to the sur-

face pressure, Π_{elec}, can be calculated using the method of Hachisu.[42] *Recall that for an aqueous solution consisting solely of surfactants having no net charge (for example, nonionic or zwitterionic surfactants), there are no diffuse or Stern regions.*

Since it has been assumed that no counterions or coions can penetrate into the monolayer (that is, into the regions between the charge layers created by the adsorbed charge-containing surfactant molecules), the charge densities in the inter-charge layer regions all vanish. As a result, the electrostatic potential, $\Psi_\phi(x)$ with $\phi = 1$ to $L-1$, is governed by the Laplace equation. Specifically,

$$\frac{d^2\Psi_\phi}{dx^2} = 0 \tag{3.13}$$

Furthermore, since it has been assumed that the electrostatic charge on the various charge layers can be smeared in the direction parallel to the interface, thus forming a uniform, two-dimensional flat charged surface, the gradient of the electrostatic potential in inter-charge layer region, ϕ, and the gradient of the electrostatic potential in the adjacent inter-charge layer region, $\phi+1$, exhibit a discontinuity at their common boundary located at $x = d_{\phi+1}$, given by:[59]

$$\varepsilon_\phi \left.\frac{d\Psi_\phi}{dx}\right|_{d_{\phi+1}} - \varepsilon_{\phi+1} \left.\frac{d\Psi_{\phi+1}}{dx}\right|_{d_{\phi+1}} = 4\pi\sigma_{\phi+1} \tag{3.14}$$

where ε_ϕ ($\varepsilon_{\phi+1}$) is the dielectric constant in inter-charge layer region ϕ ($\phi+1$), whose value will be discussed in detail in Section 3.3, and $\sigma_{\phi+1}$ is the charge density on charge layer $\phi+1$. In addition, the electrostatic potentials are required to be continuous across each charge layer, that is,

$$\Psi_\phi(d_{\phi+1}) = \Psi_{\phi+1}(d_{\phi+1}) \tag{3.15}$$

Note that Eqs. (3.14) and (3.15) each represents a set of $(L-2)$ equations, ranging from $\phi = 1$ through $\phi = L-2$ (with the L^{th} charge layer, which forms the boundary between inter-charge layer region $L-1$ and the Stern region, to be discussed below).

In the Stern region, that is, in the region between the last charge layer of the

monolayer (layer L, located at d_L) and the closest approach distance of the center of charge of the counterions (located at d_S), the charge density also vanishes due to steric repulsions associated with the Stern region. Therefore, the behavior of the electrostatic potential in the Stern region, Ψ_S, is also governed by the Laplace equation, that is, by:

$$\frac{d^2\Psi_s}{dx^2} = 0 \tag{3.16}$$

Similar to Eqs. (3.14) and (3.15), the following two boundary conditions must be satisfied between the (L-1)th inter-charge layer region and the Stern region at their common boundary located at x=d_L:

$$\varepsilon_{L-1} \left.\frac{d\Psi_{L-1}}{dx}\right|_{d_L} - \varepsilon_s \left.\frac{d\Psi_s}{dx}\right|_{d_L} = 4\pi\sigma_L \tag{3.17}$$

and

$$\Psi_{L-1}(d_L) = \Psi_s(d_L) \tag{3.18}$$

where ε_s is the dielectric constant in the Stern region, whose value will be discussed in detail in Section 3.3. Finally, under the assumptions discussed above that: (i) the diffuse region can be treated by smearing out the charges of all the ions into a uniform charge density that varies with x, (ii) the ions can be treated as point ions without any physical size, and (iii) the solvent has a uniform dielectric constant, ε_D (assumed to be that of pure water), one obtains the well-known Poisson-Boltzmann equation which governs the behavior of the electrostatic potential in the diffuse region, Ψ_D. Specifically,[28,14]

$$\frac{d^2\Psi_D}{dx^2} = \frac{-4\pi\rho_{elec}}{\varepsilon_D} = \frac{-4\pi e}{\varepsilon_D}\sum_{i=1}^{n} z_i n_i(x) = \frac{-4\pi e}{\varepsilon_D}\sum_{i=1}^{n} z_i n_i^w \exp\left(\frac{-z_i e\Psi_D(x)}{k_B T}\right) \tag{3.19}$$

where ρ_{elec} is the charge density in the diffuse region, $n_i(x)$ is the number density of molecules of type i, and n_i^w is the bulk number density of molecules of type i (limit of $n_i(x)$ as $x \to \infty$). Similar to Eqs. (3.14) and (3.15), with the difference that there is no charge on the layer that separates the Stern region from the diffuse region (recall

that it has been assumed that the counterions do not bind or physically adsorb to the monolayer), the following two boundary conditions must be satisfied between the Stern region and the diffuse region at their common boundary located at $x = \mathrm{d}_S$:

$$\varepsilon_s \left.\frac{\mathrm{d}\Psi_s}{\mathrm{d}x}\right|_{d_s} = \varepsilon_{\mathrm{D}} \left.\frac{\mathrm{d}\Psi_{\mathrm{D}}}{\mathrm{d}x}\right|_{d_s} \tag{3.20}$$

and

$$\Psi_{\mathrm{s}}\left(\mathrm{d_s}\right) = \Psi_{\mathrm{D}}\left(\mathrm{d}_s\right) \tag{3.21}$$

Finally, due to overall electroneutrality of the system, the gradient of the electrostatic potential must vanish far away from the charged monolayer ($x \to \infty$). Specifically,[14]

$$\left.\frac{\mathrm{d}\Psi_{\mathrm{D}}}{\mathrm{d}x}\right|_{x\to\infty} = 0 \tag{3.22}$$

The zero point of the electrostatic potential has been selected to be at infinity, that is,

$$\Psi_{\mathrm{D}}\left(x \to \infty\right) = 0 \tag{3.23}$$

There are now $L+1$ second-order ordinary differential equations {the set of $(L-1)$ equations given in Eq. (3.13) [corresponding to the $(L-1)$ inter-charge layer regions], as well as Eq. (3.16) [corresponding to the Stern region], and Eq. (3.19) [corresponding to the diffuse region]}. To solve these equations, there are also the necessary $2(L+1)$ boundary conditions {the set of $(L-2)$ equations given in Eq. (3.14), the set of $(L-2)$ equations given in Eq. (3.15), as well as Eqs. (3.17), (3.18), and (3.20)–(3.23)}.

Integrating Eq. (3.19) once from $x = \mathrm{d}_S$ to infinity, along with Eq. (3.22) as a boundary condition, the following expression is obtained:

$$\left.\frac{\mathrm{d}\Psi_{\mathrm{D}}}{\mathrm{d}x}\right|_{\mathrm{d_s}} - \left.\frac{\mathrm{d}\Psi_{\mathrm{D}}}{\mathrm{d}x}\right|_{\infty} = \left.\frac{\mathrm{d}\Psi_{\mathrm{D}}}{\mathrm{d}x}\right|_{\mathrm{d_s}} = \int_{\mathrm{d_s}}^{\infty} \frac{4\pi\rho_{\mathrm{elec}}}{\varepsilon_{\mathrm{D}}}\mathrm{d}x = \frac{4\pi}{\varepsilon_{\mathrm{D}}}\sum_{i=1}^{n}\left(\mathrm{ez}_i\int_{\mathrm{d_s}}^{\infty} n_i\left(x\right)\mathrm{d}x\right)$$

$$= \frac{4\pi}{\varepsilon_{\mathrm{D}}}\sum_{i=1}^{n}\frac{\mathrm{ez}_i\lambda_i}{A} \tag{3.24}$$

Note that in deriving Eq. (3.24), Eq. (3.3) was utilized where the lower limit of integration, $\varepsilon \to 0$, has been replaced by d_S due to the presence of the Stern region, as well as the fact that $\sum_{i=1}^{n} \mathrm{e} z_i n_i^{\mathrm{w}} = 0$ due to overall electroneutrality in the bulk solution.

Equation (3.24) can be rewritten in terms of the monolayer number densities of adsorbed surfactant species, η_i, by exploiting the electroneutrality of the entire surface phase[34] which requires that $\sum_i e z_i N_i^{\sigma}/A = \sum_i e z_i \lambda_i + \sum_i e z_i \eta_i = 0$. Specifically, one obtains:

$$\left.\frac{\mathrm{d}\Psi_{\mathrm{D}}}{\mathrm{d}x}\right|_{\mathrm{d_s}} = \frac{-4\pi}{\varepsilon_{\mathrm{D}}} \sum_{i=1}^{n} \frac{\mathrm{e} z_i \eta_i}{A} \tag{3.25}$$

Note that the governing equation for the electrostatic potential in the diffuse region, Eq. (3.19), and the two boundary conditions, Eqs. (3.23) and (3.25), are the same as those obtained when ionic surfactants are adsorbed in a single charge layer, the case considered in Chapter 2. In particular, the resulting expression for the electrostatic potential at the boundary between the diffuse and the Stern regions, located at $x = \mathrm{d}_s$, $\Psi_D(\mathrm{d}_s)$, is the same as that corresponding to the single charge layer case (see Section 2.2.2 for a detailed derivation). In particular, when only monovalent ions ($\mathrm{z}_i = \pm 1$) are considered, one obtains:

$$\Psi_{\mathrm{D}}\left(\mathrm{d}_s\right) = \frac{2\mathrm{k_B}T}{\mathrm{e}} \ln\left[\frac{2\pi \mathrm{e}\hat{\sigma}}{\varepsilon_{\mathrm{D}}\kappa \mathrm{k_B}T} + \sqrt{1 + \left(\frac{2\pi \mathrm{e}\hat{\sigma}}{\varepsilon_D \kappa \mathrm{k_B}T}\right)^2}\right] \tag{3.26}$$

where $\hat{\sigma} = \sum_i e z_i \eta_i / A = \sum_{\phi=1}^{L} \sigma_\phi$ is the total charge density of the monolayer and $\kappa^{-1} \equiv \sqrt{\mathrm{k_B}T\varepsilon_{\mathrm{D}}/(8\pi n^{\mathrm{w}} \mathrm{e}^2)}$ (where n^{w} is the bulk number density of the monovalent anions or cations) is the Debye-Hückel screening length. Note that multivalent ions were considered in Chapter 2 and in Refs. 60 and 61, and the corresponding solution of the electrostatic potential in the diffuse region could be used in place of Eq. (3.26) to treat solutions containing multivalent ions. However, this is beyond the scope of this chapter since only solutions containing monovalent ions are considered.

In the Stern region, integrating Eq. (3.16) once yields a constant value of $\mathrm{d}\Psi_s/\mathrm{d}x$,

which when combined with Eqs. (3.20) and (3.25) yields:

$$\frac{d\Psi_s}{dx} = \frac{-4\pi}{\varepsilon_s}\sum_{i=1}^{n}\frac{ez_i\eta_i}{A} = \frac{-4\pi}{\varepsilon_s}\hat{\sigma} \tag{3.27}$$

Integrating Eq. (3.27) over the Stern region ($d_L \leq x \leq d_S$), in combination with Eqs. (3.21) and (3.26), yields $\Psi_S(d_L)$ {or $\Psi_{L-1}(d_L)$, since the electrostatic potential is continuous across the boundary (at $x = d_L$) between the $(L-1)$ inter-charge layer region and the Stern region}. Specifically, one obtains:

$$\Psi_s(d_L) = \Psi_{L-1}(d_L) \tag{3.28}$$

$$= (d_s - d_L)\frac{4\pi}{\varepsilon_s}\hat{\sigma} + \frac{2k_BT}{e}\ln\left[\frac{2\pi e\hat{\sigma}}{\varepsilon_D\kappa k_BT} + \sqrt{1+\left(\frac{2\pi e\hat{\sigma}}{\varepsilon_D\kappa k_BT}\right)^2}\right]$$

Equation (3.28) will be utilized below for the evaluation of the various inter-charge layer electrostatic potentials, $\Psi_\phi(x)$. *Note that if only surfactants with no net charge are considered (for example, nonionic or zwitterionic), then $\hat{\sigma} = 0$ in Eqs. (3.26) and (3.28), which results in $\Psi_D(d_S)$=0 and $\Psi_S(d_L)$=$\Psi_{L-1}(d_L)$=0, respectively.*

Turning next to the calculation of the various inter-charge layer electrostatic potentials, $\Psi_\phi(x)$, [with $d_\phi \leq x \leq d_{\phi+1}$ for $1 \leq \phi \leq (L-1)$], Eq. (3.13) is integrated once (for each ϕ from 1 to $L-1$) which results in a constant value of $d\Psi_\phi/dx$ within each region. To determine the values of these various constants, one could start with Eq. (3.17) to determine $d\Psi_\phi/dx$ for $\phi = L-1$ with $(d\Psi_S/dx)|_{d_L}$ given in Eq. (3.27). Then, by utilizing Eq. (3.14) successively at each charge layer, one can determine the value of $d\Psi_\phi/dx$ in decreasing order from $\phi = (L-2)$ to $\phi = 1$. Alternatively, one could start with $d\Psi/dx = 0$ for $x < d_1$ (due to the electroneutrality of the system), and then utilize Eq. (3.14) successively to determine $d\Psi_\phi/dx$ in increasing order from

$\phi = 1$ to $\phi = L-1$. With either method, the following general expression is obtained:

$$\frac{\mathrm{d}\Psi_\phi}{\mathrm{d}x} = \frac{-4\pi}{\varepsilon_\phi}\sum_{\omega=1}^{\phi}\sigma_\omega \tag{3.29}$$

The inter-charge layer electrostatic potential at any of the charge layers ($x = \mathrm{d}_\phi$) can be related to the Stern layer potential, $\Psi_S(\mathrm{d}_L)$, by integrating Eq. (3.29) successively for each charge layer from $\phi = (L-1)$ to $\phi = 1$, and applying the boundary conditions given in Eq. (3.18) for $\phi = (L-1)$ and Eq. (3.15) for $\phi = (L-2)$ to $\phi = 1$. This yields:

$$\begin{aligned}\Psi(\mathrm{d}_\phi) &= \sum_{\omega=\phi}^{L-1}\left\{(\mathrm{d}_{\omega+1}-\mathrm{d}_\omega)\frac{4\pi}{\varepsilon_\omega}\sum_{\gamma=1}^{\omega}\sigma_\gamma\right\} + \Psi(\mathrm{d}_L) \\ &= \sum_{\omega=\phi}^{L-1}\left\{(\mathrm{d}_{\omega+1}-\mathrm{d}_\omega)\frac{4\pi}{\varepsilon_\omega}\sum_{\gamma=1}^{\omega}\sigma_\gamma\right\} + (\mathrm{d}_s-\mathrm{d}_L)\frac{4\pi}{\varepsilon_\mathrm{s}}\hat{\sigma} \\ &+ \frac{2\mathrm{k_B}T}{\mathrm{e}}\ln\left[\frac{2\pi\mathrm{e}\hat{\sigma}}{\varepsilon_\mathrm{D}\kappa\mathrm{k_B}T} + \sqrt{1+\left(\frac{2\pi\mathrm{e}\hat{\sigma}}{\varepsilon_\mathrm{D}\kappa\mathrm{k_B}T}\right)^2}\right]\end{aligned} \tag{3.30}$$

where Eq. (3.30) uses the definition of the total electrostatic potential, $\Psi(x)$, given in Eq. (3.10).

3.2.3.3 Calculation of the Electrostatic Surface Pressure

To calculate the electrostatic surface pressure, the method introduced by Hachisu[42] is generalized to allow for the presence of multiple charge layers. Using this method, the electrostatic surface pressure, Π_{elec}, can be written as follows:

$$\Pi_{\mathrm{elec}} = \int_{-\infty}^{\infty} P_{\mathrm{elec}}(x)\,\mathrm{d}x + \int_{-\infty}^{\infty} P_{\mathrm{osm}}(x)\,\mathrm{d}x \tag{3.31}$$

where $P_{osm}(x)$ is the osmotic pressure resulting from the excess of ions in the diffuse region, and P_{elec} is the electrostatic pressure given by:

$$P_{\text{elec}}(x) = \frac{\varepsilon}{8\pi} E^2(x) = \frac{\varepsilon}{8\pi}\left(\frac{\mathrm{d}\Psi(x)}{\mathrm{d}x}\right)^2 \tag{3.32}$$

where $E = -\mathrm{d}\Psi/\mathrm{d}x$ is the local electric field. The first integrand in Eq. (3.31) vanishes for $x < \mathrm{d}_1$ (recall that $E(x) = 0$ for $x < \mathrm{d}_1$). Accordingly, the first integral in Eq. (3.31) can be evaluated as a sum of integrals over each of the $(L-1)$ inter-charge layer regions, the Stern region, and the diffuse region. The second integrand in Eq. (3.31) vanishes for $x < \mathrm{d}_S$, and therefore, the second integral in Eq. (3.31) extends solely over the diffuse region (from $x = \mathrm{d}_S$ to ∞). With this in mind, Π_{elec} in Eq. (3.31) can be rewritten as follows:

$$\Pi_{\text{elec}} = \sum_{\phi=1}^{L-1} \int_{\mathrm{d}_\phi}^{\mathrm{d}_{\phi+1}} P_{\text{elec}}(x)\,\mathrm{d}x + \int_{\mathrm{d}_L}^{\mathrm{d}_s} P_{\text{elec}}(x)\,\mathrm{d}x + \int_{\mathrm{d}_s}^{\infty} P_{\text{elec}}(x)\,\mathrm{d}x + \int_{\mathrm{d}_s}^{\infty} P_{\text{osm}}(x)\mathrm{d}x \tag{3.33}$$

The last two terms in Eq. (3.33) were already calculated by Hachisu in Ref. 42. To evaluate the first two terms in Eq. (3.33), Eqs. (3.29) and (3.32) are utilized for the first term of Eqs. (3.27) and (3.32) is utilized for the second term. This calculation yields:

$$\Pi_{\text{elec}} = \sum_{\phi=1}^{L-1} \int_{d_\phi}^{d_{\phi+1}} \frac{\varepsilon_\phi}{8\pi}\left(\frac{4\pi}{\varepsilon_\phi}\sum_{\omega=1}^{\phi}\sigma_\omega\right)^2 \mathrm{d}x + \int_{d_L}^{d_s} \frac{\varepsilon_s}{8\pi}\left(\frac{4\pi}{\varepsilon_s}\frac{\sum_{i=1}^{n}\mathrm{e}z_i\eta_i}{A}\right)^2 \mathrm{d}x \tag{3.34}$$

$$+ \left(\frac{\varepsilon_D\kappa}{\pi}\right)\left(\frac{\mathrm{k_B}T}{\mathrm{e}}\right)^2\left[\sqrt{1+\left(\frac{2\pi\mathrm{e}}{\varepsilon_D\kappa\mathrm{k_B}T}\right)^2\left(\frac{\sum_{i=1}^{n}\mathrm{e}z_i\eta_i}{A}\right)^2}-1\right]$$

where the last term in Eq. (3.34) corresponds to the result of Hachisu.[42] By carrying out the integrations in Eq. (3.34), and using Eq. (3.8), the following expression for

Π_{elec} is obtained:

$$\Pi_{\text{elec}} = \sum_{\phi=1}^{L-1} \left\{ \frac{2\pi}{\varepsilon_\phi} \left(\sum_{\omega=1}^{\phi} \left(\sum_{i=1}^{n} \mathrm{e}\zeta_i^\omega \eta_i / A \right) \right)^2 (\mathrm{d}_{\phi+1} - \mathrm{d}_\phi) \right\} + \frac{2\pi}{\varepsilon_s} \left(\frac{\sum_{i=1}^{n} \mathrm{e}z_i\eta_i}{A} \right)^2 (\mathrm{d}_\mathrm{s} - \mathrm{d}_L)$$

$$+ \left(\frac{\varepsilon_D \kappa}{\pi} \right) \left(\frac{\mathrm{k_B}T}{\mathrm{e}} \right)^2 \left[\sqrt{1 + \left(\frac{2\pi \mathrm{e}}{\varepsilon_D \kappa \mathrm{k_B}T} \right)^2 \left(\frac{\sum_{i=1}^{n} \mathrm{e}z_i\eta_i}{A} \right)^2} - 1 \right] \tag{3.35}$$

Note that for the single ionic surfactant case where there is only one charge layer ($L = 1$), the first term in Eq. (3.35) vanishes, thus yielding the expression for Π_{elec} obtained in Section 2.2.2. If, in addition, the Stern layer is neglected (in which case $\mathrm{d}_L = \mathrm{d}_S$), then the second term in Eq. (3.35) also vanishes, leading to the well-known Davies expression for Π_{elec}.[28] If only surfactants having no net charge (for example, zwitterionic surfactants) are considered, then $\mathrm{z}_i = 0$ for all i and the last two terms in Eq. (3.35) vanish, reflecting the fact that there are no Stern or diffuse regions in this case. Finally, if only nonionic surfactant species are considered, then $\mathrm{z}_i = 0$ and $\zeta_i^\omega = 0$ for all i and ω, leading to $\Pi_{\text{elec}} = 0$ in Eq. (3.35) as expected in this case.

Equation (3.11) can now be utilized, along with Eqs. (3.12) and (3.35), to obtain the following expression for the surface equation of state, that is, for the surface pressure, Π, as a function of the temperature, T, the monolayer area, A, and the number of adsorbed surfactant molecules of each type, η_i, along with the various physical constants and molecular parameters characterizing the surfactants. Specifically,

$$\Pi = \mathrm{k_B}T \left\{ \frac{\sum_{i=1}^{n} \eta_i}{A - \sum_{i=1}^{n} \eta_i a_i} + \frac{\pi \left(\sum_{i=1}^{n} \eta_i \mathrm{r}_i \right)^2}{\left(A - \sum_{i=1}^{n} \eta_i a_i \right)^2} + \sum_{ij=1}^{n} B_{ij} \frac{\eta_i \eta_j}{A^2} \right\} + \tag{3.36}$$

$$+ \sum_{\phi=1}^{L-1} \left\{ \frac{2\pi}{\varepsilon_\phi} \left(\sum_{\omega=1}^{\phi} \left(\sum_{i=1}^{n} \mathrm{e}\zeta_i^{\omega}\eta_i/A \right) \right)^2 (\mathrm{d}_{\phi+1} - \mathrm{d}_\phi) \right\} + \frac{2\pi}{\varepsilon_s} \left(\frac{\sum_{i=1}^{n} \mathrm{e}z_i\eta_i}{A} \right)^2 (\mathrm{d}_s - \mathrm{d}_L)$$

$$+ \left(\frac{\varepsilon_D \kappa}{\pi} \right) \left(\frac{\mathrm{k_B}T}{\mathrm{e}} \right)^2 \left[\sqrt{1 + \left(\frac{2\pi \mathrm{e}}{\varepsilon_D \kappa \mathrm{k_B}T} \right)^2 \left(\frac{\sum_i \mathrm{e}z_i\eta_i}{A} \right)^2} - 1 \right]$$

Equation (3.36) can also be rewritten in intensive form as follows:

$$\Pi = \mathrm{k_B}T \left\{ \frac{1}{\alpha - \sum_{i=1}^{n} \xi_i a_i} + \frac{\pi \left(\sum_{i=1}^{n} \xi_i \mathrm{r}_i \right)^2}{\left(\alpha - \sum_{i=1}^{n} \xi_i a_i \right)^2} + \sum_{ij=1}^{n} B_{ij} \frac{\xi_i \xi_j}{\alpha^2} \right\} \tag{3.37}$$

$$+ \sum_{\phi=1}^{L-1} \left\{ \frac{2\pi}{\varepsilon_\phi} \left(\sum_{\omega=1}^{\phi} \left(\sum_{i=1}^{n} \mathrm{e}\zeta_i^{\omega}\xi_i/\alpha \right) \right)^2 (\mathrm{d}_{\phi+1} - \mathrm{d}_\phi) \right\} + \frac{2\pi}{\varepsilon_s} \left(\frac{\sum_{i=1}^{n} \mathrm{e}z_i\xi_i}{\alpha} \right)^2 (\mathrm{d}_s - \mathrm{d}_L)$$

$$+ \left(\frac{\varepsilon_D \kappa}{\pi} \right) \left(\frac{\mathrm{k_B}T}{\mathrm{e}} \right)^2 \left[\sqrt{1 + \left(\frac{2\pi \mathrm{e}}{\varepsilon_D \kappa \mathrm{k_B}T} \right)^2 \left(\frac{\sum_{i=1}^{n} \mathrm{e}z_i\xi_i}{\alpha} \right)^2} - 1 \right]$$

where $\alpha \equiv A \Big/ \sum_{i=1}^{n} \eta_i$ is the area per surfactant molecule in the monolayer, and $\xi_i \equiv \eta_i \Big/ \sum_{k=1}^{n} \eta_k$ is the monolayer mole fraction of surfactant molecules of type i. The first term in Eq. (3.37) is the contribution to the surface pressure, Π, from the non-electrostatic (that is, hard-disk and van der Waals) interactions, the second term is the contribution to Π associated with the inter-charge layer regions corresponding to the adsorbed charged surfactant molecules, the third term is the contribution to Π from the Stern region, and the last term is the contribution to Π from the diffuse region.

3.2.3.4 Calculation of the Surface Chemical Potential

As an illustration of the application of the theoretical framework developed so far, an aqueous solution containing only one monovalent ionic surfactant species (denoted by subscript s) and its oppositely-charged counterion (denoted by subscript c), along with an arbitrary number of surfactant species that have no net charge, including nonionic or zwitterionic surfactants is considered. The subscript N will be used hereafter to denote any one of these nonionic or zwitterionic surfactant species. Consideration is restricted to solutions that do not contain any added electrolyte. These restrictions simplify the mathematical analysis that follows, and allow for a description of the experimental surfactant solutions considered in Section 3.3. The analysis is also restricted to surfactant solutions below the critical micelle concentration (CMC). Although one could utilize a bulk thermodynamic theory of micellization to make predictions for surfactant solutions above the CMC, as was done in Chapter 2, the focus here will instead be on the interfacial properties at surfactant concentrations below the CMC. Note that this does not pose a serious limitation, since it is below the CMC that one observes the largest variation in the interfacial properties of the surfactant solution.

As was shown in detail in Section 2.2.2 and Ref. 12, the surface chemical potential of surfactant molecules of type N, μ_N^σ, which have a net electrostatic charge of zero, and are therefore characterized by $N_N^\sigma = \eta_N$ [see Eq. (3.5)], is given by:

$$\mu_N^\sigma = \frac{\partial}{\partial N_N^\sigma}\left(F^{\sigma,\mathrm{id}} - \int_\infty^A \left(\Pi - \Pi^{\mathrm{id}}\right) \mathrm{d}A\right)_{A,T,P,N_{i\neq N}^\sigma} \tag{3.38}$$

$$= \tilde{\mu}_N^{\sigma,0} + \mathrm{k_B}T\left(1 + \ln\left(\frac{\Pi^{\mathrm{id}}}{\Pi_0}\right) + \ln \xi_N\right) - \int_\infty^A \left(\frac{\partial\left(\Pi - \Pi^{\mathrm{id}}\right)}{\partial \eta_N}\right)_{A,T,P,N_{i\neq N}^\sigma} \mathrm{d}A$$

where $F^{\sigma,\mathrm{id}}$ is the ideal surface free energy given by:

$$F^{\sigma,\mathrm{id}} = \sum_{i=1}^{n} N_i^{\sigma} \left(\tilde{\mu}_i^{\sigma,0} + \mathrm{k}T \ln \left(\frac{\Pi^{\mathrm{id}}}{\Pi_0} \right) + \mathrm{k_B}T \ln x_i^{\sigma} \right) \tag{3.39}$$

and Π^{id} is the ideal surface pressure given by:

$$\Pi^{\mathrm{id}} = \mathrm{k_B}T \sum_{i=1}^{n} N_i^{\sigma}/A \tag{3.40}$$

and $\tilde{\mu}_N^{\sigma,0}$ is the standard-state surface chemical potential of surfactant molecules of type N at a reference pressure, Π_0. Note that the reference pressure is chosen arbitrarily to be $1 dyn/cm$, since *cgs* units are used throughout this thesis. Note also that the choice of the reference pressure will affect the numerical value of the standard-state surface chemical potential, but will not affect the final predicted surface tensions or surface concentrations and compositions.

Utilizing Eq. (3.36) for Π (with $\mathrm{z}_N = 0$) in Eq. (3.38) leads to the following expression for the surface chemical potential of an uncharged surfactant species:

$$\begin{aligned} \mu_N^{\sigma} \;=\; & \mu_N^{\sigma,0} + \mathrm{k_B}T \left\{ \ln \left(\frac{\xi_N}{\alpha - \sum_{i=1}^{n} \xi_i \mathrm{a}_i} \right) + \frac{\mathrm{a}_N + 2\pi \mathrm{r}_N \sum_{i=1}^{n} \xi_i \mathrm{r}_i}{\alpha - \sum_{i=1}^{n} \xi_i \mathrm{a}_i} \right. \\ & \left. + \frac{\pi \mathrm{a}_N \left(\sum_{i=1}^{n} \xi_i \mathrm{r}_i \right)^2}{\left(\alpha - \sum_{i=1}^{n} \xi_i \mathrm{a}_i \right)^2} + \frac{2}{\alpha} \sum_{i=1}^{n} B_{iN} \xi_i \right\} \\ & + \sum_{\phi=1}^{L-1} \mathrm{e}\zeta_N^{\phi} \left[\sum_{\omega=\phi}^{L-1} \left\{ (\mathrm{d}_{\omega+1} - \mathrm{d}_{\omega}) \frac{4\pi}{\varepsilon_{\omega}} \sum_{\gamma=1}^{\omega} \left(\sum_{i=1}^{n} \frac{\mathrm{e}\zeta_i^{\gamma} \xi_i}{\alpha} \right) \right\} \right] \end{aligned} \tag{3.41}$$

where $\mu_N^{\sigma,0} \equiv \tilde{\mu}_N^{\sigma,0} + k_B T \{1 + \ln (k_B T/\Pi_0)\}$ has been introduced for convenience. Note that for a nonionic surfactant, $\zeta_N^{\phi} = 0$ for all values of ϕ, and therefore, the

last term in Eq. (3.41), which results from the electrostatic charges on the surfactant molecules, vanishes. On the other hand, for a zwitterionic surfactant, $\zeta_N^\phi \neq 0$ for two values of ϕ, and consequently, the last term in Eq. (3.41) does not vanish. Note also that using Eq. (3.30), along with the fact that $z_N = \sum_{\phi=1}^{L} \zeta_N^\phi = 0$ for any uncharged surfactant species (see Eq. (3.9) with i replaced by N), the last term in Eq. (3.41), the electrostatic contribution to the surface chemical potential, can be written in a more compact form as $\sum_{\phi=1}^{L} e\zeta_N^\phi \Psi(d_\phi)$. However, a more detailed expression was used in Eq. (3.41) to show that, indeed, Eq. (3.41) yields an expression for the surface chemical potential in terms of the temperature, T, the monolayer area, A, and the number of surfactant molecules of each surfactant species adsorbed in the monolayer, $\{\eta_i\}$, along with the various physical constants and molecularly-based surfactant parameters.

For the ionic surfactant (s), one must consider the combined chemical potential of the electroneutral combination of the surfactant ion and its counterion (c), μ_{sc}^σ (see Section 2.2.2 for a detailed derivation). Specifically,

$$\mu_s^\sigma + \mu_c^\sigma \equiv \mu_{sc}^\sigma = \frac{\partial}{\partial N_s^\sigma}\left(F^{\sigma,\mathrm{id}} - \int_\infty^A (\Pi - \Pi^{\mathrm{id}})\, dA\right)_{A,T,P,N_{i\neq s,c}^\sigma} \tag{3.42}$$

$$= \tilde{\mu}_{sc}^{\sigma,0} + k_B T\left(1 + \ln\left(\frac{\Pi^{\mathrm{id}}}{\Pi_0}\right) + \ln \xi_s\right) - \int_\infty^A \left(\frac{\partial\left(\Pi - \Pi^{\mathrm{id}}\right)}{\partial \eta_s}\right) dA_{A,T,P,N_{i\neq N}^\sigma}$$

Similar to Eq. (3.41), utilizing Eq. (3.36) for Π in Eq. (3.42) leads to the following expression for the surface chemical potential of the ionic surfactant and its counterion, μ_{sc}^σ:

$$\mu_{sc}^\sigma = \mu_{sc}^{\sigma,0} + k_B T\left\{\ln\left(\frac{\xi_s}{\alpha - \sum_{i=1}^{n} \xi_i a_i}\right) + \frac{a_s + 2\pi r_s \sum_{i=1}^{n} \xi_i r_i}{\alpha - \sum_{i=1}^{n} \xi_i a_i} + \right. \tag{3.43}$$

$$+ \quad \frac{\pi a_s \left(\sum_{i=1}^{n} \xi_i r_i\right)^2}{\left(\alpha - \sum_{i=1}^{n} \xi_i a_i\right)^2} + \frac{2}{\alpha} \sum_{i=1}^{n} B_{si} \xi_i \Bigg\}$$

$$+ \quad \sum_{\phi=1}^{L-1} e\zeta_s^{\phi} \left[\sum_{\omega=\phi}^{L-1} \left\{ (d_{\omega+1} - d_{\omega}) \frac{4\pi}{\varepsilon_{\omega}} \sum_{\gamma=1}^{\omega} \left(\sum_{i=1}^{n} \frac{e\zeta_i^{\gamma} \xi_i}{\alpha} \right) \right\} \right] + (d_s - d_L) \frac{4\pi e z_s}{\varepsilon_s} \sum_{i=1}^{n} \frac{e z_i \xi_i}{\alpha}$$

$$+ \quad 2 z_s k_B T \ln \left(\frac{2\pi e \sum_{i=1}^{n} e z_i \xi_i}{\varepsilon_D \kappa k_B T \alpha} + \sqrt{1 + \left(\frac{2\pi e \sum_{i=1}^{n} e z_i \xi_i}{\varepsilon_D \kappa k_B T \alpha} \right)^2} \right)$$

Note that the last two terms in Eq. (3.43) represent the contributions from the Stern and the diffuse regions, respectively. In addition, note that as in Eq. (3.41), the last three terms in Eq. (3.43) (the electrostatic contribution to the surface chemical potential) can be written in a more compact form as $\sum_{\phi=1}^{L} e\zeta_s^{\phi} \Psi(d_{\phi})$. However, the more detailed expression given in Eq. (3.43) is preferred here to stress that it is indeed an expression for the surface chemical potential of the charged surfactant and its counterion in terms of the temperature, T, the monolayer area, A, and the number of surfactant molecules adsorbed in the monolayer, $\{\eta_i\}$, along with the various physical constants and molecularly-based surfactant parameters.

3.2.3.5 Thermodynamic Equilibrium between the Surface and the Bulk Phases

In general, the bulk, aqueous chemical potential of any solute (surfactant or counterion) molecule of type i, μ_i^w, can be determined using a bulk equation of state or free energy model. For surfactant solutions below the CMC, the solute concentrations are typically sufficiently dilute that the ideal solution model provides a good

approximation. In that case,

$$\mu_i^{\mathrm{w}} = \mu_i^{\mathrm{w},0} + \mathrm{k_B}T \ln(x_i) \approx \mu_i^{\mathrm{w},0} + \mathrm{k_B}T \ln\left(\frac{n_i^{\mathrm{w}}}{n_{\mathrm{w}}^{\mathrm{w}}}\right) \tag{3.44}$$

where $\mu_i^{\mathrm{w},0}$ is the bulk standard-state chemical potential of surfactant molecules of type i, and $x_i \equiv n_i^{\mathrm{w}} \Big/ \left(\sum_{j=1}^{n} n_j^{\mathrm{w}} + n_{\mathrm{w}}^{\mathrm{w}}\right) \approx n_i^{\mathrm{w}}/n_{\mathrm{w}}^{\mathrm{w}}$ is the bulk aqueous mole fraction of surfactant molecules of type i, n_i^{w} is the bulk aqueous concentration (as a number density) of surfactant molecules of type i, and $n_{\mathrm{w}}^{\mathrm{w}}$ is the bulk concentration (as a number density) of water molecules. Note that, since the surfactant solutions are dilute, $n_{\mathrm{w}}^{\mathrm{w}}$ is approximately constant and equal to the bulk concentration of pure water. Also note that since only pre-micellar solutions are considered in this chapter, the surfactant monomer concentration, n_{1i}^{w}, which was used in Chapter 2, is equal to the total surfactant concentration, n_i^{w} used here.

For nonionic or zwitterionic surfactants (which have no net charge), thermodynamic diffusional equilibrium requires equating the bulk chemical potential, μ_N^{w}, given in Eq. (3.44), and the surface chemical potential, μ_N^{σ}, given in Eq. (3.41). This yields:

$$\begin{aligned}
\mathrm{k_B}T \ln\left(\frac{n_N^{\mathrm{w}}}{n_{\mathrm{w}}^{\mathrm{w}}}\right) &= \Delta\mu_N^0 + \mathrm{k_B}T \left\{ \ln\left(\frac{\xi_N}{\alpha - \sum_{i=1}^{n} \xi_i \mathrm{a}_i}\right) + \frac{\mathrm{a}_N + 2\pi \mathrm{r}_N \sum_{i=1}^{n} \xi_i \mathrm{r}_i}{\alpha - \sum_{i=1}^{n} \xi_i \mathrm{a}_i} \right. \\
&+ \left. \frac{\pi \mathrm{a}_N \left(\sum_{i=1}^{n} \xi_i \mathrm{r}_i\right)^2}{\left(\alpha - \sum_{i=1}^{n} \xi_i \mathrm{a}_i\right)^2} + \frac{2}{\alpha} \sum_{i=1}^{n} B_{Ni} \xi_i \right\} \\
&+ \sum_{\phi=1}^{L-1} \mathrm{e}\zeta_N^{\phi} \left[\sum_{\omega=\phi}^{L-1} \left\{ (\mathrm{d}_{\omega+1} - \mathrm{d}_{\omega}) \frac{4\pi}{\varepsilon_{\omega}} \sum_{\gamma=1}^{\omega} \left(\sum_{i=1}^{n} \frac{\mathrm{e}\zeta_i^{\gamma} \xi_i}{\alpha} \right) \right\} \right]
\end{aligned} \tag{3.45}$$

where $\Delta\mu_N^0 \equiv \mu_N^{\sigma,0} - \mu_N^{\mathrm{w},0}$. The quantities $\Delta\mu_N^0$ [along with $\Delta\mu_{sc}^0$ defined below in Eq. (3.46)] are the only parameters in the theory that are not calculated by direct

molecular modeling. Instead, $\Delta\mu_N^0$ can be found by using a single experimental surface tension measurement at a known total bulk surfactant concentration for each individual surfactant species comprising the mixture, and then fitting the solution of Eqs. (3.37) and (3.45) (or Eq. (3.46) for $\Delta\mu_{sc}^0$) to the measured surface tension value. Specifically, one can first determine the surface pressure, Π, by measuring the surface tension, σ, using $\Pi = \sigma_0 - \sigma$. This value of the surface pressure can then be used in Eq. (3.37) for a particular single surfactant type N to determine α, the interfacial area per molecule. Note that, in this case, the monolayer mole fraction of surfactant molecules of type N, ξ_N^σ, is unity, while the monolayer mole fractions of all the other surfactant types, $\xi_{i\neq N}^\sigma$, vanish since only a single surfactant type, N, is present in this case. This value of α can then be used in Eq. (3.45) to determine $\Delta\mu_N^0$ (see Section 3.3 for a discussion of the recommended total bulk surfactant concentration to be used for this surface tension measurement).

Similarly, for the ionic surfactants, equating the combined bulk chemical potential of the surfactant (s) and its counterion (c), $\mu_s^{\mathrm{w}} + \mu_c^{\mathrm{w}} \equiv \mu_{sc}^{\mathrm{w}}$, using Eq. (3.44) with $i = s$ and c, and the combined surface chemical potential of the surfactant and its counterion, μ_{sc}^σ, given in Eq. (3.43), yields the required thermodynamic diffusional equilibrium condition (see Section 2.2.2 for a detailed discussion). Specifically,

$$\begin{aligned} \mathrm{k_B}T \ln\left(\frac{n_s^{\mathrm{w}}}{n_{\mathrm{w}}^{\mathrm{w}}}\right) + \mathrm{k_B}T \ln\left(\frac{n_c^{\mathrm{w}}}{n_{\mathrm{w}}^{\mathrm{w}}}\right) &= \Delta\mu_{sc}^0 + \mathrm{k_B}T \left\{ \ln\left(\frac{\xi_s}{\alpha - \sum_{i=1}^{n} \xi_i \mathrm{a}_i}\right) + \frac{\mathrm{a}_s + 2\pi \mathrm{r}_s \sum_{i=1}^{n} \xi_i \mathrm{r}_i}{\alpha - \sum_{i=1}^{n} \xi_i \mathrm{a}_i} \right. \\ &+ \left. \frac{\pi \mathrm{a}_s \left(\sum_{i=1}^{n} \xi_i \mathrm{r}_i\right)^2}{\left(\alpha - \sum_{i=1}^{n} \xi_i \mathrm{a}_i\right)^2} + \frac{2}{\alpha} \sum_{i=1}^{n} B_{si} \xi_i \right\} \qquad (3.46) \\ &+ \sum_{\phi=1}^{L-1} \mathrm{e}\zeta_s^\phi \left[\sum_{\omega=\phi}^{L-1} \left\{ (\mathrm{d}_{\omega+1} - \mathrm{d}_\omega) \frac{4\pi}{\varepsilon_\omega} \sum_{\gamma=1}^{\omega} \left(\sum_{i=1}^{n} \frac{\mathrm{e}\zeta_i^\gamma \xi_i}{\alpha} \right) \right\} \right] + \end{aligned}$$

$$+ \quad (d_S - d_L)\frac{4\pi e z_s}{\varepsilon_s}\sum_{i=1}^{n}\frac{e z_i \xi_i}{\alpha}$$

$$+ \quad 2 z_s k_B T \ln\left(\frac{2\pi e\sum_{i=1}^{n} e z_i \xi_i}{\varepsilon_D \kappa k_B T \alpha} + \sqrt{1+\left(\frac{2\pi e\sum_{i=1}^{n} e z_i \xi_i}{\varepsilon_D \kappa k_B T \alpha}\right)^2}\right)$$

where $\Delta\mu_{sc}^{0} \equiv \mu_{sc}^{\sigma,0} - \mu_{sc}^{w,0}$ is determined by fitting to a single surface tension value, measured at a known bulk surfactant concentration, of an aqueous solution containing only the ionic surfactant and counterion of interest, as described above for $\Delta\mu_{N}^{0}$. Note that once the values of $\Delta\mu_{N}^{0}$ and $\Delta\mu_{sc}^{0}$ are determined in this manner for each surfactant species present in the solution, *no additional experimental measurements involving the surfactant mixture are necessary.*

Note that Eqs. (3.45) and (3.46) represent a set of n equations, one for each of the surfactant species present in the solution. Therefore, as will be shown in Section 3.3 for a few specific cases of interest, one can simultaneously solve this set of n equations, along with the additional constraint that the surface mole fractions sum to unity, that is, $\sum_{i=1}^{n}\xi_i = 1$, to determine the $n+1$ unknown quantities, α and $\{\xi_1,...,\xi_n\}$. One can then use these determined values of α and $\{\xi_1,...,\xi_n\}$, along with Eq. (3.37), to determine the surface pressure, Π, and hence, the surface tension, $\sigma = \sigma_0 - \Pi$.

3.3 Results and Discussion

3.3.1 Calculation of Molecular Parameters

The surface tension, σ, surface concentration, $\Gamma = 1/\alpha$, and surface composition, $\{\xi_1,...,\xi_n\}$, were predicted for: (i) aqueous solutions containing either C_{12}Maltoside, C_{12}Betaine, or SDS, (ii) aqueous solutions containing binary mixtures of C_{12}Maltoside-C_{12}Betaine and C_{12}Betaine-SDS, and (iii) an aqueous solution containing a tern-

ary mixture of C_{12}Maltoside-C_{12}Betaine-SDS. Note that the aqueous solution of C_{12}Maltoside-SDS was discussed in detail in Chapter 2, and therefore, will not be discussed here. The corresponding values of the hard-disk radii, r_i, hard-disk areas, a_i, second-order virial coefficients, B_{ii} and B_{ij}, and standard-state chemical potential differences, $\Delta\mu_i^0$, are listed in Tables 3.1 and 3.2. An analysis of the sensitivity of the theoretical predictions to the values of these parameters is presented in Appendix B. The positions of the various charge layers, d_ϕ, corresponding to the various surfactant systems examined, are listed in Table 3.3, and the corresponding charge-layer valences, ζ_i^ϕ, are listed in Tables 3.4 and 3.5. The estimation of a_i for SDS and C_{12}Maltoside was discussed in detail previously in Section 2.3.1. The hard-disk area of the C_{12}Betaine surfactant was estimated to be 29Å^2 using the bond lengths and angles of the betaine head group as estimated by the Molecular Modeling Pro software package by *ChemSW*.[62] The second-order virial coefficients were computed using the determined head area size as described in Ref. 12. For the dielectric constant values in the Stern region, ε_S, and in the inter-charge layer regions, ε_ϕ, an estimated value of 42, suggested by Bockris and Reddy,[47] which is in reasonable agreement with the experimental values, has been utilized. Note that a 10% change in the values of ε_S and ε_ϕ results in a change of less than 1% in the final predicted surface tension. Accordingly, our results are not extremely sensitive to the precise values of ε_S and ε_ϕ, with the approximate value utilized here providing sufficient accuracy. For mathematical convenience, ε_ϕ will be replaced by ε_S in the equations that follow since their values are assumed to be identical. The positions of the electrostatic charges in the sulfate and betaine heads, as well as the position of the Stern layer, measured relative to the first carbon atom in the hydrocarbon tail group, were also calculated using the Molecular Modeling Pro software by ChemSW.[62] Note that the choice of this reference point in the hydrocarbon tail is arbitrary, and will not effect the final predictions since the results depend solely on the thickness of each layer, that is, on the relative positions of the various d_ϕ's. Specifically, for aqueous solutions containing only the zwitterionic surfactant C_{12}Betaine, or aqueous solutions containing the binary mixture of the nonionic surfactant C_{12}Maltoside and the zwitterionic surfactant C_{12}Betaine, there

are two charge layers positioned at d_1=1.5Åand d_2=3.9Åcorresponding to the positive and negative charges on the dipolar Betaine head, respectively (see Table 3.3). Recall that there are no Stern or diffuse regions in this case since the surfactant molecules considered have no net charge. For aqueous solutions containing a binary surfactant mixture of C_{12}Betaine and the ionic surfactant SDS, there are three charge layers positioned at d_1=1.5Å, d_2=2.3Å, and d_3=3.9Åcorresponding to the positive charge on the betaine head, the negative charge on the sulfate head, and the negative charge on the betaine head, respectively, as well as a Stern layer positioned at d_S=7.8Å. For aqueous solutions containing a ternary surfactant mixture of C_{12}Maltoside, C_{12}Betaine, and SDS, the positions of the three charge layers and the Stern layer are the same as in the previous case (see Table 3.3).

As indicated in Section 3.2.3.5, the standard-state chemical potential differences, $\Delta\mu_i^0$, were calculated by fitting *one* measured surface tension value for each *single* surfactant solution considered. The bulk surfactant concentrations, n_i^w, chosen for this fit are $1.7 \times 10^{-8} mol/cm^3$ for C_{12}Maltoside, $6.7 \times 10^{-7} mol/cm^3$ for C_{12}Betaine, and $5.4 \times 10^{-6} mol/cm^3$ for SDS. Since the theoretically predicted surface tensions were found to be in good agreement with the experimentally measured surface tensions (see below), the precise choice of n_i^w for the fit is quite arbitrary and does not greatly affect the theoretical predictions. However, in general, one should avoid extremely low surfactant concentrations, where the percent uncertainty in the surface pressure measurement is large due to the low value of the surface pressure.

3.3.2 Comparison with Experimental Surface Tension and Adsorption Measurements

Experimentally measured surface tensions and surface concentrations and compositions (measured directly using neutron scattering) were reported for the aqueous solutions listed above in Section 3.3.1. All the reported measurements were conducted at 25°C, except for the monolayer composition measurements of the ternary surfactant solution, which were performed at 40°C.[52,56,63]

Table 3.1: Values of the hard-disk areas, a_i, second-order virial coefficients, B_{ii}, and standard-state chemical potential differences, $\Delta\mu_i^0$, corresponding to the three surfactants C_{12}Maltoside, C_{12}Betaine, and SDS.

Surfactant i	a_i (Å^2)	B_{ii} (Å^2)	$\Delta\mu_i^0$ (k_BT)
C_{12}Maltoside	32	-157	-48.6
C_{12}Betaine	29	-222	-48.1
SDS	25	-367	-59.0

Table 3.2: Values of the second-order virial coefficients, B_{ij}, for the three binary combinations corresponding to the three surfactants C_{12}Maltoside, C_{12}Betaine, and SDS.

Surfactant Pair	B_{ij} (Å^2)
C_{12}Maltoside–C_{12}Betaine	-185
C_{12}Maltoside–SDS	-225
C_{12}Betaine–SDS	-294

Table 3.3: Values of the charge layer positions, d_ϕ, and the Stern layer position, d_S, corresponding to the various surfactant systems considered.

Surfactant Pair	d_1 (Å)	d_2 (Å)	d_3 (Å)	d_S (Å)
C_{12}Maltoside–C_{12}Betaine	1.5	3.9	–	–
C_{12}Maltoside–C_{12}Betaine–SDS	1.5	2.3	3.9	7.8
C_{12}Betaine–SDS	1.5	2.3	3.9	7.8

Table 3.4: Values of the charge layer valences, ζ_i^ϕ, representing the valence of the charges of surfactant molecules of type i positioned at layer ϕ, for an aqueous single surfactant solution of C_{12}Betaine (b), or for an aqueous binary surfactant mixture of C_{12}Maltoside (m)-C_{12}Betaine (b).

Layer (ϕ)	ζ_m^ϕ	ζ_b^ϕ
1	0	+1
1	0	-1

Table 3.5: Values of the charge layer valences, ζ_i^ϕ, representing the valence of the charges of surfactant molecules of type i positioned at layer ϕ, for an aqueous binary surfactant mixture of C_{12}Betaine (b)-SDS (s), or for an aqueous ternary surfactant mixture of C_{12}Maltoside (m)-C_{12}Betaine (b)-SDS (s).

Layer (ϕ)	ζ_m^ϕ	ζ_b^ϕ	ζ_s^ϕ
1	0	+1	0
2	0	0	-1
3	0	-1	0

The predicted surface tensions of aqueous solutions containing only SDS or C_{12}-Maltoside were reported previously in Chapter 2, and are shown here again in Figure 3-2 for comparison purposes. For C_{12}Betaine (b), the monolayer area per molecule, α, for a given bulk concentration, n_b^{w}, is found by solving Eq. (3.45) for α. For this single zwitterionic surfactant, $N = b$, $L = 2$, $\xi_b = 1$, and Eq. (3.45) reduces to:

$$\mathrm{k_B}T \ln\left(\frac{n_b^{\mathrm{w}}}{n_{\mathrm{w}}^{\mathrm{w}}}\right) = \Delta\mu_b^0 + \mathrm{k_B}T\left\{\ln\left(\frac{1}{\alpha - \mathrm{a}_b}\right) + \frac{3\mathrm{a}_b}{\alpha - \mathrm{a}_b} + \frac{\mathrm{a}_b^2}{(\alpha - \mathrm{a}_b)^2} + \frac{2B_{bb}}{\alpha}\right\}$$

$$+ \quad (\mathrm{d}_2 - \mathrm{d}_1)\frac{4\pi \mathrm{e}^2}{\varepsilon_s \alpha} \tag{3.47}$$

Once α is known, the surface tension, σ, can be determined by calculating Π using Eq. (3.37). Recall that the last two terms in Eq. (3.37) vanish since there are no Stern or diffuse regions in this case. Specifically,

$$\sigma = \sigma_0 - \Pi = \sigma_0 - \mathrm{k_B}T\left\{\frac{1}{\alpha - a_b} + \frac{a_b}{(\alpha - a_b)^2} + \frac{B_{bb}}{\alpha^2}\right\} - \frac{2\pi \mathrm{e}^2}{\varepsilon_s \alpha^2}(\mathrm{d}_2 - \mathrm{d}_1) \tag{3.48}$$

Figure 3-2 shows both the predicted (lines) and experimentally measured (various symbols) values of the surface tension, σ, as a function of bulk surfactant concentration, n_i^{w}, where i= m, b, or s, for single surfactant aqueous solutions of C_{12}Maltoside (▲), C_{12}Betaine (■), and SDS (●) below the CMC. The quoted experimental error in these and the other surface tension values reported here is less than 0.1dyn/cm. In all three cases, the theoretical predictions are in good agreement with the experimental results.

For aqueous solutions containing the binary surfactant mixture of C_{12}Maltoside (m) and C_{12}Betaine (b), the monolayer area per molecule, α, and composition, ξ_m and ξ_b, for given total bulk surfactant concentration, $n_{tot}^{\mathrm{w}} \equiv n_m^{\mathrm{w}} + n_b^{\mathrm{w}}$, can be found by simultaneously solving the set of two equations given in Eq. (3.45), along with the constraint that $\xi_m + \xi_b = 1$. For this binary surfactant mixture, i = m and b, $L = 2$, $N = m$ [for Eq. (3.49)] and $N = b$ [for Eq. (3.50)], and therefore, Eq. (3.45) reduces

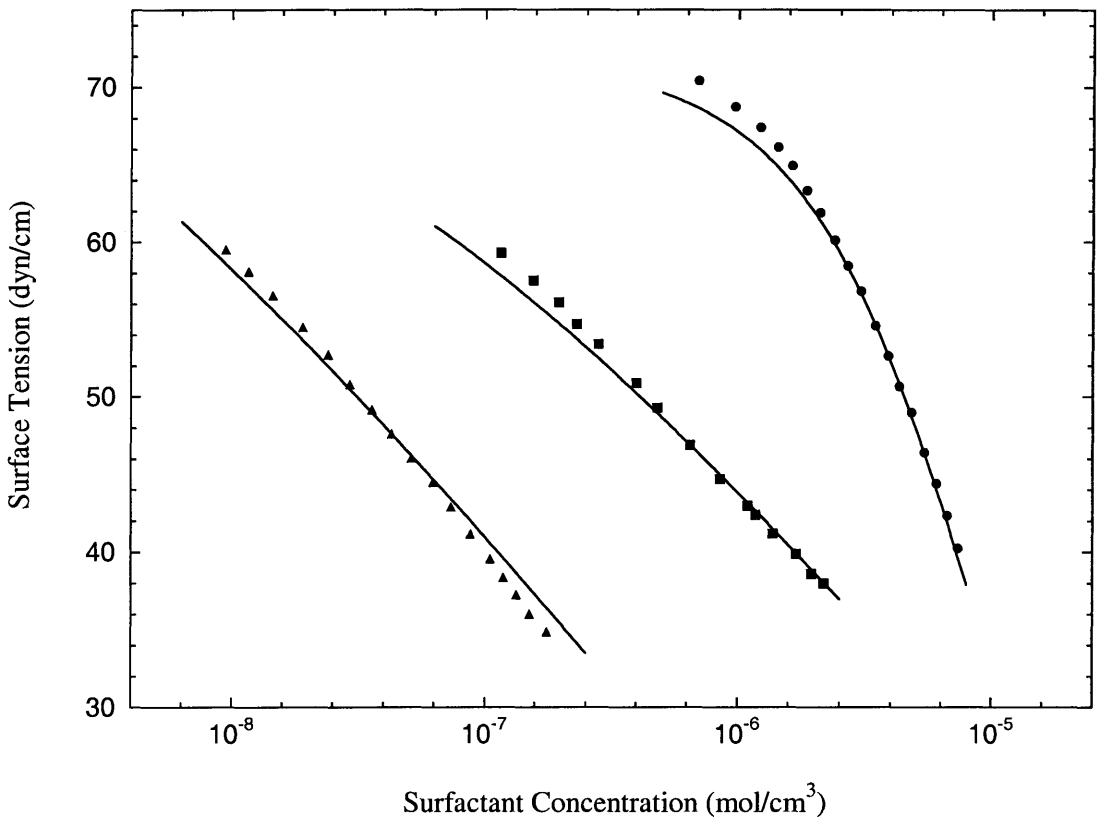

Figure 3-2: Predicted (various lines) and measured (various symbols) surface tensions, σ, as a function of the bulk surfactant concentration, n_i^w, of single surfactant aqueous solutions of C_{12}Maltoside (▲), C_{12}Betaine (■), and SDS (●) at 25°C. The reported experimental uncertainty in the surface tension values is within 0.1 dyn/cm.

to the following two equations:

$$k_B T \ln\left(\frac{n_m^w}{n_w^w}\right) = \Delta\mu_m^0 + k_B T \left\{ \ln\left(\frac{\xi_m}{\alpha - \xi_b a_b - \xi_m a_m}\right) + \frac{a_m + 2\pi r_m (\xi_b r_b + \xi_m r_m)}{\alpha - \xi_b a_b - \xi_m a_m} \right.$$

$$\left. + \frac{\pi a_m (\xi_b r_b + \xi_m r_m)^2}{(\alpha - \xi_b a_b - \xi_m a_m)^2} + \frac{2}{\alpha}(\xi_b B_{mb} + \xi_m B_{mm}) \right\} \quad (3.49)$$

and

$$k_B T \ln\left(\frac{n_b^w}{n_w^w}\right) = \Delta\mu_b^0 + k_B T \left\{ \ln\left(\frac{\xi_b}{\alpha - \xi_b a_b - \xi_m a_m}\right) + \frac{a_b + 2\pi r_b (\xi_b r_b + \xi_m r_m)}{\alpha - \xi_b a_b - \xi_m a_m} \right.$$

$$\left. + \frac{\pi a_b (\xi_b r_b + \xi_m r_m)^2}{(\alpha - \xi_b a_b - \xi_m a_m)^2} + \frac{2}{\alpha}(\xi_b B_{bb} + \xi_m B_{mb}) \right\} \quad (3.50)$$

$$+ (d_2 - d_1)\frac{4\pi e^2 \xi_b}{\varepsilon_s \alpha}$$

Once α, ξ_m, and ξ_b, are known, the surface tension, σ, can be determined by calculating Π using Eq. (3.37). Note that as in the previous case, there are no Stern or diffuse regions. Specifically,

$$\sigma = \sigma_0 - \Pi = \sigma_0 - k_B T \left\{ \frac{1}{\alpha - \xi_b a_b - \xi_m a_m} + \frac{\pi (\xi_b r_b + \xi_m a_m)^2}{(\alpha - \xi_b a_b - \xi_m a_m)^2} \right. \quad (3.51)$$

$$\left. + \frac{\xi_b^2 B_{bb} + 2\xi_b \xi_m B_{mb} + \xi_m^2 B_{mm}}{\alpha^2} \right\} - \frac{2\pi e^2 \xi_b^2}{\varepsilon_s \alpha^2}(d_2 - d_1)$$

Figure 3-3 shows both the predicted (lines) and experimentally measured (various symbols) values of the surface tension, σ, as a function of the total bulk surfactant concentration, $n_{tot}^w \equiv \sum_{i=1}^{n} n_i^w$, for an aqueous binary surfactant mixture of 50%

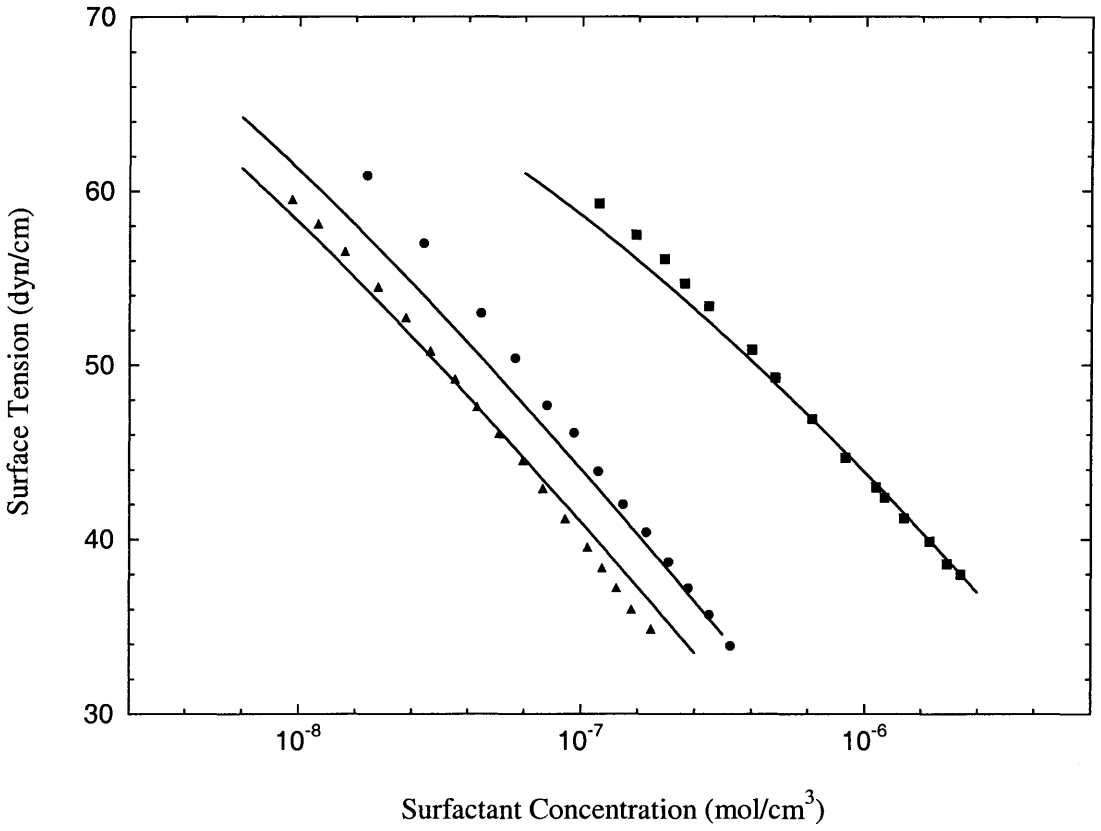

Figure 3-3: Predicted (various lines) and measured (various symbols) surface tensions, σ, as a function of the total bulk surfactant concentration, $n_m^w + n_b^w$, of aqueous solutions containing a binary surfactant mixture of 50% C_{12}Maltoside and 50% C_{12}Betaine (●) at 25°C. Also shown for comparison are the surface tensions of single surfactant aqueous solutions of C_{12}Maltoside (▲) and C_{12}Betaine (■) at 25°C. The reported experimental uncertainty in the surface tension values is within 0.1 dyn/cm.

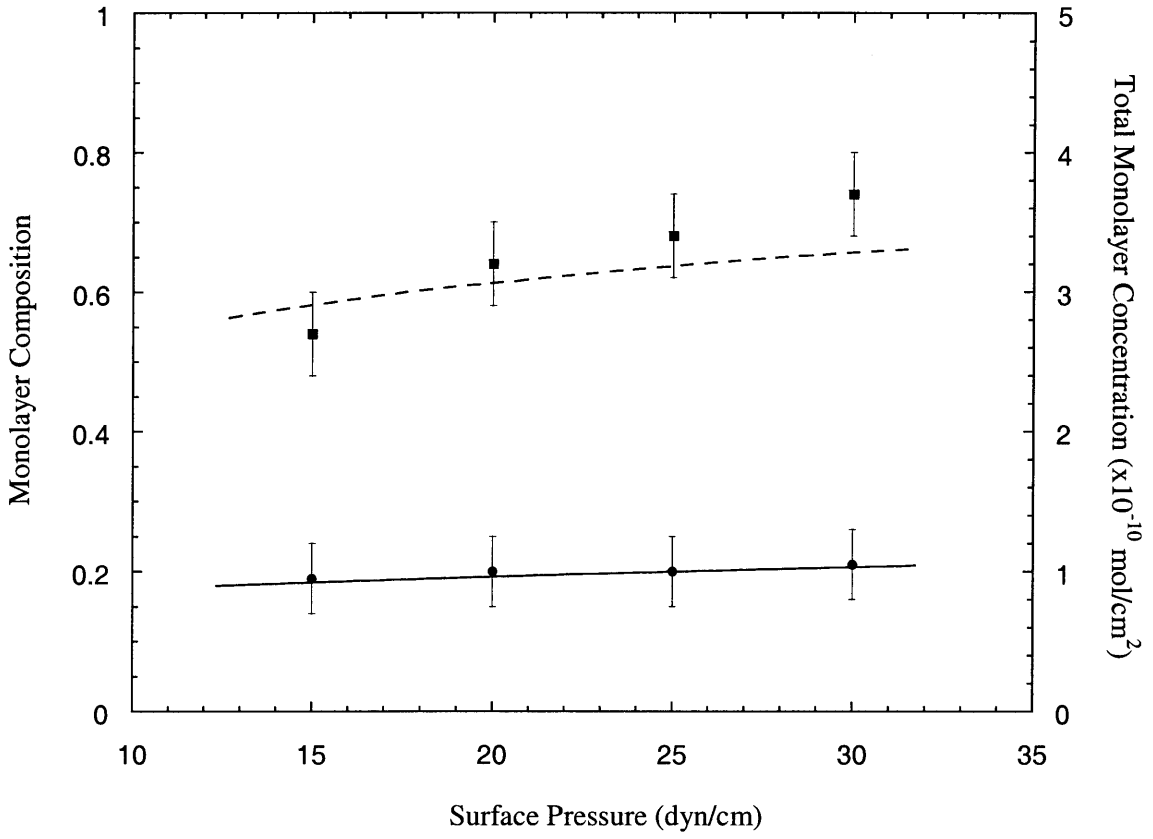

Figure 3-4: Predicted (solid line) and measured (●) monolayer compositions, $\xi_{C_{12}Betaine}$, as well as predicted (dashed line) and measured (■) total monolayer concentrations, Γ, as a function of the surface pressure, Π, of aqueous solutions containing a binary surfactant mixture of 50% C_{12}Maltoside and 50% C_{12}Betaine at 25°C.

C_{12}Maltoside and 50% C_{12}Betaine (●). For comparison purposes, the surface tension curves of aqueous solutions of the two single surfactants, C_{12}Maltoside (▲) and C_{12}Betaine (■), are also shown in Figure 3-3. Figure 3-4 shows both the predicted (solid line) and experimentally measured value (●) of the monolayer composition, ξ_b, as well as the predicted (dashed line) and experimentally measured value (■) of the total monolayer concentration, $\Gamma = 1/\alpha$, as a function of the surface pressure, Π, for an aqueous binary surfactant mixture of 50% C_{12}Maltoside and 50% C_{12}Betaine. The predicted values of the surface tension and both the monolayer composition and concentration are in reasonable agreement with the experimental results. As discussed in Section 3.1, the mixture of C_{12}Maltoside and C_{12}Betaine shows little synergism, as is evidenced by the fact that the surface tension curve of the mixed surfactant solution lies between those of the two single surfactant solutions. Note that our theory successfully predicts this lack of synergism since both the surface tension and monolayer concentration and composition predictions are in reasonable agreement with the experimental results. Note that, for clarity, only one bulk solution composition is shown, since the agreement between theory and experiment was found to be similar for other bulk solution compositions.

For aqueous solutions containing the binary surfactant mixture of SDS (s) and C_{12}Betaine (b), the monolayer area per molecule, α, and composition, ξ_s and ξ_b, for given bulk surfactant concentrations, n_b^{w} and n_s^{w}, can be found by simultaneously solving the set of two equations given in Eqs. (3.45) and (3.46), along with the constraint that $\xi_s + \xi_b = 1$. For this binary surfactant mixture, $i = b$ and s, $N = b$, $L = 3$, and Eqs. (3.45) and (3.46) reduce to the following two equations:

$$\mathrm{k_B}T \ln\left(\frac{n_b^{\mathrm{w}}}{n_{\mathrm{w}}^{\mathrm{w}}}\right) = \Delta\mu_b^0 + \mathrm{k_B}T\left\{\ln\left(\frac{\xi_b}{\alpha - \xi_b \mathrm{a}_b - \xi_s \mathrm{a}_s}\right) + \frac{\mathrm{a}_b + 2\pi \mathrm{r}_b\left(\xi_b \mathrm{r}_b + \xi_s \mathrm{r}_s\right)}{\alpha - \xi_b \mathrm{a}_b - \xi_s \mathrm{a}_s}\right.$$

$$\left. + \frac{\pi \mathrm{a_b}\left(\xi_b \mathrm{r}_b + \xi_s \mathrm{r}_s\right)^2}{\left(\alpha - \xi_b \mathrm{a}_b - \xi_s \mathrm{a}_s\right)^2} + \frac{2}{\alpha}\left(\xi_b B_{bb} + \xi_s B_{sb}\right)\right\} + \qquad (3.52)$$

$$+ \quad \frac{4\pi e^2}{\varepsilon_s \alpha} \left\{ \xi_b \left(d_3 - d_1 \right) - \xi_s \left(d_3 - d_2 \right) \right\}$$

and

$$k_B T \ln \left(\frac{n_s^w}{n_w^w} \right) + k_B T \ln \left(\frac{n_c^w}{n_w^w} \right) = \Delta \mu_{sc}^0 + k_B T \left\{ \ln \left(\frac{\xi_s}{\alpha - \xi_b a_b - \xi_s a_s} \right) \right. \tag{3.53}$$

$$\left. + \quad \frac{a_s + 2\pi r_s \left(\xi_b r_b + \xi_s r_s \right)}{\alpha - \xi_b a_b - \xi_s a_s} \frac{\pi a_s \left(\xi_b r_b + \xi_s r_s \right)^2}{\left(\alpha - \xi_b a_b - \xi_s a_s \right)^2} + \frac{2}{\alpha} \left(\xi_s B_{ss} + \xi_b B_{sb} \right) \right\}$$

$$+ \quad \frac{4\pi e^2}{\varepsilon_s \alpha} \left\{ \xi_s \left(d_s - d_2 \right) - \xi_b \left(d_3 - d_2 \right) \right\}$$

$$- \quad 2 k_B T \ln \left[\frac{-2\pi e^2 \xi_s}{\varepsilon_D \kappa k_B T \alpha} + \sqrt{1 + \left(\frac{-2\pi e^2 \xi_s}{\varepsilon_D \kappa k_B T \alpha} \right)^2} \right]$$

Once α, ξ_b, and ξ_s, are known, the surface tension, σ, can be determined from the surface pressure, Π, using Eq. (3.37) as follows:

$$\sigma = \sigma_0 - \Pi = \sigma_0 - k_B T \left\{ \frac{1}{\alpha - \xi_b a_b - \xi_s a_s} + \frac{\pi \left(\xi_b r_b + \xi_s r_s \right)^2}{\left(\alpha - \xi_b a_b - \xi_s a_s \right)^2} \right.$$

$$\left. + \quad \frac{\xi_b^2 B_{bb} + 2\xi_b \xi_s B_{bs} + \xi_s^2 B_{ss}}{\alpha^2} \right\} \tag{3.54}$$

$$- \quad \frac{2\pi e^2}{\varepsilon_s \alpha^2} \left\{ \xi_s^2 \left(d_s - d_2 \right) + \xi_b^2 \left(d_3 - d_1 \right) - 2\xi_b \xi_s \left(d_3 - d_2 \right) \right\} +$$

$$- \left(\frac{\varepsilon_D \kappa}{\pi}\right)\left(\frac{k_B T}{e}\right)^2 \left[\sqrt{1+\left(\frac{2\pi e^2 \xi_s}{\varepsilon_D \kappa k_B T \alpha}\right)^2} - 1\right]$$

Figure 3-5 shows both the predicted (lines) and experimentally measured (various symbols) values of the surface tension, σ, as a function of the total bulk surfactant concentration for an aqueous binary surfactant mixture of 50% C_{12}Betaine and 50% SDS (▲). For comparison purposes, the surface tension curves of the two single surfactant aqueous solutions, C_{12}Betaine (■) and SDS (●), are also shown in Figure 3-5. Figure 3-6 shows both the predicted (solid line) and experimentally measured values (●) of the monolayer composition, ξ_s, as well as the predicted (dashed line) and experimentally measured values (■) of the total monolayer concentration, $\Gamma = 1/\alpha$, as a function of the surface pressure, Π, for an aqueous binary surfactant mixture of 50% C_{12}Betaine and 50% SDS. The predicted values of the surface tension as well as of the monolayer composition and concentration are in reasonable agreement with the experimental results. As discussed in Section 3.1, the mixture of C_{12}Betaine and SDS shows significant synergism,[56] as is clearly reflected in Figure 3-5 by the fact that the surface tension curve of the mixed surfactant solution lies to the left of the surface tension curve of the two single surfactant solutions. Note that our theory successfully quantitatively predicts this strong synergism since both the surface tension and monolayer concentration and composition predictions are in reasonable agreement with the experimental results.

For aqueous solutions containing a ternary surfactant mixture of C_{12}Maltoside (m), C_{12}Betaine (b), and SDS (s), the monolayer area per molecule, α, and composition, ξ_m, ξ_b, and ξ_s, for given total bulk surfactant concentrations, n_m^w, n_b^w, and n_s^w, can be found by simultaneously solving the set of three equations given in Eqs. (3.45) and (3.46), along with the constraint that $\xi_m + \xi_b + \xi_s = 1$. For this ternary surfactant mixture, $i = m$, b, and s, $L = 3$, $N = m$ [for Eq. (3.55)] and $N = b$ [for Eq. (3.56)],

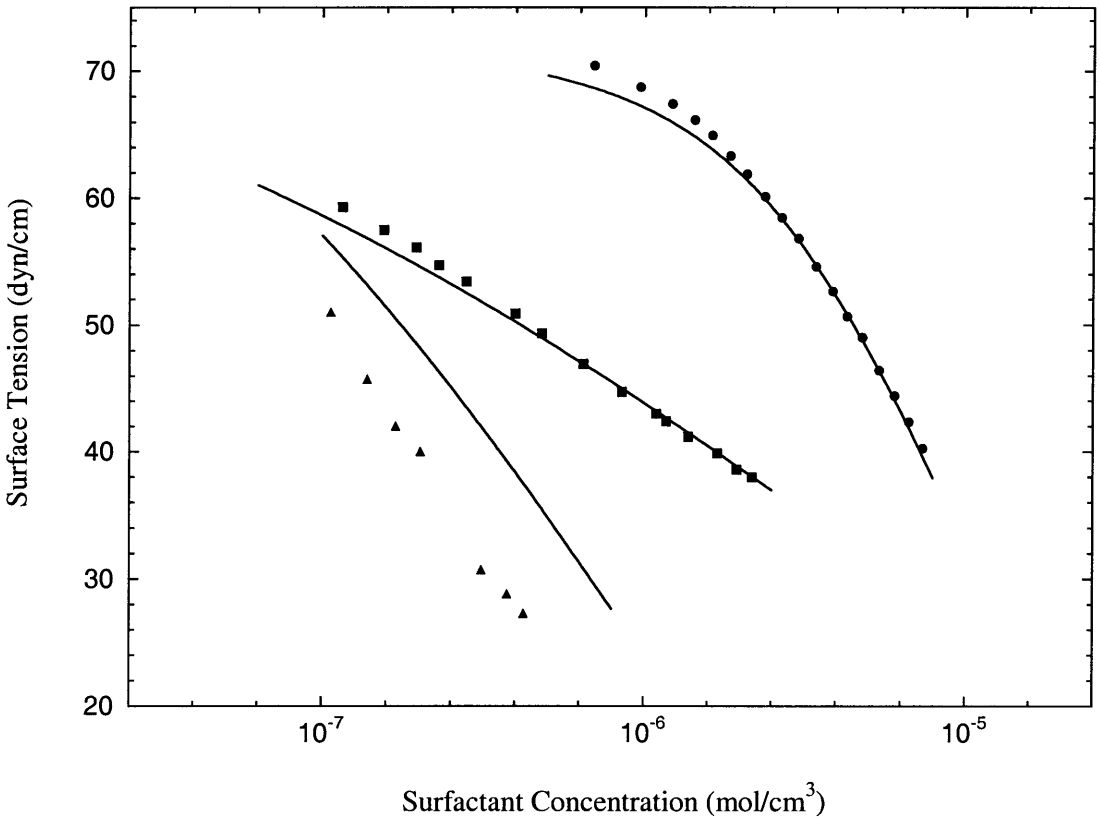

Figure 3-5: Predicted (various lines) and measured (various symbols) surface tensions, σ, as a function of the total bulk surfactant concentration, $n_b^w + n_s^w$, of aqueous solutions containing a binary surfactant mixture of 50% C_{12}Betaine and 50% SDS (▲) at 25°C. Also shown for comparison are the surface tensions of single surfactant aqueous solutions of C_{12}Betaine (■) and SDS (●) at 25°C. The reported experimental uncertainty in the surface tension values is within 0.1 dyn/cm.

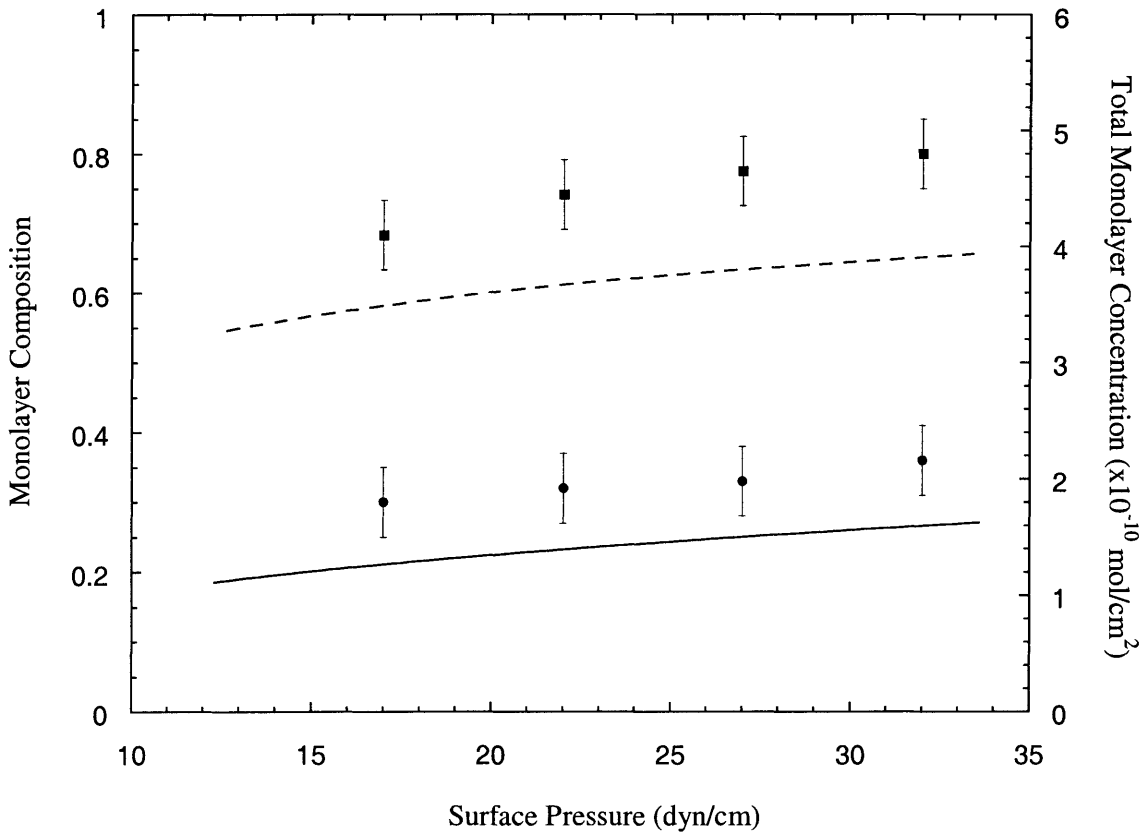

Figure 3-6: Predicted (solid line) and measured (●) monolayer compositions, ξ_{SDS}, as well as predicted (dashed line) and measured (■) total monolayer concentrations, Γ, as a function of the surface pressure, Π, of aqueous solutions containing a binary surfactant mixture of 50% C_{12}Betaine and 50% SDS at 25°C.

and Eqs. (3.45) and (3.46) reduce to the following three equations:

$$\mathrm{k_B}T\ln\left(\frac{n_m^{\mathrm{w}}}{n_{\mathrm{w}}^{\mathrm{w}}}\right) = \Delta\mu_m^0 + \mathrm{k_B}T\left\{\ln\left(\frac{\xi_m}{\alpha-\xi_m\mathrm{a}_m-\xi_b\mathrm{a}_b-\xi_s\mathrm{a}_s}\right)\right. \tag{3.55}$$

$$+\ \frac{\mathrm{a}_m+2\pi\mathrm{r}_m\left(\xi_m\mathrm{r}_m+\xi_b\mathrm{r}_b+\xi_s\mathrm{r}_s\right)}{\alpha-\xi_m\mathrm{a}_m-\xi_b\mathrm{a}_b-\xi_s\mathrm{a}_s}+\frac{\pi\mathrm{a_m}\left(\xi_m\mathrm{r}_m+\xi_b\mathrm{r}_b+\xi_s\mathrm{r}_s\right)^2}{\left(\alpha-\xi_m\mathrm{a}_m-\xi_b\mathrm{a}_b-\xi_s\mathrm{a}_s\right)^2}$$

$$\left.+\ \frac{2}{\alpha}\left(\xi_mB_{mm}+\xi_bB_{bm}+\xi_sB_{sm}\right)\right\}$$

$$\mathrm{k_B}T\ln\left(\frac{n_b^{\mathrm{w}}}{n_{\mathrm{w}}^{\mathrm{w}}}\right) = \Delta\mu_b^0 + \mathrm{k_B}T\left\{\ln\left(\frac{\xi_b}{\alpha-\xi_m\mathrm{a}_m-\xi_b\mathrm{a}_b-\xi_s\mathrm{a}_s}\right)\right. \tag{3.56}$$

$$+\ \frac{\mathrm{a}_b+2\pi\mathrm{r}_b\left(\xi_m\mathrm{r}_m+\xi_b\mathrm{r}_b+\xi_s\mathrm{r}_s\right)}{\alpha-\xi_m\mathrm{a}_m-\xi_b\mathrm{a}_b-\xi_s\mathrm{a}_s}+\frac{\pi\mathrm{a}_b\left(\xi_m\mathrm{r}_m+\xi_b\mathrm{r}_b+\xi_s\mathrm{r}_s\right)^2}{\left(\alpha-\xi_m\mathrm{a}_m-\xi_b\mathrm{a}_b-\xi_s\mathrm{a}_s\right)^2}$$

$$\left.+\ \frac{2}{\alpha}\left(\xi_mB_{mb}+\xi_bB_{bb}+\xi_sB_{sb}\right)\right\}+\frac{4\pi\mathrm{e}^2}{\varepsilon_s\alpha}\left\{\xi_b\left(\mathrm{d}_3-\mathrm{d}_1\right)-\xi_s\left(\mathrm{d}_3-\mathrm{d}_2\right)\right\}$$

and

$$\mathrm{k_B}T\ln\left(\frac{n_s^{\mathrm{w}}}{n_{\mathrm{w}}^{\mathrm{w}}}\right)\ +\ \mathrm{k_B}T\ln\left(\frac{n_c^{\mathrm{w}}}{n_{\mathrm{w}}^{\mathrm{w}}}\right)=\Delta\mu_{sc}^0+\mathrm{k_B}T\left\{\ln\left(\frac{\xi_s}{\alpha-\xi_m\mathrm{a}_m-\xi_b\mathrm{a}_b-\xi_s\mathrm{a}_s}\right)\right.$$

$$+\ \frac{\mathrm{a}_s+2\pi\mathrm{r}_s\left(\xi_m\mathrm{r}_m+\xi_b\mathrm{r}_b+\xi_s\mathrm{r}_s\right)}{\alpha-\xi_m\mathrm{a}_m-\xi_b\mathrm{a}_b-\xi_s\mathrm{a}_s}+\frac{\pi\mathrm{a_s}\left(\xi_m\mathrm{r}_m+\xi_b\mathrm{r}_b+\xi_s\mathrm{r}_s\right)^2}{\left(\alpha-\xi_m\mathrm{a}_m-\xi_b\mathrm{a}_b-\xi_s\mathrm{a}_s\right)^2}+$$

$$+ \quad \frac{2}{\alpha}\left(\xi_m B_{ms} + \xi_b B_{bs} + \xi_s B_{ss}\right)\Bigg\} + \frac{4\pi e^2}{\varepsilon_s \alpha}\left\{\xi_s\left(d_s - d_2\right) - \xi_b\left(d_3 - d_2\right)\right\}$$

$$- \quad 2k_B T \ln\left(\frac{-2\pi e^2 \xi_s}{\varepsilon_D \kappa k_B T \alpha} + \sqrt{1 + \left(\frac{-2\pi e^2 \xi_s}{\varepsilon_D \kappa k_B T \alpha}\right)^2}\right) \tag{3.57}$$

Once α, ξ_m, ξ_b, and ξ_s, are known, the surface tension, σ, can be determined from the surface pressure, Π, using Eq. (3.37) as follows:

$$\sigma = \sigma_0 - \Pi \quad = \quad \sigma_0 - k_B T\left\{\frac{1}{\alpha - \xi_m a_m - \xi_b a_b - \xi_s a_s} + \frac{\pi\left(\xi_m r_m + \xi_b r_b + \xi_s r_s\right)^2}{\left(\alpha - \xi_m a_m - \xi_b a_b - \xi_s a_s\right)^2}\right.$$

$$\left. + \quad \frac{\xi_m^2 B_{mm} + \xi_b^2 B_{bb} + \xi_s^2 B_{ss} + 2\xi_m \xi_b B_{mb} + 2\xi_m \xi_s B_{ms} + 2\xi_b \xi_s B_{bs}}{\alpha^2}\right\}$$

$$- \quad \frac{2\pi e^2}{\varepsilon_s \alpha^2}\left\{\xi_s^2\left(d_s - d_2\right) + \xi_b^2\left(d_3 - d_1\right) - 2\xi_s \xi_b\left(d_3 - d_2\right)\right\}$$

$$- \quad \left(\frac{\varepsilon_D \kappa}{\pi}\right)\left(\frac{k_B T}{e}\right)^2\left[\sqrt{1 + \left(\frac{2\pi e^2 \xi_s}{\varepsilon_D \kappa k_B T \alpha}\right)^2} - 1\right] \tag{3.58}$$

Figure 3-7 shows both the predicted (line) and experimentally measured (●) values of the surface tension, σ, as a function of the total bulk surfactant concentration for an aqueous ternary surfactant mixture of 50% C_{12}Betaine, 25% C_{12}Maltoside, and 25% SDS. Figure 3-8 shows both the predicted (solid columns) and experimentally measured (striped columns) values of the monolayer composition, ξ_m, ξ_b, and ξ_s, at the solution CMC ($n_{tot}^w = 2 \times 10^{-7} mol/cm^3$) for an aqueous ternary surfactant mixture of 50% C_{12}Betaine, 25% C_{12}Maltoside, and 25% SDS. The predicted values of the surface tension and of the monolayer composition are in reasonable agreement

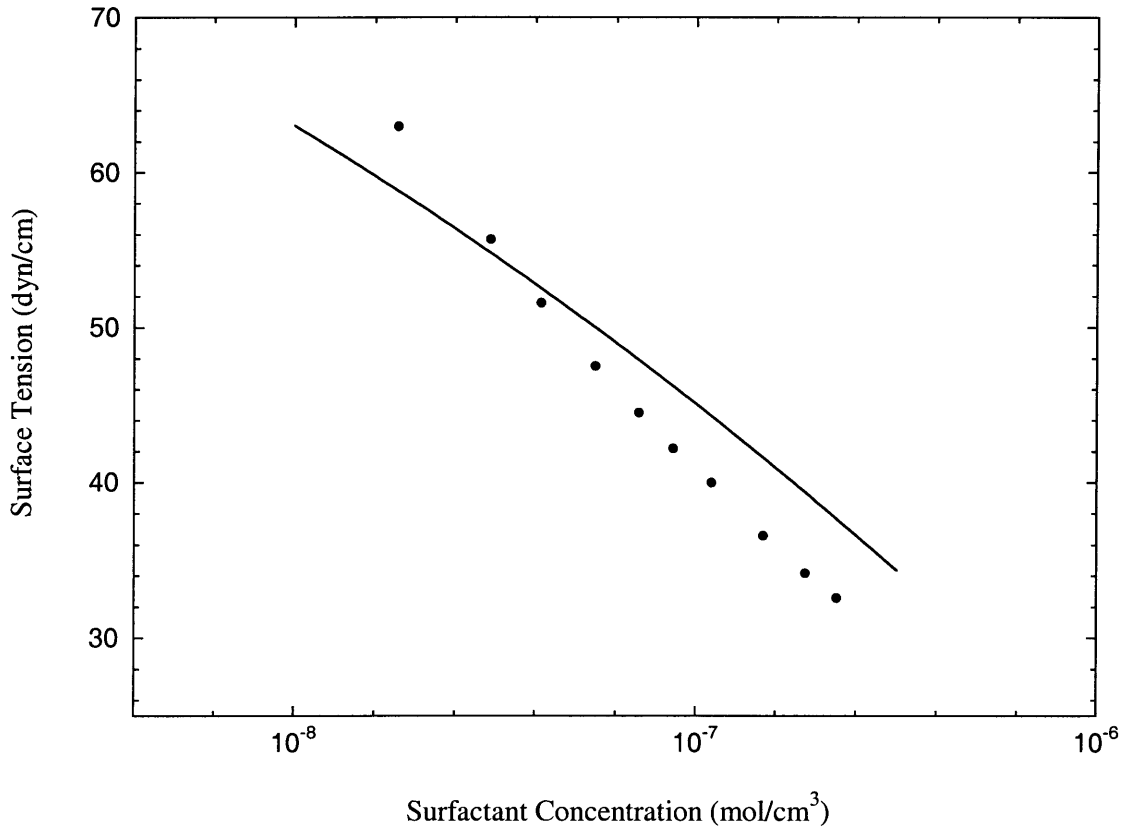

Figure 3-7: Predicted (line) and measured (●) surface tensions, σ, as a function of the total bulk surfactant concentration, $n_m^w + n_b^w + n_s^w$, of an aqueous solution containing a ternary surfactant mixture of 25% C_{12}Maltoside, 50% C_{12}Betaine, and 25% SDS at 25°C. The reported experimental uncertainty in the surface tension values is within 0.1 dyn/cm.

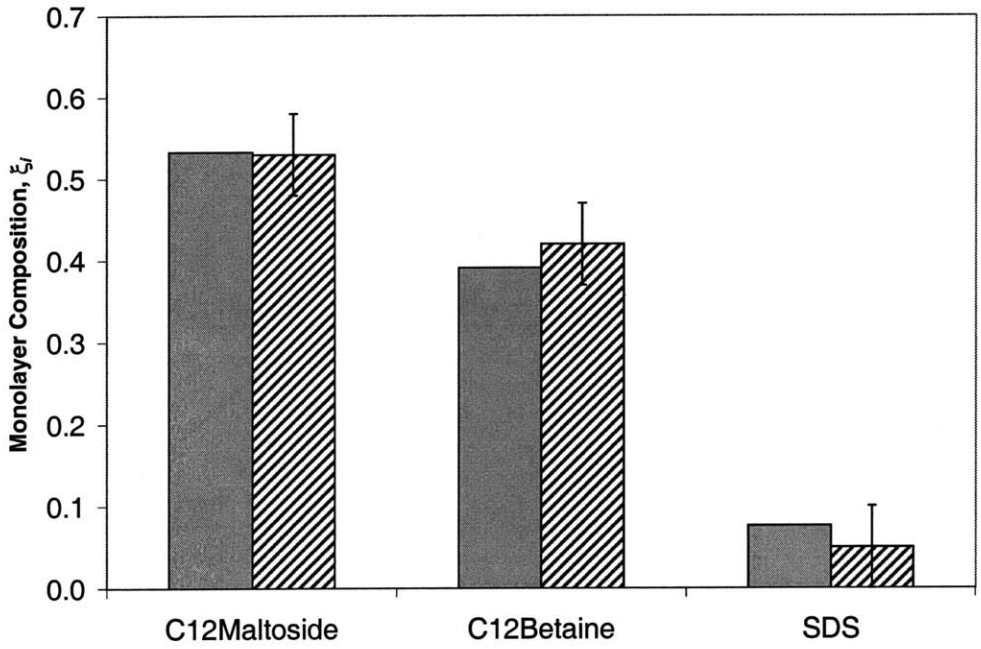

Figure 3-8: Predicted (solid) and measured (striped) monolayer composition, $\xi_{C_{12}Maltoside}$, $\xi_{C_{12}Betaine}$, and ξ_{SDS}, at the CMC ($2\times10^{-7}mol/cm^3$) of an aqueous solution containing a ternary surfactant mixture of 25% C_{12}Maltoside, 50% C_{12}Betaine, and 25% SDS at 40°C.

with the experimental results. Note that, as discussed in Section 3.1, for all the binary and ternary surfactant mixtures examined, no additional experimentally determined parameters are required in order to make predictions of the surface tension and surface concentration and composition, apart from the standard-state chemical potential differences of each single surfactant, $\Delta\mu_i^0$, which were determined from a single surface tension measurement of each single surfactant solution.

3.4 Conclusions

A theoretical framework has been presented to predict the surface tension and monolayer concentration and composition at the air-solution interface for aqueous solutions containing mixtures of nonionic, ionic, and zwitterionic surfactants, with the central theme of this chapter being the rigorous treatment of electrostatic effects associated with the adsorption of zwitterionic surfactants at the interface. Good agreement was found between the theoretical predictions and the experimentally measured surface tensions and monolayer compositions for aqueous solutions containing binary surfactant mixtures of C_{12}Maltoside-C_{12}Betaine, which exhibit a relatively small extent of synergism, and C_{12}Betaine-SDS, which exhibit a relatively large extent of synergism. Good agreement was also found between the theoretical predictions and the experimentally measured surface tensions and monolayer compositions for aqueous solutions containing the ternary surfactant mixture of C_{12}Maltoside-C_{12}Betaine-SDS, thus demonstrating that a notable advantage of the theoretical formulation presented in this chapter is that it can be readily extended to multi-component mixtures, without requiring any additional experimentally-determined parameters.

The theory presented in this chapter utilizes a molecularly-based surface equation of state developed in the context of a nonideal, two-dimensional adsorbed gas model. Nonideal interactions that are accounted for include: (i) steric, excluded-area interactions between the adsorbed surfactant molecules treated as hard-disks, (ii) attractive, van der Waals interactions between the surfactant tails that are incorporated through a virial expansion truncated at second order in surfactant surface concentration, and

(iii) electrostatic interactions in the case of ionic or zwitterionic surfactants, which are treated using a Gouy-Chapman based model. However, instead of the traditional electrostatic double layer consisting of a single two-dimensional charge layer at the interface and a diffuse region in the aqueous phase near the interface, the theory presented here allows for the presence of multiple two-dimensional charge layers at the interface, as well as for a Stern region where steric repulsions exclude the ions present in the diffuse region. By allowing for multiple two-dimensional charge layers, the theory was extended to treat electrostatic effects in solutions that contain zwitterionic surfactants, either as a single species, or when mixed with ionic or nonionic surfactants.

All the parameters appearing in the surface equation of state for the mixed surfactant monolayer can be estimated from the known molecular characteristics of the surfactants. These molecular characteristics include the cross-sectional areas of the surfactant molecules, the valence and position of each of the charged groups in the surfactant head, the distance of closest approach between an adsorbed ionic surfactant and its counterion, and the second-order virial coefficients, which can be calculated from the number of carbons in the surfactant hydrocarbon tails and the surfactant cross-sectional areas. The resulting surface equation of state can be combined with a description of the bulk surfactant solution chemical potential, including a single experimentally-determined parameter, the difference in the standard-state chemical potential of a surfactant molecule at the surface and in the bulk solution, for each single surfactant species present in the mixture, to predict the surface tension and monolayer concentration and composition. *In contrast with other existing theories for mixtures of surfactants at interfaces, there are no mixture-dependent experimentally-fitted, empirical parameters in the mixture surface equation of state presented in this chapter.* This can significantly reduce the amount of experimentation that would be necessary to predict the interfacial behavior of mixed surfactant solutions.

In the next chapter, the theory developed in Chapter 2 is extended to model the adsorption of mixtures of surfactants at the oil-water interface.

Chapter 4

Theoretical and Experimental Investigation of the Equilibrium Oil-Water Interfacial Tensions of Solutions Containing Surfactant Mixtures

4.1 Introduction

As discussed in Chapter 1, surfactant adsorption at the oil-water interface, along with the resulting lowering of the interfacial tension, plays a central role in controlling the desired interfacial properties in many practical applications involving surfactants. As a result, a molecular-based theory capable of predicting the oil-water interfacial behavior of solutions containing surfactant mixtures would be valuable for the design and optimization of surfactant systems exhibiting desirable interfacial properties, and would also help alleviate the need for costly and time consuming trial-and-error type experimentation.

There have been a number of recent theoretical and experimental investigations

of the equilibrium adsorption of surfactants at an oil-water interface. The Langmuir adsorption model is most commonly utilized to describe the equilibrium adsorption of nonionic surfactant molecules at the oil-water interface in the case of single surfactant solutions,[64–71] with the addition of a Gouy-Chapman based treatment of electrostatic effects in the case of ionic surfactants.[29,30,16,72] Recent modifications to the Langmuir adsorption model include the treatment of molecular reorientation at the interface as the interfacial concentration increases,[64,73–75] and accounting for possible clustering of the adsorbed surfactant molecules.[76] Furthermore, the Langmuir adsorption model has been extended to treat binary surfactant mixtures, either by assuming no interactions between the different adsorbed surfactant molecules,[77–79] or through the use of a Regular Solution Theory (RST) based approach to treat these interactions.[69,80,81] Note that, for a single surfactant solution, the Langmuir adsorption model requires two experimentally determined parameters, while the modified forms of this model all require three or more such parameters. In addition, the use of RST in the case of multicomponent surfactant mixtures requires introducing an additional parameter, for each surfactant pair considered, which is determined from experiments performed on that binary surfactant mixture.

In addition to the adsorption of surfactants at the oil-water interface, which can be described by an adsorption model of the type discussed above, one must also consider the equilibrium partitioning of surfactant molecules between the bulk oil phase and the bulk aqueous phase.[65] For dilute surfactant solutions below the critical micelle concentration (CMC), the bulk oil and bulk aqueous phases are commonly modeled as ideal solutions, leading to a constant ratio of the surfactant concentrations in the oil and aqueous phases (referred to as the surfactant partition coefficient, see Section 4.2.2.2 for more a more detailed description).[66,67,69–71,82–84] Note that CMC refers here to the surfactant concentration beyond which the surfactant molecules begin to aggregate (as micelles, swollen micelles, reverse micelles, or swollen reverse micelles) in either the aqueous or the oil phase. Since the surfactant concentrations in both bulk phases are typically very low, it is often difficult (although not impossible) to directly measure these concentrations to determine the surfactant partition

coefficient.[66] In addition to directly measuring the surfactant partition coefficient by measuring the surfactant concentrations in each bulk phase,[85] Ref. 66 shows that the surfactant partition coefficient can be determined by combining air-water surface tension measurements with oil-water interfacial tension measurements. Moreover, Ref. 70 describes a method to determine the surfactant partition coefficient by utilizing dynamic interfacial tension measurements, along with a detailed model describing the dynamic surfactant adsorption. In addition, Refs. 83 and 86 show that the surfactant partition coefficient can be deduced by determining the CMC through the use of oil-water interfacial tension measurements, along with an alternative method for determining the CMC (for example, through the measurement of air-water surface tensions), under the assumption that the presence of the oil phase has a negligible effect on the CMC. It should also be noted that in some cases (including those discussed in this chapter), where the surfactant molecules exhibit extreme partitioning into one of the two bulk phases, the actual determination of the surfactant partition coefficient becomes unnecessary.[69]

The theory presented in this chapter and in Ref. 87 to predict the interfacial behavior of surfactant mixtures adsorbed at the *oil-water interface* is based on the molecular-thermodynamic framework that was presented in Chapters 2 and 3 to predict the interfacial behavior of surfactant mixtures adsorbed at the *air-water interface.*[12,88,89] This theoretical framework models the adsorbed surfactant molecules as a two-dimensional, nonideal gas-like monolayer of hard disks, interacting through both attractive van der Waals interactions originating from the surfactant alkyl tails, as well as through electrostatic interactions, originating from charges present in the surfactant polar heads. More specifically, electrostatic effects are incorporated as an additive contribution to the surface pressure, which is calculated using a Gouy-Chapman based description of the diffuse layer, including a Stern layer of counterion steric exclusion.[32] The main difference between the air-water interface case considered in Chapters 2 and 3 and the oil-water interface case considered in this chapter, is in the magnitude of the attractive van der Waals interactions operating between the surfactant alkyl tails of the adsorbed surfactant molecules in each case. Specifi-

cally, in the case of surfactants consisting of linear alkyl tails interacting through an intervening linear alkane oil phase considered here, the attractive van der Waals interactions between the surfactant alkyl tails are negligible.[90,91] On the other hand, when the intervening medium is air, the van der Waals attractions between the surfactant alkyl tails are not negligible, and were modeled using a virial expansion in surfactant surface concentration truncated at quadratic order, with the resulting second-order virial coefficients computed molecularly.[12,88] However, the values of the other surfactant molecular parameters, which include the molecular cross-sectional area and the valence and location of any electrostatic charges present in the surfactant polar head, are the same as those used in the air-water interface case. As a result, *one can utilize the same theoretical framework to predict both the air-water and the oil-water interfacial tensions.*

In addition to the surfactant molecular parameters discussed above (see Section 4.2 for more details), the theory presented in this chapter also requires, for each surfactant component considered, knowledge of the standard-state chemical potential difference corresponding to a surfactant molecule adsorbed at the interface and present in either the bulk aqueous phase or the bulk oil phase, along with the oil-water surfactant partition coefficient. This standard-state chemical potential difference can be determined from a single interfacial tension measurement, at a known bulk surfactant concentration, for each single surfactant solution. As discussed in detail in Section 4.2, the surfactant partition coefficient is not needed when the surfactant molecules exhibit extreme partitioning into one of the two bulk phases. Furthermore, in those cases when the surfactant partition coefficient is needed, a new method is proposed to determine its value by conducting two interfacial tension measurements on the single surfactant solutions at two different oil-water volume ratios.

Once the required surfactant parameters have been determined, the theoretical framework presented here can be utilized to predict the interfacial tension and the interfacial concentration and composition as a function of the total bulk surfactant concentration and composition as well as of the oil-water volume ratio (that is, the total amount of each surfactant component in the mixture, and the volumes of the

aqueous phase and the oil phase) for a solution containing any number of surfactant components below the CMC, *without the need to conduct any additional measurements on the mixed surfactant solutions.*

Although many experimental measurements of oil-water interfacial tensions of single surfactant solutions have been reported, the number of reported interfacial tension measurements for mixed surfactant solutions is quite limited.[69,79–81,92] Therefore, in this chapter, the results of oil-water interfacial tension measurements of single as well as of mixed surfactant solutions are presented. Specifically, solutions of: (i) the nonionic surfactant dodecyl hexa(ethylene oxide) ($C_{12}E_6$), (ii) the ionic surfactant sodium dodecyl sulfate (SDS), and (iii) binary mixtures of $C_{12}E_6$ and SDS are considered. The two surfactants, $C_{12}E_6$ and SDS, were selected to test the theory developed in this chapter for the oil-water interface case because these same surfactants were used to test the theory for the air-water interface case. Specifically, in Chapter 2, it was shown that the theory can successfully predict the surface tensions of these surfactants and their mixtures. Accordingly, if using the same molecular parameter values for $C_{12}E_6$ and SDS as those utilized in Chapter 2, the theory can successfully predict the oil-water interfacial tensions of these two surfactants and their binary mixtures, this will provide additional support for the range of validity and applicability of the theory. To further test the theory presented here, the interfacial tension predictions are compared with the reported experimental hexadecane-water interfacial tensions of binary mixtures of the nonionic surfactants dodecyl di(ethylene oxide) ($C_{12}E_2$) and dodecyl octa(ethylene oxide) ($C_{12}E_8$).[69]

The remainder of the chapter is organized as follows. The theory of surfactant adsorption at the oil-water interface, including a description of the equilibrium distribution of the surfactant molecules among the interface, the oil phase, and the aqueous phase, as well as the determination of surfactant partition coefficients, is presented in Section 4.2. A description of the experimental technique used to carry out the interfacial tension measurements is presented in Section 4.3. In Section 4.4, the results of the experimental interfacial tension measurements, along with the results of interfacial tension measurements reported in the literature, are compared with the

interfacial tensions predictions of the theory described in Section 4.2. Finally, concluding remarks are presented in Section 4.5.

4.2 Theory

4.2.1 Surface Equation of State

An expression for the surface equation of state can be obtained by assuming that the electrostatic interactions associated with any charged surfactant molecules present at the interface form an additive contribution to the surface pressure. Specifically, the total surface pressure, $\Pi \equiv \sigma_0 - \sigma$ (where σ is the interfacial tension of the surfactant solution, and σ_0 is the interfacial tension between pure oil and water), can be written as follows:[90,88]

$$\Pi = \Pi_{\mathrm{NI}} + \Pi_{\mathrm{elec}} \tag{4.1}$$

where Π_{NI} is the contribution to the surface pressure resulting from all non-electrostatic interactions, and Π_{elec} is the contribution to the surface pressure arising from the electrostatic interactions (see Chapter 2). For the non-electrostatic contribution to the surface pressure, it is assumed that the adsorbed surfactant molecules form a two-dimensional, nonideal gas-like monolayer of hard disks. The radius, r_i, and the cross-sectional area, $\mathrm{a}_i = \pi \mathrm{r}_i^2$, of each surfactant component i in the mixture can be determined from the known chemical structure of that surfactant (see Chapter 2).[12,88,89] Furthermore, as discussed in Section 4.1, it is assumed that any attractive van der Waals interactions between the surfactant alkyl tails adsorbed at the oil-water interface are negligible. This approximation is reasonable when the oil phase has a chemical composition similar to that of the surfactant tails (this is, indeed, the case for the surfactant tails and oils considered in this chapter, which consist of linear alkane chains), but may not be appropriate in cases where the surfactant tails and the oils considered have dissimilar chemical compositions (for example, when the oil phase consists of a highly unsaturated hydrocarbon and the surfactant tails consist of a saturated hydrocarbon). In the latter case, the van der Waals attractions between

the surfactant tails through the intervening oil phase need to be accounted for (for example, by generalizing the approach presented in Ref. 12 for the air case). The nonionic contribution to the surface pressure can then be written as follows:[12]

$$\Pi_{NI} = k_B T \left\{ \frac{\sum_{i=1}^{n} \Gamma_i}{1 - \sum_{i=1}^{n} \Gamma_i a_i} + \frac{\pi \left(\sum_{i=1}^{n} \Gamma_i r_i \right)^2}{\left(1 - \sum_{i=1}^{n} \Gamma_i a_i \right)^2} \right\} \tag{4.2}$$

where k_B is the Boltzmann constant, T is the absolute temperature, r_i, and a_i are the radius and the cross-sectional area of the adsorbed surfactant molecules of type i, respectively, Γ_i is the interfacial concentration of surfactant molecules of type i, and n is the number of surfactant components comprising the mixture.

The electrostatic contribution to the surface pressure, Π_{elec}, can be estimated by making the following assumptions. First, the charge at the interface can be smeared into a single, uniform, two-dimensional charge layer in the case of a single ionic surfactant (see Chapter 2),[88] or into multiple, parallel, two-dimensional charge layers in the case of mixtures containing ionic and zwitterionic surfactants (see Chapter 3).[89] Secondly, it is assumed that the surfactant ions and the counterions are present exclusively within the aqueous phase (that is, that they are completely insoluble in the nonpolar oil phase). This assumption will be discussed further in Section 4.2.2.4, and will be substantiated in Section 4.4. Third, it is also assumed that the charges associated with the surfactant ions and the counterions which are dispersed in the bulk aqueous phase can similarly be smeared into a uniform, three-dimensional charge density which varies with the distance from the two-dimensional, planar interface (forming the so called "diffuse region"). Fourthly, it is assumed that the ions are completely dissociated, and interact within the diffuse region in a medium having uniform dielectric constant. Finally, a Stern layer is also included in the electrostatic description, that is, a distance of closest approach of the counterions, between the adsorbed surfactant molecules and the diffuse region, and assume a different, uniform dielectric constant within the Stern layer (see Chapters 2 and 3 for a more detailed discussion of these assumptions). Implementing these assumptions, the electrostatic

contribution to the surface pressure is given by:[88]

$$\Pi_{\text{elec}} = \left(\frac{\varepsilon\kappa}{\pi}\right)\left(\frac{k_B T}{e}\right)^2 \left[\sqrt{1+\left(\frac{2\pi e}{\varepsilon\kappa k_B T}\right)^2 \left(\sum_{i=1}^{n} e z_i \Gamma_i\right)^2} - 1\right] + \frac{2\pi d}{\varepsilon_s}\left(\sum_{i=1}^{n} e z_i \Gamma_i\right)^2 \tag{4.3}$$

where ε is the dielectric constant in the diffuse region (for which the value corresponding to pure water, 78, was used), κ^{-1} is the Debye-Hückel screening length, e is the charge of a proton, z_i is the valence of the surfactant molecules of type i, d is the Stern-layer thickness (which can be determined from the chemical structures of the surfactant and the counterion),[88] and ε_s is the dielectric constant in the Stern layer (for which a value of 42 was used, see Chapter 2). Note that Eq. (4.3) is written for the case of a single charge layer (that is, all the charge at the interface resides in the same two-dimensional plane), which corresponds to the adsorption of a single ionic surfactant component and any number of nonionic surfactant components, since this is the relevant case for the surfactants considered in this chapter. In the case of mixtures containing ionic and zwitterionic surfactants, the full expression for Π_{elec} given by Eq. (3.35) in Chapter 3 should be utilized instead of Eq. (4.3).

Finally, using Eqs. (4.2) and (4.3) in Eq. (4.1), along with the definition of the surface pressure, the following expression for the surface equation of state is obtained:

$$\sigma = \sigma_0 - \Pi = \sigma_0 - k_B T \left\{ \frac{\sum_{i=1}^{n} \Gamma_i}{1 - \sum_{i=1}^{n} \Gamma_i a_i} + \frac{\pi\left(\sum_{i=1}^{n} \Gamma_i r_i\right)^2}{\left(1 - \sum_{i=1}^{n} \Gamma_i a_i\right)^2} \right\} \tag{4.4}$$

$$- \left(\frac{\varepsilon\kappa}{\pi}\right)\left(\frac{k_B T}{e}\right)^2 \left[\sqrt{1+\left(\frac{2\pi e}{\varepsilon\kappa k_B T}\right)^2 \left(\sum_{i=1}^{n} e z_i \Gamma_i\right)^2} - 1\right] - \frac{2\pi d}{\varepsilon_s}\left(\sum_{i=1}^{n} e z_i \Gamma_i\right)^2$$

4.2.2 Adsorption Equilibrium

4.2.2.1 Equilibrium Among the Interface and the Two Bulk Phases for Nonionic Surfactants

Equation (4.4) relates the interfacial tension, σ, to the surface concentration, Γ_i, of each surfactant component i present in the mixture. In order to compute the dependence of the interfacial tension on the total bulk surfactant concentration and composition of the surfactant mixture, at a given temperature and pressure, it is necessary to first relate the surface concentration, Γ_i, to the total bulk surfactant concentration and composition of the surfactant mixture (the actual experimentally-controlled variables). For this purpose, one must consider the diffusional equilibrium of each surfactant component i among three coexisting phases: the aqueous phase, the oil phase, and the interfacial phase. In this section, *only nonionic* surfactants are considered, and *ionic* surfactants are discussed in Section 4.2.2.4. The diffusional equilibrium condition can be satisfied by equating the chemical potentials of each surfactant component i in each of the three coexisting phases, following the approach of Chapters 2 and 3. Specifically, the interfacial chemical potential of surfactant molecules of type i, μ_i^σ, is given by:[12]

$$\mu_i^\sigma = \mu_i^{\sigma,0} + \mathrm{k_B}T \left\{ \ln\left(\frac{\Gamma_i}{1 - \sum_{k=1}^{n} \Gamma_k \mathrm{a}_k} \right) \right. \tag{4.5}$$

$$\left. + \frac{\mathrm{a}_i + 2\pi \mathrm{r}_i \sum_{k=1}^{n} \Gamma_k \mathrm{r}_k}{1 - \sum_{k=1}^{n} \Gamma_k \mathrm{a}_k} + \frac{\pi \mathrm{a}_i \left(\sum_{k=1}^{n} \Gamma_k \mathrm{r}_k \right)^2}{\left(1 - \sum_{k=1}^{n} \Gamma_k \mathrm{a}_k \right)^2} \right\}$$

where $\mu_i^{\sigma,0}$ is the standard-state chemical potential of surfactant molecules of type i adsorbed at the interface.

Since the bulk surfactant concentrations are dilute in the pre-micellar solutions considered here, the chemical potentials of the surfactant molecules in the bulk aque-

ous and oil phases can be modeled quite accurately using the ideal-solution approximation. Specifically, the chemical potential of surfactant molecules of type i in the aqueous phase, μ_i^{w}, can be written as follows:

$$\mu_i^{\mathrm{w}} = \mu_i^{\mathrm{w},0} + \mathrm{k_B}T \ln\left(\frac{n_i^{\mathrm{w}}}{n_{\mathrm{w}}^{\mathrm{w}}}\right) \tag{4.6}$$

where $\mu_i^{\mathrm{w},0}$ is the standard-state chemical potential of surfactant molecules of type i in the aqueous phase, n_i^{w} is the concentration (as a number density) of surfactant molecules of type i in the aqueous phase, and $n_{\mathrm{w}}^{\mathrm{w}}$ is the concentration (as a number density) of water (and therefore, $n_i^{\mathrm{w}}/n_{\mathrm{w}}^{\mathrm{w}}$ is approximately equal to the mole fraction of surfactant molecules of type i in the aqueous phase). Note that, since the surfactant concentration is dilute, $n_{\mathrm{w}}^{\mathrm{w}}$ is approximately constant and equal to the molar density of pure water given by $n_{\mathrm{w}}^{\mathrm{w}} = \rho_{\mathrm{w}}/\mathrm{MW_w}$ (where ρ_{w} and $\mathrm{MW_w}$ are the density and molecular weight of water, respectively).

Similarly, the chemical potential of surfactant molecules of type i in the oil phase, μ_i^{o}, can be written as follows:

$$\mu_i^{\mathrm{o}} = \mu_i^{\mathrm{o},0} + \mathrm{k_B}T \ln\left(\frac{n_i^{\mathrm{o}}}{n_{\mathrm{o}}^{\mathrm{o}}}\right) \tag{4.7}$$

where $\mu_i^{\mathrm{o},0}$ is the standard-state chemical potential of surfactant molecules of type i in the oil phase, n_i^{o} is the concentration (as a number density) of surfactant molecules of type i in the oil phase, and $n_{\mathrm{o}}^{\mathrm{o}}$ is the concentration (as a number density) of oil (and therefore, $n_i^{\mathrm{o}}/n_o^{\mathrm{o}}$ is approximately equal to the mole fraction of surfactant molecules of type i in the oil phase). Note again that, since the surfactant concentration in the oil phase is dilute, $n_{\mathrm{o}}^{\mathrm{o}}$ is approximately constant and equal to the molar density of pure oil given by $n_{\mathrm{o}}^{\mathrm{o}} = \rho_{\mathrm{o}}/\mathrm{MW_o}$ (where ρ_{o} and $\mathrm{MW_o}$ are the density and molecular weight of the oil, respectively).

Note, however, that the surfactant concentrations in the bulk aqueous and oil phases, n_i^{w} and n_i^{o}, respectively, are not known a priori. Instead, the total number of surfactant molecules of type i in the system, N_i, along with the volumes of the aqueous

phase, V^{w}, and of the oil phase, V^{o}, are known. Since the surfactant molecules of type i are in diffusional equilibrium between the aqueous phase and the oil phase, it follows that:

$$\mu_i^{\mathrm{w}} = \mu_i^{\mathrm{o}} \tag{4.8}$$

which, through the use of Eqs. (4.6) and (4.7), yields:

$$\frac{n_i^{\mathrm{o}}}{n_i^{\mathrm{w}}} = \left(\frac{n_{\mathrm{o}}^{\mathrm{o}}}{n_{\mathrm{w}}^{\mathrm{w}}}\right) \exp\left(\frac{\mu_i^{\mathrm{w},0} - \mu_i^{\mathrm{o},0}}{\mathrm{k_B}T}\right) \equiv \mathrm{K_{p_i}} \tag{4.9}$$

where $\mathrm{K_{p_i}}$ is the oil-water partition coefficient of surfactant molecules of type i, a quantity that will be discussed in more detail in Section 4.2.2.2. As discussed in Section 4.1, when the surfactant molecules partition extremely into either the aqueous phase or the oil phase (a condition which is satisfied by the surfactants considered in this chapter, see Section 4.4), the values of n_i^{w} (or n_i^{o}) are approximately equal to N_i/V^{w} (or N_i/V^{o}), and therefore, knowledge of K_{p_i} is not required in those cases. On the other hand, when K_{p_i} needs to be determined in order to calculate n_i^{w} (or n_i^{o}), a new procedure for determining K_{p_i}, involving the measurement of interfacial tensions, will be presented in Section 4.2.2.2.

Using Eq. (4.9), along with the requirement that the total number of surfactant molecules of type i in the two-phase system, N_i, satisfies $N_i = n_i^{\mathrm{w}}V^{\mathrm{w}} + n_i^{\mathrm{o}}V^{\mathrm{o}}$, the concentration of surfactant molecules of type i in the aqueous phase, n_i^{w}, can be written as follows:

$$n_i^{\mathrm{w}} = \frac{N_i}{V^{\mathrm{w}}}\left(1 + \left(\frac{V^{\mathrm{o}}}{V^{\mathrm{w}}}\right)\mathrm{K_{p_i}}\right)^{-1} \tag{4.10}$$

Note that in deriving Eq. (4.10), it was assumed that the number of surfactant molecules adsorbed at the interface is negligible compared to the total number of surfactant molecules (that is, that $\Gamma_i A << n_i^{\mathrm{w}}V^{\mathrm{w}} + n_i^{\mathrm{o}}V^{\mathrm{o}}$). Equation (4.10) can be combined with Eq. (4.6) to obtain the following expression for the chemical potential of surfactant molecules of type i in the bulk aqueous phase:

$$\mu_i^{\mathrm{w}} = \mu_i^{\mathrm{w},0} + \mathrm{k_B}T \ln\left(\frac{N_i}{V^{\mathrm{w}}n_{\mathrm{w}}^{\mathrm{w}}}\left(1 + \left(\frac{V^{\mathrm{o}}}{V^{\mathrm{w}}}\right)\mathrm{K_{p_i}}\right)^{-1}\right) \tag{4.11}$$

$$= \mu_i^{\mathrm{w},0} - \mathrm{k_B}T \ln\left(1 + \left(\frac{V^{\mathrm{o}}}{V^{\mathrm{w}}}\right) \mathrm{K_{p_i}}\right) + \mathrm{k_B}T \ln\left(\frac{N_i}{V^{\mathrm{w}} n_{\mathrm{w}}^{\mathrm{w}}}\right)$$

Diffusional equilibrium of surfactant molecules of type i between the aqueous phase and the interfacial phase can be satisfied by equating the chemical potentials of surfactant molecules of type i in each phase, that is, by demanding that $\mu_i^{\mathrm{w}} = \mu_i^{\sigma}$. This requirement, along with Eqs. (4.5) and (4.11), yields:

$$\ln\left(\frac{N_i}{n_{\mathrm{w}}^{\mathrm{w}} V^{\mathrm{w}}}\right) = \frac{\Delta\widehat{\mu}_i^{\sigma/\mathrm{w},0}}{\mathrm{k_B}T} + \ln\left(\frac{\Gamma_i}{1 - \sum_{k=1}^{n} \Gamma_k \mathrm{a}_k}\right) + \frac{\mathrm{a}_i \sum_{k=1}^{n} \Gamma_k + 2\pi \mathrm{r}_i \sum_{k=1}^{n} \Gamma_k \mathrm{r}_k}{1 - \sum_{k=1}^{n} \Gamma_k \mathrm{a}_k}$$

$$+ \frac{\pi \mathrm{a}_i \left(\sum_{k=1}^{n} \Gamma_k \mathrm{r}_k\right)^2}{\left(1 - \sum_{k=1}^{n} \Gamma_k \mathrm{a}_k\right)^2} \tag{4.12}$$

where

$$\Delta\widehat{\mu}_i^{\sigma/\mathrm{w},0} \equiv \mu_i^{\sigma,0} - \mu_i^{\mathrm{w},0} + \mathrm{k_B}T \ln\left(1 + \left(\frac{V^{\mathrm{o}}}{V^{\mathrm{w}}}\right) \mathrm{K_{p_i}}\right) \tag{4.13}$$

is the modified standard-state chemical potential difference associated with the adsorption of surfactant molecules of type i from the aqueous phase to the interfacial phase, reflected in $\mu_i^{\sigma,0} - \mu_i^{\mathrm{w},0}$, as well as with their partitioning between the aqueous phase and the oil phase, reflected in the term containing K_{p_i}. The quantity $\Delta\widehat{\mu}_i^{\sigma/\mathrm{w},0}$ is the only parameter in the adsorption isotherm, Eq. (4.12), that is not predicted molecularly. As such, $\Delta\widehat{\mu}_i^{\sigma/\mathrm{w},0}$ needs to be determined experimentally (see Section 4.2.2.2 for a detailed description).

In the case of the surfactant molecules of type i present in the oil phase, their concentration, n_i^{o}, can be determined using Eq. (4.9), along with the mass balance

requirement that $N_i = n_i^{\mathrm{w}} V^{\mathrm{w}} + n_i^{\mathrm{o}} V^{\mathrm{o}}$. This yields:

$$n_i^{\mathrm{o}} = \frac{N_i}{V^{\mathrm{o}}} \left(1 + \left(\frac{V^{\mathrm{w}}}{V^{\mathrm{o}}} \right) \mathrm{K}_{\mathrm{p}_i}^{-1} \right)^{-1} \tag{4.14}$$

Using Eq. (4.14) in Eq. (4.7) for μ_i^{o}, and then demanding that $\mu_i^{\mathrm{o}} = \mu_i^{\sigma}$ to satisfy the condition of diffusional equilibrium of surfactant molecules of type i between the oil phase and the interfacial phase, one obtains:

$$\begin{aligned} \ln \left(\frac{N_i}{n_{\mathrm{o}}^{\mathrm{o}} V^{\mathrm{o}}} \right) &= \frac{\Delta \widehat{\mu}_i^{\sigma/\mathrm{o},0}}{\mathrm{k_B} T} + \ln \left(\frac{\Gamma_i}{1 - \sum_{k=1}^{n} \Gamma_k \mathrm{a}_k} \right) + \frac{\mathrm{a}_i \sum_{k=1}^{n} \Gamma_k + 2\pi \mathrm{r}_i \sum_{k=1}^{n} \Gamma_k \mathrm{r}_k}{1 - \sum_{k=1}^{n} \Gamma_k \mathrm{a}_k} \\ &+ \frac{\pi \mathrm{a}_i \left(\sum_{k=1}^{n} \Gamma_k \mathrm{r}_k \right)^2}{\left(1 - \sum_{k=1}^{n} \Gamma_k \mathrm{a}_k \right)^2} \end{aligned} \tag{4.15}$$

where

$$\Delta \widehat{\mu}_i^{\sigma/\mathrm{o},0} \equiv \mu_i^{\sigma,0} - \mu_i^{\mathrm{o},0} + \mathrm{k_B} T \ln \left(1 + \left(\frac{V^{\mathrm{w}}}{V^{\mathrm{o}}} \right) \mathrm{K}_{\mathrm{p}_i}^{-1} \right) \tag{4.16}$$

is the modified standard-state chemical potential difference associated with the adsorption of surfactant molecules of type i from the oil phase to the interfacial phase, reflected in $\mu_i^{\sigma,0} - \mu_i^{\mathrm{o},0}$, as well as with their partitioning between the aqueous phase and the oil phase, reflected in the term containing K_{p_i}. As in the case of $\Delta \widehat{\mu}_i^{\sigma/\mathrm{w},0}$ in Eq. (4.12), the quantity $\Delta \widehat{\mu}_i^{\sigma/\mathrm{o},0}$ is the only parameter in the adsorption isotherm, Eq. (4.15), that is not predicted molecularly. As such, $\Delta \widehat{\mu}_i^{\sigma/\mathrm{o},0}$ needs to be determined experimentally (see Section 4.2.2.2 for a detailed description).

Note that the two adsorption isotherms, Eqs. (4.12) and (4.15), are equivalent. Indeed, by combining Eqs. (4.12) and (4.15), one simply recovers Eq. (4.9). In other words, Eqs. (4.9), (4.12), and (4.15) reflect the simultaneous equilibrium that exists among surfactant molecules of type i at the interface, in the aqueous phase, and in the oil phase. Accordingly, although either Eq. (4.12) or Eq. (4.15) may be utilized

to describe the condition of diffusional equilibrium of surfactant molecules of type i among the interface and the two bulk phases, for consistency, Eq. (4.12) will be arbitrarily utilize throughout the remainder of the chapter.

4.2.2.2 Experimental Determination of the Modified Standard-State Chemical Potential Difference

As discussed in Section 4.2.2.1, the quantity $\Delta\widehat{\mu}_i^{\sigma/\mathrm{w},0}$ in Eq. (4.12) is the only parameter in the adsorption isotherm, Eq. (4.12), that is not predicted molecularly. Below, a description of a procedure for determining $\Delta\widehat{\mu}_i^{\sigma/\mathrm{w},0}$ experimentally using interfacial tension measurements is presented. Specifically, for each surfactant component i, the measured value of the oil-water interfacial tension is used in Eq. (4.4), along with the known values of the molecular parameters, r_i and a_i, which is then solved to calculate the interfacial concentration, Γ_i. The resulting value of Γ_i can then be utilized in Eq. (4.12), along with the known value of N_i/V^{w}, to determine the quantity $\Delta\widehat{\mu}_i^{\sigma/\mathrm{w},0}$. Once the values of $\Delta\widehat{\mu}_i^{\sigma/\mathrm{w},0}$ for every surfactant component i have been determined in this manner, one can predict all the interfacial concentrations, $\{\Gamma_i\}$, as well as the interfacial tension of the surfactant mixture for any given total bulk amount of surfactant and any bulk surfactant composition for this particular oil-water volume ratio. Specifically, for a given set of n values of $\{N_i/V^{\mathrm{w}}\}$ (one for each of the n surfactant components comprising the mixture), one can solve the set of n equations given by Eq. (4.12) to calculate the set of n unknown interfacial concentrations, $\{\Gamma_i\}$. These values of $\{\Gamma_i\}$ can then be utilized in Eq. (4.4) to predict the interfacial tension of the surfactant mixture.

Since the value of $\Delta\widehat{\mu}_i^{\sigma/\mathrm{w},0}$ depends on the oil-water volume ratio (see Eq. (4.13)), if a new oil-water volume ratio is utilized, then a new value of $\Delta\widehat{\mu}_i^{\sigma/\mathrm{w},0}$ will need to be determined using the procedure described above. This, in turn, would require measuring the oil-water interfacial tension of a solution of surfactant component i for each oil-water volume ratio considered. However, an examination of Eq. (4.13) indicates that, in fact, only two interfacial tension measurements are required for each surfactant component i. Indeed, Eq. (4.13) shows that $\Delta\widehat{\mu}_i^{\sigma/\mathrm{w},0}$ depends on

$\mu_i^{\sigma,0} - \mu_i^{\mathrm{w},0}$, which is independent of the oil-water volume ratio, and on K_{p_i}, which is also independent of the oil-water volume ratio. Accordingly, if one determines the values of $\Delta\widehat{\mu}_i^{\sigma/\mathrm{w},0}$ at two different oil-water volume ratios using the procedure described above, one can deduce $(\mu_i^{\sigma,0} - \mu_i^{\mathrm{w},0})$ and K_{p_i}, and then use these values in Eq. (4.13) for any desired oil-water volume ratio. Specifically, for each surfactant component i, an interfacial tension measurement, for a known amount of surfactant i, is carried out at two different oil-water volume ratios, denoted as $\left[\frac{V^{\mathrm{o}}}{V^{\mathrm{w}}}\right]_{\mathrm{A}}$ and $\left[\frac{V^{\mathrm{o}}}{V^{\mathrm{w}}}\right]_{\mathrm{B}}$, respectively. Denoting the corresponding deduced values of $\Delta\widehat{\mu}_i^{\sigma/\mathrm{w},0}$ as $\left[\Delta\widehat{\mu}_i^{\sigma/\mathrm{w},0}\right]_{\mathrm{A}}$ and $\left[\Delta\widehat{\mu}_i^{\sigma/\mathrm{w},0}\right]_{\mathrm{B}}$, respectively, one can then simultaneously solve Eq. (4.13) at the two volume ratios to obtain the two unknown quantities, K_{p_i} and $(\mu_i^{\sigma,0} - \mu_i^{\mathrm{w},0})$. This yields:

$$\mathrm{K_{p_i}} = \frac{Y - 1}{\left[\frac{V^{\mathrm{o}}}{V^{\mathrm{w}}}\right]_{\mathrm{A}} - Y\left[\frac{V^{\mathrm{o}}}{V^{\mathrm{w}}}\right]_{\mathrm{B}}} \tag{4.17}$$

where

$$Y \equiv \exp\left(\frac{\left[\Delta\widehat{\mu}_i^{\sigma/\mathrm{w},0}\right]_{\mathrm{A}} - \left[\Delta\widehat{\mu}_i^{\sigma/\mathrm{w},0}\right]_{\mathrm{B}}}{\mathrm{k_B}T}\right) \tag{4.18}$$

and

$$\Delta\mu_i^{\sigma/\mathrm{w},0} \equiv \mu_i^{\sigma,0} - \mu_i^{\mathrm{w},0} = \left[\Delta\widehat{\mu}_i^{\mathrm{w},0}\right]_{\mathrm{A}} - \mathrm{k_B}T\ln\left(1 + \left[\frac{V^{\mathrm{o}}}{V^{\mathrm{w}}}\right]_{\mathrm{A}}\mathrm{K_{p_i}}\right) \tag{4.19}$$

Note that for a more accurate estimation of K_{p_i} and $\Delta\mu_i^{\sigma/\mathrm{w},0}$, one can measure interfacial tensions at more than two volume ratios, and then utilize a least-squares fit to determine the best values of K_{p_i} and $\Delta\mu_i^{\sigma/\mathrm{w},0}$.

The ability to determine oil-water partition coefficients of surfactants using only interfacial tension measurements should be of general interest. To demonstrate that interfacial tension measurements are indeed sensitive enough to enable the determination of the surfactant oil-water partition coefficient using the procedure described above, Figure 4-1 shows the predicted interfacial tension as a function of N_i/V^{w} for a hypothetical nonionic surfactant at three different oil-water volume ratios: 0.5 (- – - – -), 1 (———), and 2 (— — —). The surfactant molecular parameters

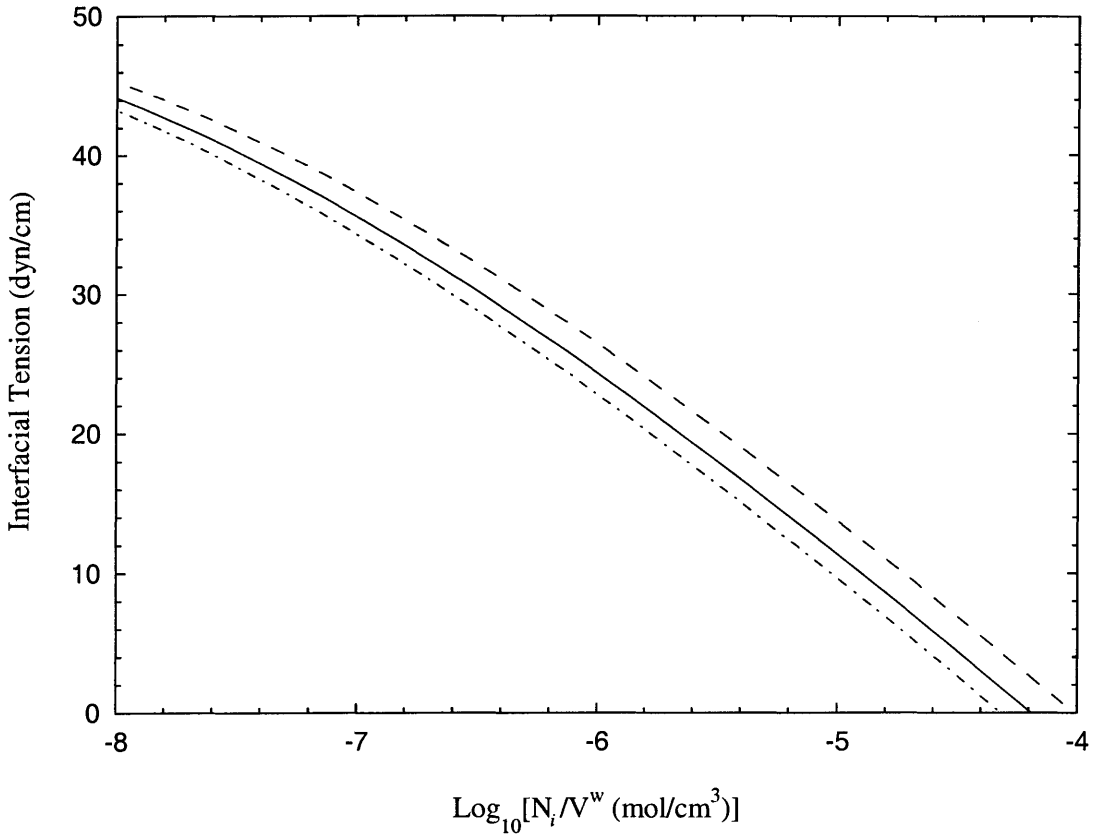

Figure 4-1: Predicted oil-water interfacial tensions as a function of N_i/V^w at three different oil-water volume ratios, 0.5 (- – - – -), 1 (———), and 2 (— — —), for single surfactant solutions of a hypothetical nonionic surfactant having an oil-water partition coefficient of 1 at T=25°C (see text for details).

used in the predictions are: $a_i = 42\text{Å}^2$ (which is the value corresponding to $C_{12}E_6$ used in Section 4.4), $\Delta\mu_i^{\sigma/w,0} = -50k_BT$, $K_{p_i} = 1$, $T = 25°C$, and $\sigma_0 = 50.4 dyn/cm$. Note that as the volume of the oil phase increases (which corresponds to an increase in the oil-water volume ratio), the surfactant is effectively diluted in the aqueous phase, since some of the surfactant molecules will diffuse from the aqueous phase to the oil phase in order to maintain a concentration ratio of $K_{p_i} = 1$. The dilution of the surfactant in the aqueous phase leads to a decrease in the interfacial concentration, with an associated increase in the interfacial tension. This can be seen in Figure 4-1 where, for a given value of N_i/V^w, the interfacial tension values increase as the oil-water volume ratio increases. Note that even for the relatively moderate variations in the oil-water volume ratios examined (0.5 – 2), the predicted interfacial tension variations shown in Figure 4-1 (approximately 3 to 4 dyn/cm) are experimentally measurable. This, in turn, demonstrates the use of the method proposed above to determine oil-water partition coefficients of surfactants.

Once K_{p_i} and $\Delta\mu_i^{\sigma/w,0}$ have been determined as discussed above, the value of $\Delta\widehat{\mu}_i^{\sigma/w,0}$ for any oil-water volume ratio can be computed using Eq (4.13). In this manner, the interfacial concentrations, $\{\Gamma_i\}$, along with the interfacial tension of the surfactant mixture, can be predicted as a function of the total bulk amount and composition of surfactant *for any oil-water volume ratio* by utilizing Eqs. (4.12) and (4.4), as described earlier in this section.

4.2.2.3 Limiting Cases

Two important limiting cases corresponding to the expressions derived in Section 4.2.2.2 can be considered:

Case I

$$\left(\frac{V^o}{V^w}\right) K_{p_i} << 1 \tag{4.20}$$

For systems where the oil-water volume ratio is of order unity (such as in the experiments carried out using the ring method described in Section 4.3.2), the inequality

in Eq. (4.20) is satisfied when $K_{p_i} << 1$. This corresponds to the case of a surfactant that partitions extremely into the aqueous phase, or equivalently, is almost completely insoluble in the oil phase. In addition, the inequality in Eq. (4.20) is satisfied in the case of a very small oil-water volume ratio. This is the case typically encountered when interfacial tensions are measured using experimental techniques that utilize a small drop of oil in a large aqueous phase, including the spinning-drop, the drop-weight, and the pendant-drop methods.[93] Physically, the case $V^{o}/V^{w} << 1$ corresponds to most of the surfactant molecules being in the aqueous phase simply because of the much larger volume of that phase, irrespective of the value of K_{p_i}. In either case, when Eq. (4.20) is satisfied, Eq. (4.12) indicates that $\Delta\widehat{\mu}_i^{\sigma/w,0} = \Delta\mu_i^{\sigma/w,0}$, and consequently that:

$$\ln\left(\frac{N_i}{n_w^w V^w}\right) = \frac{\Delta\mu_i^{\sigma/w,0}}{k_B T} + \ln\left(\frac{\Gamma_i}{1-\sum_{k=1}^{n}\Gamma_k a_k}\right) + \frac{a_i\sum_{k=1}^{n}\Gamma_k + 2\pi r_i\sum_{k=1}^{n}\Gamma_k r_k}{1-\sum_{k=1}^{n}\Gamma_k a_k}$$

$$+ \frac{\pi a_i\left(\sum_{k=1}^{n}\Gamma_k r_k\right)^2}{\left(1-\sum_{k=1}^{n}\Gamma_k a_k\right)^2} \qquad (4.21)$$

Note that the oil-water volume ratio, V^{o}/V^{w}, does not appear in Eq. (4.21). Indeed, for a solution containing only surfactant molecules of type i that partition extremely into the aqueous phase, the interfacial concentration, Γ_i, does not depend on the volume of the oil phase, or equivalently, on the oil-water volume ratio. This is physically intuitive, since there are essentially no surfactant molecules of type i in the oil phase, and therefore, its volume cannot affect their adsorption. In addition, the resulting interfacial tension is also independent of the volume of the oil phase, since, according to Eq. (4.4), the interfacial tension depends solely on the interfacial concentration, Γ_i, of surfactant molecules of type i.

Similar to the method described in Section 4.2.2.2, the value of $\Delta\mu_i^{\sigma/w,0}$ in Eq. (4.21)

can be determined from a single interfacial tension measurement carried out on a surfactant solution of surfactant component i. Specifically, the measured interfacial tension value can be used in Eq. (4.4), along with the known surfactant molecular parameters, r_i and a_i, to determine the value of Γ_i. The resulting value of Γ_i can then be used in Eq. (4.21), along with the known value of N_i/V^w, to determine $\Delta\mu_i^{\sigma/w,0}$. Once the values of $\Delta\mu_i^{\sigma/w,0}$ for every surfactant component satisfying Eq. (4.20) have been determined in this manner, one can predict the interfacial concentrations, $\{\Gamma_i\}$, as well as the interfacial tension of the surfactant mixture for any given total bulk amount and composition of surfactant *for any oil-water volume ratio.* Specifically, for a given set of n values of $\{N_i/V^w\}$ (one for each of the n surfactant components comprising the surfactant mixture), one can solve the set of n equations given by Eq. (4.21), along with the known surfactant molecular parameters, r_i and a_i, to calculate the set of n unknown interfacial concentrations, $\{\Gamma_i\}$. The resulting $\{\Gamma_i\}$ values can then be utilized in Eq. (4.4) to predict the interfacial tension of the surfactant mixture.

Case II

$$\left(\frac{V^o}{V^w}\right) K_{p_i} >> 1 \tag{4.22}$$

For systems where the oil-water volume ratio is of order unity (such as in the experiments carried out using the ring method described in Section 4.3.2), the inequality in Eq. (4.22) is satisfied when $K_{p_i} >> 1$, and corresponds to the extreme partitioning of surfactant molecules of type i into the oil phase, or equivalently, to their almost complete insolubility in the aqueous phase. In addition, the inequality in Eq. (4.22) is satisfied in the case of an extremely large oil-water volume ratio. This is the case typically encountered when interfacial tensions are measured using experimental techniques that utilize a small drop of water in a large oil phase (including the drop-weight or pendant-drop methods for a drop of water). In either case, when Eq. (4.22)

is satisfied, Eq. (4.16) indicates that $\Delta\widehat{\mu}_i^{\sigma/o,0} = \Delta\mu_i^{\sigma/o,0}$, and Eq. (4.12) reduces to:

$$\ln\left(\frac{N_i}{n_o^o V^o}\right) = \frac{\Delta\mu_i^{\sigma/o,0}}{k_B T} + \ln\left(\frac{\Gamma_i}{1-\sum_{k=1}^{n}\Gamma_k a_k}\right) + \frac{a_i\sum_{k=1}^{n}\Gamma_k + 2\pi r_i\sum_{k=1}^{n}\Gamma_k r_k}{1-\sum_{k=1}^{n}\Gamma_k a_k}$$

$$+ \frac{\pi a_i\left(\sum_{k=1}^{n}\Gamma_k r_k\right)^2}{\left(1-\sum_{k=1}^{n}\Gamma_k a_k\right)^2} \tag{4.23}$$

Note that the oil-water volume ratio does not appear in Eq. (4.23). Indeed, for a solution containing only surfactant molecules of type i that partition extremely into the oil phase, the interfacial concentration, Γ_i, does not depend on the volume of the aqueous phase, or equivalently, on the oil-water volume ratio. This is physically intuitive, since there are essentially no surfactant molecules of type i in the aqueous phase, and therefore, its volume cannot affect their adsorption. In addition, the resulting interfacial tension is also independent of the volume of the aqueous phase since, according to Eq. (4.4), the interfacial tension depends solely on the interfacial concentration, Γ_i, of surfactant molecules of type i.

Similar to the method described above for Case I, the value of $\Delta\mu_i^{\sigma/o,0}$ in Eq. (4.23) can be determined from a single interfacial tension measurement carried out on a solution of surfactant component i. Specifically, the measured interfacial tension can be used in Eq. (4.4), along with the known values of the surfactant molecular parameters, r_i and a_i, which can then be used to calculate the value of Γ_i. The resulting values of Γ_i can then be used in Eq. (4.23), along with the known value of N_i/V^o, to determine the quantity $\Delta\mu_i^{\sigma/o,0}$. Once the values of $\Delta\mu_i^{\sigma/o,0}$ for every surfactant component i satisfying Eq. (4.22) have been determined in this manner, one can predict the interfacial concentrations, $\{\Gamma_i\}$, as well as the interfacial tension of the surfactant mixture for any given bulk total amount and composition of surfactant *for any oil-water volume ratio.* Specifically, for a given set of n values of $\{N_i/V^o\}$ (one

for each of the n surfactant components comprising the mixture), one can solve the set of n equations given by Eq. (4.23), along with the known values of the surfactant molecular parameters, r_i and a_i, to calculate the set of n unknown interfacial concentrations, $\{\Gamma_i\}$. The resulting values of $\{\Gamma_i\}$ can then be used in Eq. (4.4) to compute the interfacial tension of the surfactant mixture.

One should note that when either Case I or Case II are satisfied, one cannot utilize the method described in Section 4.2.2.2 to determine the oil-water partition coefficients of surfactants. Indeed, as stressed above, in both cases, the interfacial tension does not depend on the oil-water volume ratio. As shown above, one can nevertheless predict interfacial tensions in these two limiting cases by utilizing Eq. (4.21) or Eq. (4.23) as the equilibrium adsorption isotherms.

If one nevertheless needs to determine the partition coefficient of surfactant molecules of type i, K_{p_i}, for other purposes, one can first adjust the oil-water volume ratio such that $\left(\frac{V^{\mathrm{o}}}{V^{\mathrm{w}}}\right)\mathrm{K}_{\mathrm{p}_i}$ becomes of order unity, and then utilize the method described in Section 4.2.2.2 to determine the value of K_{p_i} using interfacial tension measurements. Alternatively, one can carry out a single interfacial tension measurement at an *extremely small* oil-water volume ratio such that Eq. (4.20) is satisfied (Case I), and then use this measured value to determine the value of $\Delta\mu_i^{\sigma/\mathrm{w},0}$ as described above. Subsequently, one can carry out a second interfacial tension measurement at an *extremely large* oil-water volume ratio such that Eq. (4.22) is satisfied (Case II), and then use this measured value to determine the value of $\Delta\mu_i^{\sigma/\mathrm{o},0}$ as described above. For example, these two measurements could be carried out using the drop-weight method where, in the first case, an oil drop in a large aqueous phase is utilized, and in the second case, a water drop in a large oil phase is utilized. Once $\Delta\mu_i^{\sigma/\mathrm{w},0}$ and $\Delta\mu_i^{\sigma/\mathrm{o},0}$ have been determined, the partition coefficient of surfactant molecules of type i, K_{p_i}, can then be determined using Eq. (4.9) as follows:

$$\mathrm{K}_{\mathrm{p}_i} = \left(\frac{n_{\mathrm{o}}^{\mathrm{o}}}{n_{\mathrm{w}}^{\mathrm{w}}}\right)\exp\left(\frac{\Delta\mu_i^{\sigma/\mathrm{o},0} - \Delta\mu_i^{\sigma/\mathrm{w},0}}{\mathrm{k_B}T}\right) \tag{4.24}$$

4.2.2.4 Equilibrium Among the Interface and the Two Bulk Phases for Ionic Surfactants

Sections 4.2.2.1–4.2.2.3 dealt with nonionic surfactants where electrostatic effects are absent, and electroneutrality considerations are therefore not required. The derivation of the adsorption equilibrium equations for ionic surfactants is quite similar, and therefore, will only be discussed briefly in this section. The key difference between the ionic and the nonionic surfactant cases is in the requirement of electroneutrality in the ionic surfactant case. A convenient way to account for electroneutrality in the interfacial phase, as well as in the bulk aqueous and oil phases, is to consider the simultaneous adsorption and partitioning of the surfactant ion and its counterion in these phases.[43] In addition, the electrostatic contribution to the interfacial chemical potential of the surfactant needs to be accounted for. Recall that since the aqueous phase is dilute in surfactant, the ideal solution approximation can be utilized to model the bulk chemical potentials of the surfactant ions and their counterions. In the case of a single, monovalent ionic surfactant, denoted below by the subscript s, and its counterion, denoted below by the subscript c, with or without any other nonionic surfactants, and with no added electrolyte (which corresponds to the cases considered in Section 4.4, for SDS and for a binary surfactant mixture of SDS and $C_{12}E_6$), the interfacial chemical potential of the ionic surfactant and its counterion, $\mu_s^\sigma + \mu_c^\sigma \equiv \mu_{sc}^\sigma$, can be written as follows:[88]

$$\mu_{sc}^{\sigma} = \mu_{sc}^{\sigma,0} + \mathrm{k_B}T \left\{ \ln\left(\frac{\Gamma_s}{1 - \sum_{k=1}^{n} \Gamma_k \mathrm{a}_k} \right) + \frac{\mathrm{a}_s \sum_{k=1}^{n} \Gamma_k + 2\pi \mathrm{r}_s \sum_{k=1}^{n} \Gamma_k \mathrm{r}_k}{1 - \sum_{k=1}^{n} \Gamma_k \mathrm{a}_k} \right. \tag{4.25}$$

$$\left. + \frac{\pi \mathrm{a}_s \left(\sum_{k=1}^{n} \Gamma_k \mathrm{r}_k \right)^2}{\left(1 - \sum_{k=1}^{n} \Gamma_k \mathrm{a}_k \right)^2} \right\} + 2\mathrm{k_B}T \mathrm{z}_s \ln\left[\frac{2\pi \mathrm{e}^2}{\varepsilon \kappa \mathrm{k_B}T} \mathrm{z}_s \Gamma_s + \sqrt{1 + \left(\frac{2\pi \mathrm{e}^2}{\varepsilon \kappa \mathrm{k_B}T} \mathrm{z}_s \Gamma_s \right)^2} \right] +$$

$$+ \quad \frac{4\pi \mathrm{d}\,(\mathrm{z}_s \mathrm{e})^2}{\varepsilon_{\mathrm{s}}} \Gamma_s$$

where $\mu_{sc}^{\sigma,0} \equiv \mu_s^{\sigma,0} + \mu_c^{\sigma,0}$, and $\sum_{k=1}^{n}$ indicates summation over all surfactant types (which includes the ionic surfactant species and any nonionic surfactant species, if present).

Similar to the nonionic surfactant case considered in Section 4.2.2.1, the simultaneous equilibrium of the surfactant molecules among the three phases (the interface, the bulk aqueous phase, and the bulk oil phase), can be accounted for by first treating the equilibrium partitioning of the surfactant molecules between the two bulk phases. Note that although on physical grounds, one may expect that the solubility of any electrolyte should be extremely low in a nonpolar oil phase, in this section, the more general case where the ionic surfactant molecules and their counterions are allowed to partition into the oil phase is treated. Subsequently, in Section 4.4 it is shown that, as expected, the ionic surfactant considered in this chapter, SDS, does indeed partition extremely into the aqueous phase.

Electroneutrality of the bulk aqueous and the bulk oil phases requires that the concentration of the surfactant ions be equal to the concentration of the counterions in each of these bulk phases (that is, that $n_s^{\mathrm{w}} = n_c^{\mathrm{w}}$ and $n_s^{\mathrm{o}} = n_c^{\mathrm{o}}$). Similar to the nonionic surfactant case, the concentrations in either phase in the pre-micellar solutions considered here are dilute, and therefore, the ideal solution approximation can be utilized to model the chemical potentials of the surfactant molecules or the counterions in either the aqueous phase or the oil phase (see Eqs. (4.6) and (4.7), with $i = s$ or $i = c$). Diffusional equilibrium demands that $\mu_s^{\mathrm{w}} + \mu_c^{\mathrm{w}} = \mu_s^{\mathrm{o}} + \mu_c^{\mathrm{o}}$, which along with Eqs. (4.6) and (4.7) and the fact that $n_s^{\mathrm{w}} = n_c^{\mathrm{w}}$ and $n_s^{\mathrm{o}} = n_c^{\mathrm{o}}$, yields:

$$\frac{n_s^{\mathrm{o}}}{n_s^{\mathrm{w}}} = \frac{n_c^{\mathrm{o}}}{n_c^{\mathrm{w}}} \equiv \mathrm{K}_{\mathrm{p}_{sc}} = \frac{n_{\mathrm{o}}^{\mathrm{o}}}{n_{\mathrm{w}}^{\mathrm{w}}} \exp\left(\frac{\mu_{sc}^{\mathrm{w},0} - \mu_{sc}^{\mathrm{o},0}}{2\mathrm{k}_{\mathrm{B}} T}\right) \tag{4.26}$$

where $K_{p_{sc}}$ is the oil-water partition coefficient for the ionic surfactant and its counterion, $\mu_{sc}^{\mathrm{w},0} \equiv \mu_s^{\mathrm{w},0} + \mu_c^{\mathrm{w},0}$, and $\mu_{sc}^{\mathrm{o},0} \equiv \mu_s^{\mathrm{o},0} + \mu_c^{\mathrm{o},0}$. By utilizing an overall mass balance of the surfactant and its counterion (that is, by demanding that $N_s = n_s^{\mathrm{w}} V^{\mathrm{w}} + n_s^{\mathrm{o}} V^{\mathrm{o}}$ and $N_c = n_c^{\mathrm{w}} V^{\mathrm{w}} + n_c^{\mathrm{o}} V^{\mathrm{o}}$, where N_s is the total number of ionic surfactant molecules

and $N_c = N_s$ is the total number of counterions), the concentrations of the ionic surfactant and its counterion in the aqueous phase can be written as follows:

$$n_s^{\mathrm{w}} = \frac{N_s}{V^{\mathrm{w}}} \left(1 + \left(\frac{V^{\mathrm{o}}}{V^{\mathrm{w}}} \right) \mathrm{K}_{\mathrm{p}_{sc}} \right)^{-1} \tag{4.27}$$

and

$$n_c^{\mathrm{w}} = \frac{N_c}{V^{\mathrm{w}}} \left(1 + \left(\frac{V^{\mathrm{o}}}{V^{\mathrm{w}}} \right) \mathrm{K}_{\mathrm{p}_{sc}} \right)^{-1} \tag{4.28}$$

Finally, diffusional equilibrium of the surfactant ion s and its counterion c between the aqueous phase and the interfacial phase, including electroneutrality, requires that $\mu_s^{\mathrm{w}} + \mu_c^{\mathrm{w}} = \mu_s^{\sigma} + \mu_c^{\sigma}$, which along with the use of Eqs. (4.25), (4.6), (4.27), and (4.28), yields the following expression for the adsorption isotherm of an ionic surfactant s and its counterion c:

$$\ln \left(\frac{N_s}{n_{\mathrm{w}}^{\mathrm{w}} V^{\mathrm{w}}} \right) + \ln \left(\frac{N_c}{n_{\mathrm{w}}^{\mathrm{w}} V^{\mathrm{w}}} \right) = 2 \ln \left(\frac{N_s}{n_{\mathrm{w}}^{\mathrm{w}} V^{\mathrm{w}}} \right) \tag{4.29}$$

$$= \frac{\Delta \widehat{\mu}_{sc}^{\sigma/\mathrm{w},0}}{\mathrm{k_B} T} + \ln \left(\frac{\Gamma_s}{1 - \sum_{k=1}^{n} \Gamma_k \mathrm{a}_k} \right) + \frac{\mathrm{a}_s \sum_{k=1}^{n} \Gamma_k + 2\pi \mathrm{r}_s \sum_{k=1}^{n} \Gamma_k \mathrm{r}_k}{1 - \sum_{k=1}^{n} \Gamma_k \mathrm{a}_k}$$

$$+ \frac{\pi \mathrm{a}_s \left(\sum_{k=1}^{n} \Gamma_k \mathrm{r}_k \right)^2}{\left(1 - \sum_{k=1}^{n} \Gamma_k \mathrm{a}_k \right)^2} + 2\mathrm{z}_s \ln \left\{ \frac{2\pi \mathrm{e}^2}{\varepsilon \kappa \mathrm{k_B} T} \mathrm{z}_s \Gamma_s + \sqrt{1 + \left(\frac{2\pi \mathrm{e}^2}{\varepsilon \kappa \mathrm{k_B} T} \mathrm{z}_s \Gamma_s \right)^2} \right\}$$

$$+ \frac{4\pi \mathrm{d} \left(\mathrm{z}_s \mathrm{e} \right)^2}{\mathrm{k_B} T \varepsilon_{\mathrm{s}}} \Gamma_s$$

where

$$\Delta \widehat{\mu}_{sc}^{\sigma/\mathrm{w},0} \equiv \mu_{sc}^{\sigma,0} - \mu_{sc}^{\mathrm{w},0} + \mathrm{k_B} T \ln \left(1 + \left(\frac{V^{\mathrm{o}}}{V^{\mathrm{w}}} \right) \mathrm{K}_{\mathrm{p}_{sc}} \right) \tag{4.30}$$

Equation (4.29) can now be used for ionic surfactants in the same way that Eq. (4.12) was used for nonionic surfactants. Specifically, $\Delta\widehat{\mu}_{sc}^{\sigma/\mathrm{w},0}$ can be determined from one experimental interfacial tension measurement, and the values of $\mathrm{K}_{\mathrm{p}_{sc}}$ and $\Delta\mu_{sc}^{\sigma/\mathrm{w},0}$ can be determined from two interfacial tension measurements using the method described in Section 4.2.2.2. Once the values of $\mathrm{K}_{\mathrm{p}_{sc}}$ and $\Delta\mu_{sc}^{\sigma/\mathrm{w},0}$ have been obtained, Eq. (4.29) can be utilized to determine the surface concentration of the ionic surfactant, Γ_s, at any bulk surfactant concentration and composition and oil-water volume ratio. In the case of a mixture of ionic and nonionic surfactants, Eqs. (4.29) and (4.12) can be solved simultaneously to determine the interfacial concentrations of all the surfactant components. Once the interfacial concentrations of all the surfactant components present in the mixture have been determined, the interfacial tension of the surfactant mixture can be predicted using Eq. (4.4).

Furthermore, the same limiting cases considered in Section 4.2.2.3 can be applied to Eq. (4.29) to arrive at similar conclusions. Specifically, one can show that if Case I is satisfied (that is, if the surfactant ions and the counterions partition extremely into the aqueous phase), then the interfacial tension will not depend on the volume of the oil phase (that is, the interfacial tension will depend only on N_s/V^{w} and not on the oil-water volume ratio). Therefore, if one measures the interfacial tension at a constant amount of surfactant, N_s, and a constant aqueous phase volume, V^{w}, but at various oil phase volumes, V^{o} (while maintaining an oil-water volume ratio that is of order unity), and observes that the interfacial tension is constant, one can conclude that Eq. (4.20) is satisfied, and hence, that $\mathrm{K}_{\mathrm{p}_{sc}} << 1$. Physically, this corresponds to approximately all the surfactant ions and their counterions partitioning into the aqueous phase, which was an assumption made in Section 4.2.1.

4.3 Materials and Methods

4.3.1 Materials

The nonionic surfactant used in this study, dodecyl hexa(ethylene oxide) ($C_{12}E_6$) was obtained from Nikko Chemicals, Japan (lot number 4023) and, due to its high purity (as indicated by the absence of a minimum in the experimental surface tension versus $C_{12}E_6$ concentration curve), was used as received. The ionic surfactant used in this study, sodium dodecyl sulfate (SDS) was obtained from Sigma chemicals (99% purity, lot number 57H1242), and was further purified by foam fractionation until no minimum in the experimental surface tension versus SDS concentration curve was observed. All water used in the experiments was purified using a Millipore Milli-Q system and had a specific resistance of 18 MΩ cm. The decane used as the oil phase in the experiments was obtained from Aldrich Chemicals (99+% purity, lot number 01618PY), and was used as received. All glassware was carefully cleaned by soaking in a 1 M NaOH-Ethanol bath for at least 8 hours, followed by soaking in a 1 M nitric acid bath for at least another 8 hours, rinsing copiously with Milli-Q water, and finally drying in an oven overnight. The platinum ring used in the interfacial tension measurements was cleaned by a thorough rinsing in Milli-Q water, followed by a thorough rinsing in acetone, and finally held in a flame until an orange glow was observed.

4.3.2 Methods

The equilibrium oil-water interfacial tension was measured using a Krüss K-10 tensiometer with a platinum ring. Figure 4-2 shows a schematic illustration of this technique. A ring made out of thin platinum wire is immersed in the lower, aqueous phase. It is then pulled upwards and as it crosses from the aqueous phase to the oil phase, the meniscus acts to pull down on the ring as shown in Figure 4-2. The force on the ring is then measured by an electronic scale. The surface tension is then calculated by the tensiometer by dividing this force by twice the perimeter of

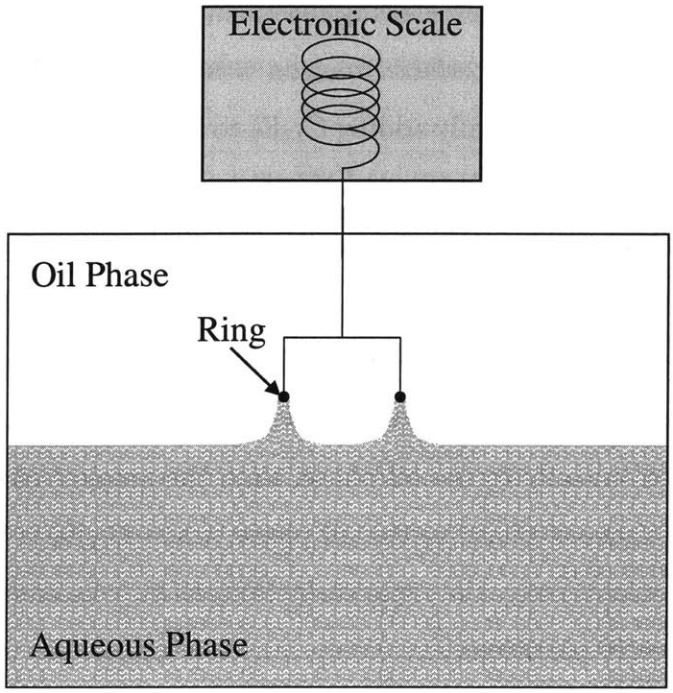

Figure 4-2: Schematic illustration of the ring method for determining the oil-water interfacial tension.

the ring. The value of the surface tension is then modified slightly, as instructed by the manufacturer, by the inclusion of a correction factor first tabulated in detail by Harkins and Jordan.[94]

Each surface tension measurement was repeated three times, and the average result is reported. The experimental uncertainty in the equilibrium interfacial tension measurements was approximately 0.1dyn/cm. The temperature was held constant at $25.0 \pm 0.1°C$ by a thermostatically controlled jacket around the sample. Attainment of equilibrium was verified by taking multiple measurements at various times until a constant interfacial tension value was obtained, which typically occurred within one to two hours. For the nonionic surfactant, $C_{12}E_6$, a solution containing the desired

amount of surfactant was prepared using decane as the solvent. This was then mixed with a pure water phase, and the resulting interfacial tension was measured. It was observed that the equilibrium interfacial tension was reached faster if this procedure was implemented, instead of initially adding $C_{12}E_6$ to the water phase. Note, however, that the same value of the equilibrium interfacial tension was obtained regardless of the phase into which $C_{12}E_6$ was added initially. This behavior is consistent with the fact that $C_{12}E_6$ partitions more readily into the oil phase than into the aqueous phase, which will be discussed further in Section 4.4. That is, for equilibrium to be reached, a smaller amount of $C_{12}E_6$ needs to diffuse from the oil phase to the water phase, when $C_{12}E_6$ is added initially to the oil phase, than the amount of $C_{12}E_6$ that needs to diffuse from the aqueous phase to the oil phase, when $C_{12}E_6$ is added initially to the aqueous phase. Conversely, the ionic surfactant, SDS, was added initially to the aqueous phase, since it partitions extremely into this phase. In fact, a solution of SDS in decane could not be prepared reliably due to its extremely low solubility in this nonpolar oil phase.

4.4 Results

Figure 4-3 shows the predicted (line) and the measured (symbols) decane–water interfacial tensions as a function of $N_{\mathrm{SDS}}/V^{\mathrm{w}}$ for single surfactant solutions of SDS at three different oil-water volume ratios: 10mL/20mL ($\triangle$), 10mL/10mL ($\circ$), and 20mL/10mL ($\diamond$) at T = 25°C. Figure 4-3 clearly shows that the interfacial tensions corresponding to the three oil-water volume ratios examined lie on the same curve, and therefore, that the interfacial tension is independent of the oil-water volume ratio. As discussed in Sections 4.2.2.3 and 4.2.2.4, this indicates that $\left[\frac{V^{\mathrm{o}}}{V^{\mathrm{w}}}\right] \mathrm{K}_{\mathrm{pSDS}} << 1$. Since the oil-water volume ratio is of order unity, one can conclude that $\mathrm{K}_{\mathrm{pSDS}} << 1$, or physically, that the majority of the SDS molecules reside in the aqueous phase. This corroborates the assumption made in Section 4.2.1 that all the ionic species are located in the aqueous phase. Therefore, for SDS, Eq. (4.21) can be utilized as the equilibrium adsorption isotherm. To determine the value of $\Delta\mu_{\mathrm{SDS}}^{\sigma/\mathrm{w},0}$ in Eq. (4.21), the

Table 4.1: Cross-sectional areas, a_i, and standard-state chemical potential differences, $\Delta\mu_i^{0,\sigma/\mathrm{w}}$ and $\Delta\mu_i^{0,\sigma/\mathrm{o}}$, for the surfactants considered in this investigation.

Surfactant i	a_i (Å^2)	$\Delta\mu_i^{0,\sigma/\mathrm{w}}$ (k_BT)	$\Delta\mu_i^{0,\sigma/\mathrm{o}}$ (k_BT)	d (Å)
SDS	25	-67.9	–	4.05
$C_{12}E_6$	42	–	-49.3	–
$C_{12}E_2$	25	-49.2	–	–
$C_{12}E_8$	53	-57.0	–	–

measured interfacial tension at $N_{\mathrm{SDS}}/V^{\mathrm{w}} = 10^{-6} mol/cm^3$ was utilized as described in Section 4.2.2.3. The resulting value of $\Delta\mu_{\mathrm{SDS}}^{\sigma/\mathrm{w},0}$ and of the SDS molecular parameters are listed in Table 4.1. The value used for the pure decane-water interfacial tension, σ_0, was the measured value of 50.4 dyn/cm. *Note that the values of the SDS molecular parameters utilized here for the oil-water interface case are the same as those utilized in Chapter 2 for the air-water interface case.* Note also that the predicted interfacial tension as a function of SDS concentration in Figure 4-3 is in good agreement with the experimental values. In Chapter 2, good agreement was also found between the predicted and the measured surface tensions of an aqueous SDS solution as a function of SDS concentration. One can therefore conclude that *the same theoretical framework, utilizing the same SDS molecular parameters, is capable of accurately predicting both the air-water and the oil-water interfacial tensions in the SDS case.*

Figure 4-4 shows the predicted (line) and the measured (symbols) decane–water interfacial tensions as a function of $N_{\mathrm{C_{12}E_6}}/V^{\mathrm{o}}$ for single surfactant solutions of $C_{12}E_6$ at four different oil-water volume ratios: 10mL/10mL (○), 10mL/20mL (◇), 10mL/30mL (×), and 20mL/10mL (△) at T=25°C. Figure 4-4 clearly shows that the interfacial tensions corresponding to the four oil-water volume ratios examined lie on the same curve, and therefore, that the interfacial tension is independent of the oil-water volume ratio. As discussed in Section 4.2.2.3, this indicates that $\left[\frac{V^{\mathrm{o}}}{V^{\mathrm{w}}}\right] \mathrm{K}_{\mathrm{p_{C_{12}E_6}}} >> 1$. Since

the oil-water volume ratio is of order unity, one can conclude that $K_{p_{C_{12}E_6}} >> 1$, or physically, that the majority of the $C_{12}E_6$ molecules reside in the oil phase. Therefore, for $C_{12}E_6$, Eq. (4.23) can be utilized as the equilibrium adsorption isotherm. To determine the value of $\Delta\mu^{\sigma/o,0}_{C_{12}E_6}$ in Eq. (4.23), the measured interfacial tension at $N_{C_{12}E_6}/V^o = 10^{-6.9} mol/cm^3$ was utilized as described in Section 4.2.2.2. The resulting value of $\Delta\mu^{\sigma/o,0}_{C_{12}E_6}$ and of the $C_{12}E_6$ molecular parameters are listed in Table 4.1. Note that, as in the case of SDS, *the values of the $C_{12}E_6$ molecular parameters utilized here for the oil-water interface case are the same as those utilized in Chapter 2 for the air-water interface case.* Note also that the predicted interfacial tension as a function of $C_{12}E_6$ concentration in Figure 4-4 is in good agreement with the experimental values. In Ref. 12, good agreement was also found between the predicted and the measured surface tensions of an aqueous $C_{12}E_6$ solution as a function of $C_{12}E_6$ concentration. It can therefore be concluded, as in the case of SDS, that *the same theoretical framework, using the same $C_{12}E_6$ molecular parameters, is capable of accurately predicting both the air-water and the oil-water interfacial tensions in the $C_{12}E_6$ case.*

Figure 4-5 shows the predicted (lines) and the measured (symbols) decane–water interfacial tensions as a function of $(N_{SDS} + N_{C_{12}E_6})/V^w = (N_{SDS} + N_{C_{12}E_6})/V^o$ for: (i) single surfactant solutions of SDS (△) and $C_{12}E_6$ (○), and (ii) binary surfactant solutions of 50% SDS–50% $C_{12}E_6$ (□) and 85% SDS–15% $C_{12}E_6$ (◇) at T=25°C. In all cases, the oil phase volume, V^o, and water phase volume, V^w, are equal to 10mL. The surfactant molecular parameters used in the predictions of the interfacial tensions are listed in Table 4.1. Recall that *there are no mixture dependent parameters*, and therefore, that the interfacial tension predictions for the mixed surfactant solutions were made without any fit to the corresponding measurements. Note, again, the good agreement between the predicted interfacial tensions and the experimentally measured values in Figure 4-5.

Finally, Figure 4-6 shows the predicted (lines) and measured (symbols) hexadecane–water interfacial tensions as a function of $(N_{C_{12}E_2} + N_{C_{12}E_8})/V^w$ for: (i) single surfactant solutions of $C_{12}E_2$ (△) and $C_{12}E_8$ (○), and (ii) binary surfactant solutions

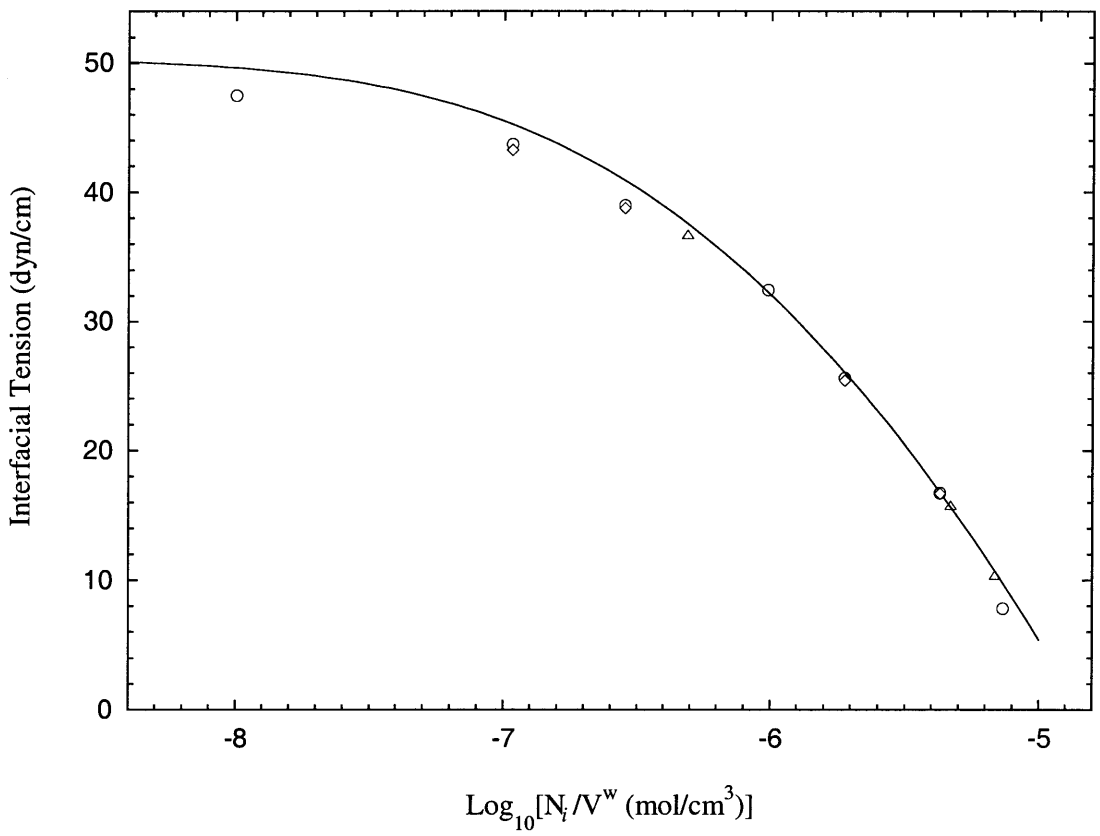

Figure 4-3: Predicted (line) and measured (symbols) decane-water interfacial tensions as a function of $N_{\mathrm{SDS}}/V^{\mathrm{w}}$ for single surfactant solutions of SDS for three different oil-water volume ratios: 10mL/10mL (○), 10mL/20mL (△), and 20mL/10mL (◇) at T=25°C.

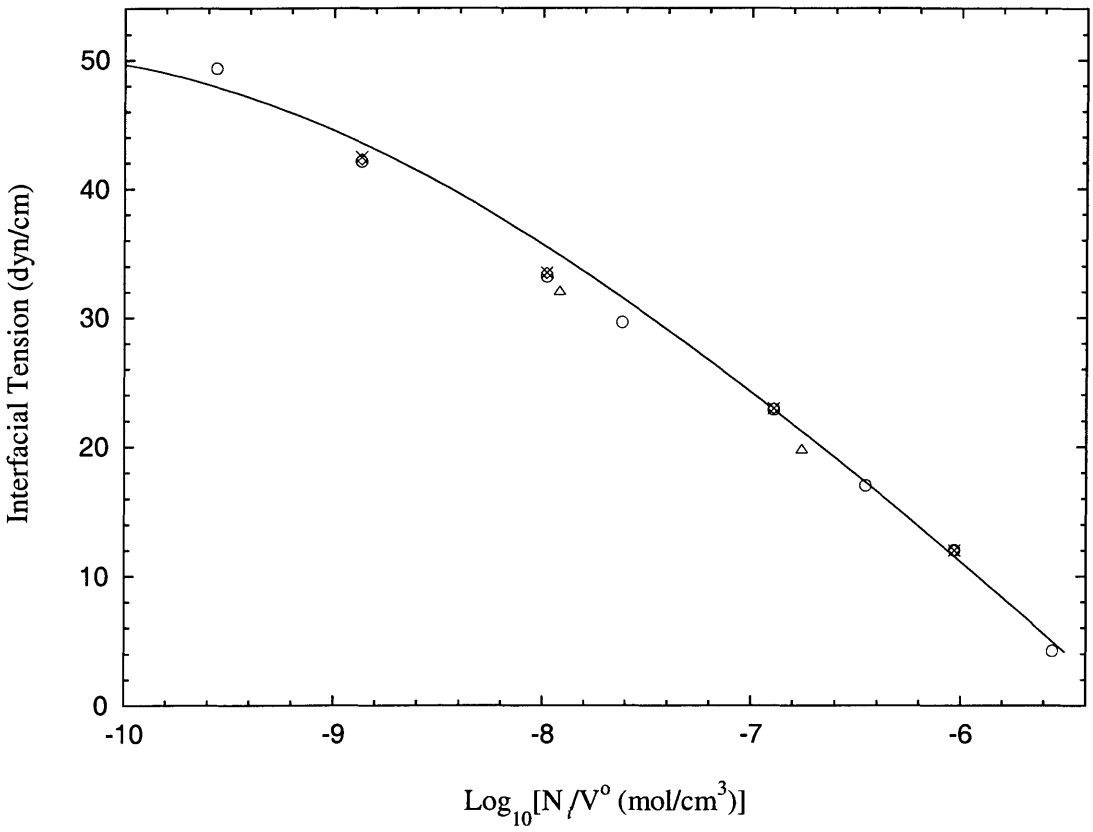

Figure 4-4: Predicted (line) and measured (symbols) decane-water interfacial tensions as a function of $N_{C_{12}E_6}/V^o$ for single surfactant solutions of $C_{12}E_6$ for four different oil-water volume ratios: 10mL/10mL (○), 10mL/20mL (◇), 10mL/30mL (×), and 20mL/10mL (△) at T=25°C.

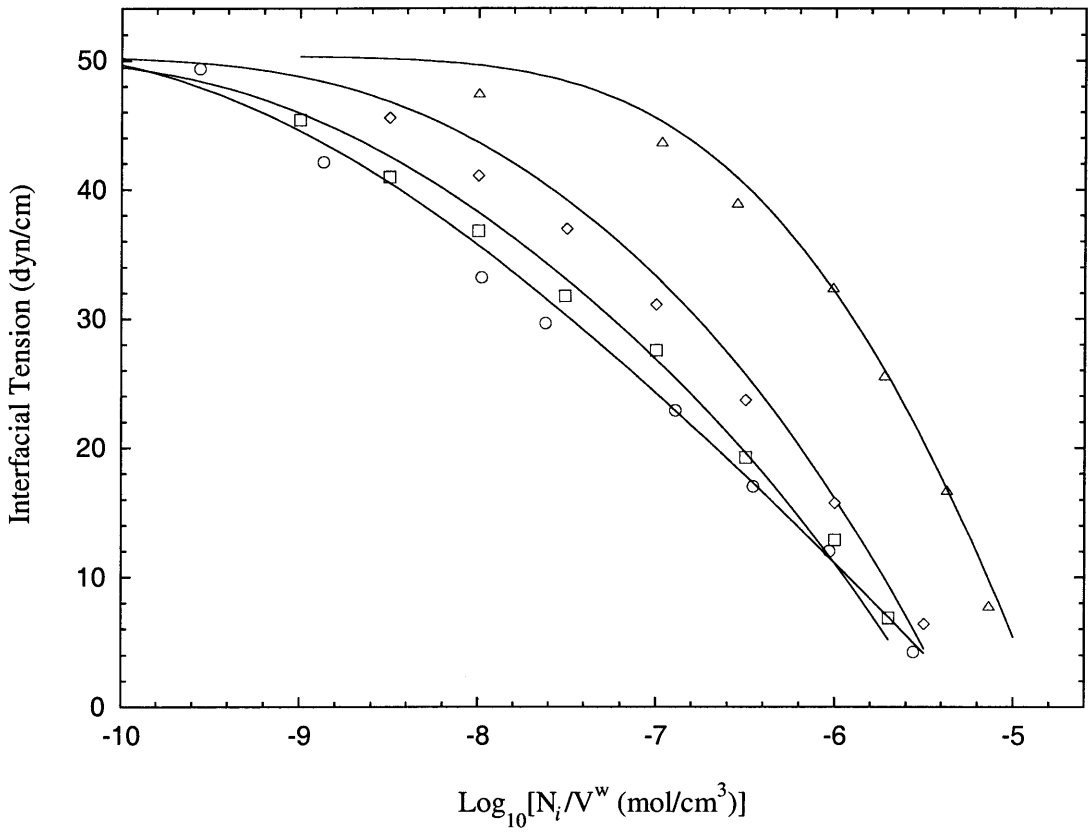

Figure 4-5: Predicted (lines) and measured (symbols) decane–water interfacial tensions as a function of $(N_{\mathrm{SDS}} + N_{\mathrm{C_{12}E_6}})/V^{\mathrm{w}} = (N_{\mathrm{SDS}} + N_{\mathrm{C_{12}E_6}})/V^{\mathrm{o}}$ for: (i) single surfactant solutions of SDS (△, ———) and $C_{12}E_6$ (○, - — - - — -), and (ii) binary surfactant solutions of 50% SDS–50% $C_{12}E_6$ (□, — — —) and 85% SDS–15% $C_{12}E_6$ (◇, ▪ ▪ ▪ ▪) at T=25°C. In all cases, the oil phase volume, V^{o}, and the water phase volume, V^{w}, are equal to 10mL.

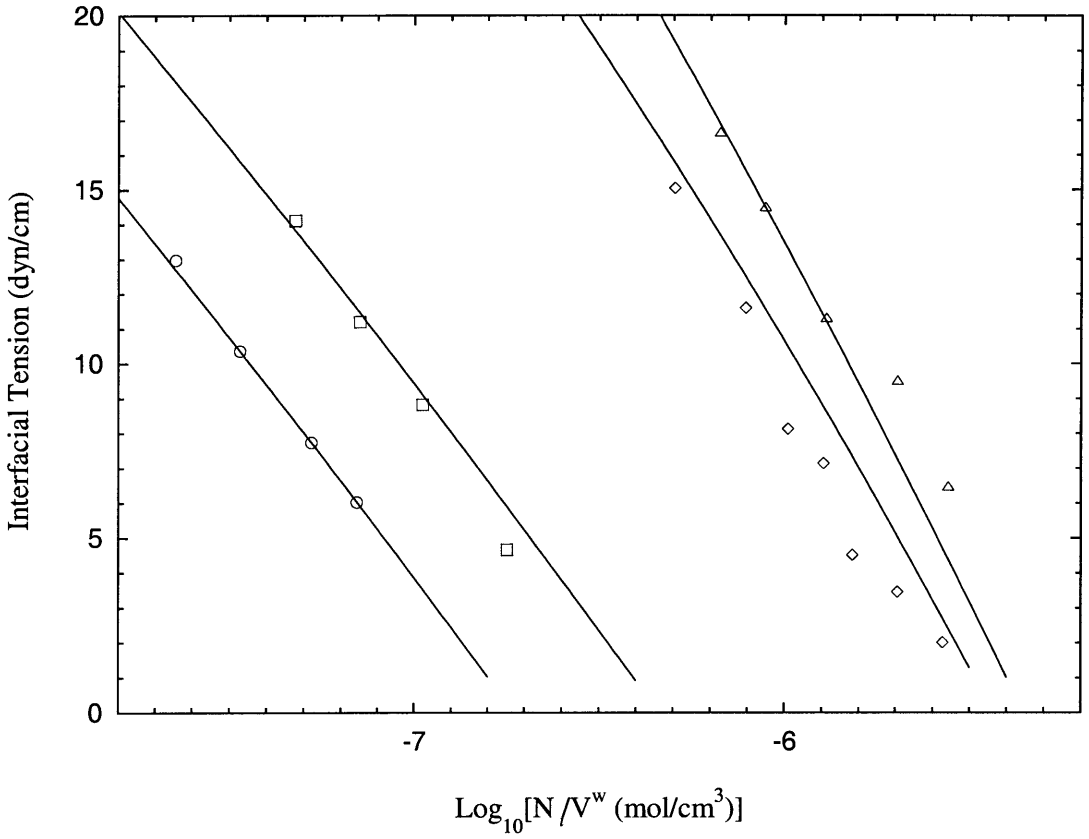

Figure 4-6: Predicted (lines) and measured (symbols) hexadecane–water interfacial tensions as a function of $(N_{C_{12}E_2} + N_{C_{12}E_8})/V^w$ for: (i) single surfactant solutions of $C_{12}E_2$ (△, ———) and $C_{12}E_8$ (○, - — - — -), and (ii) binary surfactant solutions of 62% $C_{12}E_2$–38% $C_{12}E_8$ (□, — — —) and 99% $C_{12}E_2$–1% $C_{12}E_8$ (◇, ▪ ▪ ▪ ▪) at T=25°C. The experimental interfacial tension values are those reported by Rosen and Murphy in Ref. 69.

of 62% $C_{12}E_2$–38% $C_{12}E_8$ (□) and 99% $C_{12}E_2$–1% $C_{12}E_8$ (◇). The experimental measurements are those reported by Rosen and Murphy in Ref. 69, and were made using the spinning-drop technique, where the oil-water volume ratio was extremely small (0.025). Accordingly, as discussed in Section 4.2.2.3, Eq. (4.20) is satisfied and Eq. (4.21) can be used as the equilibrium adsorption isotherm. Note that Eq. (4.20) is satisfied in this case as a result of the extremely small oil-water volume ratio and not as a result of an extremely small surfactant partition coefficient. The values of the surfactant molecular parameters used in the interfacial tension predictions shown in Figure 4-6 are listed in Table 4.1. The value used for the pure hexadecane-water interfacial tension, σ_0, is the measured value of 52.1 dyn/cm.[69] Note that the cross-sectional areas of both surfactants were determined using the computational method described in Ref. 12. To determine the values of $\Delta\mu^{\sigma/w,0}_{C_{12}E_2}$ and $\Delta\mu^{\sigma/w,0}_{C_{12}E_8}$ in Eq. (4.21), the measured interfacial tensions at: $N_{C_{12}E_2}/V^w = 1.3 \times 10^{-6} mol/cm^3$ for $C_{12}E_2$ and $N_{C_{12}E_8}/V^w = 3.4 \times 10^{-8} mol/cm^3$ for $C_{12}E_8$ were utilized as described in Section 4.2.2.2. Note again that, although *there are no parameters fitted to measurements carried out on the mixed $C_{12}E_2$–$C_{12}E_8$ solutions,* there is good agreement between the predicted interfacial tensions and the experimentally measured values in Figure 4-6.

4.5 Conclusions

In this chapter, a molecular-thermodynamic framework to predict the interfacial tension and the interfacial concentration and composition at the oil-water interface of solutions containing mixtures having any number of surfactant components was presented. Because this theoretical framework is based on the molecular characteristics of the surfactants considered, the surface equation of state contains no experimentally determined parameters. Specifically, the surfactant molecular parameters in the equation of state include the molecular cross-sectional area, and, in the case of charged surfactants, the valence and the location of any electrostatic charges in the surfactant polar head. The equilibrium adsorption isotherm contains only one exper-

imentally determined parameter for each surfactant component i in the mixture –the modified standard-state chemical potential difference of a surfactant molecule of type i adsorbed at the interface and one present in either the bulk oil phase or the bulk aqueous phase. This parameter can be determined from a single interfacial tension measurement carried out on a solution of surfactant component i.

Furthermore, when applicable, the oil-water partition coefficient of surfactant component i can be determined by conducting a second interfacial tension measurement on the solution of surfactant component i. Note that the surfactant oil-water partition coefficients are not required to predict the interfacial tensions when the oil-water volume ratio is held constant, or when the surfactant molecules partition extremely into one of the two bulk phases.

A notable practical advantage of the theoretical framework presented in this chapter is that it contains *no mixture dependent experimentally determined parameters.* Indeed, no measurements on the mixed surfactant solutions are required. The predictions made by the theory presented here include the interfacial tension and the interfacial concentration and composition as a function of the total bulk surfactant concentration and composition and the oil-water volume ratio (that is, the total amount of each surfactant component present in the mixture, and the volumes of the aqueous and the oil phases), for a solution containing any number of surfactant components below the CMC.

Good agreement was found between the theoretically predicted interfacial tensions and the experimentally measured ones for solutions containing SDS, $C_{12}E_6$, as well as their binary mixtures. Furthermore, in Chapter 2, good agreement was found between the theoretically predicted and the experimentally measured air-water surface tensions of solutions containing these same surfactants using the same molecular parameters. Moreover, good agreement was also found between the theoretically predicted and the experimentally measured[69] interfacial tensions of solutions containing $C_{12}E_2$, $C_{12}E_8$, and their binary mixtures, utilizing molecular parameters that were determined using a previously developed computational procedure applicable to C_iE_j type nonionic surfactants adsorbed at the air-water interface.[12] This ability to ac-

curately predict both surface and interfacial tensions of solutions containing single surfactants and their binary mixtures, using the same theoretical framework and surfactant molecular parameters, demonstrates the broad range of validity and applicability of the molecular-thermodynamic interfacial theory presented in Chapters 2, 3, and 4.

By reducing the number of experimentally determined parameters (as compared to other commonly used theoretical approaches, such as those based on the Langmuir adsorption model), as well as by eliminating altogether the need for any mixture dependent parameters (such as the interaction parameters in Regular Solution Theory based models), the theoretical framework presented in Chapters 2, 3, and 4 can significantly reduce the amount of experimentation required to predict the interfacial properties of mixed surfactant solutions. This predictive ability, in turn, can help in the design and optimization of surfactant solutions of practical relevance that display desirable interfacial behavior by reducing the amount of trial-and-error type experimentation.

In the next chapter, the equilibrium theoretical framework developed in Chapter 2 is utilized as a basis to predict the dynamic surface tensions of surfactant mixtures where adsorption at the air-water interface is diffusion controlled.

Chapter 5

Theoretical Investigation of the Dynamic Interfacial Adsorption in Aqueous Surfactant Mixtures

5.1 Introduction

The dynamic interfacial properties of aqueous surfactant solutions, including the surface tension, the surface concentration, and the surface composition, often play a key role in many practical applications involving surfactants. As discussed in Chapter 1, the dynamic, as opposed to the equilibrium, interfacial properties are important for applications that have a timescale that is smaller than, or on the order of, the timescale for adsorption of the surfactant. Such applications include the stabilization of foams in small-scale household applications involving detergents, as well as in large-scale applications of fire-fighting foams, the rapid spreading of an active ingredient in agricultural sprays or paints, where spreading must occur prior to the evaporation of the solvent, and others (for an overview of applied aspects of dynamic interfacial phenomena, see Ref. 95).

As a result of the importance of dynamic interfacial properties, this research area has received considerable attention following the pioneering work of Ward and

Tordai[96] (see Refs. 13, 97, and 98 for recent reviews). A number of researchers have solved the Ward and Tordai model by assuming that the diffusion of the surfactant molecules in the bulk solution constitutes the limiting barrier to adsorption.[99–103] This assumption results in an instantaneous equilibrium between the surfactant molecules adsorbed at the interface and those present in the aqueous phase adjacent to the interface (referred to as the "sublayer"). This relationship between the surfactant molecules at the interface and those in the sublayer is specified by a particular *equilibrium adsorption model.* Experimental observations in many surfactant systems (primarily those of the nonionic type) have shown good agreement with the diffusion-controlled model.[101,104–106] Several researchers have added a kinetic adsorption barrier, and found that this better describes the dynamic adsorption behavior of some surfactants (for example, ionic surfactants and nonionic surfactants at higher concentrations).[107–109,31,110–115,98] Specifically, if the timescale for diffusion is large, such as in the case of a very dilute surfactant solution (see Section 5.2.2), then diffusion becomes the rate-determining process (see Refs. 116–118 for a more detailed discussion). More generally, the diffusion-controlled model provides a useful limiting rate, in that adsorption cannot occur faster than diffusion. Note that the previous work cited above has been concerned primarily with the dynamic interfacial adsorption of a *single* surfactant species.

The examination of mixed surfactant solutions is of great interest since virtually all practical applications of surfactants involve the use of surfactant mixtures. In some cases, the use of mixed surfactants results from a desire to take advantage of synergism between the individual surfactant species. In other cases, environmental or health concerns dictate that a mixture of known and approved surfactants be used instead of developing a new surfactant. Finally, the prohibitively high cost of separating a single, pure surfactant often dictates that mixtures be used even in cases when they are not employed intentionally.

The diffusion-limited dynamic adsorption in aqueous *binary* surfactant mixtures has been investigated recently both theoretically and experimentally.[119–122] The primary difference among the theories in Refs. 119–122, including the theory presented

in this chapter, is in the *equilibrium adsorption model* utilized to relate the concentrations of the various surfactant molecules present at the interface to those present in the sublayer. Specifically, Fainerman and Miller[119,120] utilized a generalized Langmuir model that makes use of an experimentally determined partial molar area for each surfactant component, and assumes no interactions between the adsorbed surfactant molecules. Siddiqui and Franses[121] utilized the Nonideal Adsorbed Solution model which makes use of a Langmuir-type isotherm for the individual surfactant components, and treats interactions between the different surfactant components with a regular solution theory-based approach which adds an experimentally determined parameter for the binary surfactant mixture. Finally, Ariel et al.[122] utilized an equilibrium model based on a free-energy formalism that is similar to the generalized Langmuir approach with the addition of experimentally fitted parameters accounting for the interactions between surfactant molecules of the same type, as well as between the different surfactant components.

In this chapter, the Ward and Tordai model is further extended to include mixtures that contain *any number* of surfactant components.[123] This is accomplished through the use of the equilibrium adsorption model developed in Chapter 2 (which forms the underlying basis for the dynamic model) that is capable of treating mixtures containing any number of surfactant components.[12,88,89] Furthermore, as discussed in Chapter 2, the equilibrium adsorption model used here is based on the molecular characteristics of the surfactants. As a result, insight is provided as to how these surfactant molecular characteristics, especially the molecular size, can lead to interesting dynamic adsorption behavior. Another significant advantage of utilizing the equilibrium adsorption model adopted in this chapter is in the ability to predict both the equilibrium and the dynamic adsorption behavior of surfactant mixtures without utilizing any mixture dependent parameters. In other words, no additional experiments on the mixed surfactant system are necessary. As a result, the theoretical framework presented here leads to a significant reduction in the amount of experimentation required to predict the dynamic interfacial properties of surfactant mixtures. A simplified timescale approach designed to allow "quick" insight into the relation-

ship between the molecular structure of the surfactants and their dynamic interfacial properties is developed for both single surfactants and surfactant mixtures.

Specifically, in this chapter, Fickian diffusion of all the surfactant components is utilized to obtain a generalized version of the Ward and Tordai equation appropriate for the treatment of surfactant mixtures. Only surfactants below the critical micelle concentration (CMC) are considered, and it is assumed that surfactant diffusion in the bulk solution constitutes the rate limiting process. The dynamic adsorption behavior of micellar solutions is discussed in Appendix D.

Note that we restrict ourselves to nonionic surfactants so that the electric field that would be generated in the case of adsorbed ionic surfactants, including its effect on the diffusion of ionic surfactants, does not need to be accounted for. However, one can extend the theoretical framework presented here to solutions containing ionic surfactants by utilizing the quasi-equilibrium approximation (see Refs. 124 and 125 for a detailed discussion).

The surfactant molecular parameters required as inputs to the theoretical framework presented here include those which appear in the equilibrium adsorption theory (see Chapter 2). These include (for each surfactant component in the mixture): (i) the molecular cross-sectional area (which can be deduced from the known surfactant chemical structure), (ii) the second-order virial coefficients (which, for surfactants having linear alkane tails, can be computed from the number of carbon atoms in the appropriate surfactant tails), and (iii) the free energy of adsorption (see below). The only other required surfactant molecular parameters are the diffusion coefficients of each surfactant component which, in principle, can be estimated theoretically (for example, by using the Stokes-Einstein theory or a scaling-law model[126]), or can be obtained experimentally.[111] The predictions of the theoretical framework presented here include the surface tension, the surface concentration, and the surface composition, all as a function of time, for a given total bulk surfactant concentration and composition.

The remainder of the chapter is organized as follows. In Section 5.2, the theoretical model of the dynamic adsorption of surfactant mixtures is developed, and a

simplified timescale approach for both single surfactants and surfactant mixtures is presented. In Section 5.3, this theoretical framework, as well as physical insight, is utilized to analyze four illustrative examples of interesting dynamic interfacial behavior exhibited by hypothetical surfactant mixtures where the surfactant molecular parameters can be varied to demonstrate a range of interesting dynamic interfacial behavior. These examples are also utilized to implement and test the simplified timescale approach. In Section 5.4, concluding remarks are provided. A detailed comparison of dynamic surface tensions predicted utilizing the theoretical framework presented in this chapter, with experimentally measured dynamic surface tensions of aqueous solutions containing binary nonionic surfactant mixtures is presented in the next chapter.

5.2 Theoretical Framework

5.2.1 Diffusion Controlled Adsorption Model

First, the case of an aqueous surfactant solution containing a mixture of n nonionic surfactants below the critical micelle concentration (CMC) is examined. As in the case examined by Ward and Tordai, it is assumed here that the interface is initially clean (that is, an interface where the surface concentrations of all the surfactant components are zero at $t = 0$). This chapter specifically treats the case of a flat interface (see Chapter 6 and Refs. 111 and 127 for a detailed treatment of the spherical interface case), and assumes that the mass transport of each surfactant component obeys Fickian diffusion. Under these assumptions, the mass transport in the aqueous phase is given by:

$$\frac{\partial n_i}{\partial t} = D_i \frac{\partial^2 n_i}{\partial x^2} \tag{5.1}$$

where n_i is the concentration (as a number density) of surfactants of type i, D_i is the diffusion coefficient of surfactants of type i, t is time, and x is the distance from the

flat interface. A mass balance at the interface yields:

$$\frac{\partial \Gamma_i}{\partial t} = D_i \left. \frac{\partial n_i}{\partial x} \right|_{x=0} \tag{5.2}$$

where $\Gamma_i = n_i^\sigma / A$ is the surface concentration of surfactants of type i (n_i^σ is the number of surfactant molecules of type i adsorbed at the surface and A is the surface area). Furthermore, the assumption that the interface is initially clean and created instantaneously yields:

$$\Gamma_i (t = 0) = 0 \tag{5.3}$$

and

$$n_i (t = 0, x) = n_i^{\mathrm{w}} \tag{5.4}$$

where n_i^{w} is the bulk number density of surfactants of type i. Finally, the infinite nature of the aqueous phase leads to the following boundary condition:

$$n_i (t, x \to \infty) = n_i^{\mathrm{w}} \tag{5.5}$$

Note that Eqs. (5.1)–(5.5) each represents a set of n equations corresponding to $i = 1$ to n. Equations (5.1)–(5.5) can be solved in a manner analogous to the single surfactant case, leading to a form of the Ward and Tordai equation generalized for surfactant mixtures. Specifically,

$$\Gamma_i (t) = 2\sqrt{\frac{D_i}{\pi}} \left[n_i^{\mathrm{w}} \sqrt{t} - \int_0^{\sqrt{t}} n_i^0 \left(t - \tilde{t} \right) d\sqrt{\tilde{t}} \right] \tag{5.6}$$

where $n_i^0 (t) = n_i (t, x = 0)$ is the sublayer concentration of surfactants of type i. Note that Eq. (5.6) is also a set of n equations corresponding to $i = 1$ to n.

As in the case of a single surfactant solution, in the mixed surfactant case, the set of n equations given in Eq. (5.6) can be solved through the use of the set of n initial conditions given by Eq. (5.3), along with a closure relationship between the surface concentration, $\Gamma_i (t)$, and the sublayer concentration, $n_i^0 (t) \equiv n_i (t, x = 0)$, for each

surfactant component. As stated in Section 5.1, it is assumed that the surfactant adsorption is diffusion controlled, that is, that the surfactant molecules at the surface remain in equilibrium with those in the sublayer at all times. Using the equilibrium adsorption theory developed in Chapter 2, this equilibrium condition can be expressed as follows:[12,88,89]

$$\ln\left(\frac{n_i^0}{n_w^0+\sum_{k=1}^{n} n_k^0}\right) = \frac{\Delta\mu_i^0}{\mathrm{k_B}T} + \ln\left(\frac{\Gamma_i}{1-\sum_{k=1}^{n}\Gamma_k \mathrm{a}_k}\right) + \frac{\mathrm{a}_i\sum_{k=1}^{n}\Gamma_k + 2\pi \mathrm{r}_i\sum_{k=1}^{n}\Gamma_k \mathrm{r}_k}{1-\sum_{k=1}^{n}\Gamma_k \mathrm{a}_k}$$

$$+ \frac{\pi \mathrm{a}_i\left(\sum_{k=1}^{n}\Gamma_k \mathrm{r}_k\right)^2}{\left(1-\sum_{k=1}^{n}\Gamma_k \mathrm{a}_k\right)^2} + 2\sum_{k=1}^{n} B_{ik}\Gamma_k \tag{5.7}$$

where $n_i^0 \Big/ \left(n_w^0 + \sum_{k=1}^{n} n_k^0\right) \approx n_i^0/n_w^0$ is the mole fraction of surfactant molecules of type i in the sublayer (n_w^0 is the number density of water in the sublayer, which is approximately a constant since the surfactant concentration is dilute), a_i and r_i are the cross-sectional area and radius of the adsorbed surfactant molecules of type i, respectively, modeled as hard discs, B_{ij} is the second-order virial coefficient between surfactant molecules of type i and j, $\Delta\mu_i^0$ is the difference in standard-state chemical potential of a surfactant molecule of type i at the interface and in the bulk aqueous phase[12] (also referred to as the free energy of adsorption of surfactant molecules of type i), $\mathrm{k_B}$ is the Boltzmann constant, and T is the absolute temperature. Note that the free energy of adsorption, $\Delta\mu_i^0$, is the one fitted parameter for the equilibrium adsorption isotherm. In addition, note that Eq. (5.7) represents a set of n equations corresponding to $i = 1$ to n.

The surfactant surface concentrations as a function of time, $\Gamma_i(t)$, can be efficiently solved for numerically using an explicit iterative scheme similar to the one used in Ref. 100 for the single surfactant case. Specifically, starting with $\Gamma_i(t=0) = 0$ from Eq. (5.3), the set of n surface concentrations, $\{\Gamma_i(t)\}$, and the set of n sublayer

concentrations, $\{n_i^0(t)\}$, at subsequent discrete time intervals can be calculated by simultaneously solving the set of n equations given in Eq. (5.6) and the set of n equations given in Eq. (5.7). The value of the step size in time should be much smaller than the time scale for adsorption, τ_D, which will be discussed in detail in Sections 5.2.2 and 5.2.3. For the predictions made in this chapter, a step size value of $10^{-3}s$ was used. For surfactant systems that involve very different timescales for adsorption, such as in the case of a mixture of a very fast adsorbing surfactant and a very slow adsorbing surfactant, an implicit technique can be utilized (see Refs. 102 and 128 for details) to improve the stability of the numerical method. However, it was found that this is not necessary for the surfactant systems considered here. Once the set of $\{\Gamma_i(t)\}$ values is calculated, the dynamic surface tension can be predicted using the equilibrium surface equation of state,[110,129] which for the nonionic surfactant mixtures considered here can be written as follows:[12,88,89]

$$\sigma = \sigma_0 - \mathrm{k_B}T \left\{ \frac{\sum_{k=1}^{n} \Gamma_k}{1 - \sum_{k=1}^{n} \Gamma_k \mathrm{a}_k} + \frac{\pi \left(\sum_{k=1}^{n} \Gamma_k \mathrm{r}_k \right)^2}{\left(1 - \sum_{k=1}^{n} \Gamma_k \mathrm{a}_k \right)^2} + \sum\nolimits_{jk} \mathrm{B}_{jk} \Gamma_j \Gamma_k \right\} \tag{5.8}$$

where σ_0 is the surface tension of pure water.

Note that the *equilibrium* surface tension and surface concentrations can be calculated by utilizing Eqs. (5.7) and (5.8) without solving for the dynamic surface tension and surface concentrations. This is accomplished by first calculating the equilibrium surface concentrations, Γ_i^{eq}, by solving Eq. (5.7) with $n_i^0 = n_i^{\mathrm{w}}$, since, at equilibrium, the sublayer concentration is equal to the bulk concentration. Finally, the equilibrium surface tension can be calculated by substituting the equilibrium values of the surface concentrations in Eq. (5.8). Results obtained using this theory will be discussed in detail in Section 5.3 for various hypothetical surfactant mixtures where the surfactant molecular parameters can be varied to demonstrate a range of interesting dynamic interfacial behavior.

5.2.2 Simplified Timescale Analysis: Single Surfactants

It is often valuable to have a simplified theory that can be utilized to quickly estimate the time required for the surface tension (or surface concentration) to reach equilibrium. In this section, the case of a single surfactant solution will be discussed, and the relationship between the various molecular parameters in the theory and the resulting the dynamic surface adsorption will be examined. Mixed surfactant solutions will be discussed in detail in Section 5.2.3.

For a single surfactant solution, Eq. (5.6) can be made dimensionless by using the bulk surfactant concentration, n^{w}, as the characteristic bulk concentration, the equilibrium surface concentration, Γ^{eq}, as the characteristic surface concentration, and the following expression for the characteristic time, τ_D (see Refs. 116, 117, and 127 for a detailed description):

$$\tau_D = \frac{(\Gamma^{eq}/n^{\mathrm{w}})^2}{D} \tag{5.9}$$

Note that the subscript i has been omitted from Γ^{eq}, n^{w}, and D, since Eq. (5.9) applies only a single surfactant solution. In addition, note that in Eq. (5.9), the quantity $(\Gamma^{eq}/n^{\mathrm{w}})$ is the characteristic length of adsorption. This can be understood physically by noting that, for a given surface area A, the number of surfactant molecules adsorbed at the interface at equilibrium is $A\Gamma^{eq}$. To obtain a volume of solution that contains the same number of surfactant molecules, one must penetrate into the solution to a thickness of L, such that, $A\Gamma^{eq} = ALn^{\mathrm{w}}$. Solving for the penetration thickness yields a length scale for adsorption of $L = \Gamma^{eq}/n^{\mathrm{w}}$.

It is important to note that, since Γ^{eq} in Eq. (5.9) is the *equilibrium surface concentration*, one can estimate the timescale for adsorption of the surfactant by simply calculating the equilibrium surface concentration as explained in Section 5.2.1, which involves significantly less numerical computation than the calculation of the entire dynamic surface concentration and surface tension profiles.

This timescale analysis is also useful in analyzing the relationship between the molecular structure of a surfactant and its dynamic interfacial properties. For ex-

ample, Eq. (5.9) clearly shows that the larger the value of the diffusion coefficient, D, the faster the adsorption (that is, the smaller the value of τ_D), as one might expect. To illustrate the effect of the surfactant molecular parameters controlling the equilibrium adsorption theory, the surface equation of state, Eq. (5.8), for a single surfactant solution at equilibrium, can be rewritten as follows:

$$\sigma = \sigma_0 - \mathrm{k_B}T \left\{ \frac{\Gamma^{eq}}{1 - \Gamma^{eq}\mathrm{a}} + \frac{\pi \left(\Gamma^{eq}\mathrm{r}\right)^2}{\left(1 - \Gamma^{eq}\mathrm{a}\right)^2} + \mathrm{B}\left(\Gamma^{eq}\right)^2 \right\} \tag{5.10}$$

where the subscript i has been omitted from the cross-sectional area, a, the radius, r, and the second-order virial coefficient, B, since Eq. (5.10) refers to a single surfactant solution. If everything else is equal, a larger surfactant cross-sectional area requires a smaller surface concentration in order to attain a given surface tension value. While physically intuitive, this can also be seen mathematically by the fact that an increase in the surfactant cross-sectional area, a, leads to an increase in the bracketed term in Eq. (5.10), which can be counteracted by a decrease in Γ^{eq}. This, in turn, leads to faster adsorption, since as Γ^{eq} decreases in Eq. (5.9), τ_D decreases. On the other hand, a smaller (or more negative, and hence more attractive) second-order virial coefficient requires a larger surface concentration in order to attain a given surface tension value. This can be seen mathematically by the fact that a decrease in B leads to a decrease in the bracketed term in Eq. (5.10), which can be counteracted by an increase in Γ^{eq}. This, in turn, leads to slower adsorption, since as Γ^{eq} increases in Eq. (5.9), τ_D increases. Finally, a more surface active surfactant will attain the desired surface tension value at a lower bulk surfactant concentration, n_i^{w}, (which is precisely what is meant by "more surface active"), and hence, τ_D in Eq. (5.9) will be larger and the adsorption will be slower. Note that, in the context of the equilibrium theory, if everything else is equal, a more surface active surfactant is characterized by a more negative (larger in absolute value) standard-state chemical potential difference, $\Delta\mu_i^0$. This can be seen in Eq. (5.7) with n_i^0 replaced by n_i^{w} (since, at equilibrium, the sublayer concentration is equal to the bulk concentration). In that case, a decrease in $\Delta\mu_i^0$ leads to a decrease in the first term on the right-hand side of Eq. (5.7), which

can be counteracted by a decrease in $n_i^0 = n_i^w$ on the left-hand side of Eq. (5.7).

5.2.3 Simplified Timescale Analysis: Surfactant Mixtures

In analogy to the single surfactant case, one can associate a timescale for adsorption, τ_{D_i}, for each surfactant component, i, in the mixture. Specifically,

$$\tau_{D_i} = \frac{(\Gamma_i/n_i^w)^2}{D_i} \tag{5.11}$$

However, as will be shown in detail in the illustrative examples presented in Section 5.3, this timescale analysis is more involved in the case of surfactant mixtures because of various possible choices of surface concentrations, Γ_i, in Eq. (5.11). As a first approximation, the *equilibrium* surface concentration value of each surfactant component, Γ_i^{eq} (see Section 5.2.1), can be used in Eq. (5.11) to estimate the adsorption timescale for that surfactant component. If the resulting timescales for adsorption corresponding to each of the surfactant components have similar values, then the timescale for adsorption for each component can be taken to be the value so obtained. However, if the values obtained are very different, then using the *equilibrium* values for the surface concentrations (that is, using $\Gamma_i = \Gamma_i^{eq}$ in Eq (5.11)) will not yield a very good estimate of the timescale for adsorption, as discussed in detail next.

For surfactant mixtures that contain components having different timescales for adsorption, the adsorption of one surfactant component may lead to the desorption of another surfactant component that had adsorbed previously. This effect is particularly large in the case of a faster, less surface active surfactant mixed with a slower, more surface active surfactant (as will be shown in Section 5.3.2) since in that case, the later arriving surfactant will significantly displace the less surface active surfactant that had already adsorbed. (Note that in the case of very strong synergism between the adsorbed surfactant components, the surface concentration of the surfactant component that adsorbs first may be subsequently *increased* by the later adsorbing surfactant component. However, this case will not be discussed in detail here since such strong synergism is most commonly observed with mixtures of ionic[130]

or zwitterionic surfactants,[56] which are not considered here). As a result, the surface concentration of some surfactant components will attain a maximum value, Γ_i^{max}, before reaching an equilibrium value, and the final equilibrium surface concentration value may be significantly lower than Γ_i^{max}. This will make Γ_i^{eq} not suitable for use in Eq. (5.11). However, a simplified methodology for treating such a case will be discussed as part of Example 2 in Section 5.3.2.

5.3 Results

In this section, the theory developed in Section 5.2, including the simplified timescale analysis, is implemented in four examples to illustrate several types of interesting and useful dynamic adsorption behavior of hypothetical surfactant mixtures where the surfactant molecular parameters can be tuned to demonstrate a range of interesting dynamic interfacial behavior. The practical implications of the various dynamic adsorption behaviors predicted in this section will be discussed in more detail in Section 5.4. The surfactant parameters corresponding to each example are described in the following subsections. In the four examples presented, any attractive interactions between the adsorbed surfactant molecules are neglected (that is, $B_{ij} = 0$ for all i and j in Eqs. (5.7) and (5.8)). This is done to emphasize that the predicted dynamic interfacial behavior, which, as will be shown below, includes examples of *dynamic synergism*, is not a manifestation of any attractive interactions between the adsorbed surfactant molecules, but instead, reflects the differences in the molecular sizes (as reflected in the a_i values) as well as in the surface activities (as reflected in the $\Delta\mu_i^0$ values) of the surfactants involved. Furthermore, in the three binary surfactant mixtures (Examples 1-3), the diffusion coefficients, D_i, where chosen to be the same for both surfactants to emphasize that the resulting dynamic interfacial behavior is only due to differences in the equilibrium properties, rather than to differences in the transport properties. Finally, in the four examples that follow, the temperature was set at 25°C.

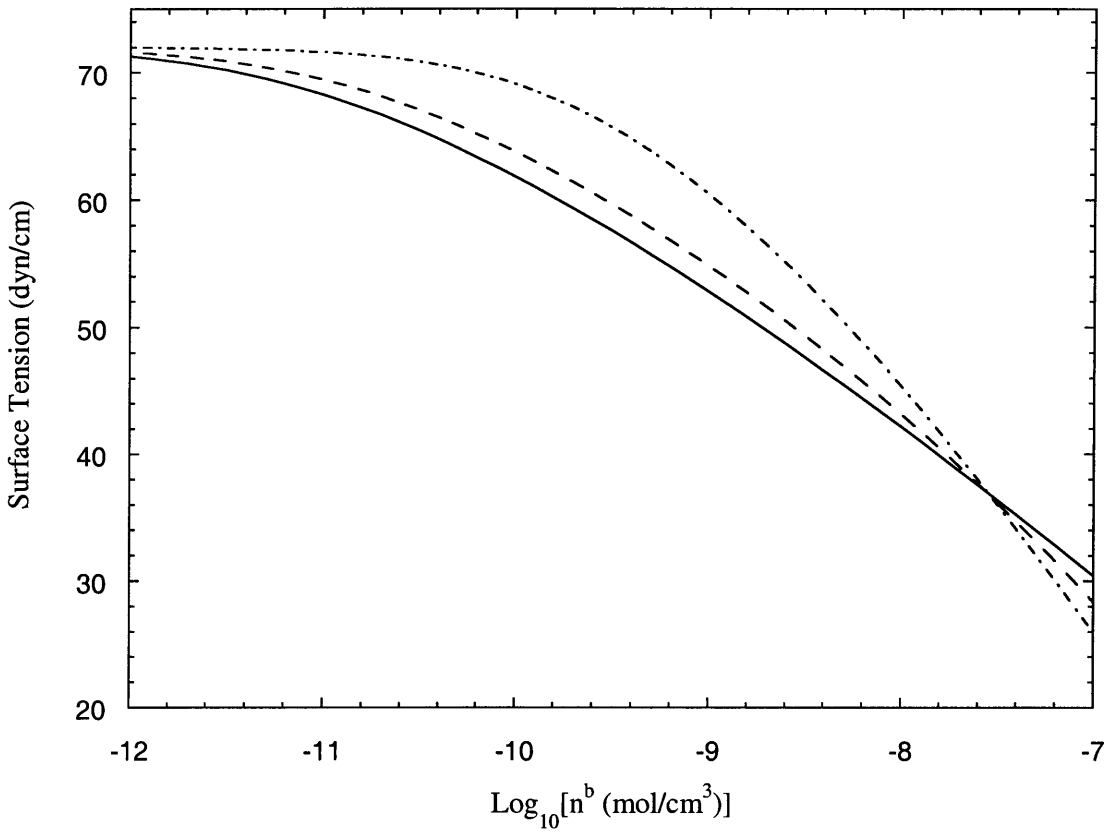

Figure 5-1: Equilibrium surface tensions as a function of total bulk surfactant concentration for aqueous solutions of: Surfactant a (———), Surfactant b (- — - — -), and a binary mixture of 50% Surfactant a – 50% Surfactant b (— — —).

5.3.1 Example 1: Binary Mixture of Surfactants Having Similar Timescales of Adsorption

In this first example, the adsorption behavior of a binary mixture of Surfactants a and b is considered. The molecular parameters corresponding to each surfactant are listed in Table 5.1. The specific choice of a_i and $\Delta\mu_i^0$ values in Table 5.1 is explained below.

Figure 5-1 shows the *equilibrium* surface tensions as a function of total bulk surfactant concentration for aqueous solutions of: (i) Surfactant a (———), (ii) Surfactant b (- — - — -), and (iii) a binary mixture of 50% Surfactant a – 50% Surfactant b

Table 5.1: Cross-sectional areas, a_i, standard-state chemical potential differences, $\Delta\mu_i^0$, and diffusion coefficients, D_i, of Surfactants a and b, corresponding to the binary surfactant mixture in Example 1.

Surfactant i	a_i (Å^2)	$\Delta\mu_i^0$ (k_BT)	D_i (cm^2/s)
a	50	-55.4	6×10^{-6}
b	25	-52.4	6×10^{-6}

(— — —), as predicted by the equilibrium theory (Eqs. (5.7) and (5.8)). Note that the predicted equilibrium surface tension behaviors of Surfactants a and b shown in Figure 5-1 are within the range of behaviors which are typically observed (see Ref. 131 for a review of the surface behavior of typical surfactants). Note also that the choice of a_i and $\Delta\mu_i$ values results in both single surfactant solutions, as well as their binary mixture, attaining the same surface tension value of 37dyn/cm at a total bulk surfactant concentration of $2.8 \times 10^{-8} mol/cm^3$ (corresponding to the point at which the three surface tension curves cross in Figure 5-1).

Figure 5-2 shows the dynamic surface tensions of the three solutions (i)–(iii) described above, all at a total bulk surfactant concentration of $2.8 \times 10^{-8} mol/cm^3$. Note that, at long times, all the three curves in Figure 5-2 approach the same surface tension value of 37 dyn/cm, since, as stressed above, the three solutions have the same equilibrium surface tension at this total bulk surfactant concentration. In addition, note that for the *single surfactant solutions*, Surfactant a has a lower equilibrium surface concentration than Surfactant b ($1.2 \times 10^{14} cm^{-2}$ and $2.0 \times 10^{14} cm^{-2}$, respectively) which leads, through the use of Eq. (5.9), to a shorter timescale of adsorption for Surfactant a as compared to Surfactant b (8.9s and 24s, respectively). This can also be seen in Figure 5-2, where the surface tension curve corresponding to Surfactant a (———) plateaus (reaches equilibrium) before that corresponding to Surfactant b (- — - — -). This difference in adsorption timescales of the two single

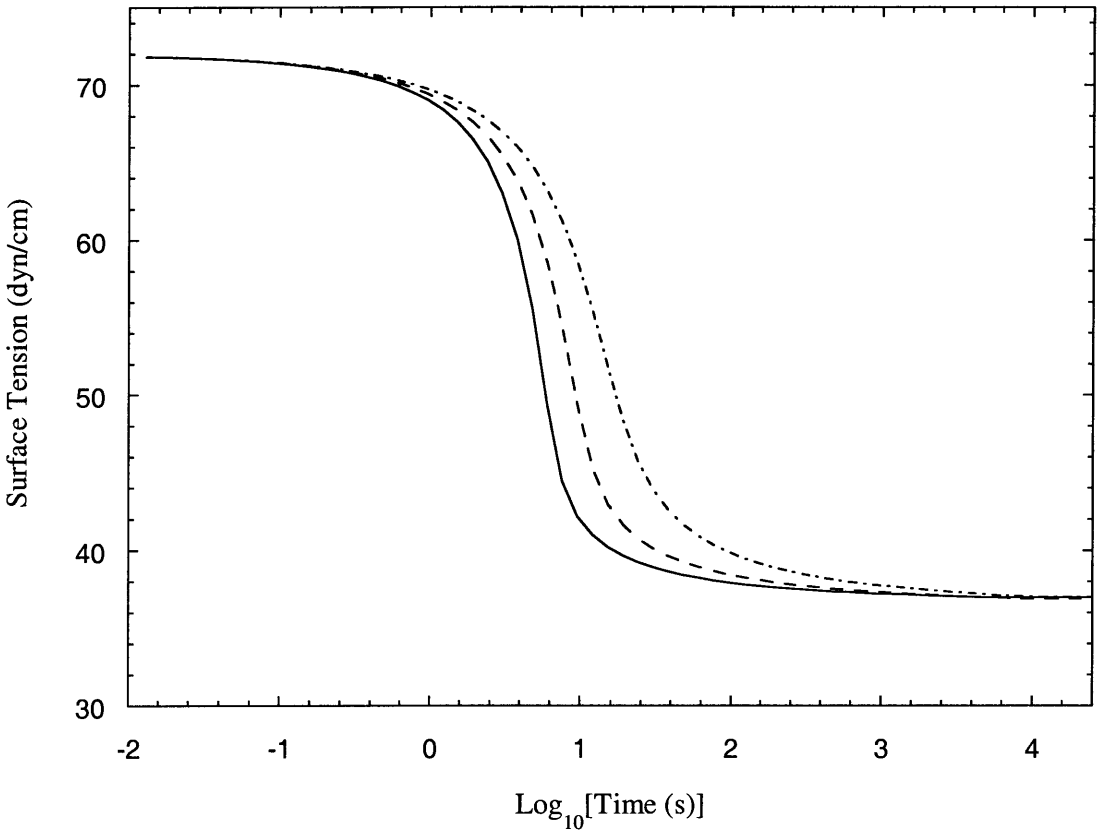

Figure 5-2: Dynamic surface tensions of aqueous solutions of: Surfactant a (———), Surfactant b (- — - — -), and a binary mixture of 50% Surfactant a – 50% Surfactant b (— — —), all at a total bulk surfactant concentration of $2.8 \times 10^{-8} mol/cm^3$.

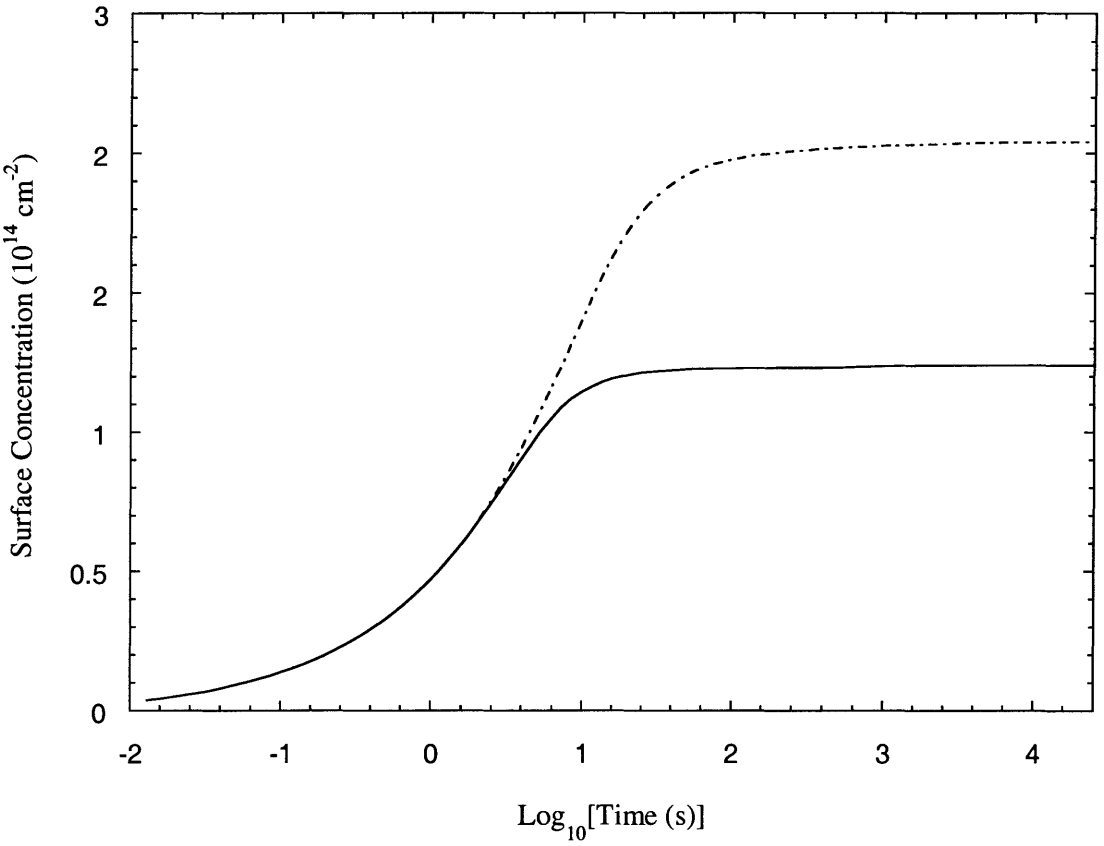

Figure 5-3: Surface concentrations, Γ_i, of aqueous single surfactant solutions of Surfactant a (———) and Surfactant b (- — - — -) as a function of time, both at a total bulk surfactant concentration of $2.8 \times 10^{-8} mol/cm^3$.

surfactant solutions is also reflected in Figure 5-3, which shows the surface concentration, Γ_i, as a function of time for the aqueous solutions of Surfactant a (———) and Surfactant b (- — - — -), both at the same total bulk surfactant concentration of $2.8 \times 10^{-8} mol/cm^3$. Figure 5-3 shows that, initially ($t < 10s$), both surfactants adsorb at the same rate, since $n_a^{\mathrm{w}} = n_b^{\mathrm{w}}$, and $D_a = D_b$ in this example, and Γ is initially proportional to $n^{\mathrm{w}}\sqrt{Dt}$ (see Ref. 13). However, the surface concentration of Surfactant a plateaus before that of Surfactant b as it approaches its lower equilibrium value.

To clarify the dynamic surface tension behavior of the binary surfactant mixture shown in Figure 5-2, Figure 5-4 shows the surface concentrations of Surfac-

tant a (———) and Surfactant b (- – - – -) as a function of time for the 50% Surfactant a – 50% Surfactant b mixture at a total bulk surfactant concentration of $2.8 \times 10^{-8} mol/cm^3$. Note that the *equilibrium* surface concentrations of each surfactant component in the mixture are the same in this example ($\Gamma_a^{eq} = \Gamma_b^{eq} = 0.8 \times 10^{14} cm^{-2}$). This equality is again a result of the choice of the surfactant molecular parameters, a_i and $\Delta\mu_i^0$, for the equilibrium theory (see Table 5.1). Specifically, in this example, the equality of the equilibrium surface concentrations follows from the fact that although Surfactant a has a larger cross-sectional area than Surfactant b (which would tend to make Γ_a^{eq} smaller than Γ_b^{eq}), Surfactant a is also more surface active than Surfactant b, that is, $\Delta\mu_a^0$ is more negative than $\Delta\mu_b^0$ (which would tend to make Γ_a^{eq} larger than Γ_b^{eq}). This equality of the equilibrium surface concentrations, in turn, leads to an equality of the individual timescales for adsorption. Specifically, since $D_a = D_b$, $n_a^{\mathrm{w}} = n_b^{\mathrm{w}}$, and $\Gamma_a^{eq} = \Gamma_b^{eq}$, using their values in Eq. (5.11) leads to $\tau_{D_a} = \tau_{D_b}$=13.8s. This timescale provides a reasonable estimate for the time required for the surfactant mixture to reach equilibrium at the interface. Indeed, the surface concentrations of both surfactant components (see Figure 5-4) and the surface tension of the surfactant mixture (see Figure 5-2) all reach a plateau within this timescale. As discussed in Section 5.2.3, the success of using the equilibrium surface concentrations, Γ_i^{eq}, in Eq. (5.11) in predicting the timescales for adsorption follows from the fact that, in this example, both surfactant components in the mixture have the same individual timescales for adsorption. However, as will be shown in the subsequent examples, using the equilibrium surface concentrations in Eq. (5.11) will not yield good estimates for the timescale for adsorption when the surfactant components have very different timescales for adsorption. In addition, note that one observes only one characteristic decrease in the surface tension as a function of time for this surfactant mixture (see Figure 5-2). This is a result of both surfactant components in the mixture adsorbing at the same time, since both possess the same timescales for adsorption. Contrasting cases where the surfactant components in the mixture have very different individual timescales for adsorption, leading to multiple characteristic decreases in the surfactant mixture surface tension as a function of time, will be presented and discussed in

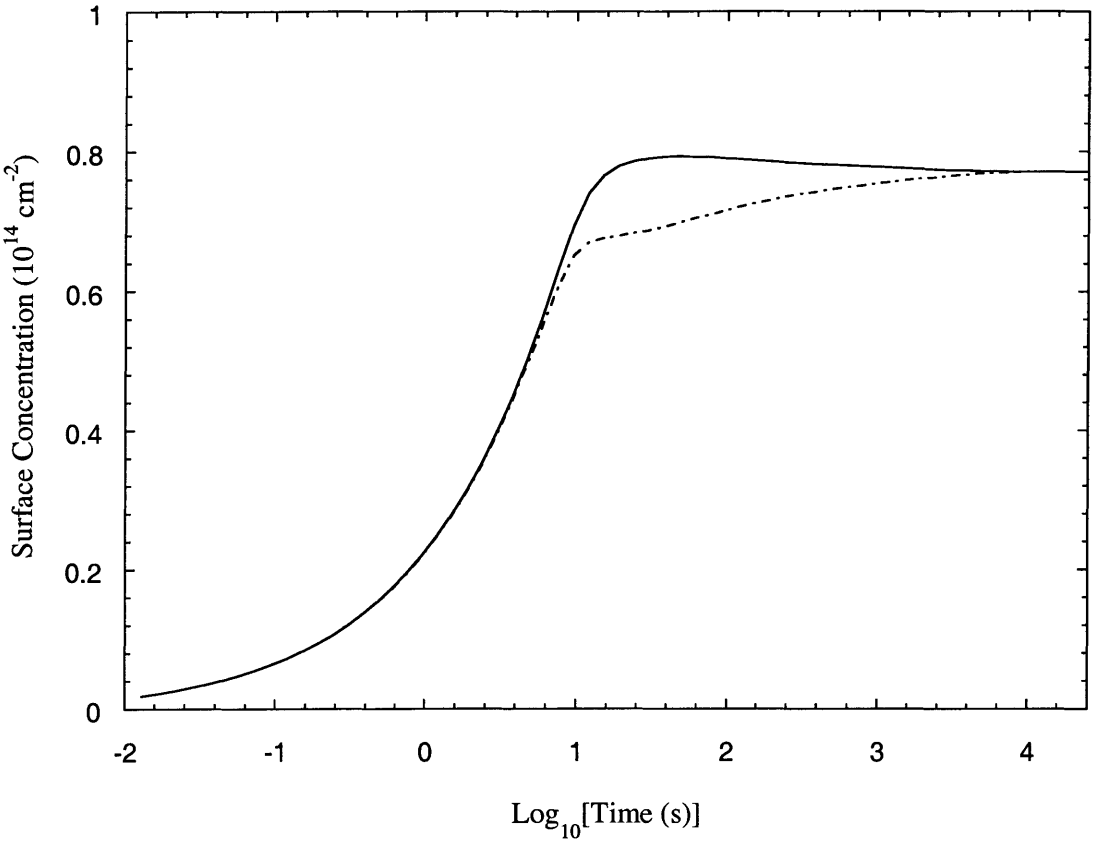

Figure 5-4: Surface concentrations, Γ_i, of Surfactant a (———) and Surfactant b (- — - — -) as a function of time in a binary mixture of 50% Surfactant a – 50% Surfactant b, at a total bulk surfactant concentration of $2.8 \times 10^{-8} mol/cm^3$.

the following illustrative examples.

5.3.2 Example 2: Binary Surfactant Mixture Exhibiting Competitive Adsorption

Another interesting case to investigate is one where the two surfactant components in the mixture have significantly different individual timescales for adsorption. Specifically, in this example, a binary mixture of Surfactants 1 and 2 is considered, where the more surface active component has the longer timescale for adsorption. In that case, the less surface active component will begin to fill up the interface first, but

Table 5.2: Cross-sectional areas, a_i, standard-state chemical potential differences, $\Delta\mu_i^0$, and diffusion coefficients, D_i, of Surfactants 1 and 2, corresponding to the binary surfactant mixture in Example 2.

Surfactant i	a_i (Å^2)	$\Delta\mu_i^0$ (k_BT)	D_i (cm^2/s)
1	75	-50.7	6×10^{-6}
2	25	-52.4	6×10^{-6}

subsequently, it will be displaced significantly by the later arriving, more surface active component. The surfactant molecular parameters corresponding to this example are listed in Table 5.2. Note that the surfactant mixture in this example consists of a larger (in terms of its cross-sectional area, a_i), less surface active (in terms of its free energy of adsorption, $\Delta\mu_i^0$) component (Surfactant 1) mixed with a smaller, more surface active component (Surfactant 2). Figure 5-5 shows the equilibrium surface tensions as a function of total bulk surfactant concentration for aqueous solutions of: (i) Surfactant 1 (———), (ii) Surfactant 2 (- — - — -), (iii) a binary mixture of 50% Surfactant 1 – 50% Surfactant 2 (— — —), and (iv) a binary mixture of 95% Surfactant 1 – 5% Surfactant 2 (▪ ▪ ▪ ▪), as predicted by the equilibrium theory (Eqs. (5.7) and (5.8)). Note that, as expected, the surface tension curve of the more surface active component (Surfactant 2) lies to the left of that of the less surface active component (Surfactant 1), with the two mixture surface tension curves lying in between according to their composition.

Figure 5-6 shows the dynamic surface tensions of the four solutions (i)–(iv) described above, all at a total bulk surfactant concentration of $2.8 \times 10^{-8} mol/cm^3$. An examination of the dynamic surface tensions of the two *single* surfactant solutions indicates that, initially ($t < 1s$), the surface tension of the solution of Surfactant 1 decreases more rapidly with time than that of the solution of Surfactant 2. This can be explained through an analysis of the dynamic surface concentrations, Γ_i, shown in

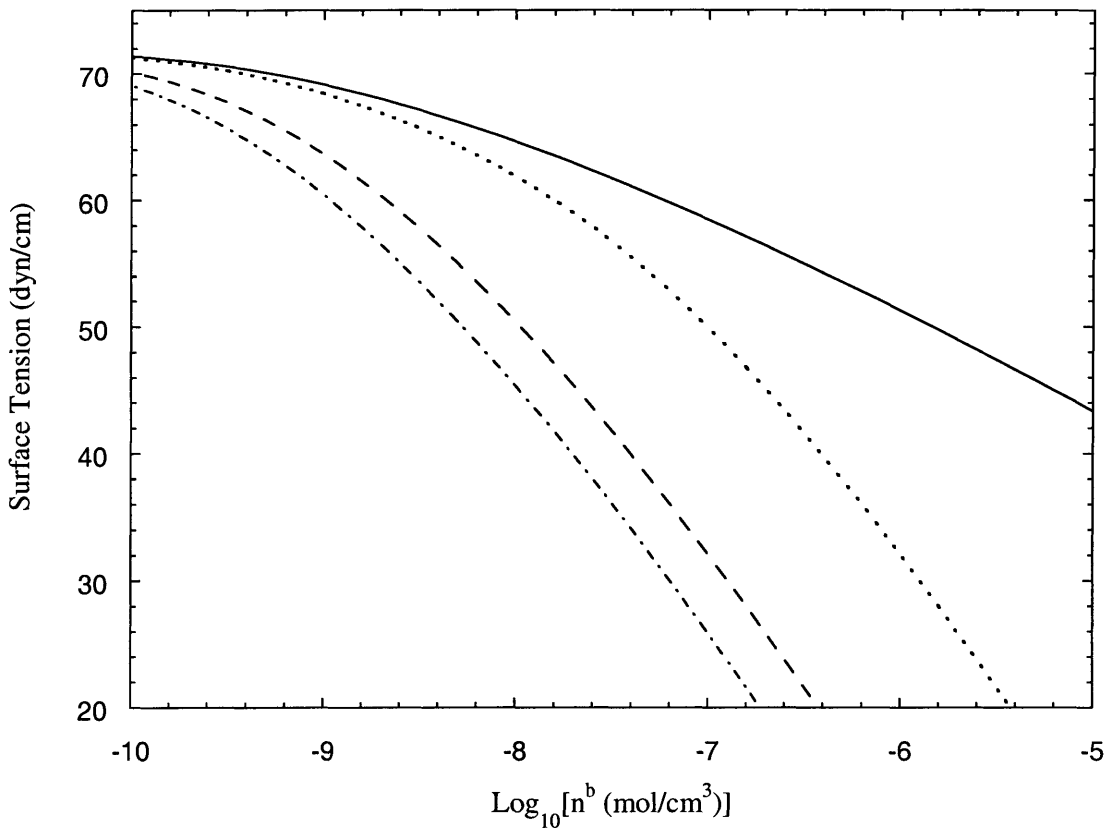

Figure 5-5: Equilibrium surface tensions as a function of total bulk surfactant concentration for aqueous solutions of: Surfactant 1 (———), Surfactant 2 (- — - — -), a binary mixture of 50% Surfactant 1 – 50% Surfactant 2 (— — —), and a binary mixture of 95% Surfactant 1 – 5% Surfactant 2 (▪ ▪ ▪ ▪).

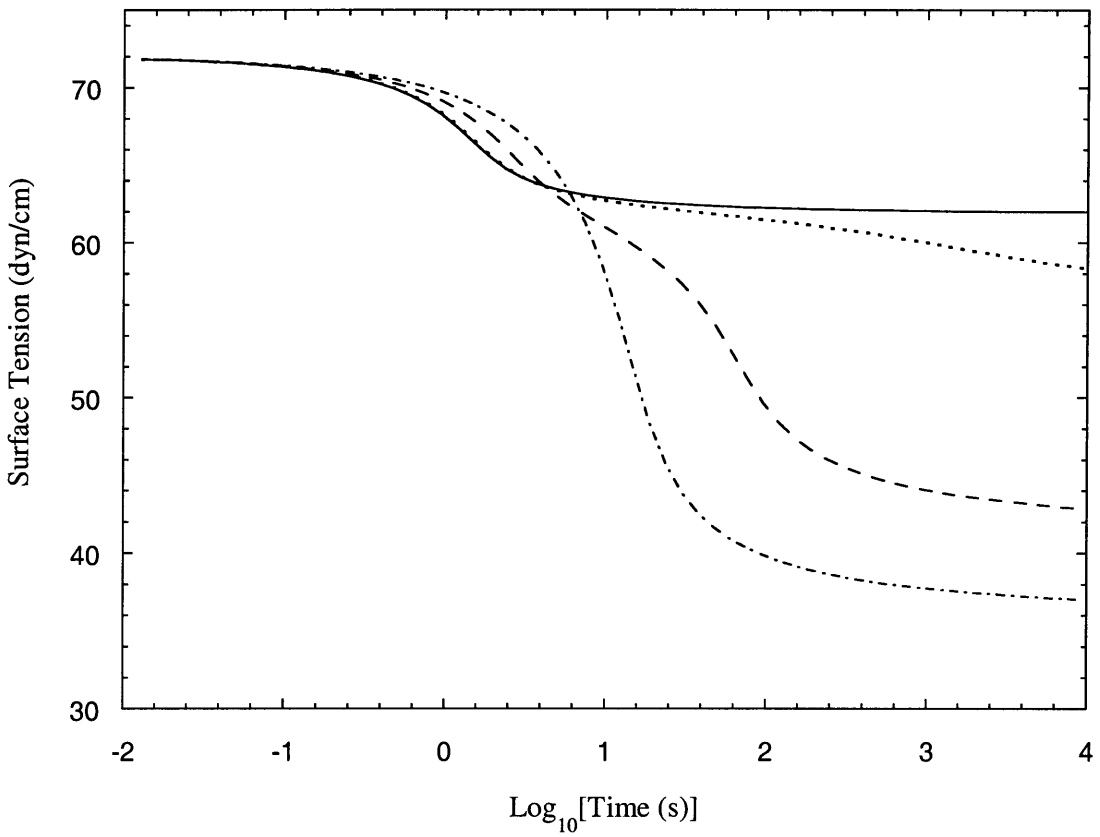

Figure 5-6: Dynamic surface tensions of aqueous solutions of: Surfactant 1 (———), Surfactant 2 (- — - — -), a binary mixture of 50% Surfactant 1 – 50% Surfactant 2 (— — —), and a binary mixture of 95% Surfactant 1 – 5% Surfactant 2 (▪ ▪ ▪ ▪), all at a total bulk surfactant concentration of $2.8 \times 10^{-8} mol/cm^3$.

Figure 5-7 and the dynamic surface coverages, $\Gamma_i a_i$, shown in Figure 5-8 for the single surfactant solutions. Figure 5-7 shows that, initially ($t < 1s$), the surface concentrations of both surfactants increase at identical rates since, initially, Γ_i is proportional to $n_i^w\sqrt{D_i t}$ (see Ref. 13), and in this example, both surfactants have identical diffusion coefficients and bulk concentrations. However, as shown in Figure 5-8, the surface coverage corresponding to the solution containing Surfactant 1 increases more rapidly with time during this initial time period as a result of the larger cross-sectional area of Surfactant 1. In other words, for a given surface concentration, Γ_i, the surface coverage, $\Gamma_i a_i$, is larger for Surfactant 1 than for Surfactant 2. This, in turn, leads to smaller denominators in the first two terms contained within the brackets in Eq. (5.8), which leads to a lower surface tension of the solution containing Surfactant 1 relative to that of Surfactant 2. Using the timescale analysis presented in Section 5.2.2, the timescale for adsorption of Surfactant 1, $\tau_D = 2.4s$, is less than that of Surfactant 2, $\tau_D = 24.1s$, due to the lower equilibrium value of the surface concentration of Surfactant 1 ($6.5 \times 10^{13} cm^{-2}$) compared to Surfactant 2 ($2.0 \times 10^{14} cm^{-2}$).

To clarify the dynamic surface tension behavior of the binary mixture of 50% Surfactant 1 – 50% Surfactant 2 (see Figure 5-6), Figures 5-9 and 5-10 show, respectively, the surface concentrations, Γ_1 (———), Γ_2 (- – - – -), and $\Gamma_1 + \Gamma_2$ (— — —), and surface coverages, $\Gamma_1 a_1$ (———), $\Gamma_2 a_2$ (- – - – -), and $\Gamma_1 a_1 + \Gamma_2 a_2$ (— — —), as a function of time. Note that in Figure 5-9, initially (for $t < 1s$), the surface concentrations of both surfactants increase at identical rates, reflecting as before, the identical diffusion coefficients and bulk concentrations of both surfactants. At these short times, the surface is virtually empty (that is, $\Gamma_1 a_1 + \Gamma_2 a_2 << 1$, see Figure 5-10), so that for both surfactants, the majority of the surfactant molecules that diffuse to the surface can adsorb onto it with minimal steric hindrance. However, eventually (at around $t = 6s$), the surface begins to saturate (that is, the total surface coverage is no longer small, see Figure 5-10). Beyond this point, the more surface active component (Surfactant 2) begins to displace the less surface active component (Surfactant 1). This results in a subsequent decrease in the surface concentration, Γ_1, and surface coverage, $\Gamma_1 a_1$, of Surfactant 1. In other words, the surface concentration and sur-

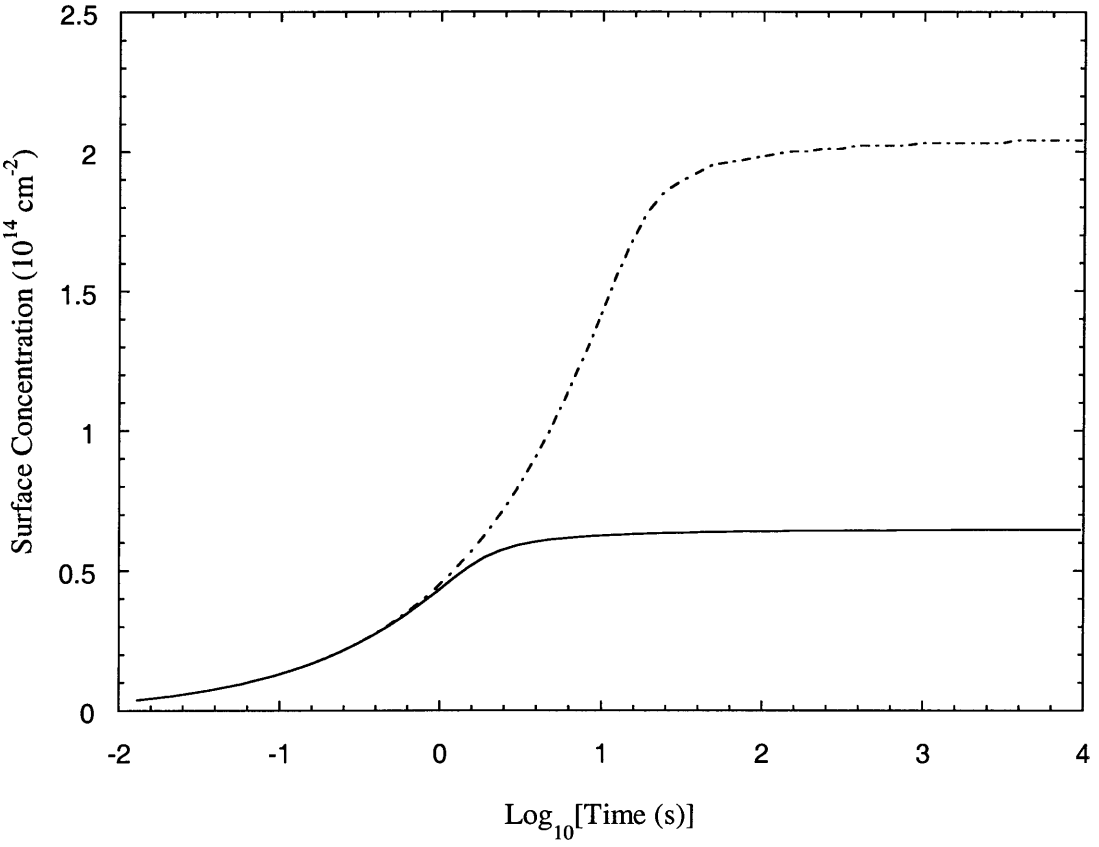

Figure 5-7: Surface concentrations, Γ_i, of aqueous single surfactant solutions of Surfactant 1 (———) and Surfactant 2 (- — - — -) as a function of time, at a total bulk surfactant concentration of $2.8 \times 10^{-8} mol/cm^3$.

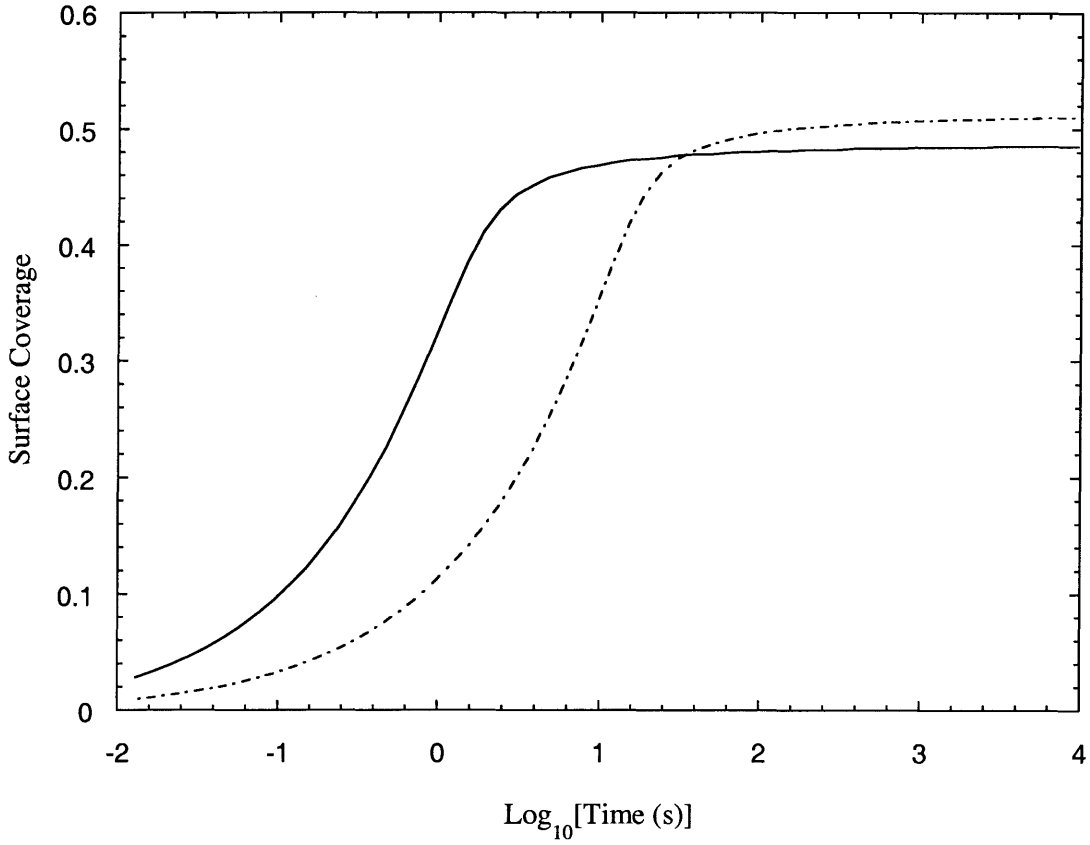

Figure 5-8: Surface coverages, $\Gamma_i a_i$, of aqueous single surfactant solutions of Surfactant 1 (———) and Surfactant 2 (- — - — -) as a function of time, at a total bulk surfactant concentration of $2.8 \times 10^{-8} mol/cm^3$.

face coverage of Surfactant 1 go through a maximum, which can be clearly seen in Figures 5-9 and 5-10.

One can also identify two characteristic decreases in the surface tension as a function of time for this 50%–50% surfactant mixture (see Figure 5-6). The first decrease, occurring at $t \approx 6s$, is caused primarily by the (relatively fast) adsorption of Surfactant 1, which can be seen by the increase in surface coverage of Surfactant 1 at $t \approx 6s$ (see Figure 5-10). Similarly, the second decrease, between $t \approx 6s$ and $t \approx 100s$, is caused primarily by the (relatively slow) adsorption of Surfactant 2 (and corresponding desorption of Surfactant 1), which can be seen by the increase in surface coverage of Surfactant 2 and the decrease in surface coverage of Surfactant 1 (resulting in the peak for Γ_1 at $t \approx 6s$ in Figure 5-10). Since the first decrease in surface tension with time in Figure 5-6 corresponds to the adsorption of Surfactant 1, one can define a timescale associated with this first decrease by using Eq. (5.11) with $i = 1$. For an initial estimate, one could try to use the equilibrium value of Γ_1 in Eq. (5.11). However, as discussed in Section 5.2.3, if the timescales for adsorption of each surfactant component are very different, as in this example, then using the equilibrium values of Γ_i in Eq (5.11) will not result in a very good estimate of the timescale for adsorption, as discussed below.

If one tried to utilize the equilibrium value of Γ_1 in Eq. (5.11), one would underestimate the timescale for adsorption of Surfactant 1 resulting in a value of $\tau_{D_1} = 1.6 \times 10^{-4}s$. This is due to the fact that the surface concentration of Surfactant 1 during this initial time period, which peaks at $\Gamma_1^{peak} = 4 \times 10^{13} cm^{-2}$ at $t = 6s$, is much larger than the equilibrium value of $\Gamma_1^{eq} = 2.5 \times 10^{11} cm^{-2}$ (see Figure 5-9). A better choice for Γ_1 in Eq (5.11) is to utilize the peak value of Γ_1, since this better represents the surface concentration during this initial adsorption period. This would lead to an estimate of the timescale for adsorption associated with the peak in surface concentration of Surfactant 1 which corresponds to the timescale of the first characteristic drop in surface tension. However, to obtain this peak value, one would need to implement the complete theory presented in Section 5.2.1. In that case, of course, one could simply generate the entire Figure 5-6, thus obtaining the complete

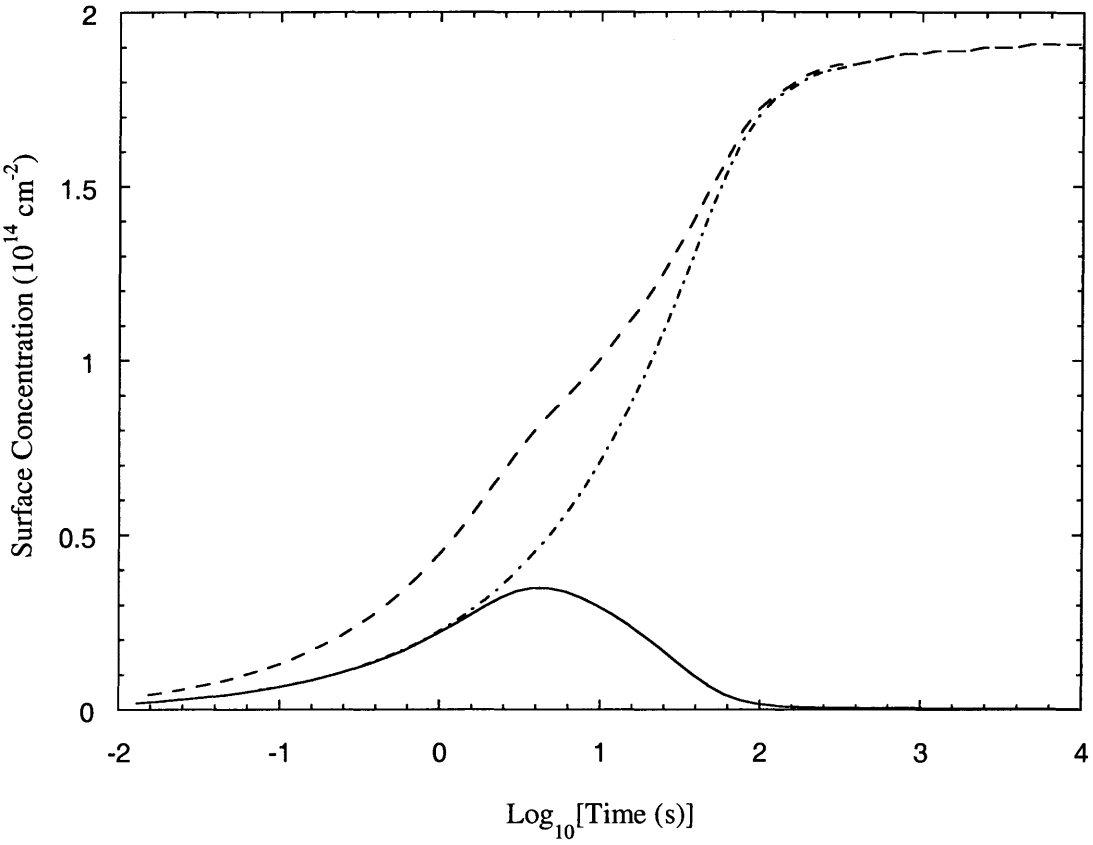

Figure 5-9: Surface concentrations, Γ_i, as a function of time in an aqueous binary mixture of 50% Surfactant 1 and 50% Surfactant 2 at a total bulk surfactant concentration of $2.8 \times 10^{-8} mol/cm^3$. Shown are the surface concentrations of Surfactant 1, Γ_1, (———), of Surfactant 2, Γ_2, (- — - — -), as well as the total surface concentration, $\Gamma_1 + \Gamma_2$, (— — —).

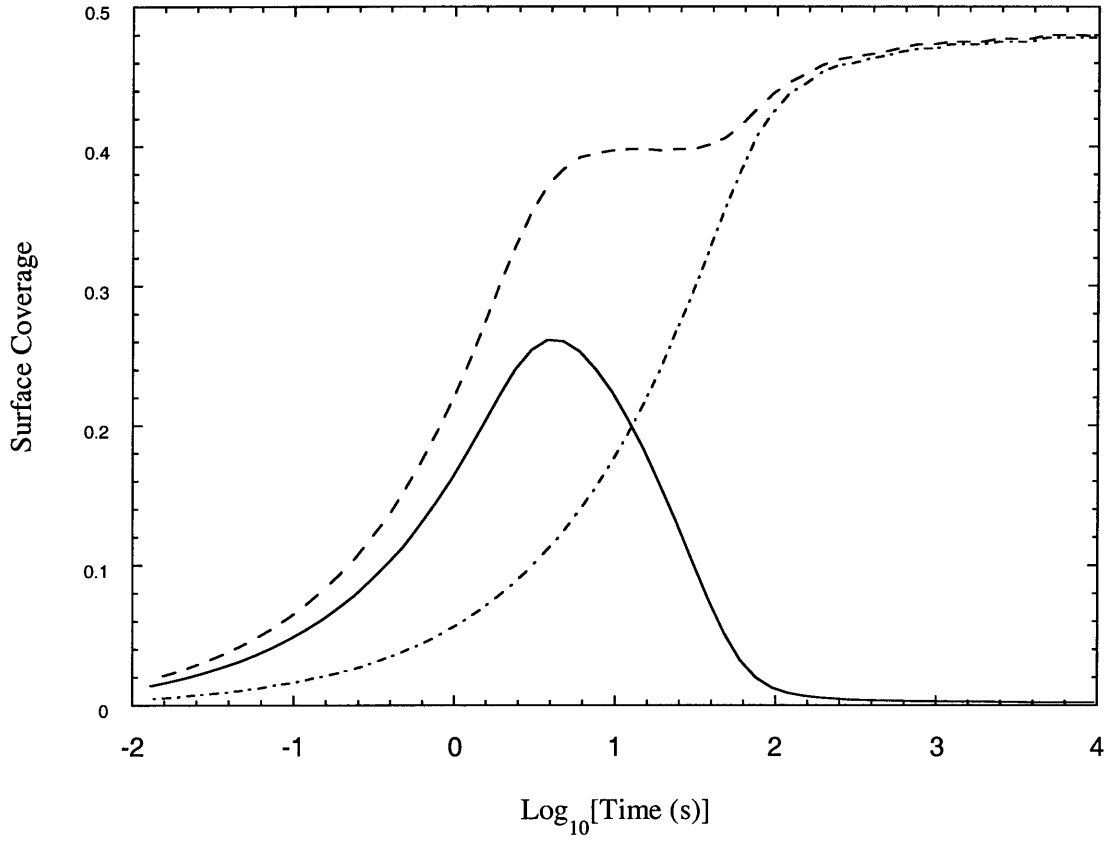

Figure 5-10: Surface coverages, $\Gamma_i a_i$, as a function of time in an aqueous binary mixture of 50% Surfactant 1 and 50% Surfactant 2 at a total bulk surfactant concentration of $2.8 \times 10^{-8} mol/cm^3$. Shown are the surface coverages of Surfactant 1, $\Gamma_1 a_1$, (———), of Surfactant 2, $\Gamma_2 a_2$, (- — - — -), as well as the total surface coverage, $\Gamma_1 a_1 + \Gamma_2 a_2$, (— — —).

dynamic surface tension profile.

Alternatively, as an approximation, one could use the *equilibrium* value of Γ_1 for a solution containing *only Surfactant 1* at the same bulk concentration as that corresponding to the surfactant mixture of interest (that is, one would solve Eq. (5.7) with $i = 1$ and $\Gamma_2 = 0$). In other words, since the interface is initially clean, the "faster" surfactant will initially behave as if it were adsorbing onto a clean interface. In that case, this yields a value of $\Gamma_1 = 6 \times 10^{13} cm^{-2}$ which is reasonably close to the precise value of $\Gamma_1^{peak} = 4 \times 10^{13} cm^{-2}$ in Figure 5-9. Using this value ($6 \times 10^{13} cm^{-2}$) of Γ_1 in Eq. (5.11) then yields a value of $\tau_{D_1} = 8.4s$, which represents a good approximation for the time at which the surface tension of this 50%–50% surfactant mixture exhibits its first decrease in Figure 5-6. Note that, in general, identifying the "faster" surfactant does not require the use of the complete theory, but instead, can be done by simply using Eq. (5.11), with Γ_i given by the equilibrium value corresponding to a solution containing only Surfactant i. However, note also that this approximation works best for surfactants that exhibit widely spaced individual timescales for adsorption.

The time corresponding to the second characteristic decrease in surface tension, which reflects the adsorption of Surfactant 2 (see Figures 5-6, 5-9, and 5-10), can similarly be determined by using Eq. (5.11) with $i = 2$. Note that here, unlike the case of Surfactant 1, the maximum surface concentration of Surfactant 2 is equal to the equilibrium surface concentration (that is, $\Gamma_2(t)$ does not go through a peak, but rather approaches the equilibrium value monotonically from below). Therefore, the equilibrium surface concentration ($\Gamma_2^{eq} = 1.9 \times 10^{14} cm^{-2}$) can be used in Eq. (5.11). In this example, this yields a value of $\tau_{D_2} = 85.1s$, which corresponds well with the adsorption equilibrium of Surfactant 2 in Figures 5-9 and 5-10, as well as with the second characteristic time at which the surface tension of the 50%–50% surfactant mixture decreases in Figure 5-6.

It is also interesting to note that although no attractive interactions operate between Surfactants 1 and 2 in this example ($B_{12} = 0$), and there is no synergism in the equilibrium surface tension (see Figure 5-5), this surfactant mixture does exhibit

dynamic surface tension synergism. That is, this mixture displays a time interval, between $t = 4s$ and $t = 6s$, where the dynamic surface tension of the surfactant mixture is lower than those of each single surfactant solution (see Figure 5-6). Note that during this time interval, the surface concentration of Surfactant 1 is much higher than its equilibrium value (see Figure 5-9). Hence, physically, one may view this excess lowering of the dynamic surface tension as a result of the excess adsorption of Surfactant 1 (relative to its equilibrium value).

The 95% Surfactant 1 – 5% Surfactant 2 binary mixture shown in Figure 5-6 serves to illustrate the effect of an impurity on the dynamic surface tension of a surfactant solution. Indeed, since Surfactant 2 is more surface active than Surfactant 1, and is also present at a relatively low concentration, it fits the classic description of an "impurity" in a surface tension experiment. Note, however, that this case, as well as a similar one presented in Section 5.3.3 below, demonstrates that initially, the surface tension of the "impure" surfactant mixture, (- - - -) in Figure 5-6, is very close to that of the "pure" surfactant solution, (———) in Figure 5-6, even though the long time ($t > 100$s) surface tension values, as well as the ultimate equilibrium surface tension values, are significantly different for the two solutions. Indeed, the equilibrium surface tension values are 57.3 dyn/cm and 62.1 dyn/cm for the 95%–5% surfactant mixture and the pure Surfactant 1 solution, respectively (see Figure 5-5 and recall that $n^{\mathrm{w}} = 2.8 \times 10^{-8} mol/cm^3$). This behavior is a result of Surfactant 2 (the "impurity") having an extremely long timescale for adsorption ($\tau_{D_2} = 2250s$) due to the small value of n_2^{w} in Eq. (5.11). This is similar to the explanation given in Refs. 132 and 133 for the observed behavior of an impure sample of sodium dodecyl sulfate.

5.3.3 Example 3: Binary Surfactant Mixture where the Adsorption is Dominated by One Surfactant

In contrast to the example considered in Section 5.3.2, a binary mixture of Surfactants A and B is considered next, where the more surface active component has the shorter

Table 5.3: Cross-sectional areas, a_i, standard-state chemical potential differences, $\Delta\mu_i^0$, and diffusion coefficients, D_i, of Surfactants A and B, corresponding to the binary surfactant mixture in Example 3.

Surfactant i	a_i (Å^2)	$\Delta\mu_i^0$ (k_BT)	D_i (cm^2/s)
A	25	-48.7	6×10^{-6}
B	75	-58.3	6×10^{-6}

timescale for adsorption. The surfactant molecular parameters corresponding to this example are listed in Table 5.3. Note that the surfactant mixture in this example consists of a larger (in terms of its cross-sectional area, a_i), more surface active (in terms of its free energy of adsorption, $\Delta\mu_i^0$) component (Surfactant B) mixed with a smaller, less surface active component (Surfactant A).

Figure 5-11 shows the equilibrium surface tensions as a function of total bulk surfactant concentration for aqueous solutions of: (i) Surfactant A (———), (ii) Surfactant B (- — - — -), (iii) a binary mixture of 50% Surfactant A - 50% Surfactant B (— — —), and (iv) a binary mixture of 95% Surfactant A - 5% Surfactant B (▪ ▪ ▪ ▪), as predicted by the equilibrium theory (Eqs. (5.7) and (5.8)). Note that, as expected, the surface tension curve of the more surface active component (Surfactant B) lies to the left of that of the less surface active component (Surfactant A), with the two mixture surface tension curves lying in between according to their composition.

Figure 5-12 shows the dynamic surface tensions of the four solutions (i)–(iv) described above, all at a total bulk surfactant concentration of $2.8 \times 10^{-8} mol/cm^3$. Note that, similar to Example 2, the surface tension initially decreases faster with time for the single surfactant solution of the surfactant having the larger cross-sectional area (Surfactant B) relative to the surface tension of the single surfactant solution of the surfactant having the smaller cross-sectional area (Surfactant A). Like in Example 2, this is due to the fact that Surfactant A has a larger timescale for adsorption

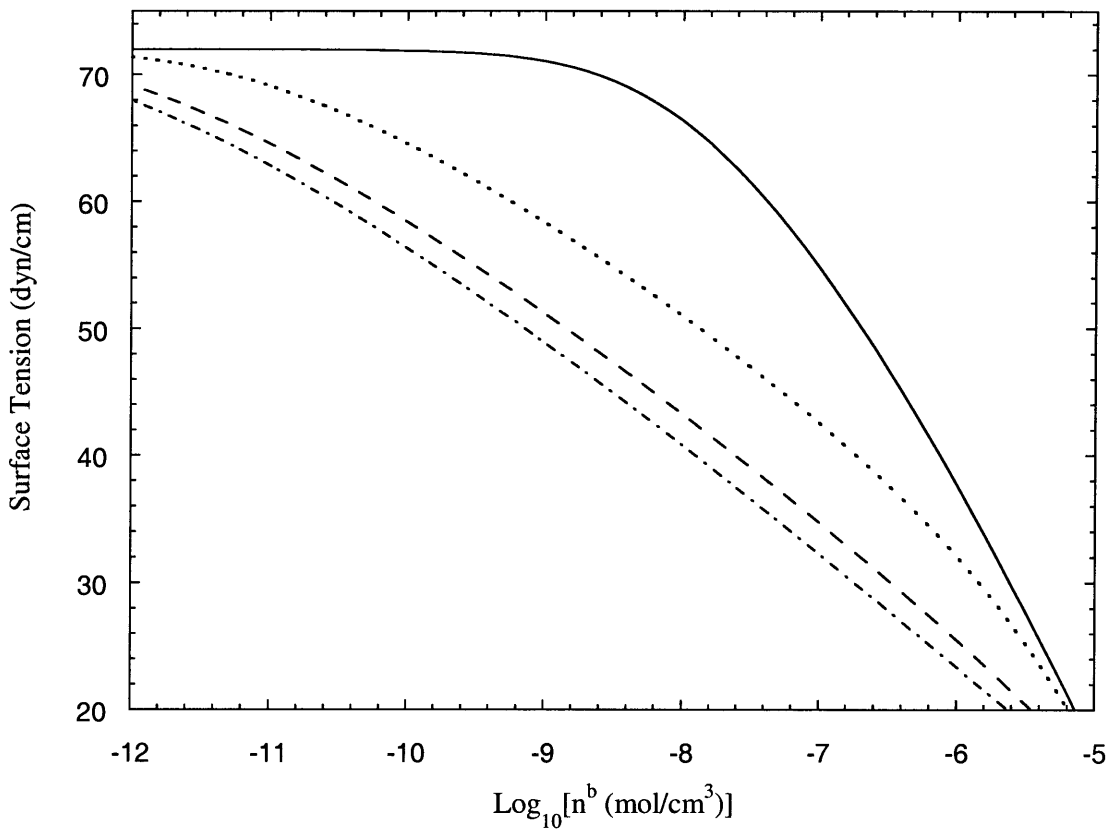

Figure 5-11: Equilibrium surface tensions as a function of total bulk surfactant concentration for aqueous solutions of: Surfactant A (———), Surfactant B (- — - — -), a binary mixture of 50% Surfactant A – 50% Surfactant B (— — —), and a binary mixture of 95% Surfactant A – 5% Surfactant B (▪ ▪ ▪ ▪).

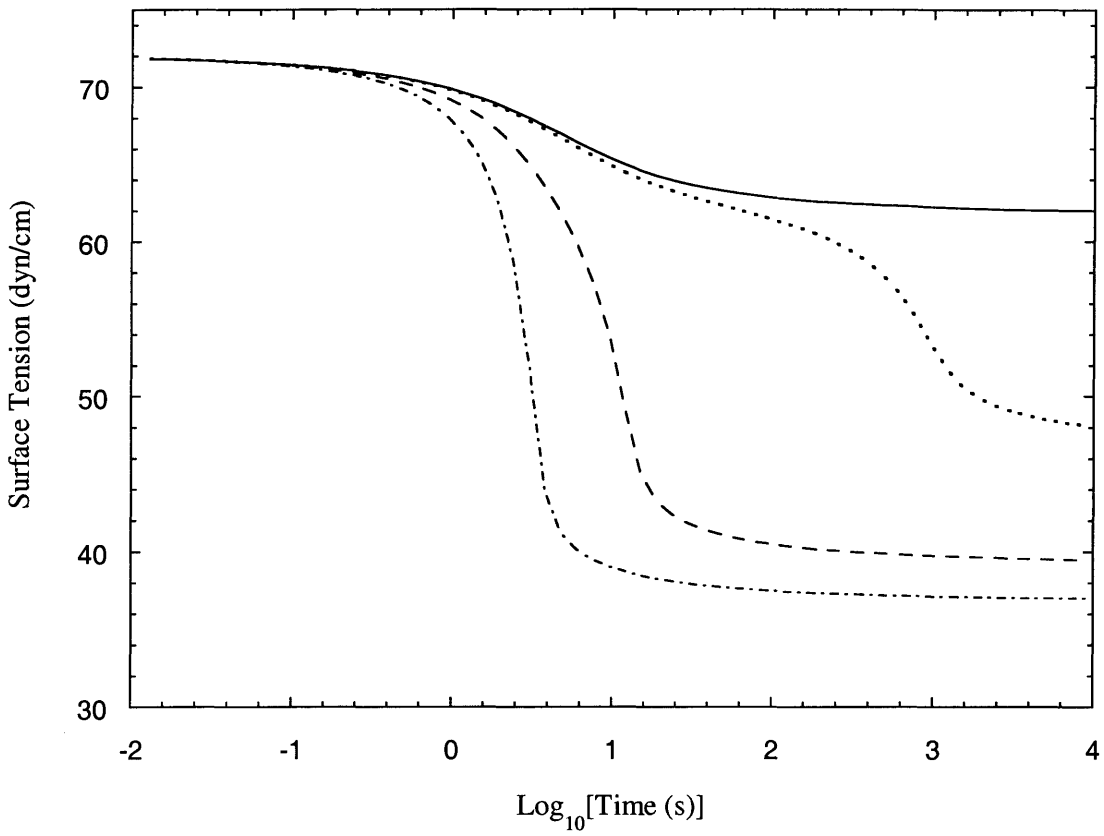

Figure 5-12: Dynamic surface tensions of aqueous solutions of: Surfactant A (———), Surfactant B (- — - — -), a binary mixture of 50% Surfactant A – 50% Surfactant B (— — —), and a binary mixture of 95% Surfactant A – 5% Surfactant B (▪ ▪ ▪ ▪), all at a total bulk surfactant concentration of $2.8 \times 10^{-8} mol/cm^3$.

($\tau_D = 8.3s$) than Surfactant B ($\tau_D = 4.7s$), see Eq. (5.9). Since the dynamic behaviors corresponding to the surface concentrations and surface coverages of the single surfactant solutions in Example 3 are analogous to those found and discussed in Example 2 (see Figures 5-7 and 5-8), they are not shown or discussed here.

To clarify the dynamic surface tension behavior of the binary mixture of 50% Surfactant A – 50% Surfactant B (see Figure 5-12), Figure 5-13 shows the surface coverages of each surfactant component, $\Gamma_A a_A$ (———) and $\Gamma_B a_B$ (- — - — -), as well as the total surfactant coverage, $\Gamma_A a_A + \Gamma_B a_B$ (— — —), all as a function of time. Because the "faster" component (Surfactant B) is also the more surface active in this example, it begins to fill up the surface first (which can be clearly seen by the much faster increase in the surface coverage of Surfactant B (shown in Figure 5-13), but is not subsequently displaced by the later arriving Surfactant A (which can be seen by the fact that the surface coverage of Surfactant B does not go through a peak in Figure 5-13). Consequently, the surface is dominated by Surfactant B, and one only observes one significant decrease in the surface tension with time (which corresponds to the adsorption of Surfactant B, since the small amount of Surfactant A that subsequently adsorbs has a negligible effect on the surface tension, see Figure 5-12). Because Surfactant B is much more surface active than Surfactant A in this example, at the same bulk surfactant concentration, the equilibrium values of Γ_B for the binary surfactant mixture and for the single surfactant solution of Surfactant B are similar ($8.8 \times 10^{13} cm^{-2}$ and $8.9 \times 10^{13} cm^{-2}$, respectively). Therefore, in this case, one can use either value in Eq. (5.11) to obtain a good estimate of the timescale for adsorption of Surfactant B. This yields a value of $\tau_{D_B} = 18s$, which corresponds well with the decrease in the surface tension of this 50%–50% surfactant mixture (see Figure 5-12). Note that there is no need to calculate a timescale for adsorption corresponding to Surfactant A since, as stressed above, this component has little effect on the dynamic mixture surface tension.

Note that only in the case of a surfactant mixture containing a large proportion of Surfactant A in the bulk (such as mixture (iv) corresponding to the extreme 95% - 5% case), in which the surface composition of Surfactant A has been increased

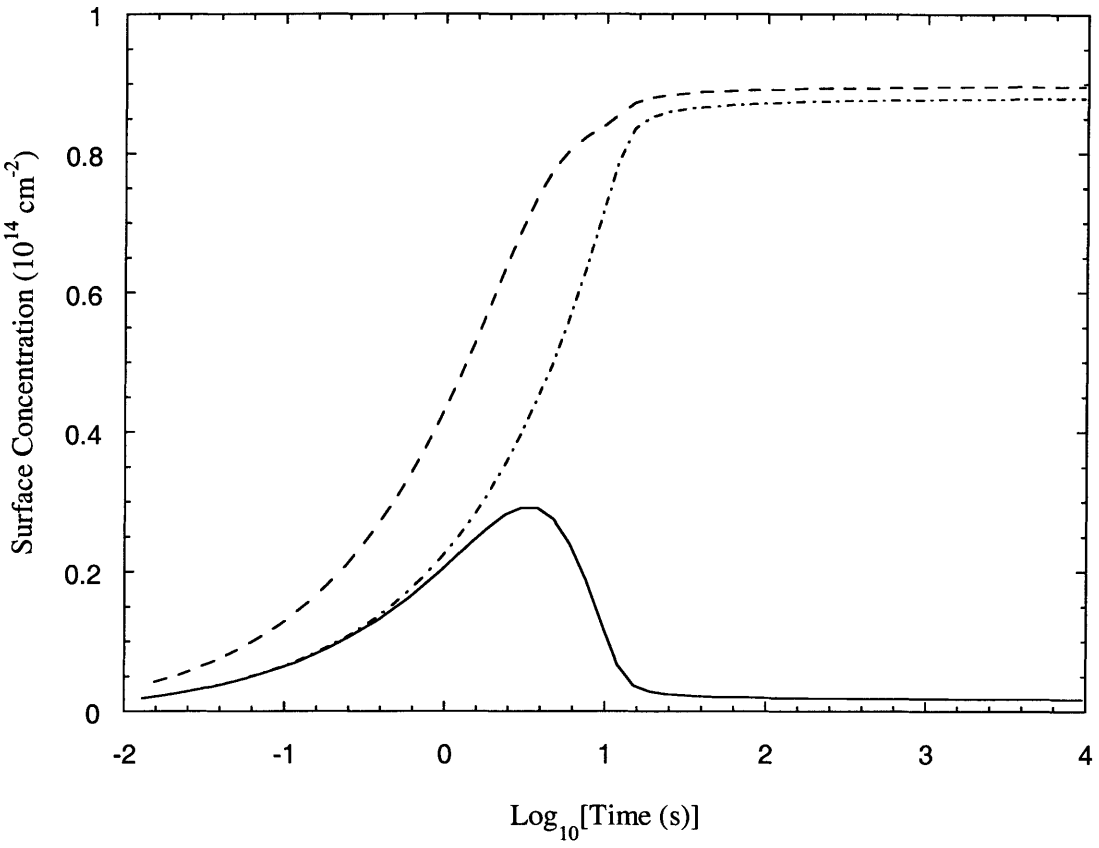

Figure 5-13: Surface coverages of the two surfactant components, $\Gamma_A a_A$ (———) and $\Gamma_B a_B$ (- — - — -), as well as the total surface coverage, $\Gamma_A a_A + \Gamma_B a_B$, (— — —), as a function of time in an aqueous binary mixture of 50% Surfactant A and 50% Surfactant B at a total bulk surfactant concentration of $2.8 \times 10^{-8} mol/cm^3$.

and the adsorption timescale of Surfactant B has been increased (as a result of the decrease in n_B^w in Eq. (5.11)), does one observe the two characteristic timescales in the dynamic surface tension (the first at $t \approx 10s$ and the second at $t \approx 1000s$, see Figure 5-12). Note also that this 95% - 5% surfactant mixture represents an example (along with the one discussed above in Example 2) of solutions containing a small amount of an "impurity" (that is, a more surface active component present at low concentrations, as is the case for Surfactant B). In this case, Figure 5-12 shows that the initial dynamic surface tension behavior of the 95%–5% surfactant solution is similar to that of a solution containing no impurity, even though the long time, equilibrium surface tension values are quite different (47.3 dyn/cm and 62.0 dyn/cm for the surfactant mixture and the single surfactant solution respectively; see Figure 5-11, and recall that $n_b = 2.8 \times 10^{-8} mol/cm^3$).

5.3.4 Example 4: Ternary Surfactant Mixture

Finally, to illustrate the flexibility of the theoretical framework presented here, a ternary mixture of Surfactants α, β, and γ is considered. The surfactant molecular parameters corresponding to this example are listed in Table 5.4. Note that these parameters were chosen such that each single surfactant will have distinctly different timescales for adsorption with the resulting timescales increasing as the surface activity increases. In other words, choosing $a_\alpha > a_\beta > a_\gamma$, leads to $\Gamma_\alpha < \Gamma_\beta < \Gamma_\gamma$. This combined with $D_\alpha > D_\beta > D_\gamma$, leads to $\tau_{D_\alpha} < \tau_{D_\beta} < \tau_{D_\gamma}$ in Eq. (5.9). Quantitatively, for single surfactant solutions at a bulk surfactant concentration of $2.8 \times 10^{-8} mol/cm^3$, the resulting equilibrium surface concentrations are $5.7 \times 10^{13} cm^{-2}$, $1.1 \times 10^{14} cm^{-2}$, and $2.2 \times 10^{14} cm^{-2}$, and the corresponding timescales for adsorption are $1.1s$, $7.3s$, and $430s$, for Surfactants α, β, and γ, respectively. Furthermore, since $\Delta\mu_\alpha^0 > \Delta\mu_\beta^0 > \Delta\mu_\gamma^0$, it follows that Surfactant γ is the most surface active, followed by Surfactant β, and then by Surfactant α. The surfactant molecular parameters were chosen in this manner so that the adsorption of each individual surfactant component in the ternary mixture is clearly reflected in the dynamic surface tension behavior of the ternary surfactant mixture.

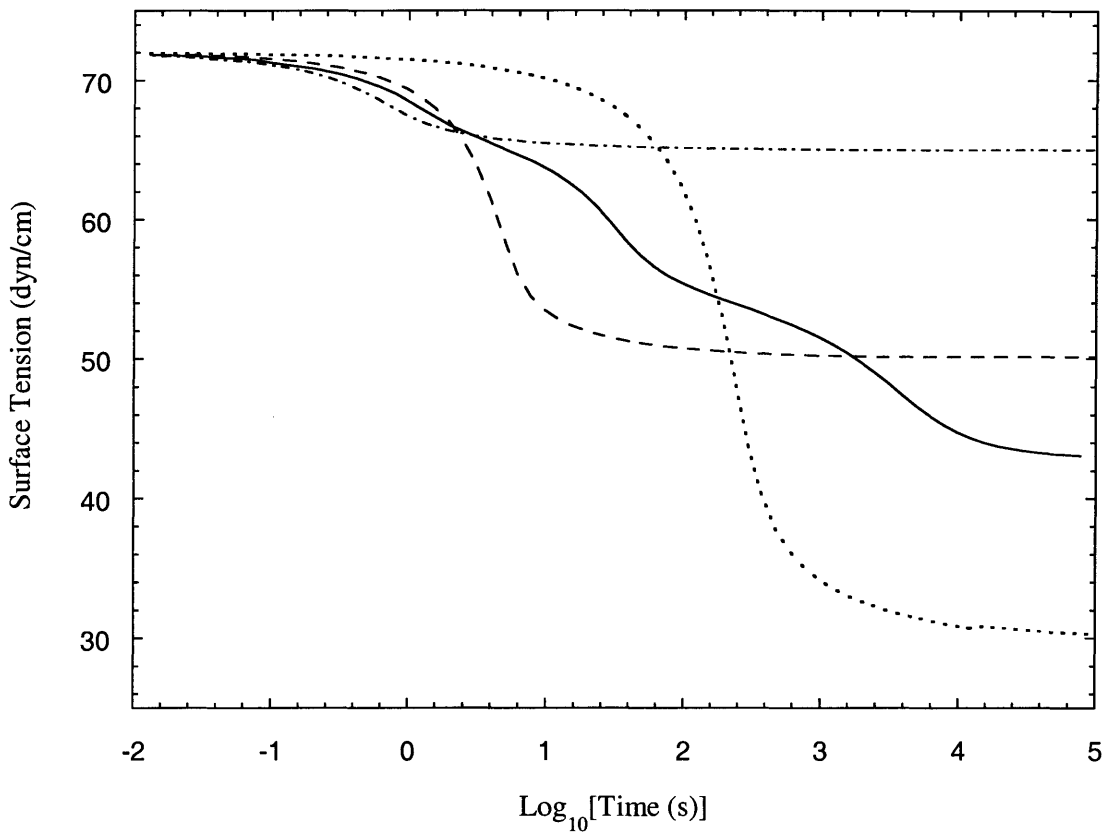

Figure 5-14: Dynamic surface tensions of aqueous solutions of: Surfactant α (- - - - -), Surfactant β (— — —), Surfactant γ (▪ ▪ ▪ ▪), and a ternary mixture of 50% Surfactant α – 30% Surfactant β – 20% Surfactant γ (———), all at a total bulk surfactant concentration of $2.8 \times 10^{-8} mol/cm^3$.

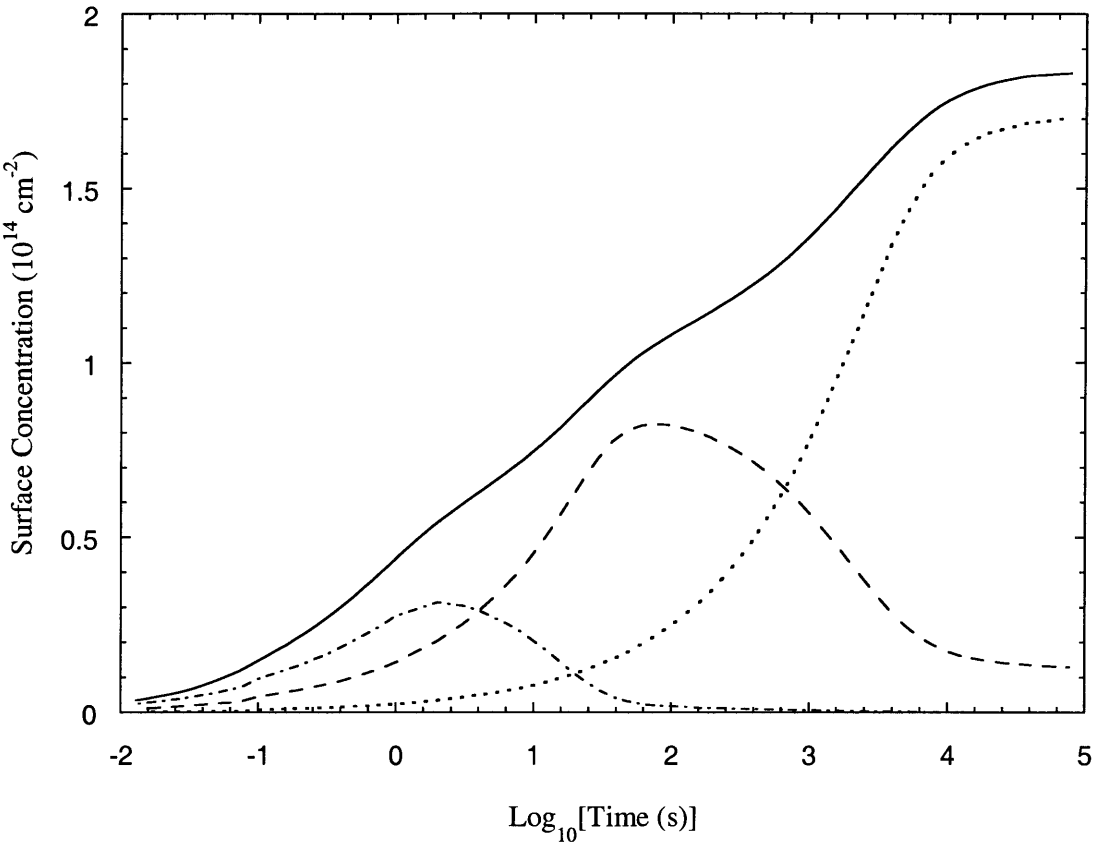

Figure 5-15: Surface concentrations of each component, Γ_i, as a function of time in a ternary mixture of 50% Surfactant α – 30% Surfactant β – 20% Surfactant γ (———), at a total bulk surfactant concentration of $2.8\times10^{-8} mol/cm^3$. Shown here are the surface concentrations of Surfactant α,Γ_α, (- — - — -), of Surfactant β, Γ_β, (— — —), of Surfactant γ, Γ_γ, (▪ ▪ ▪ ▪), as well as the total surface concentration, $\Gamma_\alpha + \Gamma_\beta + \Gamma_\gamma$, (———).

Table 5.4: Cross-sectional areas, a_i, standard-state chemical potential differences, $\Delta\mu_i^0$, and diffusion coefficients, D_i, of Surfactants α, β, and γ, corresponding to the ternary surfactant mixture in Example 4.

Surfactant i	a_i (Å^2)	$\Delta\mu_i^0$ (k_BT)	D_i (cm^2/s)
α	75	-50.7	10×10^{-6}
β	50	-52.7	6×10^{-6}
γ	25	-53.2	0.4×10^{-6}

Figure 5-14 shows the dynamic surface tensions of aqueous solutions of: (i) Surfactant α (- — - — -), (ii) Surfactant β (— — —), (iii) Surfactant γ (▪ ▪ ▪ ▪), and (iv) a ternary mixture of 50% Surfactant α - 30% Surfactant β- 20% Surfactant γ (———), all at a total bulk surfactant concentration of $2.8 \times 10^{-8} mol/cm^3$. Note that the timescales for adsorption associated with the solutions of Surfactants α, β, and γ (1.1s, 7.3s, and 430s, respectively) correspond well with the onset of the three plateaus observed in the dynamic surface tension curves of the three single surfactant solutions shown in Figure 5-14. To clarify the dynamic surface tension behavior of the ternary surfactant mixture, Figure 5-15 shows the surface concentrations of each surfactant component, Γ_α (- — - — -), Γ_β (— — —), and Γ_γ (▪ ▪ ▪ ▪), as well as the total surface concentration, $\Gamma_\alpha + \Gamma_\beta + \Gamma_\gamma$ (———). Note that, similar to Example 2, Surfactant β is more surface active than Surfactant α, and when Surfactant β arrives at the surface, it displaces Surfactant α. As a result, $\Gamma_\alpha(t)$ goes through a maximum at $t \approx 2s$. Similarly, Surfactant γ is more surface active than Surfactant β, and therefore, when Surfactant γ arrives at the surface, it displaces Surfactant β. As a result, $\Gamma_\beta(t)$ goes through a maximum at $t \approx 60s$. Finally, complete adsorption of Surfactant γ takes place at $t \approx 10^4 s$, as reflected in the observed plateau of Γ_γ. This series of dynamic adsorption events, shown in Figure 5-15, helps clarify the observed dynamic surface tension of the ternary surfactant mixture shown in Figure 5-14. Specifically,

three surface tension decreases are observed at $t \approx 2s, 60s$, and $10^4 s$.

The simplified timescale analysis for binary surfactant mixtures presented in Section 5.3.2 can, in principle, be extended to multi-component mixtures such as the ternary one considered in this example. One could imagine treating initially the ternary surfactant solution as a single surfactant solution consisting of the fastest adsorbing surfactant, followed by treating it as a binary surfactant mixture consisting of the two fastest adsorbing surfactants, etc. However, this will generally complicate the analysis to the point that it would probably be simpler to calculate the entire surface tension verses time profile using the complete theory presented in Section 5.2.1. Note, however, that one can still make use of the simplified timescale analysis to estimate the timescale for adsorption of the slowest adsorbing surfactant component (which, in turn, implies equilibrium of the surface tension). This can be done by noting that the surfactant component having the longest individual timescale for adsorption does not exhibit a maximum in the surface concentration versus time profile. Indeed, because this component is the last one to arrive at the interface, there is no subsequent arriving surfactant to displace it. Accordingly, the timescale for adsorption of the slowest adsorbing surfactant is simply given by Eq. (5.11) with Γ_i correspond to the equilibrium value of component i in the mixture under consideration. For example, in the case of the ternary surfactant mixture considered here, the slowest adsorbing component is Surfactant γ, which has an equilibrium surface concentration of $\Gamma_\gamma^{eq} = 1.4 \times 10^{14} cm^{-2}$. Using this value in Eq. (5.11) yields a value of $\tau_{D_\gamma} = 4500s$, which represents a reasonable approximation to the timescale required to attain complete surface tension equilibrium of the ternary surfactant mixture (see Figure 5-14).

5.4 Conclusions

A theoretical framework to predict the dynamic adsorption behavior of surfactants at the air-aqueous solution interface for mixtures containing any number of nonionic surfactant components was presented. The work presented in this chapter builds on an extension of the Ward-Tordai model which assumes Fickian diffusion of the surfac-

tant molecules in the bulk aqueous phase. Specifically, the case of diffusion-limited adsorption, which assumes that the adsorbed surfactant molecules are in instantaneous equilibrium with those present in the sublayer, was treated. This equilibrium relationship was determined using a previously developed molecular-thermodynamic theory for the equilibrium adsorption of surfactant mixtures. A significant advantage of this theory is that it is based on the molecular characteristics of the surfactants, and does not contain any mixture dependent parameters. This should be contrasted with other theoretical descriptions of mixed surfactant adsorption, such as those based on the Regular Solution Theory, which do require experimental inputs on every surfactant mixture considered. Since the Fickian diffusion model utilized here does not contain mixture dependent parameters either, the theoretical framework presented in this chapter can be used to predict the dynamic interfacial behavior of the mixed surfactant system without the need for any experimental inputs on the mixed surfactant system.

Although the theoretical framework developed in this chapter can be used to fully predict the surface tension and surface concentration and composition of a surfactant mixture as a function of time, a simplified timescale analysis was also provided which can be used to quickly estimate the time required to attain adsorption equilibrium (including the resulting surface tension equilibrium). While the timescale analysis is more complicated in the case of surfactant mixtures, it is generally quicker to implement than the solution of the complete theory. Accordingly, the simplified timescale analysis could be utilized to screen a large number of single surfactants and their mixtures to identify the desired dynamic interfacial behavior. The simplified timescale analysis is also useful in allowing quick prediction of the relationship between the surfactant molecular structure and the dynamic adsorption properties of that surfactant.

The theoretical framework and timescale analysis was then utilized to examine four illustrative examples of hypothetical surfactant mixtures where the surfactant molecular parameters can be varied to demonstrate a range of interesting dynamic interfacial behavior. In the first example, a binary surfactant mixture was consid-

ered where both surfactant components have the same timescale for adsorption. The results show a single characteristic decrease in the surface tension with time, corresponding to the simultaneous adsorption of both surfactants. In the second example, a binary surfactant mixture of a faster, less surface active surfactant mixed with a slower, more surface active surfactant was considered. The predicted dynamic surface tension of the binary surfactant mixture shows two characteristic decreases. The first decrease occurs at a timescale similar to the timescale for adsorption corresponding to a single surfactant solution containing only the first, faster surfactant. The second characteristic decrease lowers the surface tension further to the final equilibrium value of the surfactant mixture, and occurs at a timescale equal to the timescale for adsorption of the second, slower surfactant. In general, in the limiting case of a mixture of surfactants having very different adsorption timescales, the system will behave like a single surfactant solution of the first ("faster") surfactant at short times and like a solution of the surfactant mixture at long times.

This example also provided some insight into the behavior of surfactant solutions that contain trace amounts of a highly surface active material (an "impurity"), which is often a problem for experimental investigations of what is desired to be a pure surfactant. In that case, the impurity will typically have a very long timescale for adsorption (because it is present in such dilute amounts, the lengthscale for adsorption is very long). In this limiting mixed surfactant case, it was shown that the impurity does not pose a significant concern at short times, since the mixture will approximate the behavior of a pure surfactant solution. It is only at long times that the impurity affects the surface tension behavior.

In the third example, the contrasting dynamic interfacial behavior of a faster, more surface active surfactant mixed with a slower, less surface active surfactant was examined. This example showed that the effect of the later arriving surfactant is small when that surfactant is less surface active, since it will not significantly displace the surfactant that adsorbs first. Accordingly, the surfactant mixture shows only one characteristic decrease in the dynamic surface tension corresponding to the adsorption of the first surfactant. Finally, in the fourth example, a ternary surfactant

mixture where the adsorption of all three surfactant components is clearly reflected in the dynamic surface tension of the surfactant mixture was considered. This example illustrated the versatility of the theoretical framework presented here, in that it can be utilized to model the dynamic interfacial properties of surfactant mixtures containing any number of surfactant components.

There are numerous practical applications where the dynamic interfacial properties are important, and where the use of surfactant mixtures could be very beneficial. For example, one may be interested in a process where the desired equilibrium surface tension is known, but the time to reach that equilibrium needs to be varied continuously. Example 1 in Section 5.3.1 shows how this may be achieved by utilizing a surfactant mixture where varying the bulk surfactant composition changes the time required to reach equilibrium, but does not alter the equilibrium value of the surface tension. Another practical application of a surfactant mixture is a two-in-one shampoo plus conditioner personal care product, where one requires a cleaning surfactant to adsorb quickly, and then a conditioning surfactant to adsorb subsequently and displace the cleaning surfactant. Example 2 in Section 5.3.2 illustrates just such a case. Finally, one may be interested in a process where, say, foam stability varies with time. Any of the illustrative examples presented in Section 5.3 may be appropriate in this case, if the various surfactant components all had different foam stabilizing capabilities. In all these applications, and others, the theoretical framework presented in this chapter would be quite valuable in choosing appropriate surfactants, as well as in selecting the required solution conditions (including the total bulk surfactant concentration and composition), to tune the desired dynamic interfacial properties.

A detailed comparison of dynamic surface tensions predicted utilizing the theoretical framework presented in this chapter, with experimentally measured dynamic surface tensions of aqueous solutions containing binary nonionic surfactant mixtures is presented in the next chapter.

Chapter 6

Experimental Investigation of the Dynamic Surface Tensions of Aqueous Surfactant Mixtures

6.1 Introduction

The dynamic interfacial properties of aqueous surfactant solutions, including the surface tension, the surface concentration, and the surface composition, often play a central role in many practical applications involving surfactants (for an overview of applied aspects of dynamic interfacial phenomena, see Ref. 95). As a result of the importance of dynamic interfacial properties, this research area has received considerable attention following the pioneering work of Ward and Tordai[96] (see Refs. 98, 13, and 97 for recent reviews). Note that most of the previous work in this area has been concerned primarily with the dynamic interfacial adsorption of a *single* surfactant species. However, the examination of mixed surfactant solutions is of great practical interest, since virtually all applications of surfactants involve the use of surfactant mixtures.[130]

In Chapter 5, a theoretical framework was developed to molecularly predict the diffusion-controlled dynamic adsorption of surfactants in aqueous mixed surfactant so-

lutions.[123] The primary difference among the theory in Chapter 5 and those developed previously to predict mixed surfactant adsorption[119–122] is in the *equilibrium adsorption model* utilized to relate the concentrations of the various surfactant molecules present at the interface to those present in the sublayer (the region of the aqueous phase adjacent to the interface). Specifically, in Chapter 5, the equilibrium adsorption model used was based on the molecular characteristics of the surfactants (see Chapter 2).[12,88,89] As a result, insight could be provided as to how these surfactant molecular characteristics, specially the molecular size, can lead to interesting dynamic interfacial behavior. Another notable advantage of utilizing the equilibrium adsorption model adopted in Chapter 5 is in the ability to predict both the equilibrium and the dynamic adsorption behaviors of surfactant mixtures *without utilizing any mixture dependent parameters.* In other words, no additional experiments need to be conducted on the mixed surfactant system considered. As a result, the theoretical framework presented in Chapter 5 leads to a significant reduction in the amount of experimentation required to predict the dynamic interfacial properties of surfactant mixtures. In addition to the complete solution of the dynamic adsorption model, in Chapter 5, a simplified timescale approach designed to allow "quick" insight into the relationship between the molecular structure of the surfactants and their dynamic interfacial properties was developed for both single surfactants and surfactant mixtures.

In this chapter, the experimentally measured equilibrium and dynamic surface tensions of two nonionic surfactants, as well as of their binary mixture, is presented.[134] The measured surface tension values are then compared with those predicted using the equilibrium and the dynamic theories developed in Chapters 2 and 5, respectively. Although there have been numerous experimental investigations of the dynamic surface tensions of single surfactant solutions, previous experimental work on mixed surfactant solutions is quite limited.[119–121] The two nonionic surfactants investigated here were selected to test the validity of the theory developed in Chapter 5. Specifically, two highly purified alkyl ethoxylate surfactants, dodecyl penta(ethylene oxide) ($C_{12}E_5$), and decyl octa(ethylene oxide) ($C_{10}E_8$), whose molecular characteris-

tics have been described previously,[12] were selected. This pair of surfactants was also selected because it corresponds to a smaller, more surface active surfactant ($C_{12}E_5$) mixed with a larger, less surface active surfactant ($C_{10}E_8$), which was one of the interesting illustrative examples (Example 1) discussed theoretically in Chapter 5. In addition, these surfactants were selected because their adsorption occurs over a time range which can be measured by the pendant bubble apparatus utilized here (see Section 6.2.2). It is noteworthy that the bulk concentrations of the surfactant solutions investigated in this study were chosen to be well below the corresponding critical micelle concentrations (CMC's), where surfactant adsorption is expected to be in the diffusion-limited regime. That is, one expects a shift in surfactant adsorption mechanism as one increases the solution surfactant concentration from being dilute, where surfactant diffusion is relatively slow and therefore constitutes the rate determining step, to being concentrated, where surfactant diffusion is relatively fast and hence is no longer the rate determining step (see Refs. 135,118,117,116 for a detailed discussion).

The experimental results reveal that the adsorption of the surfactants examined here, including their binary mixtures, is consistent with diffusion-controlled adsorption, and that the theoretical framework developed in Chapter 5 is capable of quantitatively predicting the dynamic surface tension of the surfactant solutions examined. Moreover, the experimental results presented here also show that the simplified timescale analysis developed in Chapter 5 can indeed provide a relatively quick and quantitatively accurate estimation of the rate of adsorption of a single nonionic surfactant or of a surfactant component in a binary nonionic surfactant mixture.

The remainder of the chapter is organized as follows. In Section 6.2, the materials and the experimental techniques utilized to measure the equilibrium as well as the dynamic surface tensions are described. In Section 6.3, a brief overview of the equilibrium and the dynamic interfacial theories utilized here to predict the equilibrium and the dynamic surface tensions is provided. In Section 6.4, a comparison between the theoretically predicted and the experimentally measured equilibrium and dynamic surface tensions, including the simplified timescale analysis, is presented. Finally, in

Section 6.5, concluding remarks are provided.

6.2 Experimental Techniques

6.2.1 Materials

The two nonionic surfactants studied in this chapter, dodecyl penta(ethylene oxide) ($C_{12}E_5$), and decyl octa(ethylene oxide) ($C_{10}E_8$), were obtained from Nikko Chemicals, Japan (lot numbers 0054 and 0018, respectively) and, due to their high purity (as indicated by the absence of a minimum in the equilibrium surface tension versus surfactant concentration curves), were used as received. All water used in the measurements was purified using a Millipore Milli-Q system and had a specific resistance of 18 MΩ cm. All glassware was carefully cleaned either: (i) by soaking in a 1 M NaOH-Ethanol bath for at least 8 hours, followed by soaking in a 1 M nitric acid bath for at least another 8 hours, rinsing copiously with Milli-Q water, and finally drying in an oven overnight, or (ii) by soaking in a Nochromix solution for at least 8 hours, rinsing copiously with Milli-Q water, and then drying in a cabinet. The needle used in the pendant bubble measurements was cleaned by sonicating repeatedly in Milli-Q water. The platinum Wilhelmy plate used in the equilibrium surface tension measurements was cleaned by rinsing with Milli-Q water, followed by rinsing with acetone, and finally held in a flame until an orange glow was obtained.

6.2.2 Methods

The equilibrium surface tension measurements were made using a Krüss K10 tensiometer with a platinum Wilhelmy plate.[93] A schematic illustration of this apparatus is shown in Figure 6-1. To measure the equilibrium air-aqueous solution surface tension using this method, the plate is brought into contact with the surfactant solution of interest. Because the plate is made of platinum, which has an extremely high surface energy (σ_S in Eq. (1.1) in Chapter 1), the solution will fully wet the platinum plate (that is, the contact angle will nearly be zero). Therefore, the force on the plate

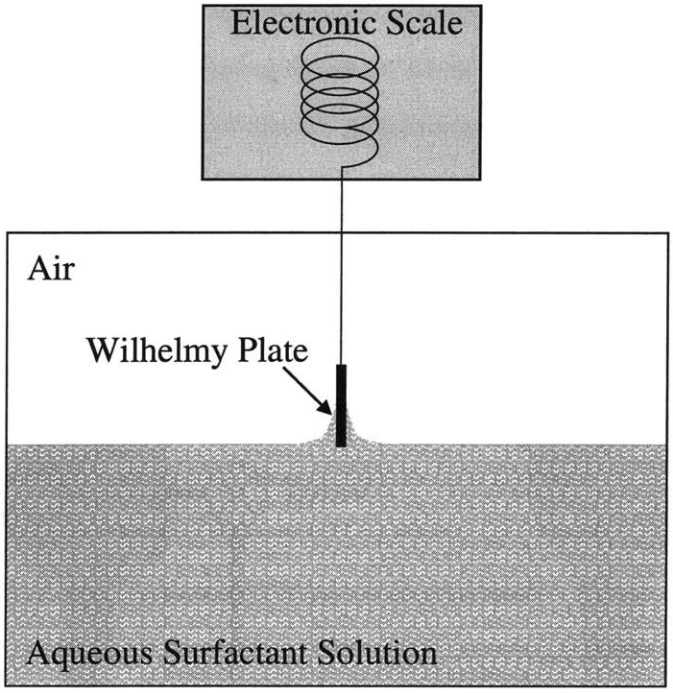

Figure 6-1: Schematic illustration of the Wilhelmy plate method for measuring the equilibrium air–aqueous surfactant solution surface tension.

will be equal to the product of the surface tension of the solution of interest and the perimeter of the plate. By measuring the force using an electronic scale, and then dividing by the known perimeter of the plate, the surface tension can be deduced. Each measurement was repeated three times and the average result is reported. For the equilibrium measurements, the temperature was held constant at 21.7 ± 0.1°C by a thermostatically controlled jacket around the sample. The experimental uncertainty in these equilibrium surface tension measurements was approximately 0.1 dyn/cm

The dynamic surface tension measurements were made using a pendant bubble apparatus (for a detailed description of this apparatus and the measuring procedure, see Refs. 107 and 127). A schematic illustration of this method for measuring the

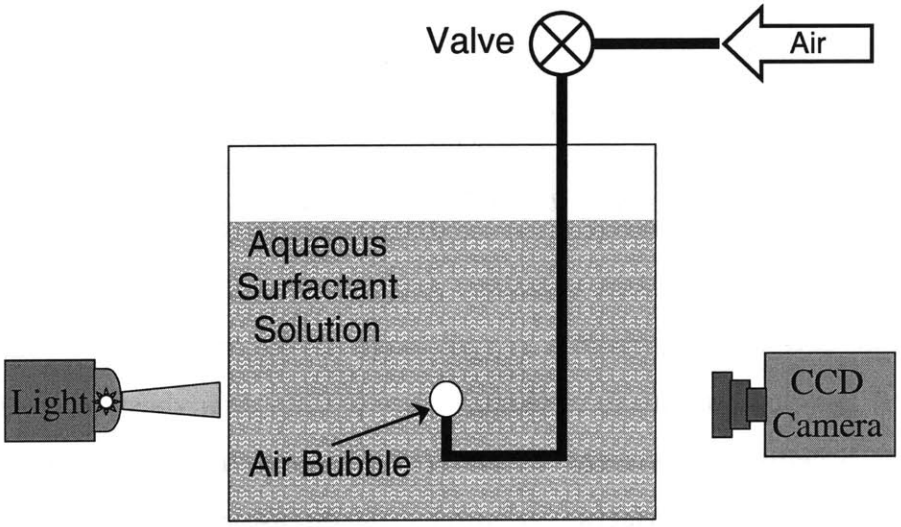

Figure 6-2: Schematic illustration of the pendant bubble method for measuring the dynamic air–aqueous surfactant solution surface tension.

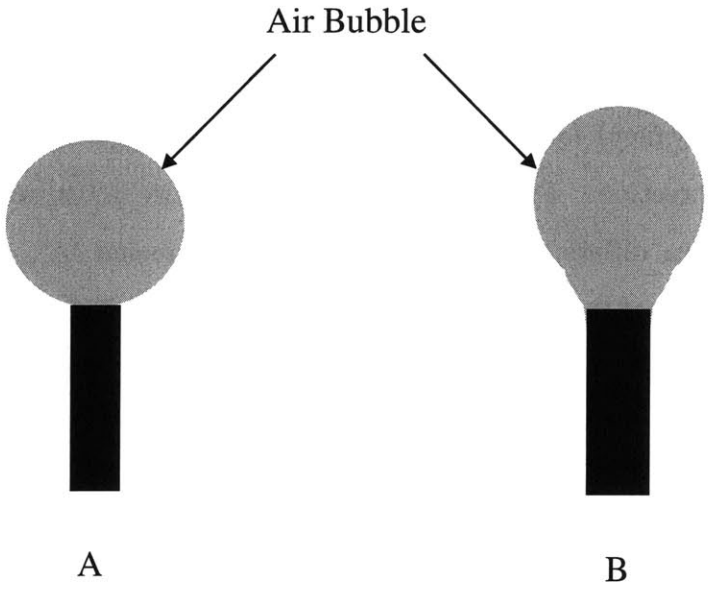

Figure 6-3: Schematic illustration of the bubble shape in the pendant bubble method for measuring the dynamic air–aqueous surfactant solution surface tension. Bubble 'A' corresponds to a relatively large value of the surface tension, where the interfacial forces dominate, and therefore, the bubble is approximately spherical in shape. Bubble 'B' corresponds to a lower value of the surface tension, where the interfacial forces no longer dominate, and hence, the bubble has elongated along the vertical direction.

dynamic air-aqueous surfactant solution surface tension is shown in Figure 6-2. First, an air bubble at the tip of an inverted steel needle is immersed in a quartz cell filled with the surfactant solution of interest. Collimated light is passed through the quartz cell, and a digital image of the bubble silhouette is captured by a CCD camera and recorded.

The instantaneous surface tension is then calculated from the profile of the bubble. That is, the shape of the bubble is determined by a balance of the interfacial force, which tends to minimize the surface area leading to a spherical bubble, and the gravitational (buoyancy) force, which tends to make the less dense bubble elongate in the vertical direction. Figure 6-3 shows a schematic illustration of the shape of a bubble in two different cases. The first case, labeled 'A', corresponds to a relatively large value of the surface tension, where the interfacial forces dominate, and therefore, the bubble is approximately spherical in shape. The second case, labeled 'B', corresponds to a lower value of the surface tension, where the interfacial forces no longer dominate, and hence, the bubble elongates along the vertical direction. Mathematically, the profile of the bubble is described by the Young-Laplace equation. Specifically,

$$\Delta \mathrm{P} = \Delta \rho \mathrm{g} z = \sigma \left(1/r_1 + 1/r_2\right) \tag{6.1}$$

where ΔP is the pressure difference across the bubble surface, $\Delta\rho$ is the density difference between the solution and air, g is the gravitational constant, z is the vertical coordinate measured from the apex of the bubble, and r_1 and r_2 are the two local principal radii of curvature.

The surface tension corresponding to the time of any given image can be determined by numerically matching the solution of the Young-Laplace equation to the measured bubble profile of that image. In this manner, the surface tension as a function of time can be determined by taking a periodic series of images, and then using these to calculate the surface tension corresponding to the time elapsed since the bubble was created. A precise timing for the creation of the bubble can be attained by using a syringe pump to blow the air through the needle, which allows for a rapid

($\approx 0.03s$) creation of the interface. Furthermore, a second beam of light, perpendicular to the first, is passed through the quartz cell and focused on a photo-diode. When the bubble is formed, its shadow causes a decrease in the voltage of the photo-diode, which can then be used to trigger the stoppage of air flowing through the needle and the commencement of the collection of the bubble profile images. In this manner, the surface tension of surfaces with ages as short as 0.06s can be measured. The pendant bubble measurements were all performed at room temperature, which varied from 21.2°C to 22.2°C. The experimental uncertainty in these dynamic surface tension measurements was approximately 0.1 dyn/cm.

6.3 Theory

6.3.1 Prediction of the Equilibrium Surface Tensions of Aqueous Nonionic Surfactant Solutions

For the prediction of the equilibrium surface tensions of aqueous nonionic surfactant solutions, the molecular-thermodynamic theory for the equilibrium interfacial behavior of nonionic surfactants developed in Chapter 2 was utilized. Since this theory for nonionic surfactants has been described in detail in Chapter 2, only a brief overview is presented here. The surface equation of state developed in the context of this theory is given by:

$$\sigma = \sigma_0 - \mathrm{k_B}T \left\{ \frac{\sum_{i=1}^{n} \Gamma_i}{1 - \sum_{i=1}^{n} \Gamma_i \mathrm{a}_i} + \frac{\pi \left(\sum_{i=1}^{n} \Gamma_i \mathrm{r}_i \right)^2}{\left(1 - \sum_{i=1}^{n} \Gamma_i \mathrm{a}_i \right)^2} + \sum_{i,j=1}^{n} \mathrm{B}_{ij} \Gamma_i \Gamma_j \right\} \tag{6.2}$$

where σ is the surface tension of the surfactant solution, σ_0 is the surface tension of pure water, $\mathrm{k_B}$ is the Boltzmann constant, T is the absolute temperature, a_i and $\mathrm{r}_i = \sqrt{\mathrm{a}_i/\pi}$ are the cross-sectional area and radius of the adsorbed surfactant molecules of type i, respectively, B_{ij} is the second-order virial coefficient between surfactant molecules of type i and j (which, for surfactants consisting of linear alkyl

tails, can be calculated from the number of carbon atoms in the tail of each surfactant[12]), $\sum_{i,j=1}^{n}$ indicates summation over all possible pairs of surfactants, while avoiding double counting, Γ_k is the surface concentration of surfactant molecules of type k, and n is the number of surfactant components comprising the mixture. The equilibrium adsorption isotherm of each surfactant component i (that is, the equilibrium relationship between the surface concentration and the bulk concentration of surfactant component i) is given by:

$$\ln\left(\frac{n_i^{\mathrm{w}}}{n_w^{\mathrm{w}}+\sum_{k=1}^{n} n_k^{\mathrm{w}}}\right) = \frac{\Delta\mu_i^0}{\mathrm{k_B}T} + \ln\left(\frac{\Gamma_i}{1-\sum_{k=1}^{n}\Gamma_k \mathrm{a}_k}\right) + \frac{\mathrm{a}_i\sum_{k=1}^{n}\Gamma_k + 2\pi \mathrm{r}_i \sum_{k=1}^{n}\Gamma_k \mathrm{r}_k}{1-\sum_{k=1}^{n}\Gamma_k \mathrm{a}_k}$$

$$+ \frac{\pi \mathrm{a}_i\left(\sum_{k=1}^{n}\Gamma_k \mathrm{r}_k\right)^2}{\left(1-\sum_{k=1}^{n}\Gamma_k \mathrm{a}_k\right)^2} + 2\sum_{k=1}^{n} B_{ik}\Gamma_k \qquad (6.3)$$

where $n_i^{\mathrm{w}} \Big/ \left(n_w^{\mathrm{w}} + \sum_{k=1}^{n} n_k^{\mathrm{w}}\right) \approx n_i^{\mathrm{w}}/n_w^{\mathrm{w}}$ is the bulk mole fraction of surfactant molecules of type i (n_w^{w} is the bulk number density of water, which is approximately constant, since the surfactant concentration is dilute), and $\Delta\mu_i^0$ is the difference between the standard-state chemical potentials of a surfactant molecule of type i at the interface and in the bulk aqueous phase[12] (also referred to as the free energy of adsorption of surfactant molecules of type i). Note that Eq. (6.3) represents a set of n equations corresponding to $i = 1$ to n. Accordingly, for a given bulk surfactant concentration and composition (that is, for a given value of the bulk surfactant mole fraction, $n_i^{\mathrm{w}}/n_w^{\mathrm{w}}$), the set of n unknown quantities, $\{\Gamma_i\}$, can be calculated by simultaneously solving the set of n equations given in Eq. (6.3). Once these surface concentrations, $\{\Gamma_i\}$, have been determined, one can predict the surface tension of the surfactant solution using Eq. (6.2). Note also that the free energies of adsorption, $\Delta\mu_i^0$, are the only unknown parameters in this theory, and can be calculated by fitting the predicted surface tension to one experimentally measured surface tension value for

each single surfactant component comprising the mixture.

6.3.2 Prediction of the Dynamic Surface Tensions of Aqueous Nonionic Surfactant Solutions

The dynamic surface tension predictions were made using the theory described in Chapter 5, which utilizes the equilibrium adsorption theory described in Chapter 2 as its basis. Specifically, the Ward and Tordai equation for spherical interfaces[103] (which most accurately describes the pendant bubble experimental conditions), extended to treat mixtures of surfactants, is given by:

$$\Gamma_i(t) = 2\sqrt{\frac{D_i}{\pi}}\left[n_i^{\mathrm{w}}\sqrt{t} - \int_0^{\sqrt{t}} n_i^0\left(t-\tilde{t}\right)d\sqrt{\tilde{t}}\right] + \frac{D_i}{R}\left[n_i^{\mathrm{w}}t - \int_0^t n_i^0\left(\tilde{t}\right)d\tilde{t}\right] \qquad (6.4)$$

where n_i^0 is the concentration of surfactant molecules of type i in the sublayer (the region of the aqueous phase adjacent to the interface), D_i is the diffusion coefficient of surfactant molecules of type i, and R is the radius of the bubble (which, for the results presented in Section 6.4, has a value of $R = 0.1cm$, corresponding to the approximate bubble radius in the pendant bubble apparatus). Note that Eq. (6.4) represents a set of n equations. Note also that in the limit of a large bubble (in particular, when $R >> \Gamma_i/n_i^{\mathrm{w}}$), Eq. (6.4) reduces to the expression corresponding to a flat interface given in Chapter 5 (see Refs. 127 and 111 for a more detailed discussion).

In the limit of *diffusion-controlled adsorption*, one can assume instantaneous equilibrium between the adsorbed surfactant molecules and those present in the sublayer. This assumption allows one to use the equilibrium adsorption isotherm, Eq. (6.3), with the sublayer concentrations, $\{n_i^0\}$, replacing the bulk concentrations, $\{n_i^{\mathrm{w}}\}$, along with the initial condition of $\{\Gamma_i(t=0)=0\}$, to iteratively solve for the surface concentration of each surfactant component as a function of time, $\{\Gamma_i(t)\}$, using Eq. (6.4). Once the surface concentrations have been determined, the dynamic surface tension can be predicted by utilizing Eq. (6.2) at every time point of interest (see Chapter 5 for a detailed description of the calculation procedure).

In addition to the complete prediction of the surface tension as a function of time, in Chapter 5, a simplified analysis was presented where the diffusion-limited timescale for adsorption of each surfactant component can be estimated without explicitly solving Eq. (6.4). Specifically, the timescale for adsorption of surfactant molecules of type i, τ_{D_i}, can be written as follows:

$$\tau_{D_i} = \frac{(\Gamma_i / n_i^{\mathrm{w}})^2}{D_i} \tag{6.5}$$

For single surfactant solutions, the value of Γ_i in Eq. (6.5) should be the equilibrium value, Γ_i^{eq}, obtained by solving Eq. (6.3) for surfactant component i. For mixtures of surfactants, one can obtain an initial estimate of the timescale for adsorption of each surfactant component by using the equilibrium value of Γ_i in Eq. (6.5). If the timescales for adsorption of each surfactant component are similar, then this procedure will provide a good estimate for τ_{D_i}. However, if the timescales for adsorption of each surfactant component are significantly different, then this procedure will not yield a good estimate for τ_{D_i}. For example, considering a binary surfactant mixture, for the surfactant having the shortest timescale for adsorption, one should use in Eq. (6.5) the equilibrium value of Γ_i corresponding to a surfactant solution containing only that surfactant component at the same bulk surfactant concentration as that corresponding to the binary surfactant mixture. For the second, later adsorbing surfactant, one should use the equilibrium value of Γ_i corresponding to the binary surfactant mixture (see Chapter 5). In this manner, one can quickly estimate the timescales for adsorption of the various surfactant components through the use of the computationally less intensive equilibrium model. Examples of all of these predictions, as well as a comparison of the predicted and the experimentally measured dynamic surface tensions, including the timescale analysis, are presented in Section 6.4.

6.4 Results

Figure 6-4 shows both the experimentally measured (symbols) and the predicted (lines) equilibrium surface tensions as a function of bulk surfactant concentration for: (i) aqueous single surfactant solutions of $C_{12}E_5$ (●) and $C_{10}E_8$ (■), and (ii) aqueous binary surfactant solutions of 50% $C_{12}E_5$ – 50% $C_{10}E_8$ (♦) and 16.7% $C_{12}E_5$ – 83.3% $C_{10}E_8$ (▲). The surfactant molecular parameters, a_i, $\Delta\mu_i^0$, and B_{ij}, used for the predictions shown in Figure 6-4 are listed in Tables 6.1 and 6.2. Note the cross-sectional areas, a_i, and the virial coefficients, B_{ij}, were calculated from the number of ethylene oxide groups, j, in the surfactant E_j heads and the number of carbon atoms in the surfactant tails, respectively, as described in detail in Ref. 12. The single surface tension measurement that was used for the fitting of the standard-state chemical potential difference, $\Delta\mu_i^0$, corresponds to the surface tension value at $1.0 \times 10^{-8} mol/cm^3$ for $C_{12}E_5$ and at $1.0 \times 10^{-6} mol/cm^3$ for $C_{10}E_8$. Recall that there are no fitted parameters for the mixed surfactant solutions. Figure 6-4 shows that the surface tension vs. surfactant concentration curve of the more surface active surfactant, $C_{12}E_5$, (which corresponds to the fact that $\Delta\mu^0_{C_{12}E_5} < \Delta\mu^0_{C_{10}E_8}$) lies to the left of that corresponding to the less surface active surfactant, $C_{10}E_8$, as expected, with the surface tension curves of the binary surfactant mixtures lying in between according to their composition. Figure 6-4 also shows that the surfactant with the smaller cross-sectional area, $C_{12}E_5$, exhibits a surface tension vs. surfactant concentration curve with a steeper slope. This is due to the fact that the slope of this curve, according to the Gibbs adsorption equation, is proportional to the surface concentration,[41] and that the smaller surfactant ($C_{12}E_5$) gives rise to a larger value of the surface concentration. Although the agreement between the predicted and the experimental surface tension measurements is quite good for the four systems examined, note that the theory does a better job at predicting the surface tension of $C_{12}E_5$ than that of $C_{10}E_8$. This may be attributed to the fact that $C_{10}E_8$ has a larger, more flexible polymeric (polyethylene oxide) E_j head, and therefore, the hard-disk description underlying the surface equation of state adopted here may better describe the shorter E_5 heads.

Table 6.1: Cross-sectional areas, a_i, and standard-state chemical potential differences, $\Delta\mu_i^0$, corresponding to $C_{12}E_5$ and $C_{10}E_8$.

Surfactant i	a_i (Å^2)	$\Delta\mu_i^0$ (k_BT)
$C_{12}E_5$	36.6	-51.9
$C_{10}E_8$	47.9	-51.0

Table 6.2: Values of the second-order virial coefficients, B_{ij}, used in the equilibrium and the dynamic surface tension predictions of solutions of $C_{12}E_5$, $C_{10}E_8$, and their binary mixtures.

Surfactant i	Surfactant j	B_{ij} (Å^2)
$C_{12}E_5$	$C_{12}E_5$	-108
$C_{10}E_8$	$C_{10}E_8$	-47
$C_{12}E_5$	$C_{10}E_8$	-69

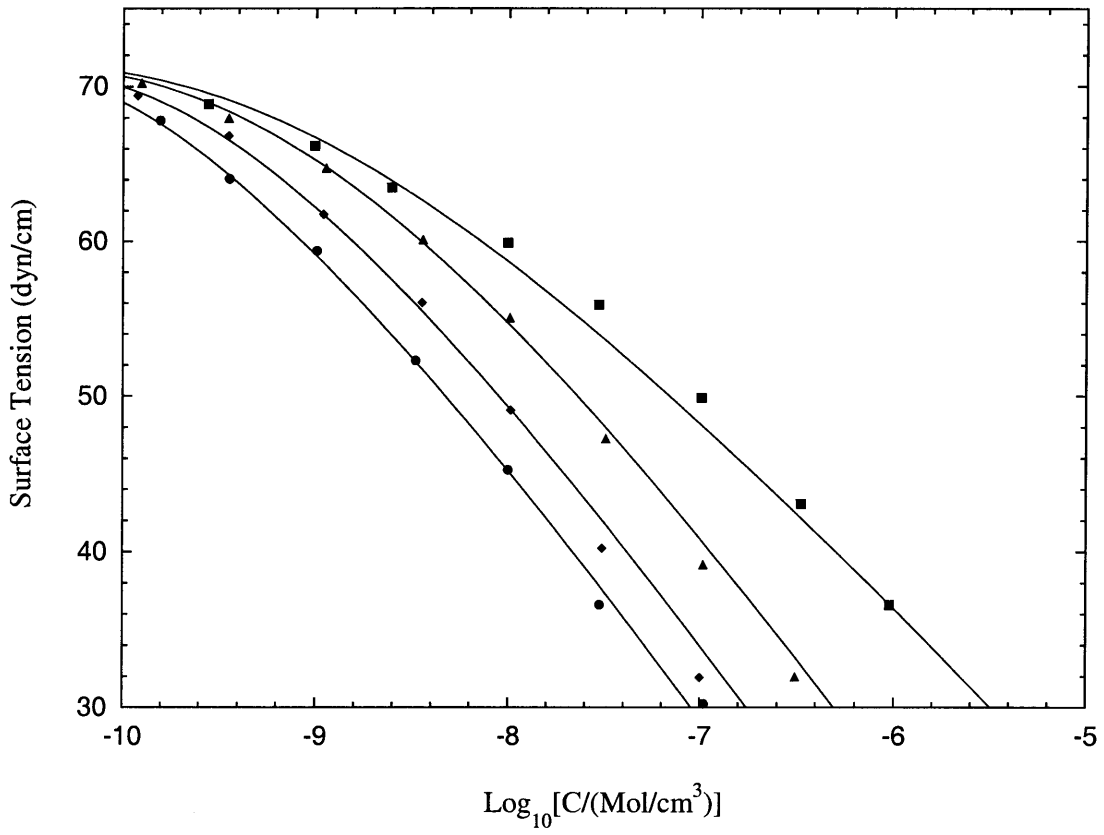

Figure 6-4: Predicted (lines) and experimentally measured (symbols) equilibrium surface tensions as a function of total bulk surfactant concentration for aqueous single surfactant solutions of: (i) $C_{12}E_5$ (●) and $C_{10}E_8$ (■), and (ii) binary surfactant mixtures of 50% $C_{12}E_5$ – 50% $C_{10}E_8$ (♦) and 16.7% $C_{12}E_5$ – 83.3% $C_{10}E_8$ (▲).

Figure 6-5 shows both the experimentally measured (symbols) and the predicted (solid lines) dynamic surface tension profiles of an aqueous solution of $C_{12}E_5$ at a bulk surfactant concentration of $4.0 \times 10^{-9} mol/cm^3$ (filled symbols), and at a bulk surfactant concentration of $16 \times 10^{-9} mol/cm^3$ (open symbols). Note that the various types of filled and open symbols correspond to different runs under the same experimental conditions. The diffusion coefficient of $C_{12}E_5$, $6.5 \times 10^{-6} cm^2/s$, was determined by fitting the predicted dynamic surface tension profile to the experimentally measured surface tension profile for the $4.0 \times 10^{-9} mol/cm^3$ solution. This value of $D_{C_{12}E_5}$ was then used to predict the dynamic surface tension of the more concentrated $C_{12}E_5$ aqueous solution. The fact that the predicted dynamic surface tensions are in good agreement with the experimental results shown in Figure 6-5 for both bulk $C_{12}E_5$ concentrations, along with the fact that the fitted value of $D_{C_{12}E_5}$ is within the range of values typically encountered for surfactants,[13] provides strong support for the assumption that the adsorption of the surfactant molecules in these solutions is indeed diffusion limited.[13]

Instead of relying on dynamic surface tension measurements to fit D, the diffusion coefficient can instead be estimated theoretically. For example, using the Wilke-Chang model[136] (which is a correlation based on the molecular weight of the solute, $C_{12}E_5$ in the present case, and the viscosity of the solvent, water in the present case) the diffusion coefficient of $C_{12}E_5$ can be estimated to be $4.2 \times 10^{-6} cm^2/s$, which is reasonably close to the value obtained by fitting to the dynamic surface tension profile ($D_{C_{12}E_5} = 6.5 \times 10^{-6} cm^2/s$). For comparison, the predicted dynamic surface tension profiles obtained using $D_{C_{12}E_5} = 4.2 \times 10^{-6} cm^2/s$ are also shown in Figure 6-5 (dashed lines). Note that these predictions are also in reasonably good agreement with the experimental measurements, specially considering that *there are no fitted parameters* in the dynamic adsorption model used to make these predictions. In addition, note that the two sets of curves in Figure 6-6, corresponding to the two different values of $D_{C_{12}E_5}$, illustrate the relatively weak sensitivity of the dynamic surface tension predictions to the value of D used. Finally, the diffusion coefficient can also be obtained by using an alternative experimental technique. For example,

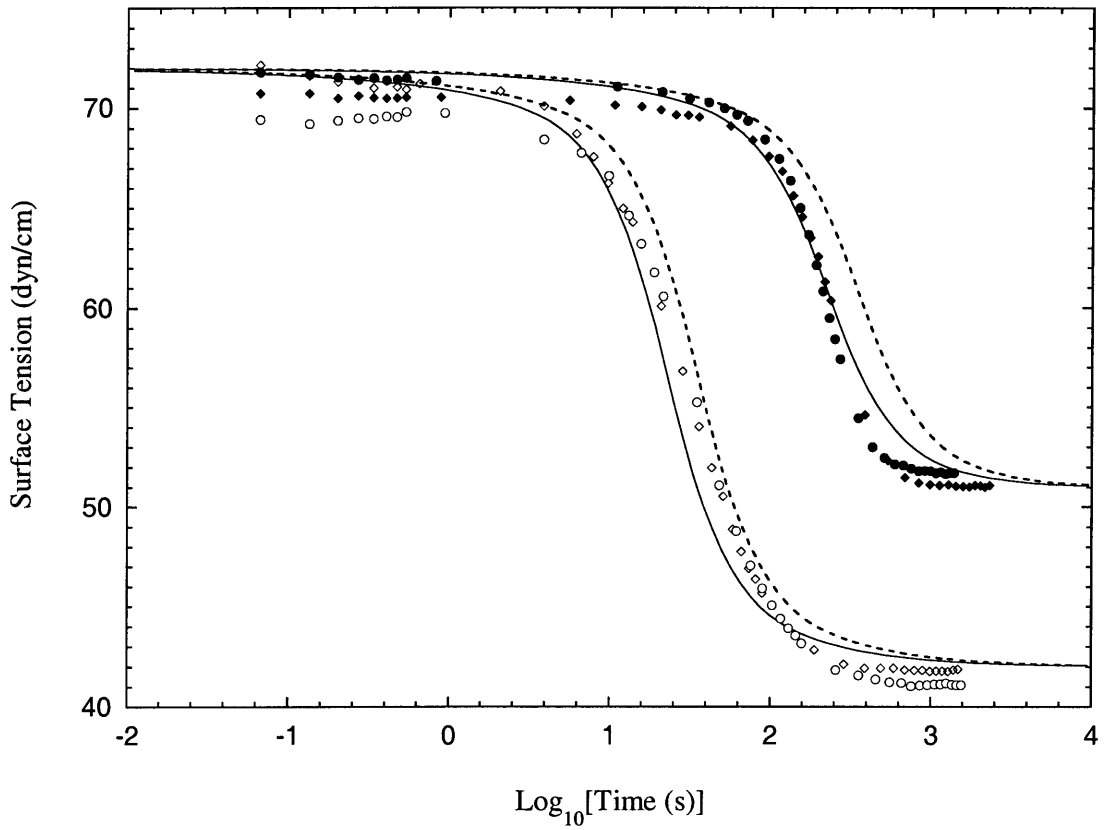

Figure 6-5: Predicted (lines) and experimentally measured (symbols) dynamic surface tensions of aqueous solutions of $C_{12}E_5$ at bulk surfactant concentrations of $4.0 \times 10^{-9} mol/cm^3$ (filled symbols) and $16 \times 10^{-9} mol/cm^3$ (open symbols). The various types of filled and open symbols correspond to different experimental runs at the same bulk surfactant concentration. The solid lines correspond to the predicted dynamic surface tensions made using the fitted value of the diffusion coefficient ($6.5 \times 10^{-6} cm^2/s$; see text). The dashed lines correspond to the predicted dynamic surface tensions made using the theoretical value of the diffusion coefficient, predicted using the Wilke-Chang model ($4.2 \times 10^{-6} cm^2/s$).

Schönhoff and Södermann[137] have measured the diffusion coefficient of $C_{12}E_5$ using NMR, and obtained a value of $3.9 \times 10^{-6} cm^2/s$, which is again reasonably close to the value obtained by fitting to the measured dynamic surface tension profile. The predicted dynamic surface tension profiles obtained when using this value of $D_{C_{12}E_5}$ are very similar to those obtained when using the value of $D_{C_{12}E_5}$ obtained from the Wilke-Chang model, and are therefore not reported in Figure 6-5.

As discussed briefly in Section 6.3 and in detail in Chapter 5, a timescale for adsorption can quickly be estimated for these solutions using Eq. (6.5). For the $4.0 \times 10^{-9} mol/cm^3$ $C_{12}E_5$ solution, the equilibrium surface concentration, $\Gamma^{eq}_{C_{12}E_5}$, calculated through the use of Eq. (6.3), is $1.51 \times 10^{-14} mol/cm^{-2}$, which, when used in Eq. (6.5) (along with the fitted value of the diffusion coefficient, $D_{C_{12}E_5} = 6.5 \times 10^{-6} cm^2/s$), yields a timescale for adsorption of $\tau_{D_{C_{12}E_5}} = 610s$. For the $16 \times 10^{-9} mol/cm^3$ solution, $\Gamma^{eq}_{C_{12}E_5}$ is $1.64 \times 10^{-14} mol/cm^{-2}$, which yields a timescale for adsorption of $\tau_{D_{C_{12}E_5}} = 45s$. Note that both of these timescales for adsorption represent reasonable estimates for the times at which the large decreases in the dynamic surface tensions of the corresponding surfactant solutions are observed in Figure 6-5.

Figure 6-6 shows both the experimentally measured (symbols) and the predicted (solid lines) dynamic surface tension profiles of an aqueous solution of $C_{10}E_8$ at a bulk surfactant concentration of $4.0 \times 10^{-9} mol/cm^3$ (filled symbols), and at a bulk surfactant concentration of $16 \times 10^{-9} mol/cm^3$ (open symbols). Note that the various types of filled and open symbols correspond to different runs under the same experimental conditions. As with $C_{12}E_5$, the diffusion coefficient of $C_{10}E_8$, $8.0 \times 10^{-6} cm^2/s$, was also determined by fitting the predicted dynamic surface tension profile to the experimentally measured surface tension profile for the $4.0 \times 10^{-9} mol/cm^3$ solution. This value of $D_{C_{10}E_8}$ was then used to predict the dynamic surface tension for the more concentrated $C_{10}E_8$ solution. As in the case of $C_{12}E_5$, the fact that the predicted dynamic surface tension profiles are in reasonably good agreement with the experimental results in Figure 6-6 for both bulk $C_{10}E_8$ concentrations, along with the fact that the fitted value of $D_{C_{10}E_8}$ is within the range of D values typically encountered for surfactants,[13] provides strong support for the assumption that the

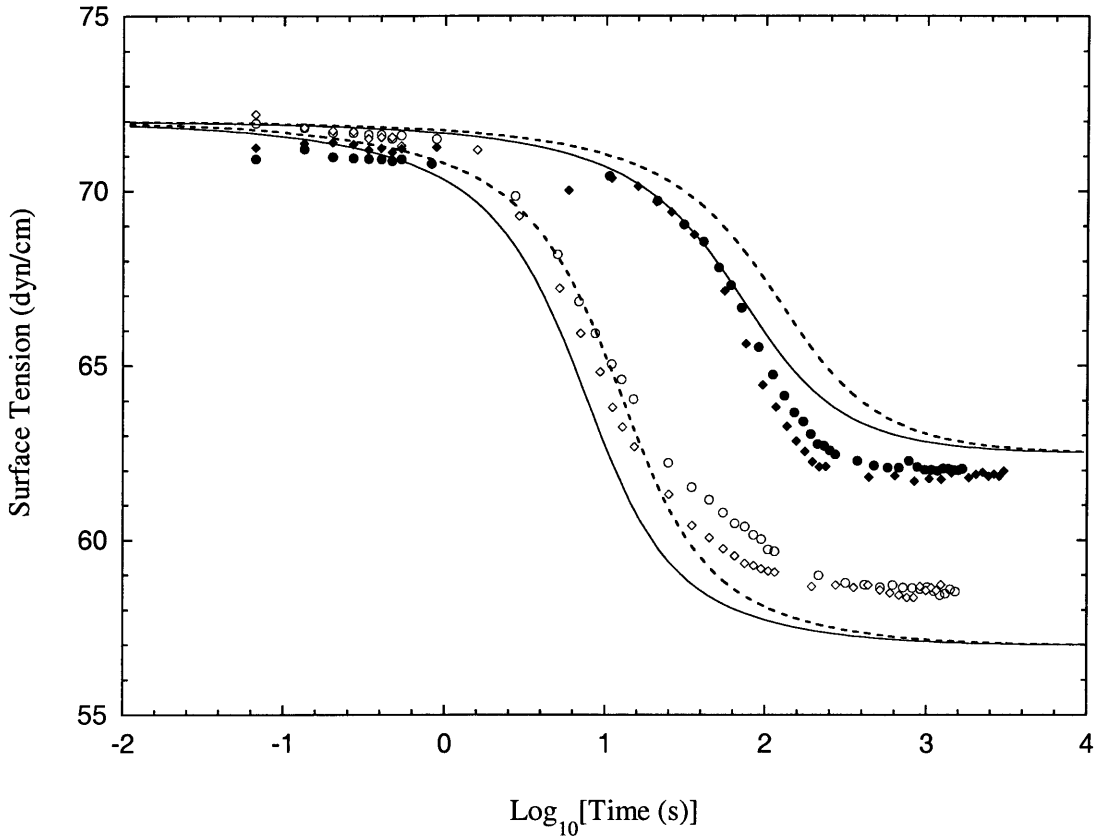

Figure 6-6: Predicted (lines) and experimentally measured (symbols) dynamic surface tensions of aqueous solutions of $C_{10}E_8$ at bulk surfactant concentrations of $4.0 \times 10^{-9} mol/cm^3$ (filled symbols) and $16 \times 10^{-9} mol/cm^3$ (open symbols). The various types of filled and open symbols correspond to different experimental runs at the same bulk surfactant concentration. The solid lines correspond to the predicted dynamic surface tensions made using the fitted value of the diffusion coefficient ($8.0 \times 10^{-6} cm^2/s$; see text). The dashed lines correspond to the predicted dynamic surface tensions made using the theoretical value of the diffusion coefficient, obtained using the Wilke-Chang model ($3.7 \times 10^{-6} cm^2/s$).

adsorption of the surfactant molecules in these solutions is indeed diffusion limited.[13] The relatively poor agreement between the predicted and the experimentally measured surface tensions in Figure 6-6 at long times ($t > 10s$) can be attributed to the difference between the actual and the predicted *equilibrium* surface tensions, which, as discussed above, may be a reflection of using the hard-disk model to describe the relatively large, flexible E_8 polymeric heads.

As in the case of $C_{12}E_5$, the diffusion coefficient can be calculated theoretically using the Wilke-Change model. In this case, this yields a value of $D_{C_{10}E_8} = 3.7 \times 10^{-6} cm^2/s$, and the predicted dynamic surface tension profiles corresponding to this value of $D_{C_{10}E_8}$ are also shown in Figure 6-6 (dashed lines). Note that these predictions are also in reasonable agreement with the experimental measurements. In addition, note that the two sets of curves in Figure 6-6, corresponding to the two different values of $D_{C_{10}E_8}$, illustrate the relatively weak sensitivity of the dynamic surface tension predictions to the value of D used.

As with $C_{12}E_5$, to determine the timescale for adsorption of $C_{10}E_8$, one proceeds as follows. For the $4.0 \times 10^{-9} mol/cm^3$ $C_{10}E_8$ solution, the equilibrium surface concentration is $\Gamma^{eq}_{C_{10}E_8} = 0.89 \times 10^{-14} mol/cm^{-2}$, which, using the fitted value of $D_{C_{10}E_8} = 8.0 \times 10^{-6} cm^2/s$ in Eq. (6.5), yields a timescale for adsorption of $\tau_{D_{C_{10}E_8}} = 170s$. For the $16 \times 10^{-9} mol/cm^3$ $C_{10}E_8$ solution, the equilibrium surface concentration is $\Gamma^{eq}_{C_{10}E_8} = 1.04 \times 10^{-14} mol/cm^{-2}$ and the corresponding timescale for adsorption is $\tau_{D_{C_{10}E_8}} = 15s$. Note that both of these timescales for adsorption represent reasonable estimates for the time at which the large decreases in the dynamic surface tensions of the corresponding solutions are observed in Figure 6-6. Note also that, at both bulk surfactant concentrations, the $C_{10}E_8$ solutions reach equilibrium faster than the $C_{12}E_5$ solutions. Physically, this reflects the fact that $C_{10}E_8$ has a larger cross-sectional area than $C_{12}E_5$ (47.9Å^2 vs. 36.6Å^2), resulting in a smaller value of its equilibrium surface concentration. This, in turn, through the use of Eq. (6.5), yields a smaller value for the timescale for adsorption of $C_{10}E_8$ (that is, $\tau_{D_{C_{10}E_8}} < \tau_{D_{C_{12}E_5}}$).

Turning next to the mixed surfactant cases, Figures 6-7 and 6-8 show both the

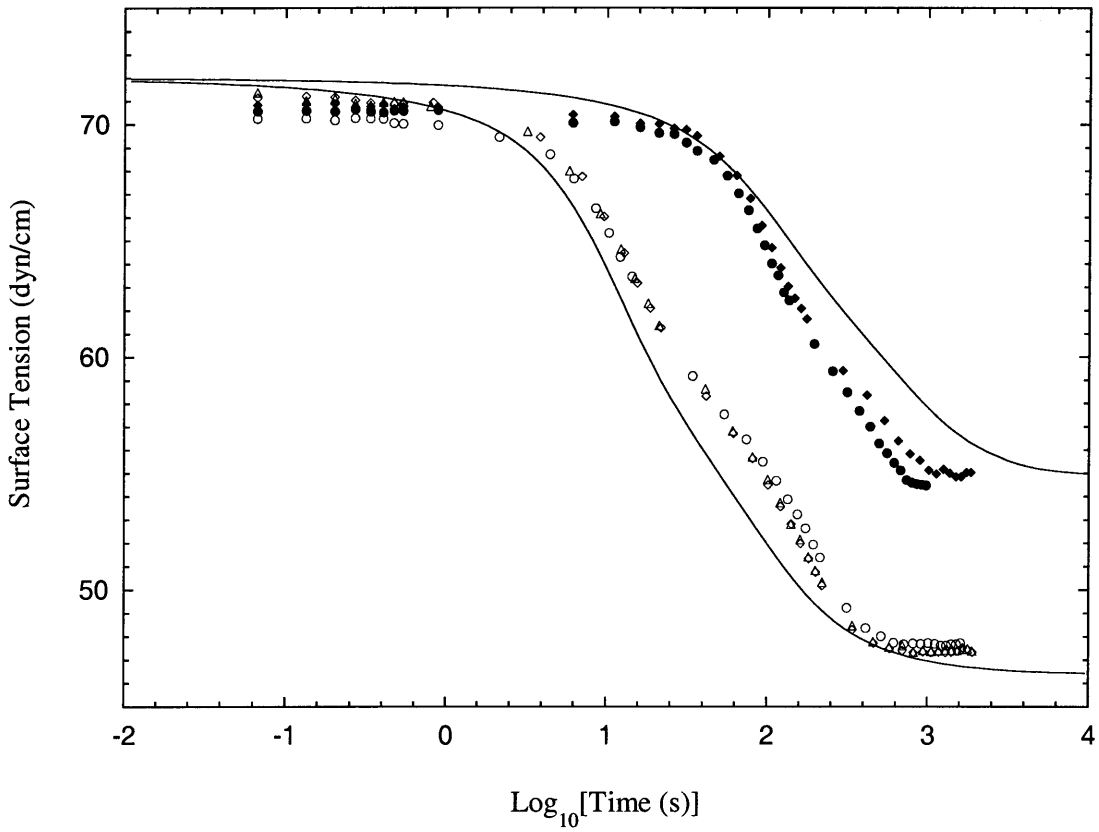

Figure 6-7: Predicted (lines) and experimentally measured (symbols) dynamic surface tensions of aqueous solutions of a binary surfactant mixture of 50% $C_{12}E_5$ – 50% $C_{10}E_8$ at total bulk surfactant concentrations of $4.0 \times 10^{-9} mol/cm^3$ (filled symbols) and $16 \times 10^{-9} mol/cm^3$ (open symbols). The various types of filled and open symbols correspond to different experimental runs at the same total bulk surfactant concentration.

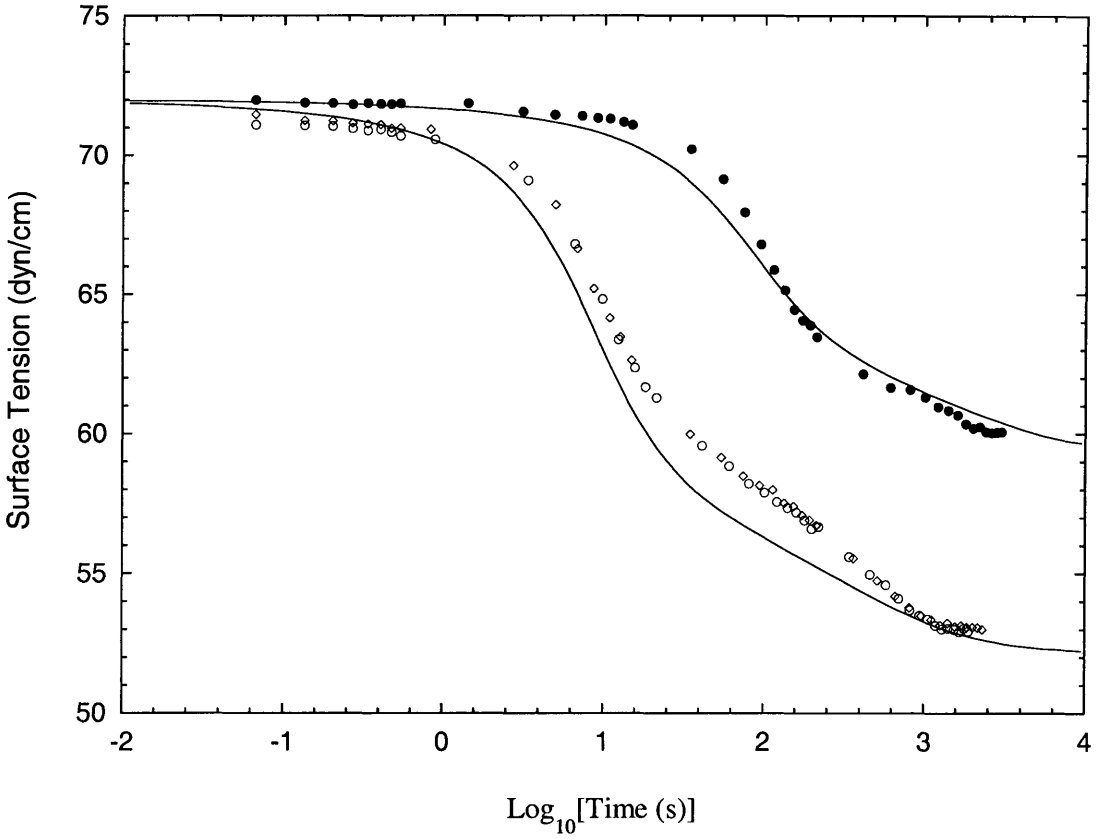

Figure 6-8: Predicted (lines) and experimentally measured (symbols) dynamic surface tensions of aqueous solutions of a binary surfactant mixture of 16.7% $C_{12}E_5$ – 83.3% $C_{10}E_8$ at total bulk surfactant concentrations of $4.0 \times 10^{-9} mol/cm^3$ (filled symbols) and $16 \times 10^{-9} mol/cm^3$ (open symbols). The various types of filled and open symbols correspond to different experimental runs at the same total bulk surfactant concentration.

experimentally measured (symbols) and the predicted (lines) dynamic surface tension profiles of a binary surfactant mixture of 50% $C_{12}E_5$ – 50% $C_{10}E_8$ (Figure 6-7), and of a binary surfactant mixture of 16.7% $C_{12}E_5$ – 83.3% $C_{10}E_8$ (Figure 6-8). For both mixtures, the filled symbols correspond to a total bulk surfactant concentration of $4.0 \times 10^{-9} mol/cm^3$, and the open symbols correspond to a total bulk surfactant concentration of $16 \times 10^{-9} mol/cm^3$. Note that the various types of filled and open symbols used in Figures 6-7 and 6-8 correspond to different runs under the same experimental conditions. Note also that all the surfactant molecular parameters used, as listed in Tables 6.1 and 6.2, are the same as those used in the predictions made for the single surfactant solutions (the diffusion coefficients used are those obtained by fitting the predicted and the experimentally measured dynamic surface tension profiles for each single surfactant solution). In other words, there are no adjustable parameters in either the equilibrium or the dynamic interfacial models, that are determined by fitting to measurements conducted on the mixed surfactant system. With this in mind, the predicted dynamic surface tension profiles shown in Figures 6-7 and 6-8 are in reasonably good agreement with the experimentally measured ones.

Note that for the binary surfactant mixtures, one can observe two characteristic decreases in the dynamic surface tensions in Figures 6-7 and 6-8. For example, for the binary surfactant mixture of 50% $C_{12}E_5$ – 50% $C_{10}E_8$ at a total bulk concentration of $16 \times 10^{-9} mol/cm^3$ (shown in Figure 6-7), the first decrease occurs at $t \approx 30s$ and the second decrease occurs at $t \approx 150s$. To clarify the observed and predicted dynamic surface tension behavior, Figure 6-9 shows the predicted surface concentrations, $\Gamma_{C_{12}E_5}$ (———), $\Gamma_{C_{10}E_8}$ (- – - – -), and $\Gamma_{C_{12}E_5} + \Gamma_{C_{10}E_8}$ (— — —) for this surfactant mixture. Figure 6-9 shows that initially, $t < 10s$, the surface concentrations of both surfactant components increase at similar rates, since initially, Γ_i is proportional to $n_i^w \sqrt{D_i t}$,[96] and both surfactant components have identical bulk concentrations and similar diffusion coefficients. However, since the cross-sectional area of $C_{10}E_8$ is larger than that of $C_{12}E_5$, the surface coverage of $C_{10}E_8$ (defined as $\Gamma_{C_{10}E_8} a_{C_{10}E_8}$) increases at a faster rate initially, and it is this initial coverage of $C_{10}E_8$ that is responsible for the first characteristic decrease in the dynamic surface tension.

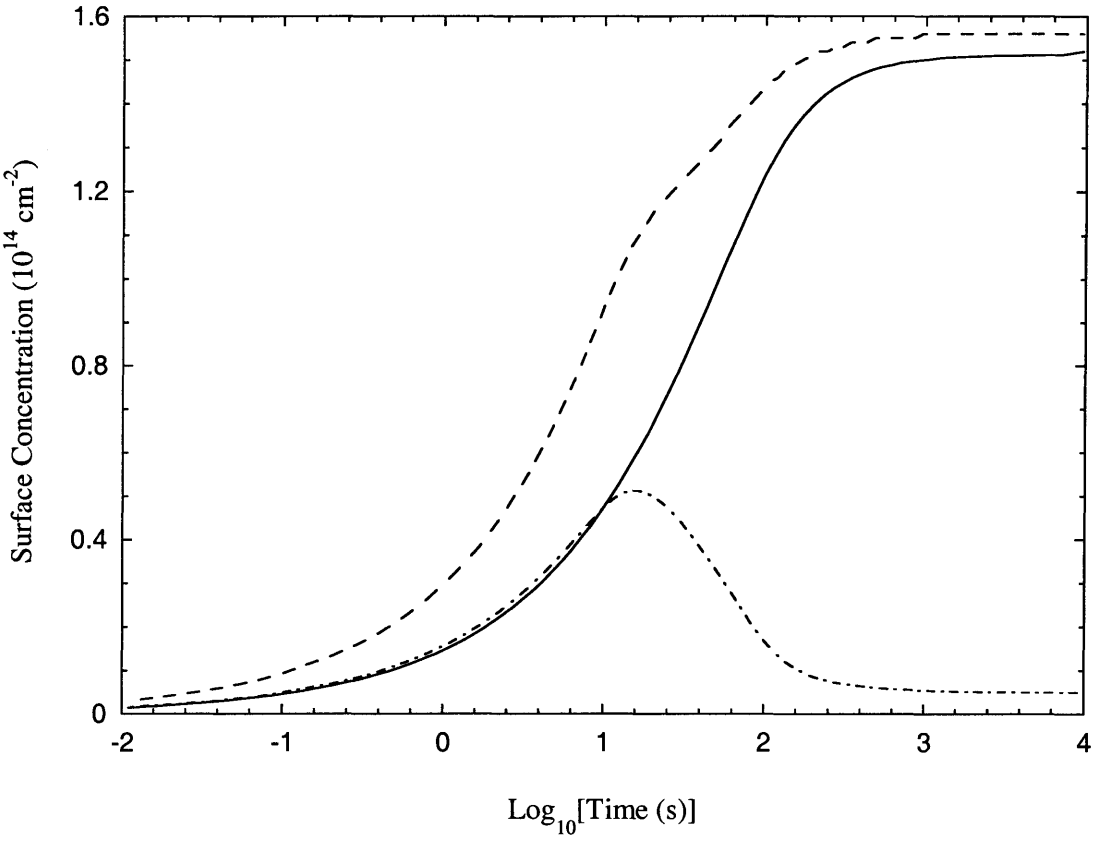

Figure 6-9: Predicted surface concentrations of $C_{12}E_5$, $\Gamma_{C_{12}E_5}$, (———), and of $C_{10}E_8$, $\Gamma_{C_{10}E_8}$, (- — - — -), as well as predicted total surface concentration, $\Gamma_{C_{12}E_5} + \Gamma_{C_{10}E_8}$, (— — —), for a binary surfactant mixture of 50% $C_{12}E_5$ – 50% $C_{10}E_8$ at a total bulk surfactant concentration of $16 \times 10^{-9} mol/cm^3$.

Eventually (around $t = 10s$), the more surface active $C_{12}E_5$ component displaces $C_{10}E_8$, leading to the second characteristic decrease in the dynamic surface tension (see Chapter 5 for a detailed discussion of this dynamic process).

Since $C_{12}E_5$ is the "slower" surfactant due to its smaller cross-sectional area ($\Gamma_{C_{12}E_5} < \Gamma_{C_{10}E_8}$, which leads to $\tau_{D_{C_{12}E_5}} > \tau_{D_{C_{10}E_8}}$, see Eq. (6.5)), as discussed in detail in Chapter 5, the timescale for adsorption of this surfactant component can be determined by using the equilibrium value of $\Gamma_{C_{12}E_5}$ corresponding to this binary surfactant mixture in Eq. (6.5). For the 50% $C_{12}E_5$ – 50% $C_{10}E_8$ surfactant solution at a

total bulk surfactant concentration of $16 \times 10^{-9} mol/cm^3$, this results in an equilibrium surface concentration of $\Gamma^{eq}_{C_{12}E_5} = 1.34 \times 10^{14} cm^{-2}$ and a corresponding timescale for adsorption of $\tau_{D_{C_{12}E_5}} = 155s$. Note that this timescale represents a good estimate for the time at which the predicted surface concentration of this component (see Figure 6-9) as well as the predicted and experimentally measured dynamic surface tensions reach equilibrium (see Figure 6-7). Since the "faster" surfactant ($C_{10}E_8$) is also the less surface active component, the timescale for adsorption of this surfactant can be determined using Eq. (6.5) with a value of $\Gamma_{C_{10}E_8}$ corresponding to the equilibrium surface concentration for a solution containing only $C_{10}E_8$ at the same surfactant concentration as in the binary surfactant mixture. For the solution of 50% $C_{12}E_5$ – 50% $C_{10}E_8$ at a total bulk concentration of $16 \times 10^{-9} mol/cm^3$, this results in an equilibrium surface concentration of $\Gamma^{eq}_{C_{10}E_8} = 0.97 \times 10^{14} cm^{-2}$ and a corresponding timescale for adsorption of $\tau_{D_{C_{10}E_8}} = 52s$. Note that this timescale is a good estimate for the time at which the surface concentration of $C_{10}E_8$ is predicted to exhibit a peak (see Figure 6-9), as well for the time at which the first characteristic decrease in both the predicted and the experimentally measured dynamic surface tensions is observed (see Figure 6-7).

The analysis of the dynamic surface tension profiles corresponding to the other three binary surfactant mixtures shown in Figures 6-7 and 6-8 are similar to the one carried out in detail above for the solution of 50% $C_{12}E_5$ – 50% $C_{10}E_8$ at a total bulk surfactant concentration of $16 \times 10^{-9} mol/cm^3$, and therefore, the preceding analysis will not be repeated for these three mixtures. Instead, as a summary, Table 6.3 lists the predicted timescales for adsorption of each surfactant component present in the four binary surfactant mixtures shown in Figures 6-7 and 6-8, as determined using the analysis described above. Note that in each case, the timescale for adsorption of $C_{10}E_8$, $\tau_{D_{C_{10}E_8}}$, provides a good estimate for the time at which the first characteristic decrease in the dynamic surface tension is observed, and that the timescale for adsorption of $C_{12}E_5$, $\tau_{D_{C_{12}E_5}}$, provides a good estimate for the time at which the second and final characteristic decrease in the dynamic surface tension is observed (see Figures 6-7 and 6-8).

Table 6.3: Timescales for adsorption of all of the single surfactant solutions and the binary surfactant mixtures examined in this chapter (see text for details).

Total Bulk Surfactant Concentration ($\times 10^{-9} mol/cm^3$)	Bulk Composition of $C_{12}E_5$	Bulk Composition of $C_{10}E_8$	$\tau_{D_{C_{12}E_5}}$ (s)	$\tau_{D_{C_{10}E_8}}$ (s)
4.0	100%	0%	610	–
16	100%	0%	45	–
4.0	0%	100%	–	171
16	0%	100%	–	15
4.0	50%	50%	1900	540
16	50%	50%	155	52
4.0	16.7%	83.3%	6100	230
16	16.7%	83.3%	710	21

6.5 Conclusions

The experimental measurements of the equilibrium and the dynamic air-aqueous solution surface tensions of solutions of two nonionic surfactants, $C_{12}E_5$ and $C_{10}E_8$, as well as of a binary mixture of 50% $C_{12}E_5$ – 50% $C_{10}E_8$ and a binary mixture of 16.7% $C_{12}E_5$ – 83.3% $C_{10}E_8$, were presented. The measured surface tensions were found to be in good agreement with the theoretical predictions made using the molecularly-based theories of equilibrium and dynamic surfactant adsorption developed in Chapters 2 and 5, respectively. Specifically, it was shown that the equilibrium interfacial theory can be used to quantitatively predict the equilibrium surface tensions of solution of single nonionic surfactants, as well as of their binary mixtures, while significantly reducing the amount of required experimental inputs. This was accomplished by utilizing a theoretical framework which is based on the molecular characteristics of the surfactants, and contains only one experimentally determined parameter for each single surfactant component comprising the mixture (obtained from one experimental surface tension measurement). No additional measurements need to be conducted on the surfactant mixtures.

Subsequently, it was shown that the diffusion-controlled dynamic adsorption theory developed in Chapter 5 can successfully predict the dynamic surface tensions of both the single nonionic surfactant solutions and the binary nonionic surfactant solutions examined. Since this dynamic adsorption theory is based on the molecular-thermodynamic equilibrium theory, it does not contain any additional experimentally determined parameters for the mixed surfactant solutions. Therefore, both the equilibrium and the dynamic surface tensions of the mixed surfactant solutions can be predicted without performing any experiments on the mixed surfactant systems.

Although the theoretical framework developed in Chapter 5 and implemented in this chapter can be used to fully predict the surface tension and the surface concentration and composition of a surfactant mixture as a function of time, a simplified time-scale analysis was provided which can be used to quickly estimate the time required to attain adsorption equilibrium (including the resulting surface tension equilibrium).

While the timescale analysis is more complicated in the case of surfactant mixtures, it is generally quicker to implement than the solution of the complete theory. Accordingly, the simplified timescale analysis could be utilized to screen a large number of single surfactants and their mixtures to select those that exhibit the desired dynamic interfacial behavior. The simplified timescale analysis is also useful in allowing quick prediction of the relationship between the surfactant molecular structure and the dynamic adsorption properties of that surfactant. In this chapter, it was shown that, in the case of $C_{12}E_5$, $C_{10}E_8$, and their binary mixtures, this simplified timescale analysis provides a reasonably accurate estimate of the timescale for adsorption of a single surfactant or of a surfactant component in the mixture.

In the next chapter, the equilibrium adsorption theories presented in Chapters 2, 3, and 4 are implemented in the user-friendly computer program, Program SURF, and the dynamic adsorption theory presented in Chapter 5 is implemented in the user-friendly computer program, Program DYNAMIC.

Chapter 7

User-Friendly Computer Programs

7.1 Introduction

The molecular-thermodynamic theories developed in Chapters 2 and 3 for the mixed surfactant adsorption at the air-water interface, as well as in Chapter 4 for the mixed surfactant adsorption at the oil-water interface, along with the theoretical framework developed in Chapter 5 for the dynamic adsorption of mixtures of surfactants, generally require a detailed knowledge and understanding of the behavior of surfactants at interfaces. Although this detailed knowledge results in useful theories, the underlying theoretical aspects are often difficult to understand and implement, particularly by those that lack the necessary theoretical foundations. In an effort to facilitate the use of the various theories developed in this thesis (Chapters 2–5) by industrial researchers, in particular, two user-friendly computer programs, Program SURF and Program DYNAMIC, were developed.

As discussed in Sections 7.2 and 7.3, the inputs to these programs are the various surfactant molecular parameters and the solutions conditions. Given these inputs, the computer programs then implement the theoretical frameworks developed in this thesis to output either the equilibrium interfacial properties, in the case of Program SURF, or the dynamic interfacial properties, in the case of Program DYNAMIC. It is hoped that this will allow an industrial researcher to screen a large number of potential surfactants for a particular application requiring desired interfacial properties, or to

find an optimum composition for a surfactant mixture exhibiting desired interfacial properties, without an explicit consideration of the underlying details of the theory. Furthermore, since the computer programs typically take only a few seconds to run, a large number of surfactant systems can be examined and screened fairly quickly. This, in turn, can lead to a considerable amount of time saving as compared to using traditional experimentation to screen or optimize surfactant systems exhibiting desired interfacial properties.

7.2 Program SURF

Program SURF predicts the equilibrium air-water or oil-water interfacial tensions, as well as interfacial concentrations and compositions, of aqueous solutions of surfactant mixtures. The surfactants can be nonionic, ionic, or zwitterionic. The program is based on the molecular-thermodynamic theories developed in Chapters 2, 3, and 4 to model mixed surfactant adsorption at interfaces. Specifically, Program SURF can deal with *any number* of surfactant components (see below), including a single surfactant. Although Program SURF deals explicitly with surfactant solutions below the critical micelle concentration (CMC), it can also be used above the CMC for: (i) *single surfactants,* provided that the user inputs the appropriate surfactant monomer concentration from Program PREDICT[53] (a user-friendly computer program that predicts bulk solution properties of single surfactants), and (ii) *binary surfactant mixtures,* provided that the user inputs the appropriate total surfactant monomer concentration and monomer composition from Program MIX2[50] (a user-friendly computer program that predicts bulk solution properties of surfactant mixtures). Note that below the CMC, the total surfactant monomer concentration and monomer composition are equal to the total bulk solution concentration and bulk surfactant composition, respectively, which are inputs to Program SURF.

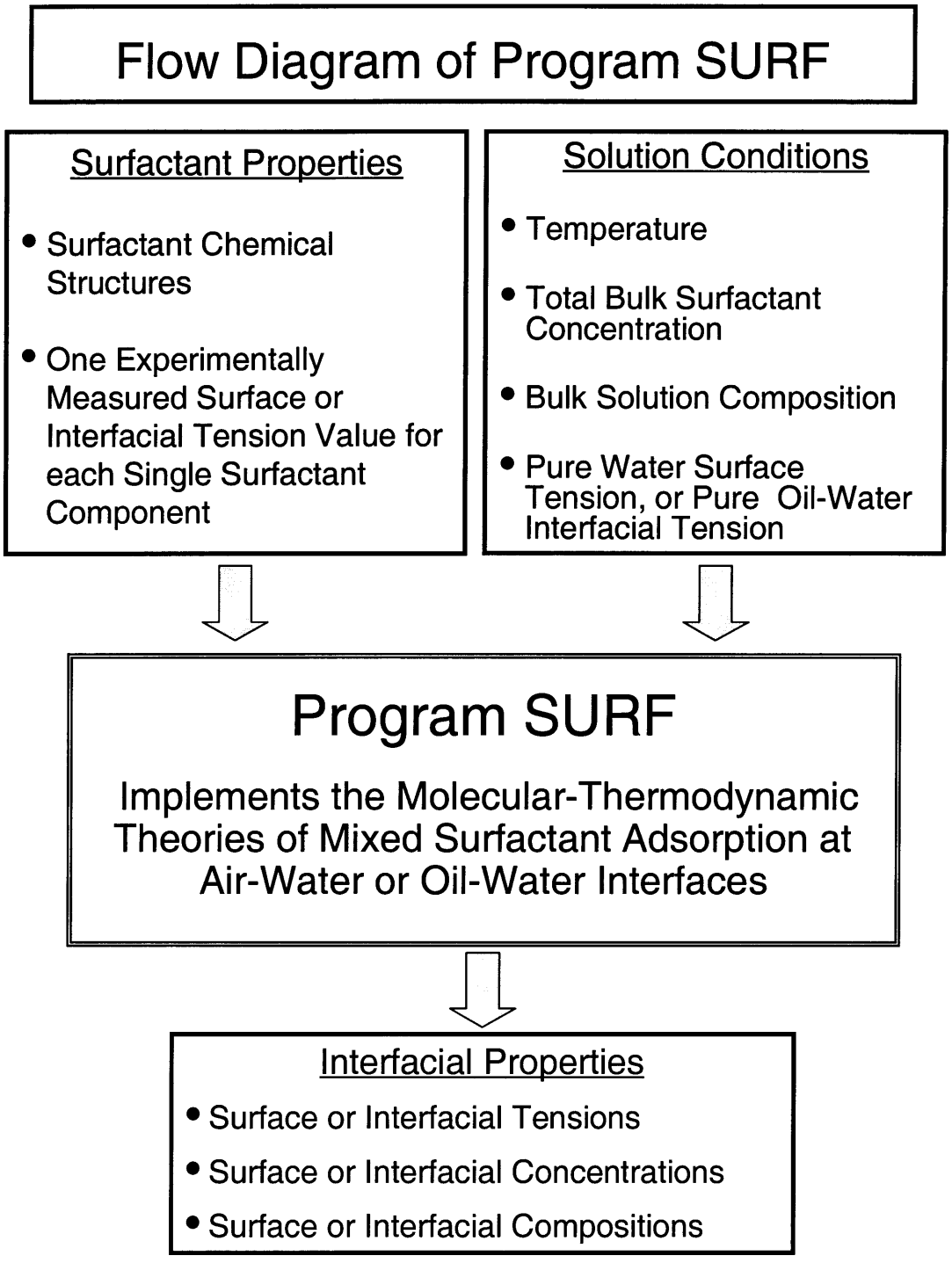

Figure 7-1: Flow diagram of Program SURF.

7.2.1 Inputs to Program SURF

The inputs to Program SURF can be divided into two classes: (i) the chemical structures of the surfactants involved, described in terms of several molecular parameters, and (ii) the solution conditions (see Figure 7-1). Inputs (i) and (ii) are discussed in detail below. Note that the required units are clearly stated by the program for each input, but in general, bulk concentrations are in mol/L, interfacial concentrations are in mol/cm^2, lengths are in Angstroms, and surface and interfacial tensions are in dyn/cm.

(i) Surfactant Chemical Structure. Program SURF will first prompt the user for the number of surfactant components, n, present in the aqueous solution. Note that, in principle, Program SURF can deal with any number of surfactant components. However, in order to conserve computer memory, the current version of Program SURF is limited to $n = 15$. The program will then ask the user for the name of the first surfactant, as well as for the various molecular parameters characterizing the chemical structure of that surfactant. The program will subsequently ask the user for similar information regarding the second surfactant, the third surfactant, up to the n^{th} surfactant.

The surfactant molecular parameters include (see Figure 7-2):

(1) The number of carbon atoms, n_c, in the surfactant tail.

(2) The head cross-sectional area, a_h.

(3) The total valence of the surfactant head (the user should enter 0 for a nonionic or zwitterionic surfactant, +1 for a monovalent cationic surfactant, and −1 for a monovalent anionic surfactant).

(4) The length of the surfactant head, l_h (measured relative to the center of the first carbon atom in the surfactant tail).

(5) The number of charged groups in the surfactant head (the user should enter 0 for a nonionic surfactant, 1 for an ionic surfactant, and 2 for a zwitterionic surfactant).

(6) The valence of each charged group in the surfactant head (typically, +1 or −1).

(7) The position of each charged group in the surfactant head, d^i_{ch}, (measured relative

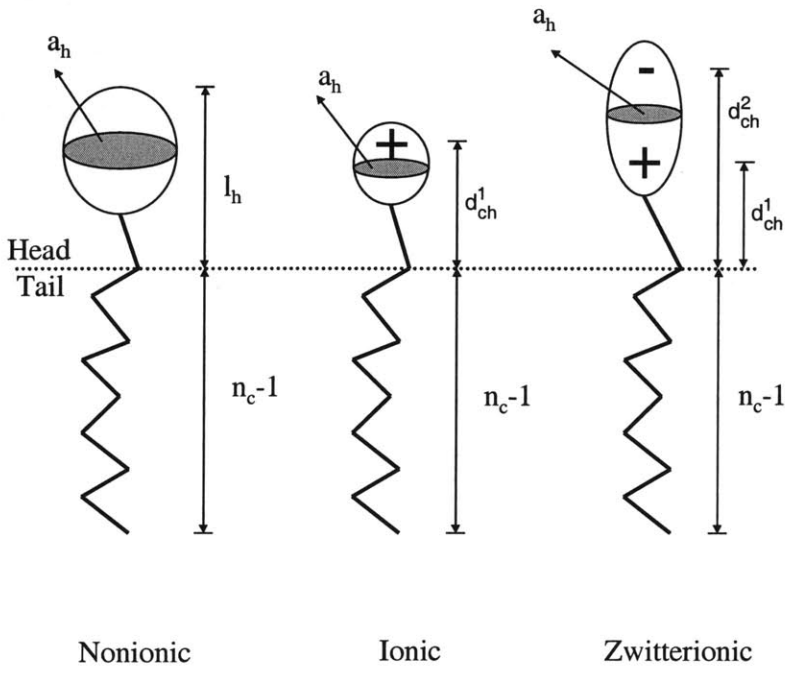

Figure 7-2: Schematic illustration of the surfactant molecular parameters.

to the center of the first carbon atom in the surfactant tail).

(8) The name, valence, and radius of the counterion, if the surfactant is ionic.

(9) A single surfactant concentration value at which the air-water or oil-water equilibrium interfacial tension of the surfactant solution is known experimentally.

(10) The air-water or oil-water equilibrium interfacial tension value at the surfactant concentration specified in item (9) above.

As a shortcut, the surfactant molecular parameters can be read from a file rather than entered manually by the user each time. This is particularly useful in order to create a library of surfactants of interest to the user for which many different mixtures involving that surfactant can be studied. This can be done by creating a file with the same name as that of the surfactant of interest. This file should be located in the *surf_dat* directory. The format of this file, which generally follows the data inputted manually by the user, can be found in the file *format.s* which is located in the *surf_dat* directory. Program SURF will then use this file to determine the molecular parameters of the surfactant. In order to revert back to manual input of the surfactant molecular parameters, the user can either use a different name for the surfactant, or delete or rename the surfactant data file.

Regarding the counterion molecular inputs in item (8) above, Program SURF can also read these inputs from a file. The file should have the same name as the counterion specified in item (8) above, and should be located in the *ion_dat* directory. The format of this file is given in the file *format.ion* located in the *ion_dat* directory. In this manner, the same counterion (for example, sodium) can be used for many surfactants without the user having to enter its molecular parameters each time.

(ii) Solution Conditions. The solution condition inputs include:

(a) The temperature.

(b) The total bulk surfactant concentration. For convenience, Program SURF will make predictions at a single total bulk surfactant concentration, or over a range of total bulk surfactant concentrations. To accomplish this, the program will first ask the user for the number of surfactant concentration data points. If only a single

surfactant concentration is desired, the user should enter 1. In that case, the user will be prompted for the specific value of the surfactant concentration of interest. If a range of surfactant concentrations is desired, the user should enter a number larger than 1 for the desired number of surfactant concentration data points (for example, 10 for a fairly coarse spacing, and 100 for a very fine spacing). The program will then ask the user for the starting (lowest) and ending (highest) surfactant concentration values. Note that the surfactant concentrations will be evenly spaced between these two selected concentrations on a $\log_{10}$ scale.

(c) The bulk solution composition, α_i. If the number of surfactant components is one ($n = 1$), then no surfactant composition is needed. In the case of surfactant mixtures ($n > 1$), the user should input the compositions of the first n-1 surfactants, with the nth surfactant composition determined automatically by $\alpha_n = 1 - \sum_{i=1}^{n-1} \alpha_i$.

(d) The surface tension of the pure air-water system or the interfacial tension of the pure oil-water system. For example, for the air-water interface at 25°C, a value of 72 dyn/cm should be used.

As a shortcut, the number of surfactant components, their names, as well as the solution condition inputs, (a)-(d) above, can be read from a file named *surf.in* located in the directory from which Program SURF is run. The format of this file is given in the file *format.in*. If a *surf.in* file is found, the user is given the option of using this file or entering the inputs manually.

After a set of predictions is completed for a given set of inputs, Program SURF will prompt the user to either: (1) change the total bulk surfactant concentration range, (2) change the bulk solution composition, or (3) quit. If other changes are desired, the user should quit and begin a new run of Program SURF. That way, a separate output file is generated, which allows the user to easily distinguish between the results from different sets of inputs.

7.2.2 Outputs of Program SURF

The file *surf.out* displays the log of the total bulk surfactant concentration, the bulk solution concentrations of each surfactant and its counterion, the predicted interfacial

concentration of each surfactant adsorbed at the interface, and the predicted interfacial tension. The bulk solution compositions of each surfactant component are also given at the beginning of this file. The output file is generally of an easy-to-read format, and can be imported into a spreadsheet in order to make plots. In addition, the interfacial tension as a function of the total bulk surfactant concentration is displayed to the screen so that the progress of the program can be monitored. If the user chooses the option to run again for a different range of total bulk surfactant concentrations (option 1), then those results are appended to the end of the *surf.out* file. If the user chooses to change the bulk solution composition (option 2), then the surfactant composition is also appended to the *surf.out* file.

7.3 Program DYNAMIC

Program DYNAMIC predicts the air-water surface tension and surface concentration and composition of aqueous solutions containing mixtures of nonionic surfactants as a function of time. The program is based on the molecular-thermodynamic theory developed in Chapter 5 to model the dynamic adsorption of surfactant mixtures at the air-water interface. Specifically, Program DYNAMIC can deal with *any number* of surfactant components (see below), including a single surfactant, below the critical micelle concentration (CMC).

7.3.1 Inputs to Program DYNAMIC

Similar to Program SURF, the inputs to Program DYNAMIC can be divided into two classes: (i) the chemical structures of the surfactants involved, described in terms of several molecular parameters, and (ii) the solution conditions (see Figure 7-3). Inputs (i) and (ii) are discussed in detail below. Note that the required units are clearly stated by the program for each input, but in general, bulk concentrations are in mol/L, surface concentrations are in mol/cm^2, lengths are in Angstroms, and surface tensions are in dyn/cm.

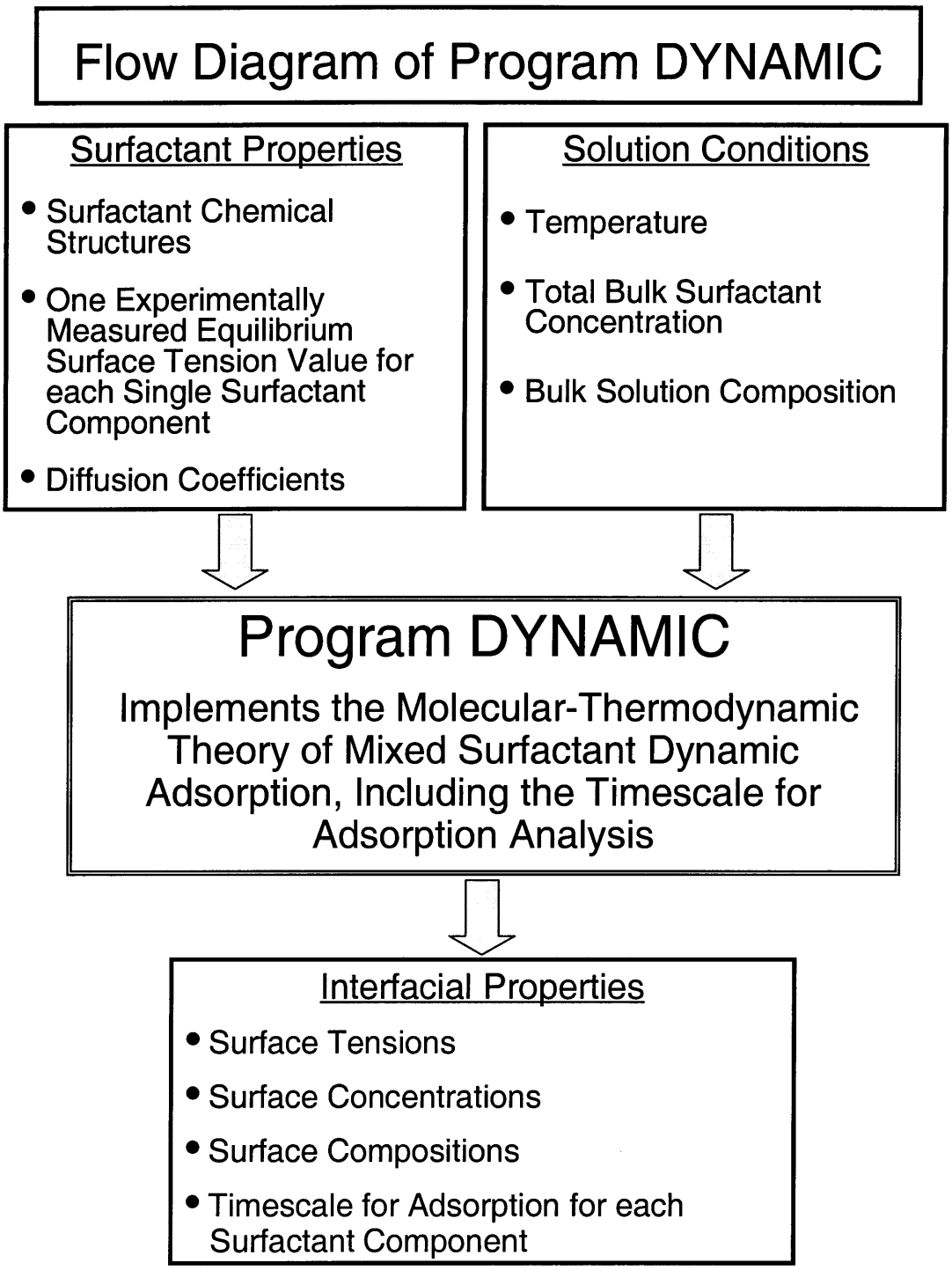

Figure 7-3: Flow diagram of Program DYNAMIC.

(i) Surfactant Chemical Structure. Program DYNAMIC will first prompt the user for the number of surfactant components, n, present in the aqueous solution. Note that, with the exception of the caveats stressed above, in principle, Program DYNAMIC can deal with any number of surfactant components. However, in order to conserve computer memory, similar to Program SURF, the current version of Program DYNAMIC is limited to $n = 15$. The program will then ask the user for the name of the first surfactant, as well as for the various molecular parameters characterizing the chemical structure of that surfactant. The program will subsequently ask the user for similar information regarding the second surfactant, the third surfactant, up to the n^{th} surfactant.

The surfactant molecular parameters include (see Figure 7-2):

(1) The number of carbon atoms, n_c, in the surfactant tail.

(2) The head cross-sectional area, a_h.

(3) The diffusion coefficient of the surfactant.

(4) A single surfactant concentration value at which the equilibrium surface tension of the surfactant solution is known experimentally.

(5) The equilibrium surface tension value at the surfactant concentration specified in item (4) above.

As a shortcut, the surfactant molecular parameters can be read from a file rather than entered manually by the user each time. This is particularly useful in order to create a library of surfactants of interest to the user for which many different mixtures involving that surfactant can be studied. This can be done by creating a file with the same name as that of the surfactant of interest. This file should be located in the *surf_dat* directory. The format of this file, which generally follows the data inputted manually by the user, can be found in the file *format.s* which is located in the *surf_dat* directory. Program DYNAMIC will then use this file to determine the molecular parameters of the surfactant. In order to revert back to manual input of the surfactant molecular parameters, the user can either use a different name for the surfactant, or delete or rename the surfactant data file.

(ii) Solution Conditions. The solution condition inputs include (see Figure 7-3):

(a) The temperature.

(b) The total bulk surfactant concentration.

(c) The bulk solution composition, α_i. If the number of surfactant components is one ($n = 1$), then no surfactant composition is needed. In the case of surfactant mixtures ($n > 1$), the user should input the compositions of the first $n - 1$ surfactants, with the nth surfactant composition determined automatically by $\alpha_n = 1 - \sum_{i=1}^{n-1} \alpha_i$.

As a shortcut, the number of surfactant components, their names, as well as the solution condition inputs, (a)-(c) above, can be read from a file named *dynamic.in* located in the directory from which Program DYNAMIC is run. The format of this file is given in the file *format.in*. If a *dynamic.in* file is found, the user is given the option of using this file or entering the inputs manually.

After a set of predictions is completed for a given set of inputs, Program DYNAMIC will prompt the user to either: (1) change the total bulk surfactant concentration, (2) change the bulk solution composition, or (3) quit. If other changes are desired, the user should quit and begin a new run of Program DYNAMIC. That way, a separate output file is generated, which allows the user to easily distinguish between the results from different sets of inputs.

7.3.2 Outputs of Program DYNAMIC

The file *surf.out* displays the surface tension and the surface concentration of each surfactant component, all as a function of time. The program also outputs the time-scale for adsorption for each surfactant component. The output file is generally of an easy-to-read format, and can be imported into a spreadsheet in order to make plots. In addition, the surface tension as a function of time is displayed to the screen so that the progress of the program can be monitored. If the user chooses the option to run again for a different range of total bulk surfactant concentrations (option 1), then those results are appended to the end of the *surf.out* file. If the user chooses to change the bulk solution composition (option 2), then the surfactant composition is also appended to the *surf.out* file.

7.4 Conclusions

The computer programs discussed in this chapter, Program SURF and Program DYNAMIC, allow an industrial surfactant scientist or formulator to quickly implement the theoretical frameworks developed throughout this thesis without a detailed knowledge or understanding of these theories. This is of value to companies that develop products containing surfactants where the interfacial properties are important (see Chapter 1), since using Programs SURF or DYNAMIC should allow industrial formulators to quickly screen or optimize a large number of surfactant mixtures, thus reducing the need for tedious and time consuming experimentation. It is hoped that by developing the computer programs described in this chapter, the theoretical frameworks developed in this thesis will have a larger and more wide spread impact. Furthermore, as these computer programs are utilized by industry, useful feedback will be provided that may help to guide future research towards more meaningful industrial directions. Accordingly, the computer programs described in this chapter provide an important link between industrial product development and the academic research presented in this thesis.

In the next chapter, a summary of the main results of this thesis is provided along with a discussion of future research directions.

Chapter 8

Thesis Summary and Future Research Directions

8.1 Thesis Summary

The main goal of this thesis was to develop theoretical frameworks to predict the interfacial behavior of mixed surfactant solutions (including both equilibrium and dynamic properties) using molecularly-based descriptions of mixed surfactant adsorption. As stressed in Chapter 2, the interfacial behavior of mixed surfactant solutions is extremely important since there are many practical application of surfactants where the interfacial properties lead to the desired behavior. Furthermore, mixtures of surfactants are important since almost every practical applications of surfactants utilizes surfactant mixtures. Therefore, the development of a predictive interfacial adsorption theory would help reduce the amount of costly and time consuming trial-and-error type experimentation that is typically associated with the design and optimization of surfactant mixtures of practical relevance. A key aspect of the theoretical frameworks developed as part of this thesis is that the number of experimentally determined parameters has been significantly reduced. In particular, all the theoretical descriptions developed in this thesis have no experimentally determined mixture dependent parameters.

Chapter 2 begins the theoretical journey of this thesis by developing a theoreti-

cal framework to model the equilibrium adsorption of surfactant mixtures containing ionic surfactants. To this end, a theory developed earlier by Nikas et al.[12] to model the adsorption of nonionic surfactants was generalized to include ionic surfactants. This theory treated the adsorbed surfactant molecules as a two-dimensional, non-ideal gas having two types of interactions: repulsive, steric interactions which were treated using a hard-disk model, and attractive, van der Waals interactions which were treated using a virial expansion truncated to second order in the surfactant surface concentration. In Chapter 2, the effect of electrostatic interactions was incorporated by adding an electrostatic contribution to the surface pressure which was computed using the Poisson-Boltzmann based model developed by Gouy, Chapman, and Stern.[29,30,32] This electrostatic model assumes that the charge at the interface, resulting from the adsorption of charged surfactants, resides on a single, two-dimensional surface of charge, and hence, can only be utilized to describe the adsorption of a single ionic surfactant species. In Chapter 3, the electrostatic model was extended further to treat the case of multiple, two-dimensional charge layers at the interface. This extended model is then capable of describing the adsorption of any number of surfactants containing any number of charged groups, and is particularly useful in predicting the interfacial behavior of zwitterionic surfactants, or mixtures of ionic and zwitterionic surfactants. The effect of the underlying assumptions of the Poisson-Boltzmann model, namely, that the ions in the aqueous phase have no physical size and that the dielectric constant is uniform within the aqueous phase, where investigated in detail in Appendix A. It was found that relaxing these two assumptions by incorporating ion size effects and dielectric saturation had little effect on the predictions of the theory, while generally increasing the computational intensity of the numerical solutions. The sensitivity of the interfacial theoretical predictions made in Chapters 2 and 3 to the surfactant molecular parameters was examined in Appendix B. Since this equilibrium adsorption theory includes both attractive and repulsive interactions among the adsorbed surfactant molecules, interfacial phase transitions are possible and can be predicted under certain conditions, a topic which was examined in detail in Appendix C. In Chapters 2 and 3, as well as in Appendix C, the theoretical predictions were compared

to experimental measurements of surface tensions, surface concentrations, and surface compositions taken from the literature. In all cases, the theoretical predictions were found to be in good agreement with the various experimental results. Of particular interest are the large extents of interfacial synergism found in a binary mixture of an ionic and a zwitterionic surfactant, shown in Chapter 2, as well as in a mixture of an anionic and a cationic surfactant, shown in Appendix C.

The theoretical frameworks developed in Chapters 2 and 3 were extended further in Chapter 4 to predict the interfacial behavior of surfactant mixtures adsorbed at the oil-water interface. Specifically, the attractive van der Waals interactions among the adsorbed surfactant tails can be neglected in this case due to the compatibility between the alkane oil phase and the alkyl tails of the surfactants. It should be noted, however, that all other molecular parameters remained unchanged in going from the air-water case to the oil-water case. Another difference between the oil-water interface case and the air-water interface case is that the surfactant molecules may partition between the bulk aqueous phase and the bulk oil phase, in addition to adsorbing at the oil-water interface. Chapter 4 describes a method to account for this partitioning, including a method for determining the surfactant oil-water partition coefficient solely from interfacial tension measurements. Since the availability of experimental data on the adsorption of surfactant mixtures at the oil-water interface is extremely limited, a series of experiments involving a pair of surfactants specifically chosen to test the range of validity and applicability of the theory developed in Chapter 4 were carried out and presented in Chapter 4. Good agreement was found between these experimental measurements and the theoretical predictions made in Chapter 4.

In Chapter 5, the theoretical descriptions developed in Chapters 2 and 3 were utilized as the basis for formulating a diffusion controlled, dynamic adsorption theory that is capable of predicting the air-water dynamic interfacial behavior (including the dynamic surface tension and the dynamic surface concentration and composition) of mixed surfactant solutions. Since the dynamic theoretical framework utilizes the equilibrium theories developed in Chapters 2 and 3 as its basis, it has the same advantages, including a reduction in the number of experimentally determined pa-

rameters and the applicability to surfactant mixtures which contain any number of components. Furthermore, a simplified timescale for adsorption analysis was developed for mixtures of surfactants that allows for the relatively quick determination of the time required for the adsorption of each surfactant component in a mixture to reach equilibrium. This, in turn, leads to a simplified understanding of the relationship between the molecular structure of a surfactant and its dynamic interfacial behavior. In Chapter 6, the dynamic adsorption theory developed in Chapter 5 was tested by comparing the dynamic surface tension predictions to measurements made using the pendant bubble apparatus. These measurements were made on a pair of surfactants that were specifically chosen to test the range of validity and applicability of the theoretical framework developed in Chapter 5, and good agreement was found between the theoretical predictions and the experimental measurements.

In order to broaden the applicability of the theories developed in this thesis, as well as to facilitate the establishment of a link between this academic work and commercial applications, the various theoretical frameworks were incorporated in two user-friendly computer programs, Program SURF and Program DYNAMIC. Program SURF utilizes the theory developed in Chapters 2 and 3 to predict the equilibrium air-water or oil-water interfacial behavior of mixed surfactant solutions. Program DYNAMIC utilizes the theory developed in Chapter 5 to predict the dynamic air-water interfacial behavior of surfactant solutions. Note that use of Programs SURF and DYNAMIC does not require a complete or detailed understanding of the underlying theories, and hence, may be used by industrial formulators to quickly screen a large number of potential surfactant candidates, or to optimize a surfactant mixture, for a given commercial interfacial application.

8.2 Future Research Directions

8.2.1 Equilibrium Interfacial Properties

8.2.1.1 Adsorption of Fluorocarbon Surfactants

The adsorption of fluorocarbon surfactants (that is, surfactants that consist of a fluorocarbon, rather than a hydrocarbon, tail) at the air-water interface is of interest because these surfactants are often able to lower the surface tension to a value that is below what is typically obtained with hydrocarbon surfactants.[138] Although there have been several experimental studies involving this class of surfactants, the theoretical analysis of their interfacial behavior usually involves the use of general empirical formulas which contain experimentally determined parameters.[139–141] Accordingly, the extension of the theoretical frameworks developed in this thesis to fluorocarbon surfactants would be of interest. This would involve primarily incorporating the van der Waals attractions between the fluorocarbon tails adsorbed at the interface, by extending the calculation of the second-order virial coefficients done in the hydrocarbon case. More specifically, an appropriate expression for the interaction potential between fluorocarbons, rather than hydrocarbons, should be utilized in Eq. (2.4). The surface tension as a function of fluorocarbon surfactant concentration could then be predicted following a similar framework as that presented in Chapters 2 and 3. The theory can also be extended to mixtures of fluorocarbon surfactants as well as to mixtures of fluorocarbon and hydrocarbon surfactants.

8.2.1.2 Insoluble Monolayers of Surfactants

The surface tension of insoluble monolayers of surfactants, that is, surfactants that are constrained to the interface only, can be predicted by utilizing the surface equations of state developed in Chapters 2 and 3. One additional area that would need to be addressed in this case is the possible occurrence of interfacial phase transitions. Specifically, the insolubility of these surfactants is usually associated with the presence of a large hydrophobic tail. These large tails may lead to relatively large van der

Waals attractive interactions between the adsorbed surfactant molecules which, as discussed in Appendix C, can induce an interfacial phase transition. In order to quantitatively predict the surface tension of these monolayers, a theoretical treatment of these interfacial phase transitions, which is more detailed than the theoretical description presented in Appendix C, may have to be developed. For example, the formation of two-dimensional clusters or aggregates may need to be considered, as was done recently by Ruckenstein[142] and Israelachvili.[143]

8.2.1.3 Oil-Water Interfacial Tension of Concentrated Surfactant Solutions

In Chapter 4, only the oil-water interfacial tension of surfactant solutions below the critical surfactant concentration where surfactant aggregates (for example, micelles or reverse micelles) begin to form in either phase was considered. However, the theoretical framework presented in Chapter 4 can be extended to these more concentrated surfactant solutions by combining the interfacial description with a bulk molecular-thermodynamic description capable of modeling the formation of these aggregates in a manner similar to what was done in the air-water surface case for surfactant solutions above the CMC.

8.2.1.4 Interfacial Tension of Solutions Containing Polymers or Surfactant-Polymer Mixtures

The adsorption of polymers, or of a mixture of polymers and surfactants, at both the air-water and the oil-water interfaces, which was not addressed in this thesis, represents another interesting and important area for possible future research.[144,145] Similar to the equilibrium adsorption of surfactant mixtures at the oil-water interface, this would involve developing both a suitable theoretical framework and measuring equilibrium surface or interfacial tensions. To this end, the interfacial theory should be combined with a molecular-thermodynamic description of the bulk polymer-surfactant complexation that may occur in solutions above the critical aggregation concentration (CAC).[146] The resulting theory could then predict the interfacial be-

havior (in particular, the surface tension) of polymer-surfactant solutions, in a manner that reflects the bulk polymer-surfactant complexation above the CAC. Along with the general predictive value of such a theory, one may also be able to probe the bulk complexation of polymers and surfactants through relatively simple surface tension measurements.

8.2.2 Dynamic Interfacial Properties

8.2.2.1 Kinetic Adsorption Barriers

In Chapter 5, it was assumed that the adsorption of the surfactant molecules is diffusion limited. However, as discussed in Chapter 5, as the surfactant solution becomes more concentrated, the adsorption controlling mechanism can shift from the bulk diffusion of the surfactant molecules to their kinetic adsorption at the interface.[116–118] The inclusion of a kinetic barrier to adsorption would be a useful modification to the theory developed in Chapter 5. This would allow one to treat more concentrated surfactant solutions, and in particular, to investigate the dynamic surface tension of micellar solutions as discussed in Appendix D. Furthermore, the inclusion of a kinetic barrier would allow for the treatment of ionic surfactants, which are typically found in solution at higher concentrations than nonionic surfactants (their surface activity is typically lower due to their ionic character), and as a result, exhibit a kinetic adsorption barrier.[124,125]

8.2.2.2 Dynamic Oil-Water Interfacial Tension

In Chapter 5, only the dynamic adsorption of surfactant molecules at the air-water interface was considered. The theoretical framework developed in Chapter 5 can be extended to model the dynamic oil-water interfacial behavior of surfactant mixtures by using the equilibrium adsorption theory for the oil-water interface developed in Chapter 4 as its basis. An additional modification to the theory presented in Chapter 5 would be accounting for the possible diffusion of surfactant molecules in both the oil phase and the aqueous phase.[67,147]

8.2.3 Applications of the Interfacial Theories

8.2.3.1 Detergency

As discussed in Chapter 1, one of the largest commercial uses of surfactants is in cleaning products, such as detergents, soaps, and shampoos. Therefore, an interesting and very important area for possible future research involves developing a theoretical description to quantify the cleaning ability of a surfactant solution. Since, as discussed in Chapter 1, the oil-water interfacial tension is a key feature that controls the cleaning ability of the surfactant solution,[148,149] the oil-water interfacial theory presented in Chapter 4 can be utilized as the basis for a theoretical quantification of detergency.

8.2.3.2 Foam Stability

As discussed in Chapter 1, another commercially important application of surfactant solutions is their stabilization of foams. Consequently, another interesting and very important area for possible future research involves developing a theoretical description to quantify the foam stability of a surfactant solution. Since, as discussed in Chapter 1, the air-water surface tension, as well as the surfactant surface concentration and composition, are essential interfacial features that control the stability of foams,[10,148] the air-water interfacial theories presented in Chapters 2 and 3 can be utilized as the basis for a theoretical quantification of foam stability induced by surfactants. In addition, dynamic aspects of surfactant induced foam stability can be addressed by making use of the dynamic surface tension theory developed in Chapter 5.

8.3 Concluding Remarks

As stressed in Section 8.1 and in Chapter 1, the central goal of this thesis was to develop a molecular-level theoretical description for the prediction of the equilibrium as well as the dynamic interfacial behaviors of mixed surfactant solutions. It is hoped that the theoretical developments presented in this thesis will facilitate the design and

optimization of surfactant solutions of practical relevance having desired interfacial properties by reducing the need for relatively costly and time-consuming experimentation. Finally, as discussed in Section 8.2, it is hoped that the work presented in this thesis will also inspire future studies of the interfacial behavior of mixed surfactant solutions and their effect on practical phenomena.

Appendix A

Effects of Ion Size and Dielectric Saturation in the Diffuse Region of the Gouy-Chapman Model

A.1 Introduction

As discussed in Section 2.1, the original Gouy-Chapman model of the diffuse region (that is, the region in the aqueous phase near a charged interface where the entropically-driven tendency of the ions in the solution to maintain a uniform concentration is balanced by the ordering effect of the decaying electric field resulting from the charges located on the adsorbed surfactant molecules) assumes that the ions in the aqueous phase have no physical size. However, as a result of this assumption, the Gouy-Chapman model predicts an extremely large concentration of counterions very close to the interface (where the electric field is strongest). In the case of highly charged interfaces, the concentration of the counterions near the interface can become unrealistically high as it exceeds the concentration corresponding to the maximum packing of the ions. Moreover, the original Gouy-Chapman model also assumes that the ions in the diffuse region interact through a medium (water) having a uniform dielectric constant. However, when an electric field acts on water, the dielectric con-

stant decreases as a result of dielectric saturation (that is, the dipoles of the water molecules align with the electric field, which effectively decreases the polarity, and hence, the dielectric constant, of water).[47,150]

The first modification to the Gouy-Chapman model, introduced to address the effect of the counterion size, was made by Stern[32] and was used in the theoretical description presented in Chapters 2–4. This modification includes a region between the charged interface and the diffuse region where the ions cannot penetrate due to steric repulsive interactions. However, this modification did not actually reduce the concentration of counterions near the interface, but instead, shifted this region of high counterion concentration from being adjacent to the interface (at $x = 0$) to the edge of the Stern region (at $x = \mathrm{d}$), since the ions are still treated as having zero size within the diffuse region. More recently, other researchers have accounted for the effect of ion size in the diffuse region by modifying the Poisson-Boltzmann equation (which is the governing equation of the diffuse region in the original Gouy-Chapman theory).[151–154] In addition, others have relaxed the assumption in the original Gouy-Chapman model of a uniform dielectric constant by accounting for dielectric saturation.[153,154] The results of these investigations indicate that the effect of relaxing these assumption depends on the charge density of the interface. That is, for a relatively low surfactant charge density, the effect of relaxing these assumptions is small, and hence, one can conclude that the original Gouy-Chapman model (which is generally much less computationally intensive to utilize) is a good approximation in that case.

In this Appendix, the validity of the two assumptions of the Gouy-Chapman model discussed above (that is, zero ion size and uniform dielectric constant in the diffuse region) is investigated by modifying the Poisson-Boltzmann based theory presented in Chapter 2. Specifically, a modified form of the Poisson-Boltzmann equation, which was derived using the Carnahan-Starling model[151,155,156] (which treats the ions in the diffuse region as finite sized hard spheres) instead of using the ideal solution model (which treats the ions in the diffuse region as point ions having no physical size), is presented in Section A.2.1. Secondly, a modified form of the Poisson-Boltzmann equation which includes the effect of dielectric saturation through the use of a model

developed by Booth[150] to predict the dielectric constant of water as a function of the electric field is presented in Section A.2.2. Comparisons of the surface tension versus surfactant concentration predictions for a model surfactant (SDS) made using the original and the modified forms of the Poisson-Boltzmann equations are presented in Section A.3. Finally, concluding remarks are presented in Section A.4.

A.2 Theory

A.2.1 Theoretical Treatment of Ion Size Effects

As in the case of the original Poisson-Boltzmann equation, the electrostatic contribution to the surface equation of state, Π_{elec} (see Section 2.2 for a detailed discussion), is computed by first calculating the electrostatic potential, Ψ, as a function of the distance from the charged interface, x, for a given electrostatic surface charge density, $\hat{\sigma}$. As was done in Chapter 2, the electrostatic potential in the Stern region, $(0 \leq x \leq \mathrm{d})$, is governed by the Laplace equation, which can be derived from the Poisson equation as follows:

$$\frac{\mathrm{d}^2\Psi}{\mathrm{d}x^2} = \frac{-4\pi\rho_{\text{elec}}}{\varepsilon_{\text{s}}} = 0 \quad , \quad \text{for} \quad 0 \leq x \leq \mathrm{d} \tag{A.1}$$

The solution to this equation is a constant value of $\mathrm{d}\Psi/\mathrm{d}x$, which, as was shown in Section 2.2.2.1, can be written as follows:

$$\frac{\mathrm{d}\Psi}{\mathrm{d}x} = -\frac{4\pi\hat{\sigma}}{\varepsilon_{\text{s}}} \quad , \quad \text{for} \quad 0 \leq x \leq \mathrm{d} \tag{A.2}$$

and

$$\Psi = \Psi_{\mathrm{d}} + \frac{4\pi\hat{\sigma}}{\varepsilon_{\text{s}}}(\mathrm{d} - x) \quad , \quad \text{for} \quad 0 \leq x \leq \mathrm{d} \tag{A.3}$$

where $\Psi_{\mathrm{d}} \equiv \Psi(x = d)$ is the value of the electrostatic potential at the boundary between the Stern region and the diffuse region, ε_{s} is the dielectric constant in the Stern region, and $\hat{\sigma}$ is the electrostatic charge density of the monolayer.

In the diffuse region, $(x > \mathrm{d})$, the Poisson equation can be reduced to the following

governing equation for the electrostatic potential:

$$\frac{\mathrm{d}^2\Psi}{\mathrm{d}x^2} = \frac{-4\pi\rho_{\mathrm{elec}}}{\varepsilon} = \frac{-4\pi\mathrm{e}}{\varepsilon}\sum_{i=1}^{m}\mathrm{z}_i n_i\left(x\right) \quad , \quad \text{for} \quad x > \mathrm{d} \tag{A.4}$$

where $n_i(x)$ is the concentration of ions of type i at a distance x from the interface, ε is the dielectric constant in the diffuse region, assumed to be that of pure water, and m is the number of ionic species (which includes surfactants, counterions, and any added salt ions). The two boundary conditions for this second-order differential equation are the same as those presented in Chapter 2. Specifically,

$$\Psi\left(x \to \infty\right) = 0 \tag{A.5}$$

and

$$\left.\frac{\mathrm{d}\Psi}{\mathrm{d}x}\right|_{x=\mathrm{d}} = \frac{-4\pi\hat{\sigma}}{\varepsilon} \tag{A.6}$$

The local concentration of ions, $n_i(x)$, which appears in Eq. (A.4), can be calculated by invoking electro-diffusional equilibrium which requires that the electrochemical potential of each ion be uniform. Specifically,

$$\mu_i^{\mathrm{w}}\left[\left\{n_j\left(x\right)\right\}\right] + \mathrm{z}_i\mathrm{e}\Psi\left(x\right) = \mu_i^{\mathrm{w}}\left[\left\{n_j^{\mathrm{w}}\right\}\right] \tag{A.7}$$

where $\mu_i\left[\left\{n_j\left(x\right)\right\}\right]$ denotes the chemical potential of ions of type i at position x (which is determined through a bulk solution equation of state from the local concentration of ions, $\left\{n_j\left(x\right)\right\}$), and $\mu_i^{\mathrm{w}}\left[\left\{n_j^{\mathrm{w}}\right\}\right]$ is the bulk aqueous chemical potential of ions of type i (that is, at $x \to \infty$, where $n_j(x) \to n_j^{\mathrm{w}}$ and $\Psi \to 0$). To determine the chemical potentials in Eq. (A.7), the Carnahan-Starling equation of state, which is derived by treating the ions as hard spheres of finite size, can be utilized. This model provides a good estimate of the effect of steric interactions associated with molecules that are reasonably spherical in nature (such as the surfactants counterions), but does not include any other type of interactions (for example, van der Waals interactions). Utilizing this model, the following expression for the chemical potential of ions of

type i as a function of the local ion concentrations is obtained:[151]

$$\mu_i^{\mathrm{w}} = \mu_i^{\mathrm{w},0} + \mathrm{k_B}T\left\{\ln\left(\frac{n_i(x)}{n_{\mathrm{w}}^{\mathrm{w}} + \sum_{j=1}^{m} n_j(x)}\right) + \left(-1 + \frac{3\chi_2^2\mathrm{r}_i^2}{\chi_3^2} - \frac{2\chi_2^3\mathrm{r}_i^3}{\chi_3^3}\right)\ln(1-\chi_3)\right.$$

$$+ \frac{\chi_0^3\mathrm{r}_i^3 + 3\chi_1\mathrm{r}_i^2 + 3\chi_2\mathrm{r}_i}{1-\chi_3} + \frac{6\chi_1\chi_2\mathrm{r}_i^3 + 9\chi_2^2\mathrm{r}_i^2}{2(1-\chi_3)^2} + \frac{3\chi_2^3\mathrm{r}_i^3}{(1-\chi_3)^3} \qquad \text{(A.8)}$$

$$\left. + \frac{3\chi_2^2\mathrm{r}_i^2}{\chi_3}\frac{(1-(3/2)\chi_3)}{(1-\chi_3)^2} - \frac{\chi_2^3\mathrm{r}_i^3}{\chi_3^2}\frac{(2-5\chi_3+4\chi_3^2)}{(1-\chi_3)^3}\right\}$$

where r_i is the hard-sphere cross-sectional radius of ions of type i, and $\chi_k \equiv \frac{\pi}{6}\sum_{j=1}^{m}\mathrm{r}_j^k n_j(x)$. Note that the hard-sphere interactions are only important when the ion concentrations are large, and hence the ions "feel" each other. That is, if the concentration of ions of type j, $n_j(x)$, is small, then its contribution in the summation of the various χ's in Eq. (A.8) will be negligible. In the case of a single ionic surfactant (denoted by the subscript s, which is the case considered in this Appendix), the local surfactant concentration will always be less than, or equal to, the bulk surfactant concentration (that is, $n_s(x) \leq n_s^{\mathrm{w}}$), since the similarly charged surfactant molecules adsorbed at the interface repel those present in the aqueous phase. Since the bulk surfactant concentration is typically dilute (below or slightly above the CMC), it follows that the concentration of the surfactant is dilute everywhere in the aqueous phase. Therefore, the hard-sphere interactions of the surfactant molecules are negligible. Since these interactions are negligible, for simplicity, the same value (and the same symbol, r_i) is used hereafter for the hard-sphere radius and the two-dimensional hard-disk radius (which is the two-dimensional projection of the surfactant molecule, and hence, strictly speaking, the two would only be equal for a spherical surfactant). The value of the radius for the surfactant considered in this Appendix, dodecyl sulfate, is 2.8Å. The counterions, however, are attracted towards the interface, and therefore, their

concentration can become large. Hence, it is the hard-sphere interaction of the counterions that is relatively important. The values of r_i for the ions considered here (other than for the dodecyl sulfate ion) are the experimentally determined values of 1.85Å for Na and 1.91Å for Cl.[47]

Note that Eq. (A.7) represents a set of m equations. Therefore, by inserting the expression for $\mu_i[\{n_j(x)\}]$ and $\mu_i[\{n_j^w\}]$ given in Eq. (A.8) into Eq. (A.7), one can solve this set of m equations for the set of m unknown local ion concentrations, $\{n_j(x)\}$, for a given value of $\Psi(x)$. This relationship between $\{n_j(x)\}$ and $\Psi(x)$ can then be utilized in Eq. (A.4), along with the boundary conditions given by Eqs. (A.5) and (A.6), to determine $\Psi(x)$. Note, however, that there is no closed form solution describing the relationship between $\{n_j(x)\}$ and $\Psi(x)$. Therefore, Eq. (A.4) needs to be solved numerically as described below.

The numerical solution to Eq. (A.4) can be obtained using a Runga-Kuta method.[48] Specifically, one can use Eq. (A.6) for the value of $(d\Psi/dx)|_{x=d}$ and guess a value of $\Psi(x = d)$. Note that the solution to the original Poisson-Boltzmann model presented in Chapter 2 can be utilized as an initial guess. One can then integrate Eq. (A.4) in discrete steps of x in the positive direction. In the case of a positively-charged monolayer (where the initial guess for $\Psi(x = d)$ should be positive), if the solution of Eq. (A.4) becomes negative as x increases, then the guess for $\Psi(x = d)$ was too small. If the solution of Eq. (A.4) never becomes negative as x increases, but rather diverges to $+\infty$, then the guess for $\Psi(x = d)$ was too large. Similarly, in the case of a negatively-charged monolayer (where the initial guess for $\Psi(x = d)$ should be negative), if the solution of Eq. (A.4) becomes positive as x increases, then the guess for $\Psi(x = d)$ was too large. If the solution of Eq. (A.4) never becomes positive as x increases, but rather diverges to $-\infty$, then the guess for $\Psi(x = d)$ was too small. In this manner, one can bracket the actual value of $\Psi(x = d)$, and thus iteratively solve Eq. (A.4) for $\Psi(x = d)$ within any desired tolerance level.

Once the value of $\Psi(x = d)$ has been determined in this manner, it can be inserted into Eq. (A.3) to obtain the value of $\Psi_0 \equiv \Psi(x = 0)$. In other words, following this procedure, the surface electrostatic potential can be calculated as a function of

the monolayer charge density. Finally, the electrostatic contribution to the surface pressure, Π_{elec}, can be calculated by numerically integrating the following expression:

$$\Pi_{\text{elec}} = \hat{\sigma}\Psi_0|_{\sum_i \text{ez}_i\eta_i/A} - \int_0^{\sum_i \text{ez}_i\eta_i/A} \Psi_0\left(\hat{\sigma}\right) \mathrm{d}\hat{\sigma} \tag{A.9}$$

This value of Π_{elec} can then be combined with the expression for the nonionic contribution to the surface pressure, Eq. (2.19), to calculate the total surface pressure as a function of the surfactant surface concentrations. However, it is the bulk solution concentrations and compositions that are typically known or controlled experimentally. Accordingly, to relate the surface concentrations and compositions to the bulk surfactant concentrations and compositions, one can invoke thermodynamic diffusional equilibrium between the surfactant molecules adsorbed at the interface and those present in the bulk aqueous solution using the theoretical description that was developed in Chapter 2.

For simplicity, and since this is the case that is examined in Section A.3, a single ionic surfactant (denoted by the subscript s) along with its counterion (denoted by the subscript c) are considered here. The surface free energy, F^σ, can be computed by numerically integrating Eq. (2.7). This can then be inserted into Eq. (2.40) to numerically compute the surface chemical potential of the surfactant and its counterion, $\mu^\sigma_{sc} \equiv \mu^\sigma_s + \mu^\sigma_c$. Finally, this numerical method for computing the surface chemical potential of the ionic surfactant and its counterion can be used in Eq. (2.11), along with the expression for the bulk aqueous chemical potentials of the surfactant and its counterion given in Eq. (A.8), to compute the equilibrium surfactant surface concentration for any given bulk surfactant concentration (after determining the standard-state chemical potential difference, $\Delta\mu^0_{sc}$, from a single surface tension measurement following the procedure presented in Chapter 2). Once the equilibrium surfactant surface concentration has been determined, the surface pressure, Π, and hence, the surface tension, $\sigma = \sigma_0 - \Pi$, can be computed using Eqs. (2.19) and (A.9) as described above. Results of these calculations are presented in Section A.3.1.

A.2.2 Theoretical Treatment of Dielectric Saturation

Including dielectric saturation in the Poisson-Boltzmann model follows similar steps to those associated with including ion size effects, which was addressed in Section A.2.1. Specifically, the electrostatic contribution to the surface equation of state, Π_{elec}, is calculated by first calculating the electrostatic potential, Ψ, as a function of the distance from the charged interface, x, for a given electrostatic surface charge density, $\hat{\sigma}$. Since the treatment of the Stern region remains unchanged, Eqs. (A.1) through (A.3) are still valid, and therefore, will not be repeated here. The diffuse region, however, is different in this case. The governing equation for the diffuse region can be derived from the Poisson equation, taking into account the fact that the dielectric "constant", ε, is not constant, but instead, is now a function of the electric field, $E(x) \equiv -\mathrm{d}\Psi/\mathrm{d}x$. Specifically,

$$\frac{\mathrm{d}^2\Psi}{\mathrm{d}x^2} = \frac{-4\pi \mathrm{e}}{\varepsilon\left(E\left(x\right)\right) + E\left(x\right)\frac{\mathrm{d}\varepsilon}{\mathrm{d}E}} \sum\nolimits_i z_i n_i\left(x\right) \tag{A.10}$$

The local concentration of ions, $n_i(x)$, in Eq. (A.10) can be calculated by invoking electro-diffusional equilibrium, which requires that the electro-chemical potential of each ion be uniform. In this case, this condition can be written as follows:[47]

$$\mu_i^{\mathrm{w}}\left[\{n_j\left(x\right)\}\right] + \mathrm{z}_i \mathrm{e}\Psi\left(x\right) + \frac{\mathrm{e}^2 \mathrm{z}_i^2}{2\mathrm{r}_i}\left(\frac{1}{\varepsilon\left(E\left(x\right)\right)} - \frac{1}{\varepsilon\left(E=0\right)}\right) = \mu_i^{\mathrm{w}}\left[\{n_j^{\mathrm{w}}\}\right] \tag{A.11}$$

where r_i is the radius of ions of type i. Note that Eq. (A.11) represents a set of m equations. Therefore, by inserting an expression for $\mu_i\left[\{n_j\left(x\right)\}\right]$ and $\mu_i\left[\{n_j^{\mathrm{w}}\}\right]$, either based on an ideal solution model which is given in Eq. (2.12), or based on the Carnahan-Starling model which is given in Eq. (A.8), into Eq. (A.11), one can solve this set of m equations for the set of m unknown local ion concentrations, $\{n_j\left(x\right)\}$, for a given value of $\Psi(x)$ and $\varepsilon(x)$. If one chooses to use the ideal solution model, one can arrive at a closed-form solution for $\{n_j\left(x\right)\}$ as a function of $\Psi(x)$ and $\varepsilon(x)$.

Specifically,

$$n_i(x) = n_i^{\mathrm{w}} \exp\left\{-\frac{\mathrm{e}z_i\Psi(x)}{\mathrm{k_B}T} - \frac{\mathrm{e}^2\mathrm{z_i^2}}{2\mathrm{r}_i\mathrm{k}T}\left(\frac{1}{\varepsilon(E(x))} - \frac{1}{\varepsilon(E=0)}\right)\right\} \tag{A.12}$$

Because the closed-form solution is generally faster to solve, and since, as will be shown below in Section A.3.1, the difference between the predicted surface tensions when using the ideal solution model and the Carnahan-Starling model is very small, the ideal solution model will be utilized here. In that case, inserting Eq. (A.12) into Eq. (A.10) yields:

$$\begin{aligned}\frac{\mathrm{d}^2\Psi}{\mathrm{d}x^2} &= \frac{-4\pi\mathrm{e}}{\varepsilon(E(x)) + E(x)\frac{\mathrm{d}\varepsilon}{\mathrm{d}E}}\sum_{i=1}^{m} z_i n_i^{\mathrm{w}} \exp\left\{-\frac{\mathrm{e}z_i\Psi(x)}{\mathrm{k_B}T}\right. \\ &\quad \left. - \frac{\mathrm{e}^2\mathrm{z_i^2}}{2\mathrm{r}_i\mathrm{k}T}\left(\frac{1}{\varepsilon(E(x))} - \frac{1}{\varepsilon(E=0)}\right)\right\}\end{aligned} \tag{A.13}$$

The boundary conditions for this second-order differential equation are given by Eqs. (A.5) and (A.6).

Finally, Eq. (A.13) requires an expression for $\varepsilon(E)$. In this Appendix, the model developed by Booth[150] will be utilized. Specifically,

$$\varepsilon = \bar{\mathrm{n}}^2 + \left(\varepsilon(\infty) - \bar{\mathrm{n}}^2\right)\left(\frac{3}{\beta E}\right)\left(\frac{1}{\tanh(\beta E)} - \frac{1}{\beta E}\right) \tag{A.14}$$

where $\bar{\mathrm{n}} = 1.33$ is the water index of refraction, and $\beta \equiv 9.25\times10^{-18}\left(\bar{\mathrm{n}}^2 + 2\right)/\left(2\mathrm{k_B}T\right)$ (when E is in *cgs* units) is a known constant at a given temperature.

Next, Eqs. (A.13) and (A.14) can be combined and solved numerically in the same manner as was done in Section A.2.1 using a Runga-Kuta method.[48] Specifically, one can use Eq. (A.6) for the value of $\left(\mathrm{d}\Psi/\mathrm{d}x\right)|_{x=\mathrm{d}}$ and guess a value of $\Psi(x=\mathrm{d})$. Note that the solution to the original Poisson-Boltzmann model presented in Chapter 2 can be utilized as an initial guess. One can then integrate Eq. (A.13) in discrete steps of x in the positive direction. In the case of a positively-charged monolayer (where the

initial guess for $\Psi(x = \mathrm{d})$ should be positive), if the solution of Eq. (A.13) becomes negative as x increases, then the guess for $\Psi(x = \mathrm{d})$ was too small. If the solution of Eq. (A.13) never becomes negative as x increases, but rather diverges to $+\infty$, then the guess for $\Psi(x = \mathrm{d})$ was too large. Similarly, in the case of a negatively-charged monolayer (where the initial guess for $\Psi(x = \mathrm{d})$ should be negative), if the solution of Eq. (A.13) becomes positive as x increases, then the guess for $\Psi(x = \mathrm{d})$ was too large. If the solution of Eq. (A.13) never becomes positive as x increases, but rather diverges to $-\infty$, then the guess for $\Psi(x = \mathrm{d})$ was too small. In this manner, one can bracket the actual value of $\Psi(x = \mathrm{d})$, and thus iteratively solve Eq. (A.13) for $\Psi(x = \mathrm{d})$ within any desired tolerance level. Once the value of $\Psi(x = \mathrm{d})$ has been determined in this manner, it can be inserted into Eq. (A.3) to obtain the value of $\Psi_0 \equiv \Psi(x = 0)$. In other words, following this procedure, the surface electrostatic potential can be calculated as a function of the monolayer charge density. Finally, the electrostatic contribution to the surface pressure, Π_{elec}, can be calculated by numerically integrating Eq. (A.9).

This value of Π_{elec} can then be combined with the expression for the nonionic contribution to the surface pressure, Eq. (2.19), to calculate the total surface pressure as a function of the surfactant surface concentrations. However, it is the bulk surfactant concentrations and compositions which are typically known or controlled experimentally. To relate the surfactant surface concentrations and compositions to the surfactant bulk concentrations and compositions, one can invoke thermodynamic diffusional equilibrium between the surfactant molecules adsorbed at the interface and those present in the bulk aqueous solution using the theoretical description that was developed in Chapter 2.

For simplicity, and since this is the case that is examined in Section A.3, a single ionic surfactant (denoted by the subscript s) along with its counterion (denoted by the subscript c) is considered here. The surface free energy, F^σ, can be computed by numerically integrating Eq. (2.7). This can then be inserted into Eq. (2.40) to numerically compute the surface chemical potential of the surfactant and its counterion, $\mu^\sigma_{sc} \equiv \mu^\sigma_s + \mu^\sigma_c$. Finally, this numerical method for computing the surface chemical

potential of the ionic surfactant and its counterion can be used in Eq. (2.11), along with the expression for the bulk aqueous chemical potentials of the surfactant and its counterion given by Eq. (2.12) (for an ideal bulk solution) or by Eq. (A.8) (for a bulk solution treated using the Carnahan-Starling model), to compute the equilibrium surfactant surface concentration for any given bulk surfactant concentration (after determining the standard-state chemical potential difference, $\Delta\mu^0_{sc}$, from a single surface tension measurement following the procedure presented in Chapter 2). Once the equilibrium surfactant surface concentration has been determined, the surface pressure, Π, and hence, the surface tension, $\sigma = \sigma_0 - \Pi$, can be computed using Eqs. (2.19) and (A.9) as described above. Results of these calculations are presented in Section A.3.2.

A.3 Results

A.3.1 Ion Size

In this section, the ionic surfactant sodium dodecyl sulfate (SDS) will be utilized to illustrate the effect of the hard-disk interactions between the ions in the diffuse region. This will be done by comparing the predicted surface tensions as a function of the bulk aqueous surfactant concentration predicted using the original Poisson-Boltzmann model, which uses the ideal solution equation of state, to those derived using the modified form of the Poisson-Boltzmann model described in Section A.2, which uses the Carnahan-Starling equation of state. The molecular parameters for SDS can be found in Table 2.1 (see Chapter 2).

Figure A-1 shows the predicted (lines) and the experimentally measured (symbols) surface tensions, σ, as a function of the bulk aqueous SDS concentration, n^{w}_s, for an aqueous solution containing no added salt. The theoretical predictions correspond to those made using the classic Poisson-Boltzmann model (———) and those made using the modified form of the Poisson-Boltzmann model, described in Section A.2, which uses the Carnahan-Starling equation of state to account for hard-

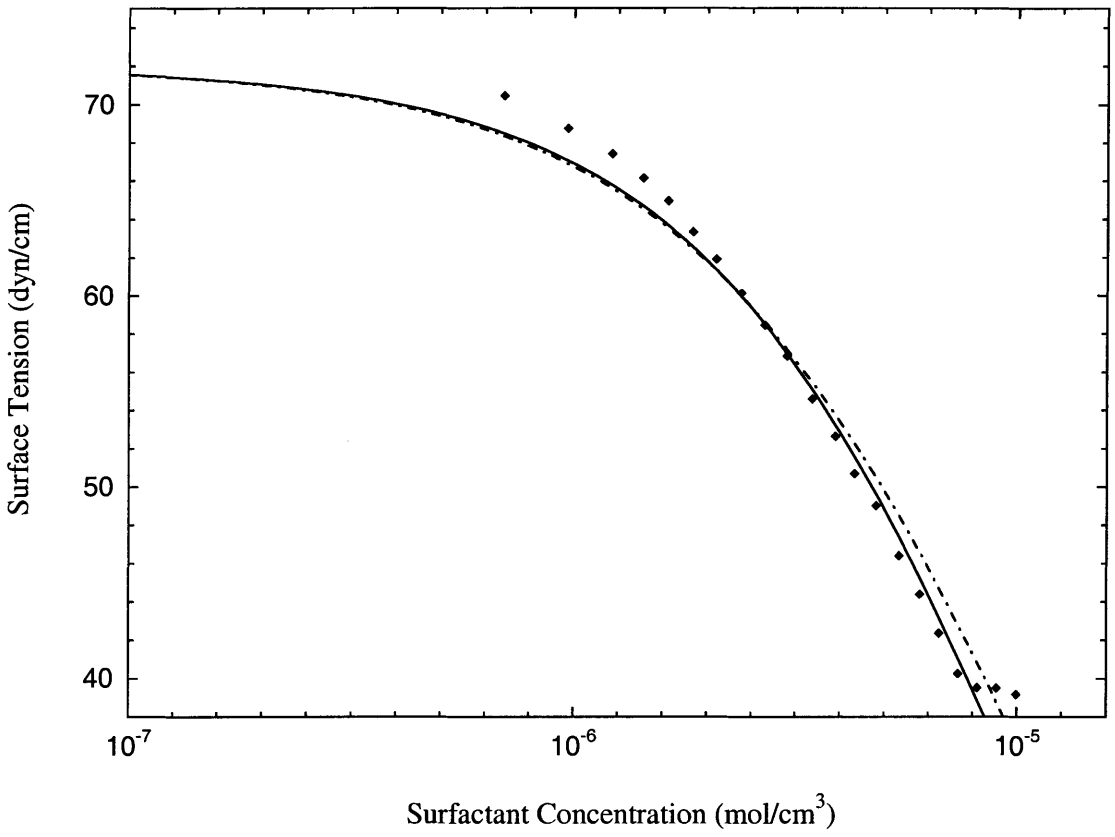

Figure A-1: Predicted (lines) and experimentally measured (symbols) surface tensions, σ, as a function of the bulk aqueous SDS concentration, n_s^w, for an aqueous solution containing no added salt at 25°C. The theoretical predictions correspond to those made using the original Poisson-Boltzmann model (———) and to those made using the modified form of the Poisson-Boltzmann model, described in Section A.2.1, which uses the Carnahan-Starling equation of state to account for hard-disk interactions between the ions in the diffuse region (- — - — -). The experimental measurements are from Ref. 52.

disk interactions between the ions in the diffuse region (- — - — -). The experimental measurements, which are shown in Figure A-1 for comparison, are from Ref. 52. Note that including the hard-disk interactions between the ions in the diffuse region has the effect of decreasing the electrostatic screening, which in turn, causes less surfactant to adsorb at the interface since there is a larger electrostatic barrier to do so. This, in turn, leads to a smaller slope of the surface tension versus bulk surfactant concentration curve (since, from the Gibbs adsorption equation, the slope of this curve is proportional to the surfactant surface concentration[41]). This can be seen in Figure A-1 by the fact that, at a given surface tension, the surface tension curve corresponding to the modified Poisson-Boltzmann theory (- — - — -) has a smaller slope. More importantly, note that the difference between the two theoretical surface tension versus surfactant concentration curves is very small. In other words, the effect of including hard-disk interactions between the ions in the diffuse region is almost negligible.

Furthermore, Figure A-2 shows the predicted (lines) and the experimentally measured (symbols) surface tensions, σ, as a function of the bulk aqueous SDS concentration, n_s^w, for an aqueous solution containing 1.0M added salt (NaCl) at 25°C. The theoretical predictions correspond to those made using the original Poisson-Boltzmann model (———) and those made using the modified form of the Poisson-Boltzmann model, described in Section A.2, which uses the Carnahan-Starling equation of state (- — - — -) to account for the hard-disk interactions between the ions in the diffuse region. The experimental measurements, which are shown in Figure A-1 for comparison, are from Ref. 33. One may expect that including the hard-disk interactions between the ions in the diffuse region should have a larger effect in this case because the high salt concentration should cause the ions to more strongly "feel each other" sterically in this more crowded solution. However, the high salt concentration also leads to much more electrostatic screening, which reduces the electrostatic potential near the interface. As a result of these competing effects, the enhancement of the counterion concentration near the interface is actually reduced. Hence, as in the no salt case, the difference between the two theoretical surface tension curves in Figure A-2 is very small.

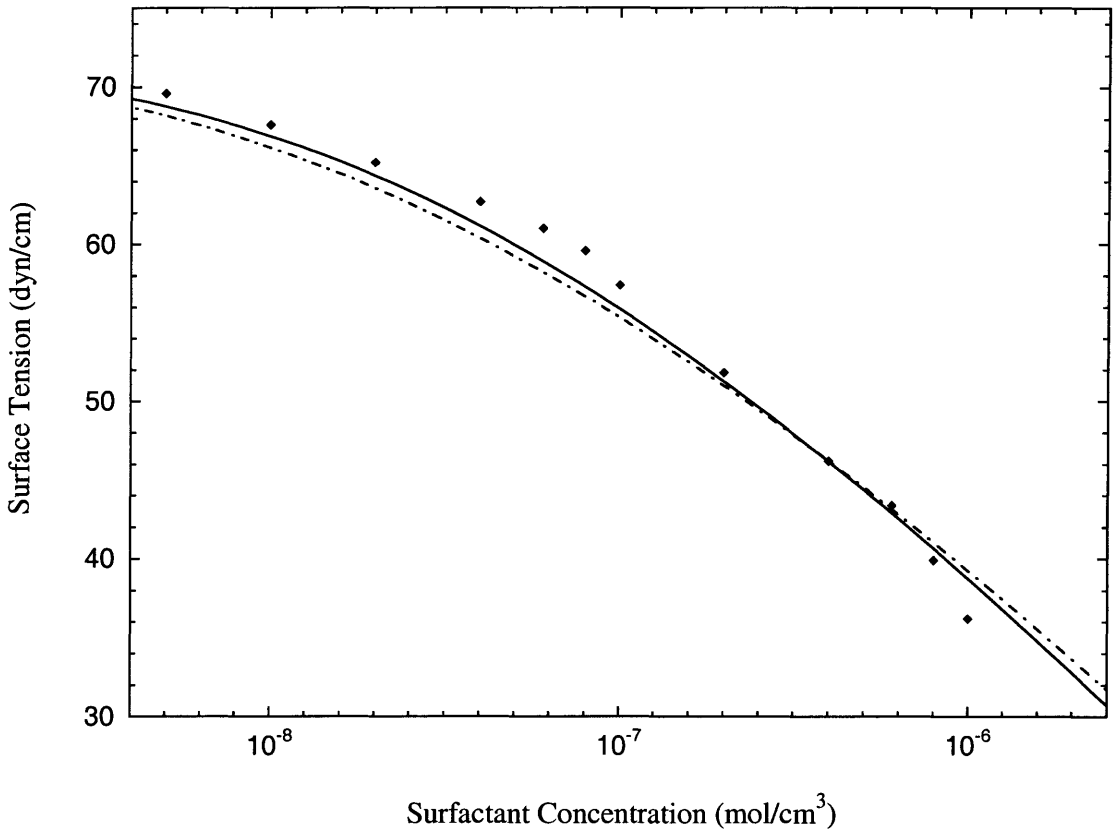

Figure A-2: Predicted (lines) and experimentally measured (symbols) surface tensions, σ, as a function of the bulk aqueous SDS concentration, n_s^w, for an aqueous solution containing 1.0M added salt (NaCl) at 25°C. The theoretical predictions correspond to those made using the original Poisson-Boltzmann model (———) and those made using the modified form of the Poisson-Boltzmann model, described in Section A.2.1, which uses the Carnahan-Starling equation of state to account for hard-disk interactions between the ions in the diffuse region (- — - — -). The experimental measurements are from Ref. 33.

A.3.2 Dielectric Saturation

In this section, as in Section A.3.1, the ionic surfactant SDS is utilized to illustrate the effect of dielectric saturation in the diffuse region. This will be done by comparing the predicted surface tensions as a function of the bulk aqueous surfactant concentration when the dielectric constant, ε, is assumed to be uniform and equal to the value corresponding to that of pure water, and when the dielectric constant is computed using the Booth model of dielectric saturation (see Eq. A.14).

Figure A-3 shows the predicted (lines) and the experimentally measured (symbols) surface tensions, σ, as a function of the bulk aqueous SDS concentration, n_s^w, for an aqueous solution containing no added salt. The theoretical predictions correspond to those made using the original Poisson-Boltzmann model (———) and to those made using the modified form of the Poisson-Boltzmann model, described in Section A.2.2, which uses the Booth model for dielectric saturation (- — - — -). The experimental measurements, which are shown in Figure A-3 for comparison, are from Ref. 52. Note that including dielectric saturation in the diffuse region has the effect of decreasing the electrostatic screening caused by the ions, which, in turn, causes less surfactant to adsorb at the interface since there is a larger electrostatic barrier to do so. This, in turn, leads to a smaller slope of the surface tensions versus surfactant concentration curve (since, from the Gibbs adsorption equation, the slope of this curve is proportional to the surfactant surface concentration[41]). This can be seen in Figure A-3 by the fact that, at a given surface tension, the surface tension curve corresponding to the modified Poisson-Boltzmann theory has a smaller slope (- — - — -). However, note that the difference between the two theoretical surface tension versus surfactant concentration curves is relatively small. In other words, neglecting dielectric saturation in the original Poisson-Boltzmann model is a reasonable assumption.

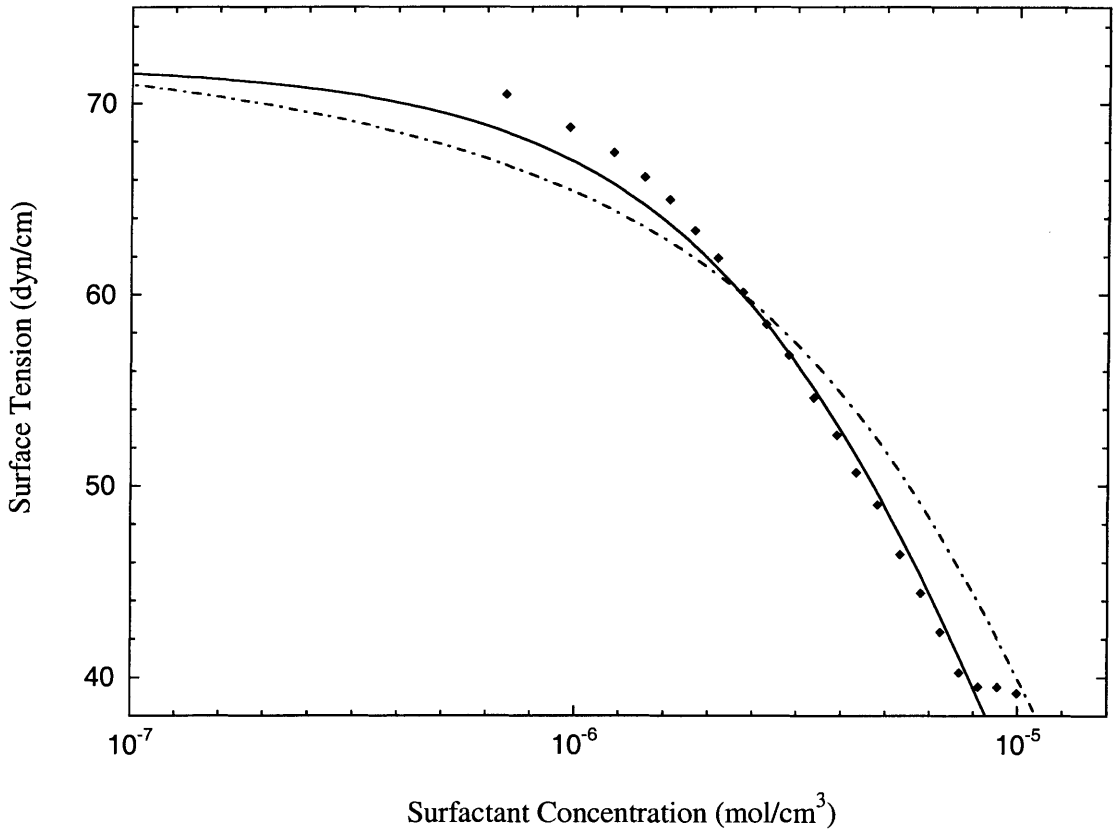

Figure A-3: Predicted (lines) and experimentally measured (symbols) surface tensions, σ, as a function of the bulk aqueous SDS concentration, n_s^w, for an aqueous solution containing no added salt at 25°C. The theoretical predictions correspond to those made using the original Poisson-Boltzmann model where the dielectric constant is assumed to be uniform and equal to the value corresponding to that of pure water (———), and those made using the modified form of the Poisson-Boltzmann model, described in Section A.2.2, which uses the Booth model of dielectric saturation (- — - — -). The experimental measurements are from Ref. 52.

A.4 Conclusions

In this Appendix, the validity of two of the assumption of the Gouy-Chapman model, that the ions in the diffuse region have no physical size, and that the dielectric constant in the diffuse region is uniform, were investigated by modifying the Poisson-Boltzmann based theory presented in Chapter 2. Specifically, a modified form of the Poisson-Boltzmann equation, which was derived using the Carnahan-Starling model[151,155,156] that treats the ions in the diffuse region as finite-sized hard spheres, was utilized to predict the surface tension of an aqueous solution of the model surfactant SDS. The results indicate that treating the ions with the Carnahan-Starling model, as opposed to the point-ion treatment of the original Poisson-Boltzmann model, has little effect on the predicted surface tension versus surfactant concentration curves, made using the theoretical framework presented in Chapter 2, of an aqueous solution of the ionic surfactant SDS.

Furthermore, a modified form of the Poisson-Boltzmann equation which incorporates the effect of dielectric saturation, through the use of a model developed by Booth[150] to predict the dielectric constant of water as a function of the electric field, was utilized to predict the surface tension as a function of bulk surfactant concentration of an aqueous solution of SDS. Again, the results indicate that dielectric saturation has little effect on the predictions.

Note that the theoretical framework presented in this Appendix requires the numerical solution of the governing electrostatic equations (Eq. (A.4) or Eq. (A.10)), whereas the original Poisson-Boltzmann equation presented in Chapter 2 can be solved analytically in closed-form. Therefore, the modified forms of the Poisson-Boltzmann equation are much more computationally intensive to solve. Since the inclusion of ion size effects and dielectric saturation was found to have little effect on the surface tension predictions, one may conclude that the treatment of the ions in the diffuse region as point ions and the assumption that the dielectric constant in the diffuse region is uniform represent reasonable approximations.

Appendix B

Analysis of the Sensitivity of the Predictions of the Equilibrium Surfactant Adsorption Models to the Surfactant Molecular Parameters

In this Appendix, the sensitivity of the theoretical predictions presented in Chapters 2 and 3 to the various surfactant molecular parameters is examined. To investigate this sensitivity, two model surfactants are chosen: one ionic, to investigate the sensitivity of the theory presented in Chapter 2, and one zwitterionic, to investigate the sensitivity of the theory presented in Chapter 3. The sensitivity to any one of the surfactant molecular parameters is then studied by varying that parameter while holding all other parameters constant. The theoretically predicted surface tension as a function of bulk surfactant concentration is then used as the response variable for the various values of the surfactant molecular parameter of interest. Note that in all the cases examined, the standard-state chemical potential difference is calculated by fitting the predicted surface tension to a single experimentally measured

surface tension at a known bulk surfactant concentration (see Chapter 2), for each set of surfactant molecular parameters. In other words, the value of the standard-state chemical potential difference is not held constant, but instead, the value of the surface tension at a particular bulk surfactant concentration is held constant. In all cases examined, the temperature is set at 25°C.

To investigate the sensitivity of the predictions made in Chapter 2 to the value of the surfactant cross-sectional area, the surfactant second-order virial coefficient, and the Stern layer dielectric constant, the surfactant dodecyl trimethyl ammonium bromide (DTAB) is utilized as a model surfactant. This surfactant was chosen because it possesses a polar head that is neither very large nor very small, and an alkyl tail that consists of a reasonable number of carbon atoms. The actual values of the molecular parameters corresponding to this surfactant are listed in Table C.1 in Appendix C. The single surface tension measurement that was utilized to compute the standard-state chemical potential difference corresponds to a bulk surfactant concentration of $1.4 \times 10^{-5} mol/cm^3$.

To investigate the sensitivity of the theoretical predictions to the surfactant cross-sectional area, Figure B-1 shows the predicted surface tensions as a function of the surfactant concentration for aqueous surfactant solutions of three illustrative surfactants. The molecular parameters for the three surfactants are those corresponding to DTAB, except for the cross-sectional area, which has values of: 25 Å^2 (- — - — -), 29Å^2 (———), and 35Å^2 (— — —). Note that, in each case, the second-order virial coefficient is computed using Eq. (2.4), with a value of 12 for the number of carbon atoms in the surfactant tail and the corresponding value of the surfactant cross-sectional area. In other words, rather than holding the value of the second-order virial coefficient constant, the value of the number of carbon atoms in the surfactant tail is held constant. Note that, as shown in Figure B-1, the predictions are not overly sensitive to the surfactant cross-sectional area.

To investigate the sensitivity of the theoretical predictions to the second-order virial coefficient, Figure B-2 shows the predicted surface tensions as a function of the surfactant concentration for aqueous surfactant solutions of three illustrative surfac-

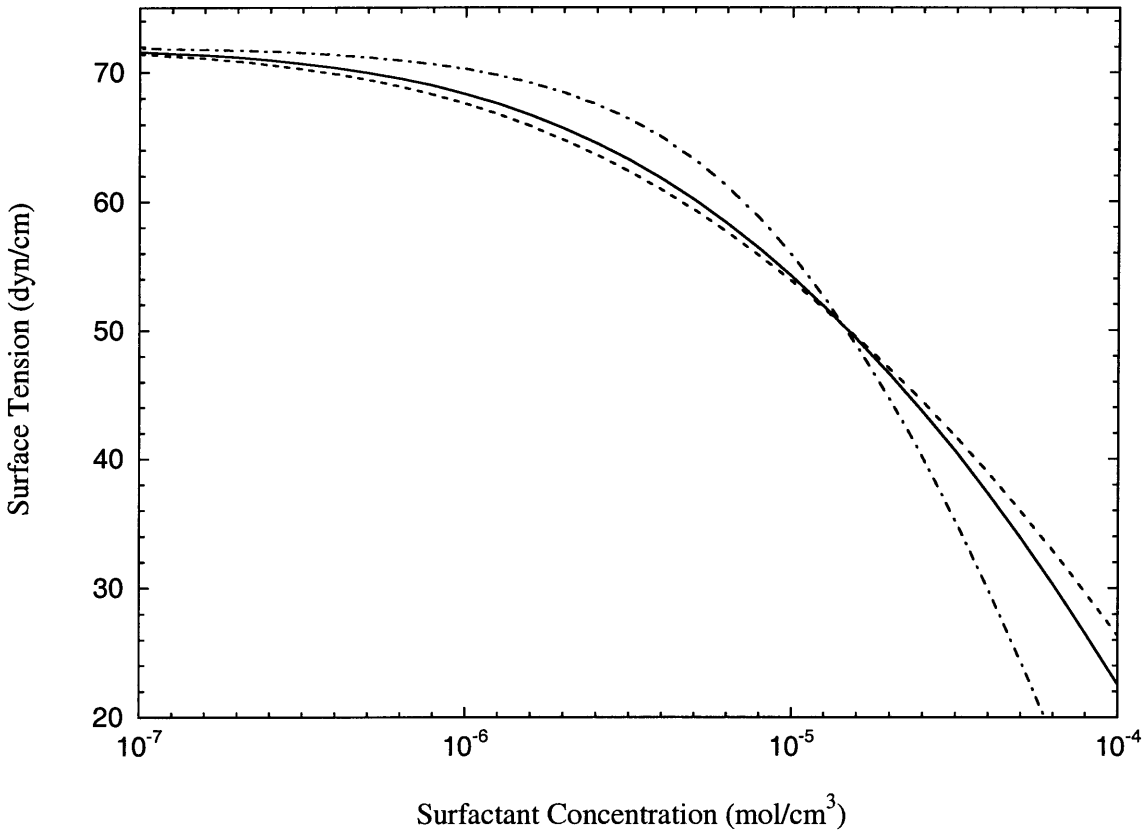

Figure B-1: Predicted surface tensions as a function of the surfactant concentration for aqueous surfactant solutions of three illustrative surfactants, showing the sensitivity of the theoretical predictions to the surfactant cross-sectional area. The molecular parameters for the three surfactants are those corresponding to DTAB, except for the cross-sectional area, which has values of: 25 Å^2 (- — - — -), 29Å^2 (———), and 35Å^2 (— — —).

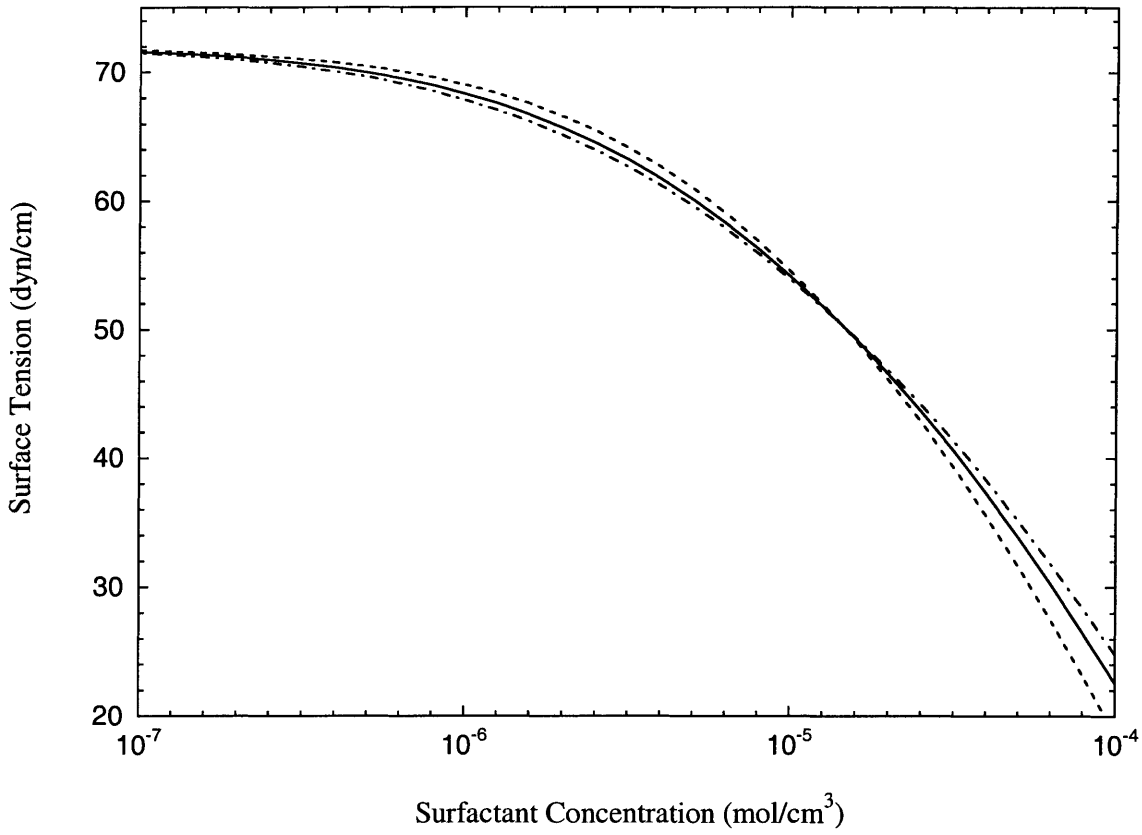

Figure B-2: Predicted surface tensions as a function of the surfactant concentration for aqueous surfactant solutions of three illustrative surfactants, showing the sensitivity of the theoretical predictions to the second-order virial coefficient. The molecular parameters for the three surfactants are those corresponding to DTAB, except for the second-order virial coefficient, which has values of: -154Å^2 (- — - — -), -222Å^2 (———), and -317Å^2 (— — —). These values of the second-order virial coefficient correspond to a surfactant with a cross-sectional area of 29Å^2, and a linear alkane tail containing 10, 12, and 14 carbon atoms, respectively.

tants. The molecular parameters for the three surfactants are those corresponding to DTAB, except for the second-order virial coefficient, which has values of: -154Å^2 (- — - — -), -222Å^2 (———), and -317Å^2 (— — —). Note that these values of the second-order virial coefficient correspond to a surfactant with a cross-sectional area of 29Å^2, and a linear alkane tail containing 10, 12, and 14 carbon atoms, respectively. In addition, note that, as shown in Figure B-2, the predictions are not very sensitive to the surfactant second-order virial coefficient.

To investigate the sensitivity of the theoretical predictions to the dielectric constant of the Stern layer, Figure B-3 shows the predicted surface tensions as a function of the surfactant concentration for aqueous surfactant solutions of three illustrative cationic surfactants. The molecular parameters for the three surfactants are those corresponding to DTAB, except for the Stern layer dielectric constant, which has values of: 35 (- — - — -), 42 (———), and 50 (— — —). Note that, as shown in Figure B-3, the predictions are not very sensitive to the dielectric constant of the Stern layer. Note that the sensitivity of the theoretical predictions to the Stern layer thickness is comparable to the sensitivity to the dielectric constant of the Stern layer, since only the ratio of these two properties affect the theoretical predictions (see Chapter 2).

Finally, to investigate the sensitivity of the theoretical predictions made in Chapter 3 to the value of the charge separation distance of a zwitterionic surfactant, the model surfactant dodecyl betaine (C_{12}Betaine) is utilized. Similar to the choice of DTAB, this surfactant was chosen because its molecular parameters are all in the moderate range. The values of the molecular parameters corresponding to C_{12}Betaine are listed in Tables 3.1 and 3.3 in Chapter 3. Recall that for a single zwitterionic surfactant, only the charge separation distance (that is, the difference between the locations of the two charge layers) is important, and not the absolute values of the locations of the two charge layers. To investigate the sensitivity of the theoretical predictions to the separation distance of the two charge layers, Figure B-4 shows the predicted surface tensions as a function of the surfactant concentration for aqueous surfactant solutions of three illustrative zwitterionic surfactants. The molecular parameters for the three surfactants are those corresponding to C_{12}Betaine, except for the charge separation

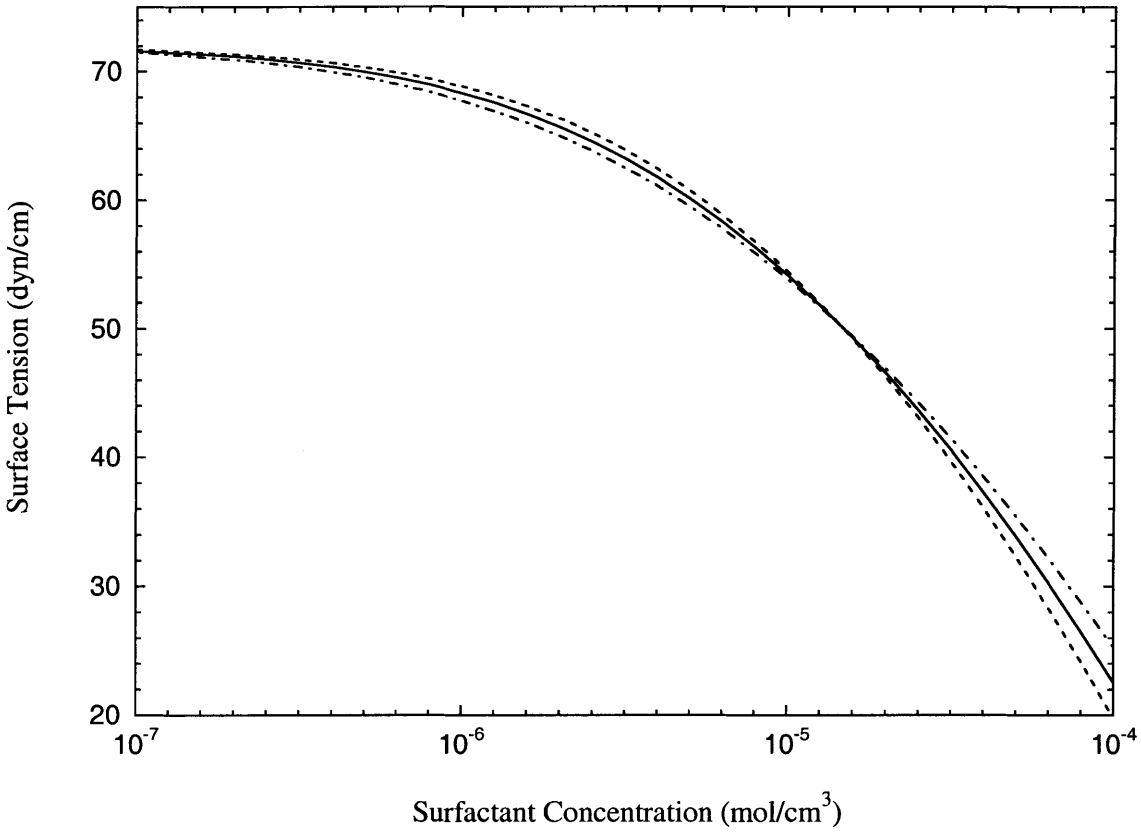

Figure B-3: Predicted surface tensions as a function of the surfactant concentration for aqueous surfactant solutions of three illustrative cationic surfactants, showing the sensitivity of the theoretical predictions to the Stern layer dielectric constant. The molecular parameters for the three surfactants are those corresponding to DTAB, except for the Stern layer dielectric constant, which has values of: 35 (- — - — -), 42 (———), and 50 (— — —).

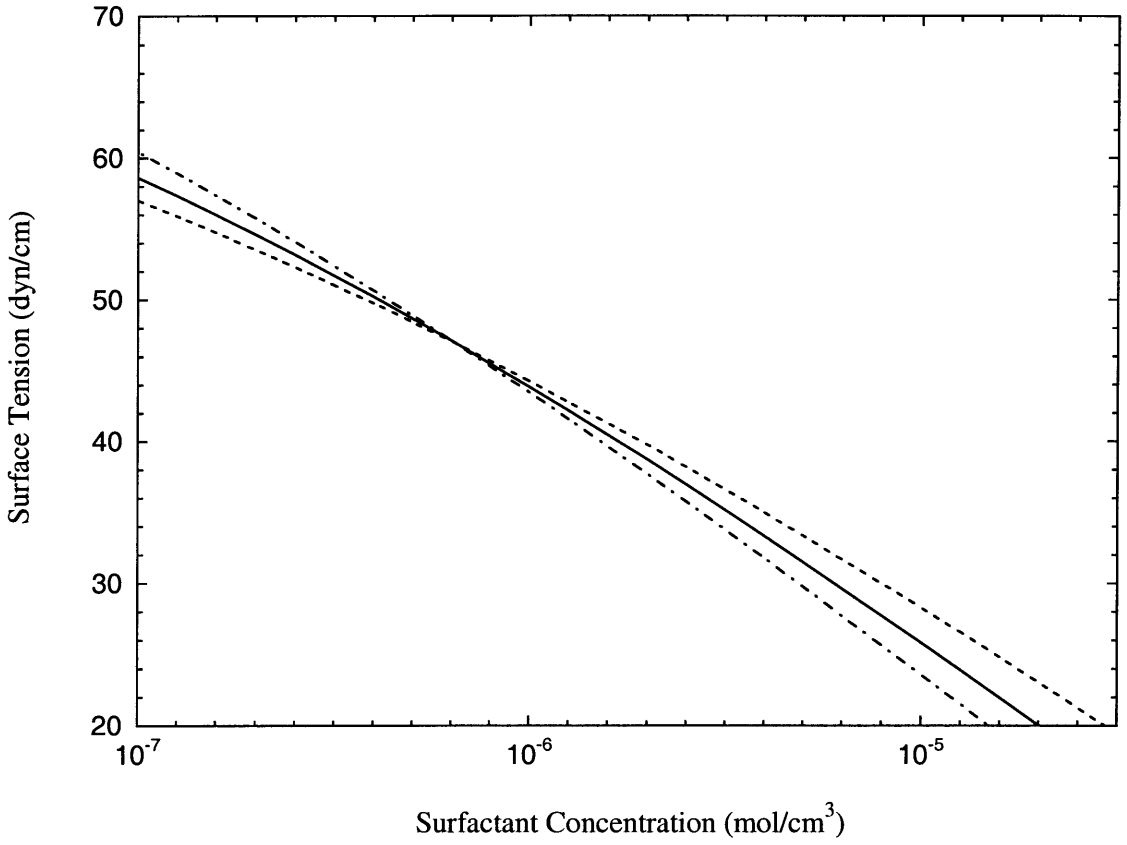

Figure B-4: Predicted surface tensions as a function of the surfactant concentration for aqueous surfactant solutions of three illustrative zwitterionic surfactants, showing the sensitivity of the theoretical predictions to the charge separation distance of a zwitterionic surfactant. The molecular parameters for the three surfactants are those corresponding to C_{12}Betaine, except for the charge separation distance, which has values of: 4.0 Å(- – - – -), 5.2Å(———), and 6.0Å(— — —).

distance, which has values of: 4.0 Å(- – - – -), 5.2Å(———), and 6.0Å(— — —). Note that, as shown in Figure B-4, the predictions are not very sensitive to the charge separation distance.

As clearly shown by the four illustrative examples examined in this Appendix, the equilibrium surface tension predictions made using the theories developed in Chapters 2 and 3 are not overly sensitive to any one surfactant molecular parameter. This finding contributes to the robustness of these theories, since the various surfactant molecular parameters need to be determined only to within a reasonable precision. Furthermore, it should be noted that the predictions are generally most sensitive to the molecular cross-sectional area of the surfactant. This can be explained physically by noting that this parameter affects both the steric repulsive interactions, as well as the attractive van der Waals interactions. For example, decreasing the molecular cross-sectional area of a surfactant has the effect of decreasing the steric repulsive interactions as well as increasing the attractive van der Waals interactions. Consequently, although the predicted surface tension is not overly sensitive to the surfactant cross-sectional area, it is more sensitive to this surfactant molecular parameter than to the other ones, as shown in Figure B-1.

Appendix C

Interfacial Phase Transitions

C.1 Introduction

In Chapters 2 and 3, it was assumed that although there are attractive van der Waals interactions between the tails of the adsorbed surfactant molecules, these interactions are not strong enough to induce an interfacial phase transition. However, it is possible for the model developed in Chapter 2, or other models that include attractive interactions, to predict an interfacial phase transition under certain conditions. Furthermore, interfacial phase transitions have been observed experimentally.[157–160] Whether or not the adsorbed surfactant molecules exhibit an interfacial phase transition is dictated by a balance between the attractive, van der Waals interactions, which tend to drive the adsorbed surfactant molecules towards a more condensed phase, and the repulsive, steric (and, possibly, electrostatic, in the case of a single charged surfactant) interactions, which tend to drive the adsorbed surfactant molecules towards a more expanded phase. Specifically, if the attractive interactions are weak, or if the repulsive steric or electrostatic interactions are strong, then the the critical temperature for phase transitions (which is the temperature above which there is no interfacial phase transition) will be low. Hence, if one is only interested in temperatures above this relatively low critical temperature (and, in particular, if this critical temperature is below the freezing point of the bulk aqueous phase), then one will never observe an interfacial phase transition experimentally or theoretically. However, if the adsorbed

surfactant molecules exhibit stronger attractive interactions, or weaker repulsive steric or electrostatic interactions, then the critical temperature will increase. If this critical temperature rises above the operating temperature of interest, then an interfacial phase transition will be observed.

The simplest theories that includes attractive interactions is the Frumkin model which contains an experimentally-determined empirical parameter to account for the attractions between the adsorbed surfactant molecules. If this parameter is small enough (that is, if it has a large negative value), then a first-order interfacial phase transition will be predicted.[161,162] More recently, several theoretical model have been developed specifically to treat interfacial phase transitions by assuming that the adsorbed surfactant molecules form surfactant "clusters".[163,164,142,165–168] While these theories have been shown to successfully predict the surface tension of surfactant solutions that undergo an interfacial phase transition, they all contain a number of additional experimentally determined parameters.

In this Appendix, it will be shown that the theoretical framework developed in Chapters 2 and 3 can be used to predict interfacial phase transitions without the addition of any parameters. Specifically, by using a thermodynamic framework to model interfacial phase transitions (see Section C.2), the surface equation of state developed in Chapters 2 and 3 can be used to predict the surface tension of surfactant solutions that undergo an interfacial phase transition. Furthermore, the development of a theoretical framework to model interfacial phase transitions also allows one to predict the interfacial properties of mixtures of anionic and cationic surfactants. These mixtures are of particular interest because, as discussed in Section C.3, single surfactant solutions of either of the two ionic surfactants do not exhibit an interfacial phase transition, while binary mixtures of these oppositely-charged surfactants do exhibit an interfacial phase transition. In addition, there is a very large interfacial synergistic relationship between the two oppositely-charged surfactants.

In Section C.3, a comparison is presented between the theoretically predicted and the experimentally measured surface tensions of: (i) single surfactant solutions of two linear alkane alcohols, octanol and decanol (where, due to their relative small

head sizes, there are strong enough van der Waals attractions between the tails of the adsorbed surfactant molecules to induce an interfacial phase transition), and (ii) a mixture of the anionic surfactant SDS and the cationic surfactant DTAB (which illustrates the case of an anionic–cationic surfactant mixture discussed above). Finally, concluding remarks are presented in Section C.4.

C.2 Theory

C.2.1 Interfacial Phase Transitions for Single Surfactants

First, to demonstrate that the equilibrium equation of state developed in Chapters 2 and 3 can predict an interfacial phase transition, two hypothetical nonionic surfactants are considered. The molecular parameters of the two surfactants are listed in Table C.1. Note that the molecular cross-sectional area is 30Å^2 for Surfactant 1 and 28Å^2 for Surfactant 2, while the number of carbon atoms in the tails of both surfactants is 10. The smaller cross-sectional area of Surfactant 2 leads both to a reduction in the steric repulsive interactions as well as to an increase in the van der Waals attractions (which can be seen by the more negative value of B_{ii} for Surfactant 2 in Table C.1, see also Eq. (2.4) in Chapter 2).

Figure C-1 shows the predicted surface pressure, Π, as a function of the area per molecule, $a \equiv 1/\Gamma_i \equiv A/N_i^\sigma$, for the two hypothetical nonionic surfactants: Surfactant 1 (- – - – -) and Surfactant 2 (———), both at 25°C, as calculated using Eq. (2.5) (see Section 2.2.1). Recall that the curves in Figure C-1 are the two-dimensional analogs of the Pressure-Volume curves commonly used to analyze phase transitions in a three-dimensional system. Note that for Surfactant 1, the surface pressure decreases monotonically with an increase in the area per molecule, which indicates that there is no interfacial transition for Surfactant 1. In other words, the critical temperature for Surfactant 1 is less than 25°C, the temperature used in the predictions. Note also that this case corresponds to all the surfactants considered in this thesis, except for those considered in this Appendix. On the other hand,

Table C.1: Values of the hard-disk areas, a_i, and second-order virial coefficients, B_{ii}, corresponding to the two hypothetical nonionic surfactants, Surfactant 1 and Surfactant 2, considered in Section C.2.1.

Surfactant i	a_i (Å^2)	B_{ii} (Å^2)
1	30	-138
2	28	-173

the surface pressure versus area per molecule for Surfactant 2 is not monotonic, but instead attains a local minimum and a local maximum. As in the case of a three-dimensional system, this non-monotonic behavior of the surface pressure of Surfactant 2 indicates that there is indeed a phases transition for this surfactant. Physically, this is a result of the fact that the decrease in the steric, repulsive interactions and the increase in the van der Waals attractive interactions (as compared to Surfactant 1) led to an increase in the critical temperature of Surfactant 2 to a value above the operating temperature of 25°C. The existence of an interfacial phase transition can also be detected in the behavior of the surface chemical potential, μ_i^σ, as a function of the area per molecule, a, which is shown in Figure C-2 (where the standard-state chemical potentials have been arbitrarily set to zero). Note that there is no one-two-one relationship between μ_i^σ and a. Therefore, if one attempted to use Eq. (2.11) to solve for the equilibrium value of a for a given bulk chemical potential value (determined from the bulk aqueous surfactant concentration using Eq. (2.12)), one could arrive at two or three different solutions.

The treatment of interfacial phase transitions is very much analogous to the treatment of phase transitions in three-dimensional phases. Specifically, a tie-line can be drawn, as shown by the horizontal line (— — —) in Figures C-1 and C-2. The two endpoints of this tie-line (points 'A' and 'B') can be determined by first requiring that the surface pressure of the two coexisting interfacial phases be equal. That is,

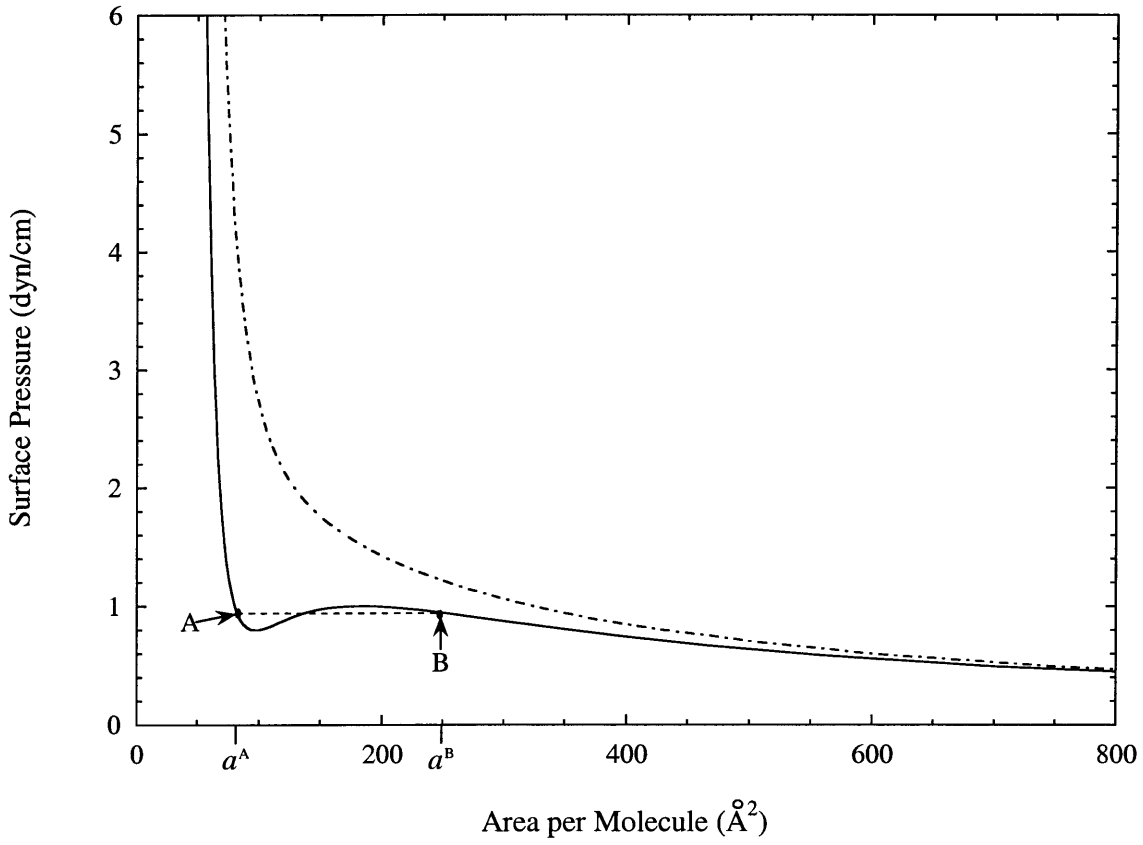

Figure C-1: Predicted surface pressure as a function of the area per molecule for two hypothetical nonionic surfactants: Surfactant 1 (- — - — -), a surfactant that does not exhibit an interfacial phase transition, and Surfactant 2 (———), a surfactant that does exhibit an interfacial phase transition. The tie-line indicating the location of the phase transition (— — —), and its endpoints, A and B, are also shown.

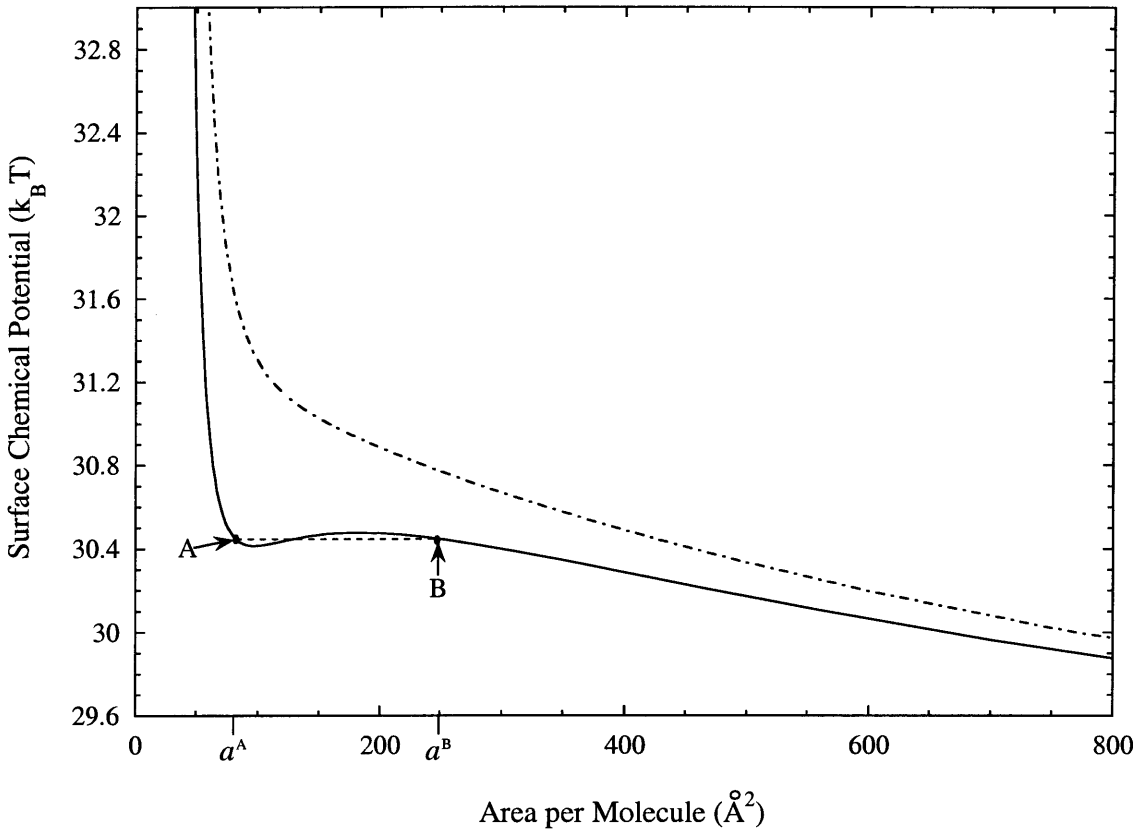

Figure C-2: Predicted surface chemical potential as a function of the area per molecule for two hypothetical nonionic surfactants: Surfactant 1 (- — - — -), a surfactant that does not exhibit an interfacial phase transition, and Surfactant 2 (———), a surfactant that does exhibit an interfacial phase transition. The tie-line indicating the location of the phase transition (— — —), and its endpoints, A and B, are also shown.

that:

$$\Pi\left(a^{\mathrm{A}}\right) = \Pi\left(a^{\mathrm{B}}\right) \tag{C.1}$$

and that the surface chemical potentials of surfactant molecules of type i in the two coexisting interfacial phases be equal as well. That is, that:

$$\mu_i^{\sigma}\left(a^{\mathrm{A}}\right) = \mu_i^{\sigma}\left(a^{\mathrm{B}}\right) \tag{C.2}$$

where a^{A} and a^{B} are the areas per molecule at points A and B, respectively, and Π is calculated using Eq. (2.5) for nonionic surfactants (or Eq. (2.37) for ionic surfactants, or Eq. (3.37) for multiply charged surfactants), and μ_i^{σ} is calculated using Eq. (2.10) for nonionic surfactants (or Eq. (2.45) for ionic surfactants, or Eq. (3.43) for multiply charged surfactants). Note that this derivation assumes that the coexisting interfacial phases are large, that is, that the ratio of the area of a phase to its perimeter is large enough that "surface" effects, such as line tensions, can be neglected. Note also that the value of the standard-state chemical potential difference in Eq. (2.10) (or in Eqs. (2.45) and (3.43)) is not needed to solve Eq. (C.2), since it appears on both sides of the equation, and hence, cancels out. Equations (C.1) and (C.2) can be solved simultaneously to determine the two unknowns, a^{A} and a^{B}. For any area per molecule between the phase transition endpoints, that is, for $a^{\mathrm{A}} \leq a \leq a^{\mathrm{B}}$, there will be a mixture of two surface phases (one corresponding to a^{A} and the other to a^{B}) with the surface pressure given by $\Pi = \Pi\left(a^{\mathrm{A}}\right) = \Pi\left(a^{\mathrm{B}}\right)$ and the surface chemical potential given by $\mu_i^{\sigma} = \mu_i^{\sigma}\left(a^{\mathrm{A}}\right) = \mu_i^{\sigma}\left(a^{\mathrm{B}}\right)$. On the other hand, if $a < a^{\mathrm{A}}$ or $a > a^{\mathrm{B}}$, then there will be only one surface phase and the surface pressure and surface chemical potential can be computed as discussed in Chapters 2 and 3.

As an illustration, suppose that the surfactant under consideration is nonionic. To implement the derivation which follows in the case of ionic surfactants, one would simply utilize Eq. (2.37) in place of Eq. (2.5), and Eq. (2.45) in place of Eq. (2.10) throughout the following derivation. Similarly, to implement the derivation which follows in the case of multiply charged surfactants (for example, zwitterionic surfactants), one would simply utilize Eq. (3.37) in place of Eq. (2.5) and Eq. (3.43) in

place of Eq. (2.10) throughout the following derivation.

Once it has been determined that the surfactant under consideration undergoes an interfacial phase transition, and the endpoints of the tieline (points 'A' and 'B') have been determined as described above, the next step is to calculate the standard-state chemical potential difference, $\Delta\mu_i^0$. As in the case of a surfactant that does not exhibit an interfacial phase transition, this is done using one experimentally measured surface tension, σ, at a known bulk surfactant concentration. The surface pressure, Π, at this bulk surfactant concentration is determined from $\Pi = \sigma_0 - \sigma$. The value of the area per molecule, a, corresponding to this surface pressure is determined by substituting this value of Π in Eq. (2.5) and then solving for a. If the measured value of Π is below the phase transition surface pressure, $\Pi\left(a^{\mathrm{A}}\right) = \Pi\left(a^{\mathrm{B}}\right)$, then the solution to Eq. (2.5) should be restricted to $a > a^{\mathrm{B}}$. If the measured value of Π is above the phase transition surface pressure, then the solution to Eq. (2.5) should be restricted to $a < a^{\mathrm{A}}$. (If the surface pressure happens to be equal to the phase transition surface pressure, then either $a = a^{\mathrm{A}}$ or $a = a^{\mathrm{B}}$ can be used.) This calculated value of a is then inserted into Eq. (2.10) which, along with the known value of the bulk surfactant concentration, can be solved to obtain $\Delta\mu_i^0$.

The surface tension can now be calculated for any bulk surfactant concentration. Specifically, for any value of n_i^{w}, one can solve Eq. (2.10) for a with the appropriate restriction that $a < a^{\mathrm{A}}$ or $a > a^{\mathrm{B}}$. This value of a is then inserted into Eq. (2.5) to compute the surface pressure, π, and hence, the surface tension, $\sigma = \sigma_0 - \Pi$.

C.2.2 Interfacial Phase Transitions for Mixtures of Surfactants

As an illustration, a binary surfactant mixture will be considered explicitly, and the extension to mixtures of more than two surfactants will be discussed at the end of this section. Also, for simplicity, this section will treat two nonionic surfactants. As in the preceding section, to implement the derivation which follows in the case of ionic surfactants, one would simply utilize Eq. (2.36) in place of Eq. (2.5) and Eq. (2.45) in

place of Eq. (2.10) throughout the following derivation. Similarly, to implement the derivation which follows in the case of multiply charged surfactants (for example, a zwitterionic surfactant or a mixture of two ionic surfactants), one would simply utilize Eq. (3.36) in place of Eq. (2.5) and Eq. (3.43) in place of Eq. (2.10) throughout the following derivation.

As in the case of surfactants that do not undergo an interfacial phase transition, in order to consider a mixture of surfactants, one must first compute the standard-state chemical potential difference of each surfactant component using a single surface tension measurement. If the single surfactant component does not undergo an interfacial phase transition, the value of this parameter can be computed using the theoretical framework presented in Section 2.2.1. If it does undergo an interfacial phase transition, the value of this parameter can be computed using the derivation presented in Section C.2.1.

As discussed in Section 2.2.1, to compute the equilibrium surface concentration, $\Gamma \equiv 1/a$, and surface composition, $x_1^\sigma \equiv \Gamma_1/(\Gamma_1 + \Gamma_2)$, for a given set of bulk surfactant monomer concentrations, n_{11}^{w} and n_{21}^{w}, one must solve the set of two equations given by Eq. (2.13) (where x_2^σ has been eliminated using $x_2^\sigma = 1 - x_1^\sigma$).

When there is no interfacial phase transition, one method of solving this set of two equations is to guess a value of x_1^σ, and then to solve Eq. (2.13) with $i = 1$ for a. This set of x_1^σ and a values can then be inserted into Eq. (2.13) with $i = 2$ and, if the equality is satisfied, then this set of x_1^σ and a values corresponds to the equilibrium values. If the equality in Eq. (2.13) with $i = 2$ is not satisfied, then a new guess for x_1^σ is made and the process is repeated. In this manner, one can eventually obtain the equilibrium values of a and x_1^σ through iteration. Once the equilibrium values of a and x_1^σ are known, one can compute the surface pressure, Π (or the surface tension, $\sigma = \sigma_0 - \Pi$), for that set of bulk surfactant monomer concentrations, using Eq. (2.6).

When there is an interfacial phase transition, one can proceed in a similar fashion. First, one guesses a value of x_1^σ. Now, however, when one attempts to solve Eq. (2.10) with $i = 1$ for a, one will find that μ_1^σ is non-monotonic in a, and therefore, that a one-to-one relationship between μ_1^σ and a does not exist in this case. Therefore, one

needs to use a procedure similar to the one described in Section C.2.1. Specifically, one can draw a tie-line where the two endpoints of this line (a^{A} and a^{B}) are determined from the set of two equations given by Eqs. (C.1) and (C.2) (with $i = 1$). Now, if a is between the two endpoint of the tie-line, then the surface chemical potential of Surfactant 1 is given by the value of the surface chemical potential at either of the two endpoints; otherwise, it is calculated using Eq. (2.10) with $i = 1$. The computed surface chemical potential of Surfactant 1, along with the bulk aqueous chemical potential of Surfactant 1 determined by utilizing Eq. (2.12), are then utilized in Eq. (2.11), which is solved for a. This value of a, along with the guessed value of x_1^σ, is then utilized in Eq. (2.10) with $i = 2$ to compute the surface chemical potential of Surfactant 2. Similarly, if one finds that μ_2^σ is non-monotonic in a, then one must again draw a tie-line, with the endpoints determined from Eqs. (C.1) and (C.2) (with $i = 2$). If a is between the two endpoint of the tie-line, then the surface chemical potential of Surfactant 2 is given by the value of the surface chemical potential at either of the two endpoints; otherwise it is calculated using Eq. (2.10) with $i = 2$. The surface chemical potential of Surfactant 2 computed using this method, along with the bulk aqueous chemical potential of Surfactant 2 determined by utilizing Eq. (2.12), are then inserted into Eq. (2.11). If the equality in Eq. (2.11) is satisfied, then this set of a and x_1^σ values corresponds to the equilibrium values; otherwise, a new guess of x_1^σ is required and the process is repeated. In this manner, one can eventually obtain the equilibrium values of a and x_1^σ through iteration. Once the equilibrium values of a and x_1^σ are known, one can compute the surface pressure, Π (or the surface tension, $\sigma = \sigma_0 - \Pi$), for that set of bulk surfactant monomer concentrations, using Eq. (2.6).

The theoretical description presented above can be extended to a mixture of $n > 2$ surfactant components. For example, one could guess values of all the surface compositions (subject to their sum being unity), solve Eq. (2.10) with $i = 1$ for a (using the tie-line procedure described above to calculate the surface chemical potential of Surfactant 1), and then check the equality in Eq. (2.10) for $i = 2, ..., n$ (using the tie-line procedure described above).

Table C.2: Values of the hard-disk areas, a_i, second-order virial coefficients, B_{ii}, Stern region thicknesses, d, and standard-state chemical potential differences, $\Delta\mu_i^0$, corresponding to the surfactants considered in Section C.3.

Surfactant i	a_i (Å^2)	B_{ii} (Å^2)	d (Å)	$\Delta\mu_i^0$ (k_BT)
Octanol	21	-230	–	-41.6
Decanol	21	-430	–	-38.1
SDS	25	-367	4.05	-59.0
DTAB	28	-257	5.2	-59.0

C.3 Results

As discussed in Section C.2, an interfacial phase transition occurs when the van der Waals attractive interactions are relatively strong, and the steric or electrostatic repulsive interactions are relatively weak, which is the case for nonionic surfactants with relatively small polar heads. Therefore, linear alkyl alcohols are good model "surfactants" to use in the investigation of interfacial phase transitions since they possess a very small head. The molecular parameters for two such alcohols, octanol and decanol, are listed in Table C.2. The standard-state chemical potential differences for each alcohol, $\Delta\mu_i^0$, were computed by fitting the experimentally measured surface tension at a bulk surfactant concentration of $1.0 \times 10^{-6} mol/cm^3$ for octanol and $5.0 \times 10^{-8} mol/cm^3$ for decanol, as discussed in Section C.2.1.

Figure C-3 shows the theoretically predicted (lines) and the experimentally measured (symbols) surface tensions as a function of bulk surfactant concentration for aqueous solutions of octanol (- – - – - , ♦) and decanol (——— , ●) at 25°C. The experimental measurements are from Ref. 159. The arrows indicate the location of the interfacial phase transition for each surfactant, which were predicted using the theoretical framework presented above. Note that there is very good agreement between the theoretically predicted surface tensions and the experimentally measured

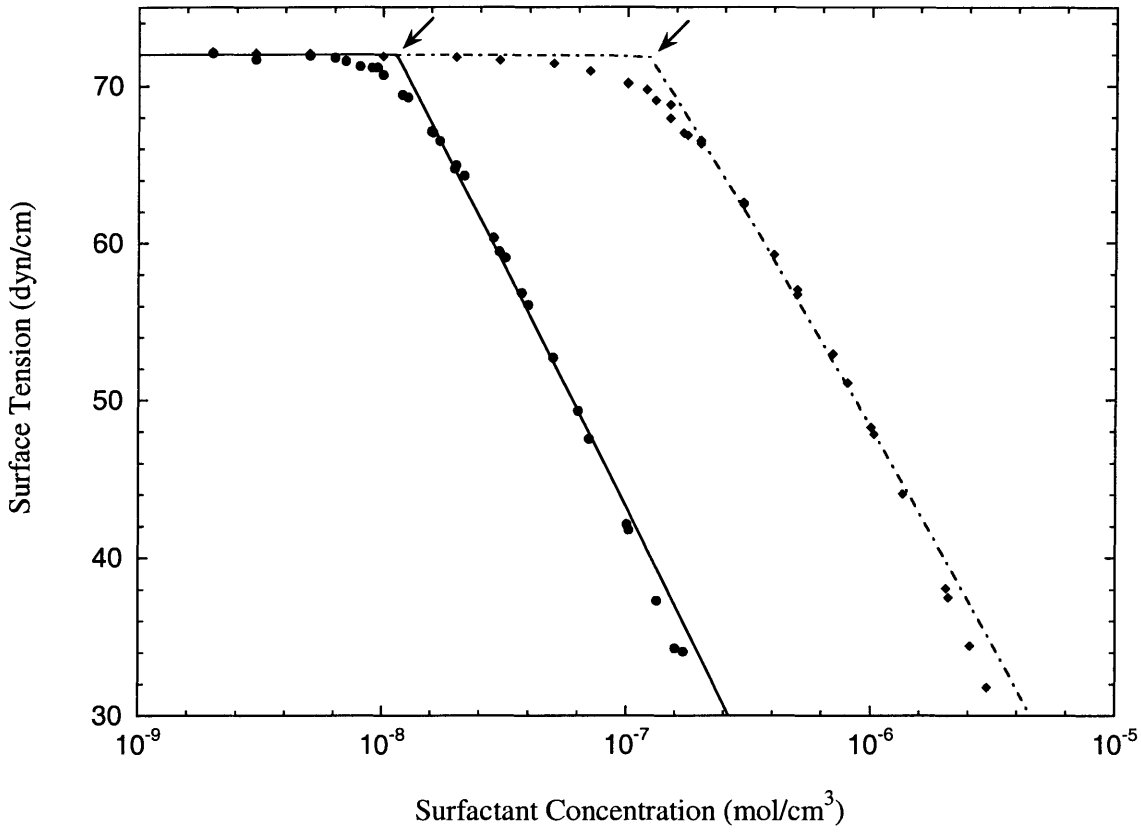

Figure C-3: Theoretically predicted (lines) and experimentally measured (symbols) surface tensions as a function of bulk surfactant concentration for aqueous solutions of octanol (- — - — - , ♦) and decanol (——— , ●) at 25°C. The experimental measurements are from Ref. 159. The arrows indicate the location of the interfacial phase transition for each surfactant.

values.

Note that the interfacial phase transition corresponds to a discontinuity in the slope of the surface tension versus surfactant concentration curve.[160] This can be explained by noting that the Gibbs adsorption equation states that the slope of this curve is proportional to the surfactant surface concentration.[41] Accordingly, at the interfacial phase transition, the surfactant surface concentration exhibits a discontinuity from the small value corresponding to the expanded phase to the large value corresponding to the condensed phase. In the context of the discussion presented in Section C.2.1, this would correspond to a transition from point 'B' to point 'A'. Note that this transition corresponds to a single value of the surface pressure (or surface tension), and hence, it occurs at just one point on the surface tension versus surfactant concentration curves shown in Figure C-3. Although a discontinuity in the slope of the experimental surface tension versus surfactant concentration curve is difficult to observe, Ref. 157 utilizes ellipsometry to show that there is indeed an interfacial phase transition for decanol at the point indicated by the arrow in Figure C-3.

Another interesting surfactant system to investigate in the context of interfacial phase transitions is a binary mixture of an anionic and a cationic surfactant. For each single surfactant, the repulsive, electrostatic interactions are so strong that an interfacial phase transition does not occur for either of the single surfactant solutions. However, in the case of a mixture of the two oppositely-charged surfactants, the electrostatic interactions are significantly reduced (for example, the electrostatic contribution to the surface pressure would actually vanish for an interface that had an equal number of adsorbed anionic and cationic surfactant molecules when their charges are positioned on the same charge layer). In the absence of the strong electrostatic, repulsive interactions, and if the van der Waals attractive interactions are strong enough, then the mixed surfactant system may undergo an interfacial phase transition even though these van der Waals attractive interactions are not strong enough to induce an interfacial phase transition in the single surfactant cases.

The anionic surfactant sodium dodecyl sulfate (SDS) and the cationic surfactant dodecyl trimethyl ammonium bromide (DTAB) provide a model system to illustrate

the case discussed above. The molecular parameters for these two surfactants are listed in Table C.2. The standard-state chemical potential differences for each surfactant, $\Delta\mu_i^0$, were computed by fitting the experimentally measured surface tension at a bulk surfactant concentration of $5.4 \times 10^{-6} mol/cm^3$ for SDS and $1.4 \times 10^{-5} mol/cm^3$ for DTAB. Note that for single surfactant solutions of either SDS or DTAB, there is only one charged group present on the surfactant head, and therefore, the theory in Chapter 2 can be used to model their interfacial behavior. However, for the mixture of these two surfactants, there are two charged groups (one on each surfactant head) which are located at different positions within the monolayer. Therefore, there are two interfacial charge layers, and the theory in Chapter 3 should be used to model the interfacial behavior. The location of the two charge layers are $d_1 = 2.3$Å (corresponding to the charge on SDS) and $d_2 = 2.5$Å(corresponding to the charge on DTAB), with the Stern layer located at $d_S = 7.7$Å. The value of the charge layer valences, ζ_i^ϕ, are: $\zeta_{SDS}^1 = -1$, $\zeta_{SDS}^2 = 0$, $\zeta_{DTAB}^1 = 0$, and $\zeta_{DTAB}^2 = 1$ (see Section 3.2.2 for a discussion of these parameters). Finally, the second-order virial coefficient for this pair of surfactants is -321Å^2.

Figure C-4 shows the theoretically predicted (lines) and the experimentally measured (symbols) surface tensions as a function of total bulk surfactant concentration for: (i) aqueous single surfactant solutions of SDS (— — —, ●) and DTAB (- — - — - , ♦), and (ii) an aqueous binary surfactant solution of 50% SDS – 50% DTAB (——— , ■), all at 25°C. The experimental measurements are from Ref. 169. The arrow indicates the location of the interfacial phase transition for the mixed surfactant case (note that there is no interfacial phase transition for the two single surfactant solutions). Furthermore, Figure C-5 shows the predicted surface composition, x_{SDS}^σ, as a function of the total bulk surfactant concentration for the 50% SDS – 50% DTAB solution at 25°C. Note that, indeed, the surface composition is nearly equal to 0.5 for any total bulk surfactant concentration, and hence, the electrostatic repulsive interactions are very small. This allows the phase transition, indicated by the arrow in Figure C-4, to occur.

In addition to this interfacial phase transition, the anionic–cationic surfactant

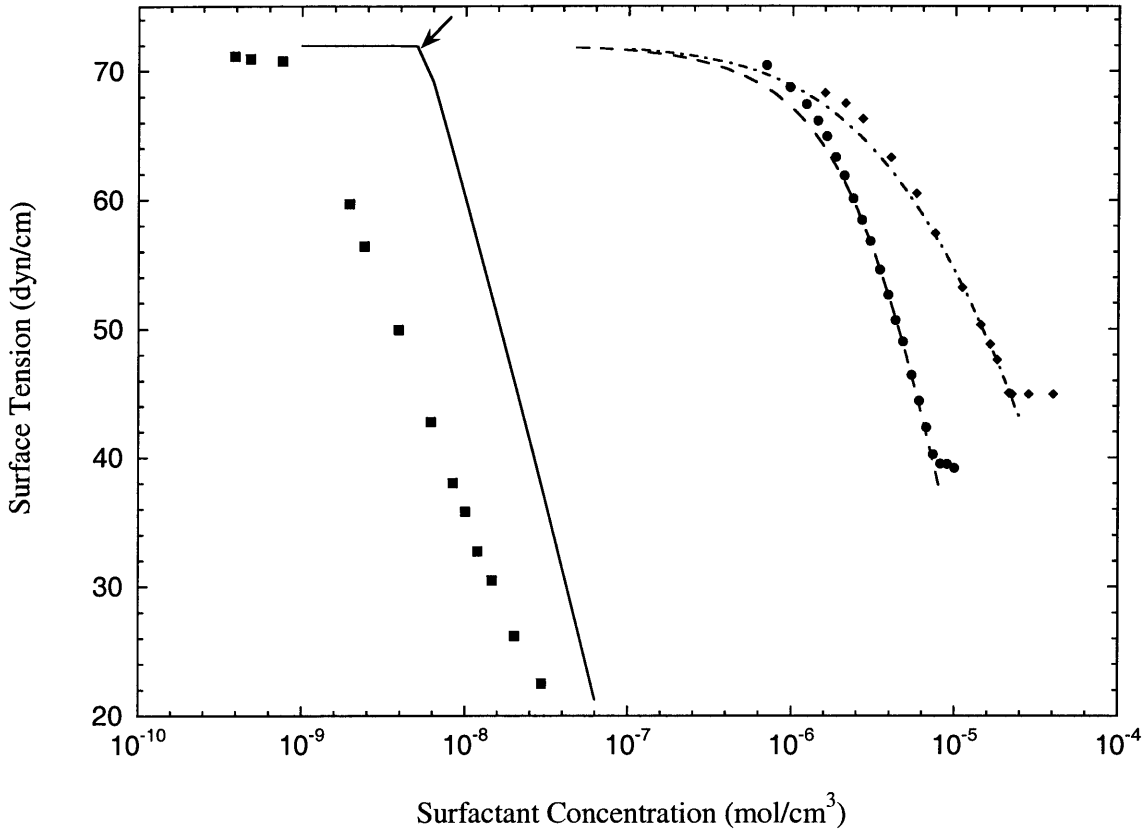

Figure C-4: Theoretically predicted (lines) and experimentally measured (symbols) surface tensions as a function of total bulk surfactant concentration for: (i) aqueous single surfactant solutions of SDS (— — —, ●) and DTAB (- — - — - , ♦), and (ii) an aqueous binary surfactant solution of 50% SDS – 50% DTAB (——— , ■), all at 25°C. The experimental measurements are from Ref. 169. The arrow indicates the location of the interfacial phase transition for the surfactant mixture (note that there is no interfacial phase transition for the two single surfactant solutions).

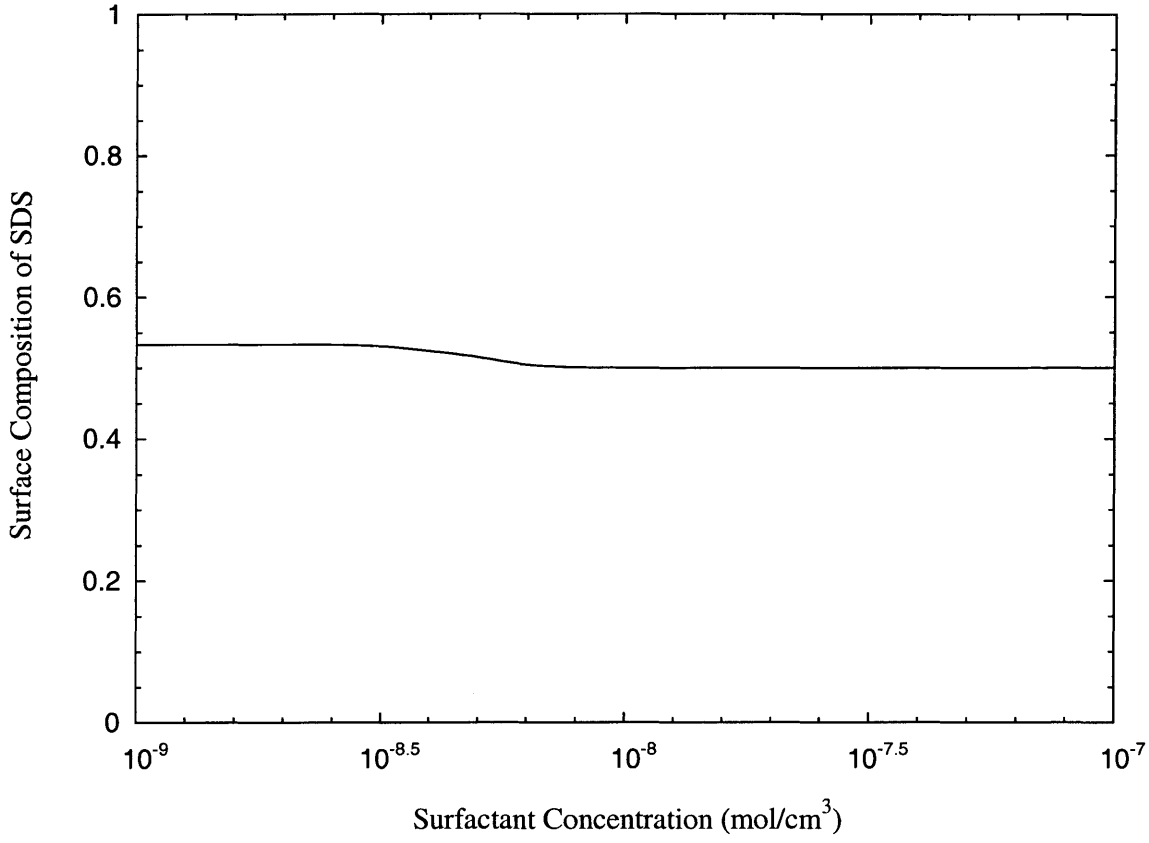

Figure C-5: Theoretically predicted surface composition of SDS, x^{σ}_{SDS}, as a function of the total bulk surfactant concentration for a 50% SDS – 50% DTAB solution at 25°C.

mixture is also of interest due to the very large extent of synergism at the interface. Indeed, as shown in Figure C-4, the surface tension versus total bulk surfactant concentration curve for the surfactant mixture lies far to the left of the corresponding curves for either of the two single surfactants. This is also a result of the fact that the repulsive, electrostatic interactions have been almost completely eliminated in the case of the surfactant mixture, and hence, the surfactant mixture can more readily adsorb at the interface, thus requiring a lower total concentration of surfactant to drive the adsorption process. Although the agreement between the theoretically predicted surface tension and the experimentally measured values is not as good as that for the other surfactant mixtures considered in Chapters 2 and 3, the agreement is still reasonably good considering the large extent of synergism between these two surfactants, and the fact that no experimentally determined parameters were utilized in the predictions.

C.4 Conclusions

In this Appendix, the surface equation of state developed in Chapters 2 and 3 was utilized to predict an interfacial phase transition. This transition will typically occur for a surfactant (or surfactant mixture) where the van der Waals, attractive interactions are relatively strong, or the repulsive, steric and electrostatic interactions are relatively weak, such that the critical temperature is higher than the operating temperature of interest.

A computational method for utilizing the previously developed equation of state, with no additional parameters, was presented, and a comparison between the theoretically predicted and the experimentally measured surface tensions for surfactant solutions that undergo an interfacial phase transition showed reasonable agreement. The surfactant solutions investigated included two linear alkyl alcohols, where the molecular cross-sectional areas are small, and therefore, the attractive, van der Waals interactions are strong and the repulsive steric interactions are weak, thus inducing an interfacial phase transition. In addition, a mixture of an anionic and a cationic

surfactant was investigated. In this case, the two single surfactants do not exhibit an interfacial phase transition because the strong electrostatic, repulsive interactions prevent one from occurring. However, in the case of a binary mixture of these two oppositely-charged surfactants, the electrostatic charges at the interface effectively cancel each other out, leading to an interfacial phase transition. This surfactant mixture is also interesting because of the large extent of interfacial synergism between the two oppositely charged surfactants. Again, this synergism results from the electrostatic charges at the interface effectively canceling each other out, thus allowing the surfactants to more readily adsorb at the interface.

Appendix D

Dynamic Adsorption Behavior of Micellar Solutions

D.1 Introduction

As discussed in Chapters 1 and 2, surfactant molecules can form aggregates, known as micelles, at concentrations above a critical concentration, known as the critical micelle concentration (CMC). In Chapter 5, the dynamic adsorption of surfactants from solutions below the CMC was considered, and therefore, the presence of micelles could be neglected. In this Appendix, the theory developed in Chapter 5 is extended to investigate the effect of micelles on the dynamic surface properties (specifically, on the dynamic air-water surface concentration and the dynamic air-water surface tension) in aqueous surfactant solutions above the CMC. The dynamic surface properties of micellar surfactant solutions have been investigated in the past by several researchers[171–174] (see also Ref. 170 for a recent review). As in the case of the pre-micellar solutions considered in Chapter 5, the central difference between the theory presented in this Appendix and those available in the literature is in the equilibrium adsorption description that forms the underlying basis for the dynamic adsorption theory. For example, Joos[171] and Miller[174] utilized the Langmuir adsorption model, while Fainerman[173] utilized the Frumkin adsorption model, where, as discussed in Chapter 2, these adsorption models contain experimentally determined parameters.

On the other hand, the theoretical framework to model the dynamic adsorption of micellar solutions presented in this Appendix utilizes the equilibrium adsorption description presented in Chapter 2 as its underlying equilibrium basis. As discussed in detail in Chapter 2, a central aspect of this equilibrium adsorption model is that it is based on the molecular characteristics of the surfactants, and hence, it minimizes the number of required experimentally determined parameters. As in Chapter 5, the dynamic adsorption description presented here assumes that the diffusion of the surfactant monomers is the rate limiting step to their subsequent adsorption at the interface. In other words, it is assumed that the surfactant molecules adsorbed at the interface are in instantaneous equilibrium with those in the sublayer (the region of the aqueous phase adjacent to the interface). The micelles affect the surfactant monomer adsorption, and therefore, the dynamic surface tension, by dissociating and supplying more surfactant monomers. In other words, as the surfactant monomers adsorb at the interface, their concentration in the aqueous phase near the interface decreases below the value that corresponds to equilibrium with the micelles. This causes a net break-up of micelles, which, in turn, supplies more surfactant monomers which can then diffuse and adsorb at the interface. In this Appendix, the kinetics of the micelle dissociation process is accounted for by using the theoretical framework developed by Aniansson and Wall,[175] which includes a single rate constant describing the relative rate of micelle dissociation. It will be shown that, if the value of this kinetic rate constant is known, then the dynamic surface tension, as well as the dynamic surface concentration, can be predicted by the theoretical framework presented in this Appendix. Alternatively, if the value of this kinetic rate constant is not known, one can utilize the theoretical framework developed here, along with experimental dynamic surface tension measurements, to estimate the value of the kinetic rate constant.

D.2 Theory

For simplicity, the case of an aqueous solution containing a *single* nonionic surfactant species is considered. As in Chapter 5, it is assumed here that: (i) the interface

is initially clean (that is, that the surface concentration of the surfactant is zero at $t = 0$), (ii) the interface is flat (see Chapter 6 and Refs. 111 and 127 for a detailed treatment of the spherical interface case), and (iii) the mass transport of both the surfactant monomers and the micelles obeys Fickian diffusion.

As discussed in Section D.1, the micelles can dissociate to generate surfactant monomers, while the surfactant monomers can associate to form micelles. To model the kinetics of this dissociation-association process, the theoretical framework developed by Aniansson and Wall[175] will be utilized here. Using this framework, the rate of generation of surfactant monomers from the break-up of micelles, R_1, as a function of the local concentration of surfactant monomers, n_1, and the local concentration of micelles, n_m, for a monodisperse micellar solution (where m is the micelle aggregation number), can be written as follows:

$$R_1 = \mathrm{k_m} \left(\frac{n_{tot}}{n_1^{\mathrm{w}}} \right) (n_1 - n_1^{\mathrm{w}}) \tag{D.1}$$

where $\mathrm{k_m}$ is the micelle kinetic rate constant, $n_{tot} \equiv n_1 + m n_m$ is the total local concentration of surfactant molecules, and n_1^{w} is the equilibrium concentration of surfactant monomers, which is approximately equal to the CMC. Note that n_1, n_m, n_{tot}, and R_1 are all functions of both x and t. Note also that the precise value of n_1^{w} can be obtained using a previously developed molecular-thermodynamic theory of micellization[35–37] (see Chapter 2 for a detailed discussion). Using the surfactant mass conservation condition, the rate of aggregation of micelles, R_m, is given by:

$$R_m = -\frac{R_1}{m} = -\frac{\mathrm{k_m}}{m} \left(\frac{n_{tot}}{n_1^{\mathrm{w}}} \right) (n_1 - n_1^{\mathrm{w}}) \tag{D.2}$$

The overall mass transport of surfactant monomers in the aqueous phase is controlled by the combination of Fickian diffusion and the kinetic generation of surfactant monomers from the break-up of micelles, which is described by the following governing equation:

$$\frac{\partial n_1}{\partial t} = D_1 \frac{\partial^2 n_1}{\partial x^2} + \mathrm{k_m} \left(\frac{n_{tot}}{n_1^{\mathrm{w}}} \right) (n_1 - n_1^{\mathrm{w}}) \tag{D.3}$$

The initial condition for Eq. (D.3) is given by Eq. (5.4), which for the single surfactant solution examined here can be written as follows:

$$n_1\left(t=0,x\right)=n_1^{\mathrm{w}} \tag{D.4}$$

Since the assumption of diffusion controlled adsorption is utilized here, as it was done in Chapter 5, the two boundary conditions for Eq. (D.3) are given by Eqs. (5.5) and (5.7), which for the single surfactant solution examined here can be written as follows:

$$n_1\left(t,x\rightarrow\infty\right)=n_1^{\mathrm{w}} \tag{D.5}$$

and

$$\begin{aligned}\ln\left(\frac{n_1^0}{n_1^0+n_{\mathrm{w}}^0}\right)\approx\ln\left(\frac{n_1^0}{n_{\mathrm{w}}^{\mathrm{w}}}\right) &= \frac{\Delta\mu_1^0}{\mathrm{k_B}T}+\ln\left(\frac{\Gamma_1}{1-\Gamma_1\mathrm{a}_1}\right)+\frac{3\mathrm{a}_1\Gamma_1}{1-\Gamma_1\mathrm{a}_1} \\ &+ \frac{\left(\mathrm{a}_1\Gamma_1\right)^2}{\left(1-\Gamma_1\mathrm{a}_1\right)^2}+2B_{11}\Gamma_1\end{aligned} \tag{D.6}$$

where $n_1^0\equiv n_1\left(x=0\right)$ is the sublayer concentration of surfactant monomers, and $n_{\mathrm{w}}^0\equiv n_{\mathrm{w}}\left(x=0\right)$ is the sublayer concentration of water molecules which is approximately equal to the bulk concentration of water molecules, $n_{\mathrm{w}}^{\mathrm{w}}$, since the surfactant concentration is dilute.

Similarly, the overall mass transport of the micelles in the aqueous phase is controlled by the combination of Fickian diffusion and the kinetic generation of micelles from monomers, which is described by the following governing equation:

$$\frac{\partial n_m}{\partial t}=D_m\frac{\partial^2 n_m}{\partial x^2}-\frac{\mathrm{k_m}}{m}\left(\frac{n_{tot}}{n_m^{\mathrm{w}}}\right)\left(n_1-n_1^{\mathrm{w}}\right) \tag{D.7}$$

The initial condition for Eq. (D.7) can similarly be written as follows:

$$n_m\left(t=0,x\right)=n_m^{\mathrm{w}} \tag{D.8}$$

where n_m^{w} is the equilibrium concentration of micelles in the bulk aqueous solution. The first boundary condition for Eq. (D.7) is obtained by requiring the concentration of micelles to approach the bulk equilibrium concentration far from the interface. Specifically,

$$n_m\left(t, x \to \infty\right) = n_m^{\mathrm{w}} \tag{D.9}$$

The second boundary condition for Eq. (D.7) is obtained by assuming that the micelles themselves do no adsorb at the interface. This leads to a vanishing flux at the interface which can be expressed as follows:

$$\left.\frac{\partial n_m}{\partial x}\right|_{x=0} = 0 \tag{D.10}$$

Finally, as in Chapter 5, the governing equation for the interface can be derived from the conservation of mass as follows:

$$\frac{\partial \Gamma_1}{\partial t} = D_1 \left.\frac{\partial n_1}{\partial x}\right|_{x=0} \tag{D.11}$$

As in Chapter 5, the initial condition for Eq. (D.11) is derived from the fact that the interface is initially free of surfactant molecules. Specifically,

$$\Gamma_1\left(t = 0\right) = 0 \tag{D.12}$$

Next, the set of three coupled differential equations given by Eqs. (D.3), (D.7), and (D.11), along with the boundary and initial conditions given above, can be solved numerically (see Ref. 48) to obtain the two bulk concentration profiles, $n_1\left(t, x\right)$ and $n_m\left(t, x\right)$, as well as the surfactant surface concentration profile, $\Gamma_1\left(t\right)$. Finally, the surface tension as a function of time, $\sigma\left(t\right)$, can be computed from the surfactant surface concentration profile, $\Gamma_1\left(t\right)$, by utilizing the surface equation of state developed in Chapter 2, which for the single nonionic surfactant case considered here can be

written as follows:

$$\sigma(t) = \sigma_0 - k_B T \left\{ \frac{\Gamma_1(t)}{1 - \Gamma_1(t) a_1} + \frac{a_1 (\Gamma_1(t))^2}{(1 - \Gamma_1(t) a_1)^2} + B_{11} (\Gamma_1(t))^2 \right\} \tag{D.13}$$

where σ_0 is the surface tension of pure water. A discussion of the values of the various molecular parameters appearing in the theoretical framework developed in this section, along with an illustrative example, are presented in the next section.

D.3 Results and Discussion

The values of the surfactant molecular parameters, a_i, r_i, and B_{ii}, can be determined from the chemical structure of the surfactant. The value of the standard-state chemical potential difference, $\Delta\mu_i^0$, can be determined from a single surface tension measurement (see Chapter 2 for a detailed discussion). The value of the diffusion coefficient of the surfactant monomer, D_1, can be determined experimentally from the measured dynamic surface tension profile of a surfactant solution below the CMC, or it can be estimated theoretically using the Wilke-Chang model[136] (see Chapter 5 for a detailed discussion). The value of the diffusion coefficient of the micelles, D_m, can be estimated theoretically using the Wilke-Chang model,[136] along with the bulk molecular-thermodynamic theory of micellization to determine the micelle aggregation number, m.[35–37] It should be noted that the predicted dynamic surface tension profiles are extremely insensitive to the precise value of the micelle diffusion coefficient, D_m (see Chapter 6 for a discussion of the sensitivity to the surfactant monomer diffusion coefficient, D_1).

If one had a method for measuring, or predicting, the micelle kinetic rate constant, k_m, one could predict the dynamic surface tension profile of a micellar solution using the theoretical framework described in Section D.2. Alternatively, one can measure the dynamic surface tension of a micellar solution and then adjust the value of k_m, such that the theoretically predicted dynamic surface tension matches the experimentally measured values. In other words, one could use dynamic surface tension

measurements, in the context of the theoretical framework developed in Section D.2, to effectively measure the value of k_m. This should be of great value, since it is generally easier to measure the dynamic surface tension than to measure the value of k_m directly.[170]

To demonstrate that it is indeed possible to deduce the value of k_m using the method outlined above, the following illustrative example is provided using the previously examined nonionic surfactant $C_{12}E_5$ (see Chapter 6). The values of the various $C_{12}E_5$ molecular parameters are given in Table 6.1. The value of the monomer diffusion coefficient utilized here is the fitted value of $6.5 \times 10^{-6} cm^2/s$. The CMC was predicted using Program PREDICT[53] to be $5 \times 10^{-8} mol/cm^3$, which also predicted a micelle aggregation number, m, of 3600. This value of the micelle aggregation number was then utilized in the Wilke-Chang model to predict a micelle diffusion coefficient of $D_m = D_1 \left(\tilde{V}_1/\tilde{V}_m\right)^{0.6} = D_1 (1/m)^{0.6} = 4.8 \times 10^{-8} cm^2/s$. Note again, that the surface tension predictions are extremely insensitive to the precise value of D_m. Indeed, changing D_m by $\pm 50\%$ has little effect on the predicted dynamic surface tensions.

Figure D-1 shows the predicted dynamic surface tensions for aqueous solutions of $C_{12}E_5$ at a concentration of ten times the CMC ($5 \times 10^{-7} mol/cm^3$). The three curves are the predicted dynamic surface tensions corresponding to k_m values of: $10 s^{-1}$ (———), $1.0 s^{-1}$ (- – - – -), and $0.1 s^{-1}$ (— — —). Note that the dynamic surface tension is indeed quite sensitive to the parameter k_m, and that the differences between the predicted dynamic surface tension curves are experimentally measurable. Note, however, that the timescales for these surface tension curves to reach equilibrium adsorption are extremely short (less than a second). Therefore, as discussed in more detail in Section D.4, the adsorption of the surfactant molecules may not be diffusion controlled, and therefore, a kinetic barrier would need to be incorporated in the theoretical framework developed in Section D.2 in order to make a meaningful comparison with actual experimental dynamic surface tension measurements.

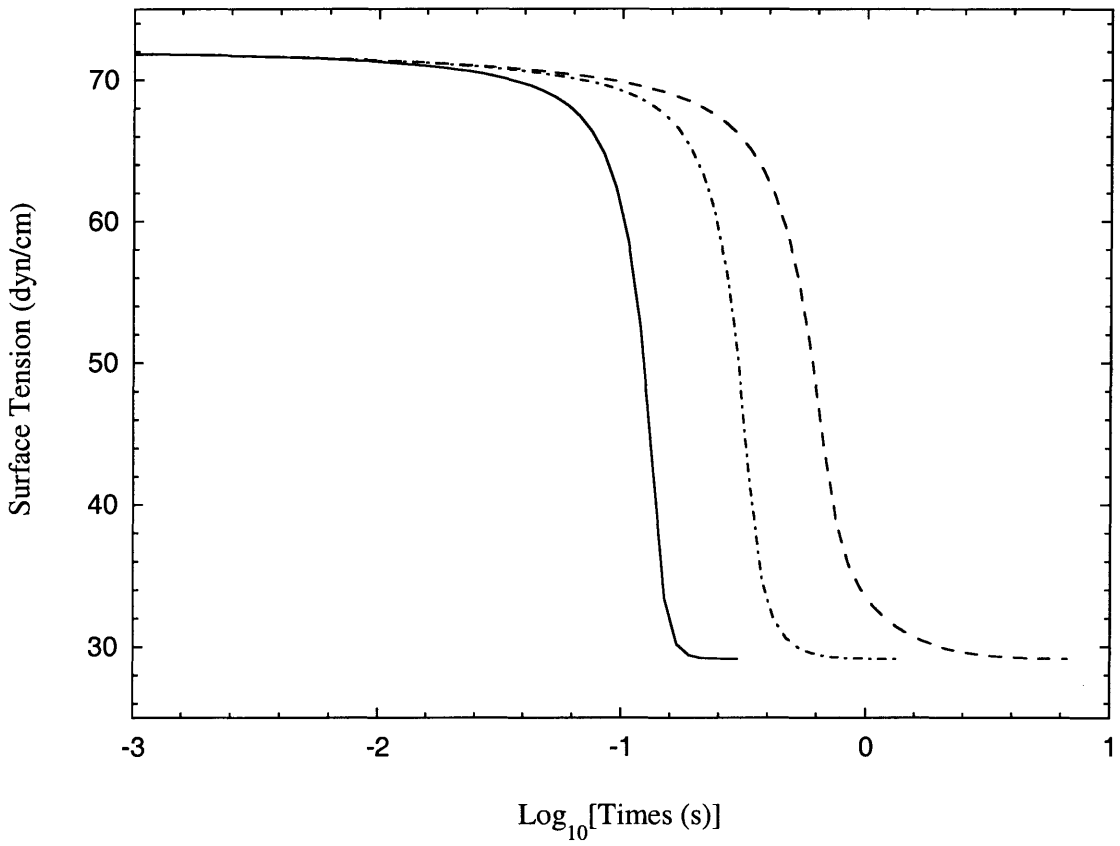

Figure D-1: Theoretically predicted surface tensions as a function of time for a micellar solution of $C_{12}E_5$ at a concentration of ten times the CMC ($5 \times 10^{-7} mol/cm^3$) at 25°C. The three curves are the predicted dynamic surface tensions corresponding to k_m values of: $10s^{-1}$ (———), $1.0s^{-1}$ (- — - — -), and $0.1s^{-1}$ (— — —).

D.4 Conclusions

In this Appendix, a theoretical framework was developed to model the diffusion controlled adsorption of surfactants at the air-water interface of an aqueous surfactant solution above the CMC. This Appendix is an extension of the theoretical framework developed in Chapter 5 for surfactant solutions below the CMC. The effect of micelles is incorporated in the theoretical framework by including a source of surfactant monomers in the governing equation for the transport of surfactant monomers in the aqueous phase that arises from the dissociation of the micelles. Since the rate of micelle dissociation depends on the local concentration of micelles, the dynamic concentration profile of the micelles in the aqueous phase is also required, and is obtained by utilizing a Fickian diffusion model. The main difference between the diffusion of the monomers and the micelles is that the micelles are assumed not to adsorb at the interface (leading to a zero flux of micelles at the interface). In Section D.3, it was shown that the predicted dynamic surface tension is indeed sensitive to the kinetic rate constant of micelle dissociation, k_m (see Figure D-1). Therefore, one could use the theoretical framework presented here, along with an experimentally measured dynamic surface tension profile of a surfactant solution above the CMC, to deduce the value of the kinetic rate constant of micelle dissociation.

As in Chapter 5, it was assumed in this Appendix that the diffusion of surfactant monomers is slow enough that it represents the rate limiting step to adsorption. In other words, although there may be a kinetic barrier to adsorption at the interface, the kinetic rate of adsorption is fast enough that the surfactant monomers at the interface are in instantaneous equilibrium with the surfactant monomers in the sublayer. While this was shown (see Chapter 6) to be a valid assumption for the relatively dilute pre-micellar solutions considered in Chapter 5 (see Chapter 6), it may not necessarily be a valid assumption in the case of the relatively concentrated micellar solutions considered here. Indeed, since the timescale for diffusion decreases as the surfactant concentration increases (see Chapter 5), one expects a shift in the controlling adsorption mechanism from diffusion controlled, to mixed kinetic-diffusion

controlled, as the surfactant concentration increases.[116–118] Therefore, as discussed in Section 8.2, an interesting area of future research could involve the incorporation of a kinetic barrier to the theoretical framework presented in Section D.2.

Bibliography

[1] E.H. Lucassen-Reynders. Adsorption at fluid interfaces. In E.H. Lucassen-Reynders, editor, *Anionic Surfactants*, chapter 1, pages 1–54. Marcel Dekker: New York, 1981.

[2] L. Thompson. The role of oil detachment mechanisms in determining optimum detergency conditions. *J. Colloid Interface Sci.*, 163:61–73, 1994.

[3] E.M. Kirschner. Soaps and detergents. *Chemical and Engineering News*, 75:30, 1997.

[4] S. Verma and V.V. Kumar. Relationship between oil-water interfacial tension and oily soil removal in mixed surfactant systems. *J. Colloid Interfacial Sci.*, 207:1–10, 1998.

[5] S.S. Dukhin, C. Kretzschmar, and R. Miller. *Dynamics of Adsorption at Liquid Interfaces.* Elsevier:Amsterdam, 1995.

[6] R.M. Giordano and J.C. Slattery. Interfacial phenomena in enhanced oil recovery. In *AIChE Symposium Series*, volume 212, page 120. 1982.

[7] J.E. Puig, L.E. Scriven, H.T. Davis, and W.G. Miller. Interfacial phenomena in enhanced oil recovery. In *AIChE Symposium Series*, volume 212, page 1. 1982.

[8] J.C. Noronha and D.O. Shah. Interfacial phenomena in enhanced oil recovery. In *AIChE Symposium Series*, volume 212, page 42. 1982.

[9] V.B. Fainerman, S.R. Khodos, and L.N. Lomazova. Generation of finely dispersed foam. *Colloid J. USSR*, 53:592–597, 1991.

[10] J.J. Bikerman. *Foams.* Springer-Verlag:New York, 1973.

[11] P.M. Holland. Mixed surfactant systems, an overview. In P.M. Holland and D.N. Rubingh, editors, *Mixed Surfactant Systems*, chapter 1, pages 2–30. American Chemical Society: Washington, DC, 1992.

[12] Y.J. Nikas, S. Puvvada, and D. Blankschtein. Surface tensions of aqueous nonionic surfactant mixtures. *Langmuir*, 8:2680–2697, 1992.

[13] Chein-Hsiang Chang and E. I. Franses. Adsorption dynamics of surfactants at the air/water interface: A critical review of mathmatical models, data, and mechanisms. *Colloids and Surfaces A*, 100:1–45, 1995.

[14] D.K. Chattoraj and K.S. Birdi. *Adsorption and the Gibbs Surface Excess*, chapters 3–5. Plenum Press:New York, 1984.

[15] S. Bae, M. Harke, A. Goebel, K. Lunkenheimer, and H. Motschmann. A critical comparison of adsorption models for soluble surfactants. *Langmuir*, 13:6274–6278, 1997.

[16] V.V. Kalinin and C.J. Radke. An ion-binding model for ionic surfactant adsorption at aqueous-fluid interfaces. *Colloids and Surfaces A*, 114:337–350, 1996.

[17] K. Lunkenheimer and R. Hirte. Another approach to a surface equation of state. *J. Phys. Chem.*, 96:8683–8686, 1992.

[18] C. Kemball, E.K. Rideal, and E.A. Guggenheim. Thermodynamics of monolayers. *Trans. Faraday Soc.*, 44:948–954, 1948.

[19] E.I. Franses, F.A. Siddiqui, D.J. Ahn, C.H. Chang, and N.H. Wang. Thermodynamically consistent equilibrium adsorption isotherms for mixtures of different-size molecules. *Langmuir*, 11:3177–3183, 1995.

[20] A.L. Myers and J.M. Prausnitz. Thermodynamics of mixed gas adsorption. *AIChE J.*, 11:121–127, 1965.

[21] B.T. Ingram. Surface tensions of non-ideal surfactant mixtures. *Colloid and Polym. Sci.*, 258:191–193, 1980.

[22] M.J. Rosen and X.Y. Hua. Surface concentrations and molecular-interactions in binary-mixtures of surfactants. *J. Colloid Interface Sci.*, 86:164–172, 1982.

[23] M.J. Rosen. Synergism in binary mixtues of surfactants at various interfaces. In P.M. Holland and D.N. Rubingh, editors, *Mixed Surfactant Systems*, chapter 21, pages 317–401. American Chemical Society: Washington, DC, 1992.

[24] P.M. Holland. Nonideality at the interface in mixed micellar systems. *Colloids and Surfaces*, 19:171–183, 1986.

[25] C.M. Nguyen and J.F. Scamehorn. Thermodynamics of mixed monolayer formation at the air water interface. *J. Colloid Interface Sci.*, 123:238–248, 1988.

[26] E.H. Lucassen. Interactions in mixed monolayers. 1. Assessment of interaction between surfactants. *J. Colloid Interface Sci.*, 42:554–562, 1973.

[27] F.A. Siddiqui and E.I. Franses. Equilibrium adsorption and tension of binary surfactant mixtures at the air/water interface. *Langmuir*, 12:354–362, 1996.

[28] J.T. Davies. The distribution of ions under a charged monolayer, and a surface equation of state for charged films. *Proc. Roy. Soc. Ser. A*, 208:224–247, 1951.

[29] P.M. Gouy. On the constitution of the electric charge on the surface on an electrolyte. *J. Phys. (Paris)*, 9:457, 1910.

[30] D.L. Chapman. *J. Phys. Radium*, 25:475, 1913.

[31] R. P. Borwankar and D. T. Wasan. The kinetics of adsorption of ionic surfactants at gas-liquid surfaces. *Chem. Eng. Sci.*, 41:199–201, 1986.

[32] O. Stern. *Elektrochem*, 30:508, 1924.

[33] P. Warszynski, W. Barzyk, K. Lunkenheimer, and H. Fruhner. Surface tension and surface potential of Na n-dodecyl sulfate at the air-solution interface: Model and experiment. *J. Phys. Chem.*, 102:10984–10957, 1998.

[34] R. Defay, I. Prigogine, and A. Bellemans. *Surface Tension and Adsorption.* Longmans: Bristol, 1966.

[35] S. Puvvada and D Blankschtein. Thermodynamic description of micellization, phase-behavior, and phase-separation of aqueous-solutions of surfactant mixtures. *J. Phys. Chem.*, 96:5567–5579, 1992.

[36] A. Shiloach and D. Blankschtein. Predicting micellar solution properties of binary surfactant mixtures. *Langmuir*, 14:1618–1636, 1998.

[37] A. Shiloach and D. Blankschtein. Measurement and prediction of ionic/nonionic mixed micelle formation and growth. *Langmuir*, 14:7166–7182, 1998.

[38] J.C. Eriksson and S. Ljunggren. A molecular theory of the surface tension of surfactant solutions. *Colloids and Surfaces*, 38:179–203, 1989.

[39] B.Q. Li and E. Ruckenstein. Adsorption of ionic surfactants on charged solid surfaces from aqueous solutions. *Langmuir*, 12:5052–5063, 1996.

[40] L. Salem. Attractive forces between long saturated chains at short distances. *J. Chem. Phys.*, 37:2100–2105, 1962.

[41] D.K. Chattoraj and K.S. Birdi. *Adsorption and the Gibbs Surface Excess*, chapter 3. Plenum Press:New York, 1984.

[42] S. Hachisu. Equation of state of ionized monolayers. *J. Colloid and Interface Sci.*, 33:445–463, 1970.

[43] W.T. Tester and M. Modell. *Thermodynamics and its Applications.* Prentice Hall: New Jersey, 1996.

[44] J.T. Davies and E.K. Rideal. *Interfacial Phenomena.* Academic Press: New York, 1963.

[45] E.M. Purcell. *Electricity and Magnetism.* McGraw-Hill: New York, 1985.

[46] E.J.W Verwey and J.T.G. Overbeek. *Theory of the Stability of Lyophobic Colloids.* Elsevier: New York, 1948.

[47] J.O.M. Bockris and A.K.N. Reddy. *Modern Electrochemistry*, volume 1. Plenum Press: New York, 1970.

[48] W.H. Press, B.P. Flannery, S.A. Teukolsky, and W.T. Vetterling. *Numerical Recipes.* Cambridge University Press: Cambridge, 1986.

[49] C. Dupuy, X. Auvray, and C. Petipas. Anomeric effects on the structure of micelles of alkyl maltosides in water. *Langmuir*, 12:3965–3967, 1997.

[50] A. Shiloach. *Theoretical Prediction and Experimental Measurement of Micellar Solution Properties of Surfactant Mixtures.* PhD thesis, Massachusettes Institute of Technology, 1998.

[51] C.J. Drummond, F. Grieser, and T.W. Healy. Effect of electrolyte on the mean interfacial solvent and electrostatic characteristics of cationic micelles. *Chem Phys Letters*, 140:493–498, 1987.

[52] J.D. Hines, R.K. Thomas, P.R. Garrett, G.K. Rennie, and J. Penfold. Investigation of mixing in binary surfactant solutions by surface tension and neutron reflection: Anionic/nonionic and zwitterionic/nonionic mixtures. *J. Phys. Chem. B*, 101:9215, 1997.

[53] N. Zoeller. *Theoretical and Experimental Investigations of Electrostatic Effects Associated with Ionic Surfactant Micelles.* PhD thesis, Massachusettes Institute of Technology, 1998.

[54] J. Penfold, E. Staples, L. Thompson, and I. Tucker. The composition of nonionic surfactant mixtures at the air/water interface as determined by neutron reflectivity. *Colloids and Surfaces A*, 102:127–132, 1995.

[55] J. Garcia Dominguez, F. Balaguer, J.L. Parra, and C.M. Pelejero. The inhibitory effect of some amphoteric surfactants on the irritation potential of alkylsulfates. *International Journal of Cosmetic Science*, 3:57–68, 1981.

[56] J.D. Hines, R.K. Thomas, P.R. Garrett, G.K. Rennie, and J Penfold. Investigation of mixing in binary surfactant solutions by surface tension and neutron reflection: Strongly interacting anionic/zwitterionic mixtures. *J. Phys. Chem. B*, 102:8834–8846, 1998.

[57] J.T. Davies. A surface equation of state for charged monolayers. *J. Colloid Sci.*, 11:377–390, 1956.

[58] R.P. Borwanker and D.T. Wasan. Equilibrium and dynamics of adsorption of surfactants at fluid-fluid interfaces. *Chem. Eng. Sci.*, 43:1323–1337, 1988.

[59] C.A. Coulson. *Electricity.* Oliver & Boyd: Edinburg, 1965.

[60] B. Abraham-Shrauner. Generalized Gouy-Chapman potential of charged phospholipid membranes with divalent cations. *J. Math. Biol.*, 2:333–339, 1975.

[61] B. Abraham-Shrauner. Erratum for generalized Gouy-Chapman potential of charged phospholipid membranes with divalent cations. *J. Math. Biol.*, 4:201, 1977.

[62] Inc ChemSW. Molecular modeling pro., 1992.

[63] J.D. Hines, R.K. Thomas, P.R. Garrett, G.K. Rennie, and J. Penfold. A study of the interactions in a ternary surfactant system in micelles and adsorbed layers. *J. Phys. Chem. B*, 102:9708, 1998.

[64] V.B. Fainerman, A.V. Makievski, and R. Miller. Surfactant adsorption isotherms considering molecular reorientation or aggregation at liquid/fluid interfaces. *Rev. Chem. Eng.*, 14:373–409, 1998.

[65] F. Ravera, M. Ferrari, and L. Liggieri. Adsorption and partitioning of surfactants in liquid-liquid systems. *Adv. Colloid Interface Sci.*, 88:129–177, 2000.

[66] F. Ravera, M. Ferrari, L. Liggieri, R. Miller, and A. Passerone. Measurement of the partition coefficient of surfactants in water/oil systems. *Langmuir*, 13:4817–4820, 1997.

[67] M. Ferrari, L. Liggieri, F. Ravera, C. Amodio, and R. Miller. Adsorption kinetics of alkylphosphine oxides at water/hexane interface: 1. Pendant drop experiments. *J. Colloid Interface Sci.*, 186:40–45, 1997.

[68] L. Liggieri, F. Ravera, and A. Passerone. Equilibrium interfacial tension of hexane/water plus Triton X-100. *J. Colloid Interface Sci.*, 169:238–240, 1995.

[69] M.J. Rosen and D.S. Murphy. Effect of the nonaqueous phase on the interfacial properties of surfactants. 2. Individual and mixed nonionic surfactants in hydrocarbon/water systems. *Langmuir*, 7:2630–2635, 1991.

[70] V.B. Fainerman, S.A. Zholob, and R. Miller. Adsorption kinetics of oxyethylated polyglycol ethers at the water-nonane interface. *Langmuir*, 13:283–289, 1997.

[71] F.K. Hansen and H. Fagerheim. The influence of oil phase on the adsorption of non-ionic surfactants investigated by the automatic sessile drop method. *Colloids and Surfaces A*, 137:217–230, 1998.

[72] M.W. Vaughn and J.C. Slattery. A surface equation of state for a partially soluble ionized surfactant. *J. Colloid Interface Sci.*, 195:1–7, 1997.

[73] V.B. Fainerman, R. Miller, and R. Wustneck. Adsorption isotherm and surface tension equation for a surfactant with changing partial molar area. 1. Ideal surface layer. *J. Phys. Chem.*, 100:7769–7675, 1996.

[74] V.B. Fainerman, R. Miller, and R. Wustneck. Adsorption isotherm and surface tension equation for a surfactant with changing partial molar area. 2. Nonideal surface layer. *J. Phys. Chem.*, 101:6479–6483, 1997.

[75] M. Ferrari, L. Liggieri, and F. Ravera. adsorption properties of $C_{10}E_8$ at the water-hexane interface. *J. Phys. Chem. B*, 102:10521–10527, 1998.

[76] V.B. Fainerman and R. Miller. Surface tension isotherms for surfactant adsorption layers including surface aggregation. *Langmuir*, 12:6011–6014, 1996.

[77] R. Miller, K. Lunkenheimer, and G. Kretzschmar. Model for diffusion-controlled adsorption of surfactant mixtures at liquid-phase boundaries. *Colloid Polym. Sci.*, 257:1118–1120, 1979.

[78] E.H. Lucassen-Reynders. Competitive adsorption of emulsifyers 1. Therory for adsorption of small and large molecules. *Colloids and Surfaces A*, 91:79–88, 1994.

[79] J.R. Campanelli and X. Wang. Dynamic interfacial tension of surfactant mixtures at liquid-liquid interfaces. *J. Colloid Interface Sci.*, 213:340–351, 1999.

[80] E. Staples, L. Thompson, I. Tucker, J. Penfold, R.K. Thomas, and J.R. Lu. Surface-composition of mixed surfactant monolayers at concentrations well in excess of the critical micelle concentration - A neutron-scattering study. *Langmuir*, 9:1651–1656, 1993.

[81] J. Chatterjee and D.T. Wasan. An interfacial tension model for mixed adsorbed layer for a ternary system - Application to an acidic oil/alkali/surfactant system. *Colloids and Surfaces A*, 132:107–125, 1998.

[82] R. Aveyard, B.P. Binks, P.D.I. Fletcher, and J.R. MacNab. Interaction of alkanes with monolayers on nonionic surfactants. *Langmuir*, 11:2515–2524, 1995.

[83] M.J. Rosen, J.H. Mathias, and L. Davenport. Aberrant aggregation behavior in cationic gemini surfactants investigated by surface tension, interfacial tension, and fluorescence methods. *Langmuir*, 15:7340–7346, 1999.

[84] L. Liggieri, F. Ravera, M. Ferrari, A. Passerone, and R. Miller. Adsorption kinetics of alkylphosphine oxides at water/hexane interface: 2. Theory of the

adsorption with transport across the interface in finite systems. *Langmuir*, 186:46–52, 1997.

[85] M.J. Rosen, Z.H. Zhu, B. Gu, and D.S. Murphy. Relationship of structure to properties of surfactants. 14. Some n-alkyl-2-pyrrolidones at various interfaces. *Langmuir*, 4:1273–1277, 1988.

[86] E.-M. Kutschmann, G.H. Findenegg, D. Nickel, and W. von Rybinski. Interfacial tension of alkylglucosides in different APG/oil/water systems. *Colloid Polym. Sci.*, 273:565–571, 1995.

[87] M. Mulqueen and D. Blankschtein. Theoretical and experimental investigation of the equilibrium oil-water interfacial tensions of solutions containing surfactant mixtures. *Submitted to Langmuir.*

[88] M. Mulqueen and D. Blankschtein. Prediction of equilibrium surface tension and surface adsorption of aqueous surfactant mixtures containing ionic surfactants. *Langmuir*, 15:8832, 1999.

[89] M. Mulqueen and D. Blankschtein. Prediction of equilibrium surface tension and surface adsorption of aqueous surfactant mixtures containing zwitterionic surfactants. *Langmuir*, 16:7640, 2000.

[90] D.K. Chattoraj and K.S. Birdi. *Adsorption and the Gibbs Surface Excess*, chapter 5. Plenum Press:New York, 1984.

[91] E.H. Lucassen-Reynders. Surface equation of state for ionized surfactants. *J. Phys. Chem.*, 70:1777–1785, 1966.

[92] E.H. Crook, D.B. Fordyce, and G.F. Trebbi. Molecular weight distribution of nonionic surfactants. I. Surface and interfacial tension of normal distribution and homogenious p,t-octylphenoxyethoxyethanols. *J. Phys. Chem.*, 67:1987–1994, 1963.

[93] A.W. Adamson and A.P. Gast. *Physical Chemistry of Surfaces.* Wiley:New York, 1997.

[94] W.D. Harkins and H.F. Jordan. A method for the determination of surface and interfacial tension from the maximum pull on a ring. *J. Am. Chem. Soc.*, 52:1751–1772, 1930.

[95] V Pillai and D.O Shah. *Dynamic Properties of Interfaces and Associated Structures.* AOCS:Champaign, Illinois, 1996.

[96] A.F.H. Ward and L. Tordai. Time-dependence of boundary tension of solutions. I. The role of diffusion in time-effects. *J. Chem. Phys.*, 14:453–461, 1946.

[97] R. Miller, P. Joos, and V. B. Fainerman. Dynamic surface and interfacial tensions of surfactant and polymer solutions. *Adv. Colloid Interface Sci.*, 49:249–302, 1994.

[98] J. Eastoe and J.S. Dalton. Dynamic surface tension and adsorption mechanisms of surfactants at the air-water interface. *Adv. Colloid Interface Sci.*, 85:103–144, 2000.

[99] K. L. Sutherland. Kinetics of adsorption at liquid surfaces. *Austr. J. Sci. Res. A*, 5:683–696, 1952.

[100] R. S. Hansen. The theory of diffusion controlled adsorption kinetics with accompanying evaporation. *J. Phys. Chem.*, 64:637–641, 1960.

[101] R. Miller and K. Lunkenheimer. Adsorption kinetics on fluid phase boundaries - numerical-solution for diffusion controlled adsorption process. *Z. Phys. Chem.*, 259:863–868, 1978.

[102] R. Miller. On the solution of diffusion controlled adsorption kinetics for any adsorption isotherms. *Colloid Polymer Sci.*, 259:375–381, 1981.

[103] K. J. Mysels. Diffusion controlled adsorption kinetics, general solution and some applications. *J. Phys. Chem.*, 86:4648–4651, 1982.

[104] G. Kretzschmar and R Miller. Dynamic properties of adsorption layers of amphiphilic substances at fluid interfaces. *Adv. Colloid Interface Sci.*, 36:65–124, 1991.

[105] S.-Y. Lin, K. McKeigue, and C. Maldarelli. Diffusion controlled surfactant adsorption studied by pendant drop digitation. *AIChE J.*, 36:1785–1795, 1990.

[106] C.-T. Hsu, M.-J. Shao, and S.-Y Lin. Adsorption kinetics of $C_{12}E_4$ at the air-water interface: Adsorption onto a fresh interface. *Langmuir*, 16:3187–3194, 2000.

[107] D. O. Johnson and K. J. Stebe. Experimental confirmation of the oscillating bubble technique with comparison to the pendant bubble method: The adsorption dynamics of 1-decanol. *J. Colloid Interface Sci.*, 182:526–538, 1996.

[108] J. F. Baret. Kinetics of adsorption from a solution: Role of diffusion and of the adsorption-desorption antagonism. *J. Phys. Chem.*, 72:2755–2758, 1968.

[109] J. F. Baret. Theoretical model for an interface allowing a kinetic study of adsorption. *J. Colloid Interface Sci.*, 30:1–12, 1969.

[110] R. P. Borwankar and D. T. Wasan. The kinetics of adsorption of surface-active agents at gas-liquid surfaces. *Chem. Eng. Sci.*, 38:1637–1649, 1983.

[111] S.-Y. Lin, K. McKeigue, and C. Maldarelli. Effect of cohesive energies between adsorbed molecules on surfactant exchange processes - shifting from diffusion control for adsorption to kinetic-diffusive control for re-equilibration. *Langmuir*, 10:3442–3448, 1994.

[112] F. Ravera, L. Liggieri, and A Steinchen. Sorption kinetics considered as a renormalized diffusion process. *J. Colloid Interface Sci.*, 156:109–116, 1993.

[113] R. S. Hansen. Diffusion and the kinetics of adsorption of aliphatic acids and alcohols at the water-air interface. *J. Colloid Sci.*, 16:549–560, 1961.

[114] C. Tsonopoulos, J. Newmann, and J. M. Prausnitz. Rapid aging and dynamic surface tension of dilute aqueous solutions. *Chem. Eng. Sci.*, 26:817–827, 1971.

[115] H. Diamant and D. Andelman. Kinetics of surfactant adsorption at fluid-fluid interfaces. *J. Phys. Chem.*, 100:13732–13742, 1996.

[116] J. K. Ferri and K. J. Stebe. Which surfactants reduce surface tension faster? A scaling argument for diffusion-controlled adsorption. *Adv. Colloid Interface Sci.*, 85:61–97, 2000.

[117] R. Pan, J. Green, and C. Maldarelli. Theory and experiment on the measurement of kinetic rate constant for surfactant exchange at an air water interface. *J. Colloid Interface Sci.*, 205:213–230, 1998.

[118] C. Dong, C.-T. Hsu, C.-H. Chiu, and S.-Y Lin. A study on surfactant adsorption kinetics: Effect of bulk concentration on the limiting adsorption rate constant. *Langmuir*, 16:4573–4580, 2000.

[119] V. B. Fainerman and R. Miller. Dynamic surface tensions of surfactant mixtures at the water-air interface. *Colloids and Surfaces A*, 97:65–82, 1995.

[120] V. B. Fainerman and R. Miller. Anamolous dynamic surface tension of mixtures of nonionic surfactants with different partial molar areas at the water-air interface. *Langmuir*, 13:409–413, 1997.

[121] F. A. Siddiqui and E. I. Franses. Dynamic adsorption and tension of nonionic binary surfactant mixture. *AIChE J.*, 43:1569–1578, 1997.

[122] G. Ariel, H. Diamant, and D. Andelman. Kinetics of surfactant adsorption at fluid-fluid interfaces: Surfactant mixtures. *Langmuir*, 15:3574–3581, 1999.

[123] M. Mulqueen and D. Blankschtein. Dynamic interfacial adsorption in aqueous surfactant mixtures: Theoretical study. *Langmuir, in press.*

[124] C. A. MacLeod and C. J. Radke. A growing drop technique for measuring dynamic interfacial-tension. *J. Colloid Interface Sci.*, 160:435–448, 1993.

[125] K.D Danov, P.M. Vlahovska, P.A. Kralchevsky, G. Broze, and A Mehreteab. Adsorption kinetics of ionic surfactants with detailed account for the electrostatic interactions: Effect of the added electrolyte. *Colloids and Surfaces, A*, 156:3389–411, 1999.

[126] R.B. Bird, W.E. Stewart, and E.N. Lightfoot. *Transport Phenomena.* Wiley:New York, 1960.

[127] J. K. Ferri and K. J. Stebe. A structure property study of the dynamic surface tension of three acetylenic diol surfactants. *Colloids and Surfaces A*, 156:567–577, 1999.

[128] R. Miller. Adsorption kinetics of surfactants from micellar solutions. *Colloid Polymer Sci.*, 259:1124–1128, 1981.

[129] R. S. Hansen and T. C. Wallace. The kinetics of adsorption of organic acids at the water-air interface. *J. Phys. Chem.*, 63:1085–1091, 1959.

[130] P.M. Holland. Nonideality at interfaces in mixed surfactant systems. In P.M. Holland and D.N. Rubingh, editors, *Mixed Surfactant Systems*, chapter 22, pages 327–341. American Chemical Society: Washington, DC, 1992.

[131] M.J. Rosen. *Surfactants and Interfacial Phenomena.* Wiley:New York, 1978.

[132] C. A. MacLeod and C. J. Radke. Charge effects in the transient adsorption of ionic surfactants at fluid interfaces. *Langmuir*, 10:3555–3566, 1994.

[133] V. B. Fainerman, A. V. Makievski, and R. Miller. The analysis of dynamic surface tension of sodium alkyl sulphate solutions, based on asymptotic equations of adsorption kinetic theory. *Colloids and Surfaces A*, 87:61–75, 1994.

[134] M. Mulqueen and D. Blankschtein. Dynamic surface tensions of aqueous surfactant mixtures: Experimental investigation. *Submitted to Langmuir.*

[135] S.-Y Lin, H.-C. Chang, and E.-M. Chen. The effect of bulk concentration on surfactant adsorption processes: The shift from diffusion-control to mixed

kinetic diffusion control with bulk concentration. *J. Chem. Eng. Japan*, 29:634–641, 1996.

[136] C.R. Wilke and P. Chang. Correlation of diffusion coefficients in dilute solutions. *A.I.Ch.E. J.*, 1:264–270, 1955.

[137] M. Schonhoff and O. Soderman. PFG-NMR diffusion as a method to investigate the equilibrium adsorption dynamics of surfactants at the solid/liquid interface. *J. Phys. Chem. B*, 101:8237–8242, 1997.

[138] E. Kissa. *Fluorinated Surfactants.* Dekker:New York, 1993.

[139] T. Takiue, T. Fukuta, H. Matsubara, N. Ikeda, and M. Aratono. Thermodynamic study on phase transition in adsorbed film of fluoroalkanol at the hexane/water interface. 8. phase transition and miscibility in the adsorbed film of fluoroalkanol mixture. *J. Phys. Chem. B.*, 105:789–795, 2001.

[140] H.J. Lehmler, M. Jay, and P.M. Bummer. Mixing of partially fluorinated carboxylic acids and their hydrocarbon analogues with dipalmitoylphosohatidylcholine at the air-water interface. *Langmuir*, 16:10161–10166, 2000.

[141] T. Yamabe, Y. Moroi, Y. Abe, and T. Takahasi. Micelle formation and surface adsorption of n-(1,1-dihydroperfluoroalkyl)-n,n,n-trimethylammonium chloride. *Langmuir*, 16:9754–9758, 2000.

[142] E. Ruckenstein and B.Q. Li. A surface equation of state based on clustering of surfactant molecules of insoluble monolayers. *Langmuir*, 11:3510–3515, 1995.

[143] J. Isrealachvili. Self-assembly in two dimensions: Surface micelles and domain formation in monolayers. *Langmuir*, 10:3774–3781, 1994.

[144] I.C. Sanchez. *Physics of Polymer Surfaces and Interfaces.* Manning: Greenwich, 1992.

[145] I.D. Robb. Polymer/surfactant interactions. In E.H. Lucassen-Reynders, editor, *Anionic Surfactants*, chapter 3, pages 109–142. Marcel Dekker: New York, 1981.

[146] Y.J. Nikas and D. Blankschtein. Complexation of nonionic polymers and surfactants in dilute aqueous solutions. *Langmuir*, 10:3512–3528, 1994.

[147] L. Liggieri, F. Ravera, M. Ferrari, A. Passerone, and R. Miller. Adsorption kinetics of alkylphosphine oxides at water/hexane interface: 2. Theory of the adsorption with transport across the interface in a finite system. *J. Colloid Interface Sci.*, 186:46–52, 1997.

[148] J. Lucassen. Dynamic properties of free liquid films and foams. In E.H. Lucassen-Reynders, editor, *Anionic Surfactants*, chapter 6, pages 217–266. Marcel Dekker: New York, 1981.

[149] M.J. Schwuger. Effects of adsorption on detergency. In E.H. Lucassen-Reynders, editor, *Anionic Surfactants*, chapter 7, pages 267–316. Marcel Dekker: New York, 1981.

[150] F. Booth. The dielectric constant of water and the saturation effect. *J. Chem. Phys.*, 19:391–394, 1951.

[151] L. Lue, N. Zoeller, and D. Blankschtein. Incorporation of nonelectrostatic interactions in the Poisson-Boltzmann equation. *Langmuir*, 15:3726–3730, 1999.

[152] I. Borukhov, D. Andelman, and H. Orland. Steric effects in electrolytes: A modified Poisson-Boltzmann equation. *Phys. Rev. Letters*, 79:435–438, 1997.

[153] S. Woelki and H.H. Kohler. A modified Poisson-Boltzmann equation: I. Basic relations. *Chemical Physics*, 261:411–419, 2000.

[154] S. Woelki and H.H. Kohler. A modified Poisson-Boltzmann equation: II. Models and solutions. *Chemical Physics*, 261:421–438, 2000.

[155] T. Boublik. Hard sphere equation of state. *J. Phys. Chem.*, 53:471–472, 1970.

[156] G.A. Mansoori, N.F. Carnahan, K.E. Starling, and T.W. Leland. Equilibrium thermodynamic properties in the mixture of hard spheres. *J. Chem. Phys.*, 54:1523–1525, 1971.

[157] B.D. Casson and C.D. Bain. Unequivocal evidence for a liquid-gas phase transition in monolayers of decanol adsorbed at the air/water interface. *J. Am. Chem. Soc.*, 121:2615–2616, 1999.

[158] J.S. Erickson, S. Sundaram, and K.J. Stebe. Evidence that the induction time in the surface pressure evolution of lysozyme solutions is caused by a surface phase transition. *Langmuir*, 16:5072–5078, 2000.

[159] S.Y. Lin, W.B. Hwang, and T.L. Lu. Adsorption kinetics of soluble surfactants and the phase transition model. 2. Experimental demonstration of 1-decanol. *Colloids and Surfaces A*, 114:143–153, 1996.

[160] M. Aratono, S. Uryu, Y. Hayami, K. Motomura, and R. Matuura. Phase-transition in the adsorbed films at the water-air interface. *J. Colloid Interface Sci.*, 98:33–38, 1984.

[161] J.K. Ferri and K.J. Stebe. Soluble surfactants undergoing surface phase transitions: A maxwell construction and the dynamic surface tension. *J. Colloid Interface Sci.*, 209:1–9, 1999.

[162] E. Ruckenstein and B.Q. Li. A simple surface equation of state for the phase transition in phospholipid monolayers. *Langmuir*, 12:2308–2315, 1996.

[163] E. Ruckenstein and B.Q. Li. Phase transition from a liquid expanded to a liquid condensed surfactant monolayer. *J. Phys. Chem.*, 100:3108–3114, 1996.

[164] E. Ruckenstein. On the nature of the liquid expanded liquid condensed phase transition in monolayers of polar molecules. *J. Colloid Interface Sci.*, 196:313–315, 1997.

[165] D. Vollhardt, V.B. Fainerman, and G. Emrich. Dynamic and equilibrium surface pressure of adsorbed dodecanol monolayers at the air/water interface. *J. Phys. Chem. B*, 104:8536–8543, 2000.

[166] V.B. Fainerman, E.V. Aksenenko, and R. Miller. Effect of surfactant aggregation in the adsorption layer at the liquid/fluid interface on the shape of the surface pressure isotherm. *J. Phys. Chem. B*, 104:5744–5749, 2000.

[167] V.B. Fainerman and D. Vollhardt. Equations of state for Langmuir monolayers with two-dimensional phase transitions. *J. Phys. Chem. B*, 103:145–150, 1999.

[168] V.B. Fainerman, D. Vollhardt, and V. Melzer. Equation of state for insoluble monolayers of aggregating amphiphilic molecules. *J. Phys. Chem.*, 100:15478–15482, 1996.

[169] T. Gilanyi, R. Meszaros, and I. Varga. Phase transition in the adsorbed layer of catanionic surfactants at the air/solution interface. *Langmuir*, 16:3200–3205, 2000.

[170] C.D. Dushkin, I.B. Ivanov, and P.A. Kralchevsky. The kinetics of the surface tension of micellar surfactant solutions. *Colloids and Surfaces*, 60:235–261, 1991.

[171] E. Rillaerts and P. Joos. Rate of demicellization from the dynamic surface tension of micellar solutions. *J. Phys. Chem.*, 86:3471–3478, 1982.

[172] V.B. Fainerman and A.V. Makievski. Micelle dissociation kinetics study by dynamic surface tension of micellar solutions. *Colloids and Surfaces*, 69:249–263, 1993.

[173] V.B. Fainerman. Adsorption kinetics from concentrated micellar solutions of ionic surfactants at the water-air interface. *Colloids and Surfaces*, 62:333–347, 1992.

[174] R. Miller. Adsorption-kinetics of surfactants from micellar solutions. *Colloid and Polymer Sci.*, 259:1124–1128, 1981.

[175] E.A.G. Aniansson and S.N. Wall. Kinetics of step-wise micelle association. *J. Phys. Chem.*, 78:1024–1030, 1974.